Chapter 1

Introduction

1.1 General Introduction

Rivers are the major natural dynamic water bodies responsible for most of the continental input to world oceans as well as exogenic cycling of elements and are the circulatory system of the continents. Although, rivers and lakes make up only a small fraction (0.006%) of the hydrosphere [1], the rate of water circulation through them is quite rapid. They are the major conveyors of water, solute, sediments and also shape much of the landscape by transporting, redistributing and depositing the weathered continental mass across the earth surface. Rivers are called "Cradles of Civilisation" as major civilisations around the world developed and flourished along the banks of the rivers. In India rivers are considered sacred and personified as deities by the people. This is mainly because the floodplain sediments are very fertile and are major natural resource capable of supporting good agriculture and thus, life.

1.2 Importance of river sediment study

Recognition of sediments both as carrier as well as potential source of nutrients as well as contaminants in aquatic systems has stimulated increasing interest in fluvial transport of sediments [2]. The sediments are delivered to the oceans by rivers from the continents which represent the records of the Earth's geological history [3]. Knowledge of the distribution of sediment sources and sinks within a catchment is also essential for recommending controls. Thus sediments are integral and inseparable parts of the river ecosystem, so any environmental program concerning river water quality would be incomplete without the proper study of its sediments. Information on sediment chemistry may also be of value in elucidating the processes operating within the upstream drainage basin. Clay mineralogy has, for example, been successfully used to distinguish sediment contributions from individual tributary basins, or from field and channel sources [4]. Metal pollution in sediments has been a particular focus of concern and study, which may be derived from agricultural fields, urban effluent , industrial and mining activities and may be incorporated into flood plain materials. Under natural conditions floodplains benefit from nutrient enrichment, but pollution effects may become significant in downstream environments.

The deposition and active reworking of freshly eroded and highly weatherable material in a system with water and sediment residence times substantially longer than the upstream source areas creates potential for additional silicate weathering and CO2 consumption [5, 6]. Provenance studies [7, 8] are also central to the understanding of river dynamics because floodplains are the primary storage sites for river sediments during floods. Fluvial sediments provide an enhanced source of rock-derived nutrients to floodplain soils. They are products of the less-weathered upstream watershed, undergo physical alteration while entrained in the fluvial system, and then are subjected to intense chemical weathering in soil [9]. More geochemical data from diverse geological environments are needed to understand the efficacy of surface processes in element distribution and migration and to apply on older sediments. Assessing the sediment budgets of "large rivers" is essential for reconstructing sediment redistributions, rearrangement of drainages due to tectonic or climatic changes, global geochemical cycles, and sediment fluxes into the oceans as well as weathering rates and burial of organic carbon in floodplains [10, 11, 12, 13, 14]. However, rapid growth in world population, economic development and changing climate over the last few decades have drastically altered the health, form and functioning of river ecosystems. Therefore, there is an urgent need to understand the response of these fragile ecosystems to the above changes in detail and in systematic manner.

1.3 Himalayan rivers

Many large rivers draining the continents originate in the Himalayas which are characterized by large catchment size, length, and large volumes of water and sediment discharges [15, 16, 17]. This region is characterized by a monsoonal climate, and more than 90% of water and sediments are transported in just four months of the year. Because of younger age of sediments, its recent upliftment and Cenozoic climate change, these rivers have received attention and are extensively studied [18, 19, 20, 13, 21]. The considerable morphodynamic energy provided by the continuing tectonic evolution of the Himalaya is expressed in high erosional potentials and very high rates of sediment production [3]. Sediments derived by erosion of these lithotectonic units were delivered to the Himalayan foreland to make the Indogangetic alluvial plains [8, 22].

1.4 The Brahmaputra

The Brahmaputra is one of the major rivers of India. Along with the Ganga, it forms the Ganga-Brahmaputra basin which constitutes the second largest hydrologic region in the world. Draining the north and south slopes of the Himalayas respectively the Brahmaputra and the Ganga rivers coalesece to form the largest delta fan system in the world [23, 24, 25]. It originates in the Kailash Mountain in the Transhimalaya and flows with a very gentle slope eastward for ∼1200 km in Tibet as Yarlung Tsangpo or Tsangpo. The Tsangpo in Tibet and the Brahmaputra in India were recognized as the same river only in the late nineteenth century [26]. Its origin has been attributed to rapid erosion, followed by uplift and knickpoint formation [27]. The Tsangpo takes a U-turn after Pai around Namche Barwa, the Eastern Syntaxis, where it makes the deepest gorge of the world and turns south to enter Arunachal Pradesh, where it acquires the name Siang or Dihang. The Brahmaputra turns south near Dhubri at the Indo-Bangladesh border and flows as the river Jamuna until it meets the Ganga at Arichaghat.

It is the single largest river system draining the Himalaya and southern Tibetan plateau and transports a significant portion of all physically and chemically weathered material in this region.).In spite of a much smaller catchment area than the

Indus and the Ganga, the Brahmaputra has a significantly larger sediment discharge (suspended load 540-1157 million tons/yr), surpassed only by the Huanghe and the Amazon [28, 29].

The Brahmaputra River receives many tributaries along its course. In Tibet, the Tsangpo receives the Lhasa He (Zangbo), Doilung, and Nyang Qu [30, 31] in addition to tributaries from the northern slope of the Himalaya. After Pai, the river Parlung Zangbo [30] merges with it. The slope of this tributary is very high and comparable to that of the Siang in this section. In the Assam plain the Brahmaputra receives the Dibang and the Lohit from the east and the Subansiri, the Ranganadi, the Jiabharali, the Puthimari, the Manas, and the Tipkai from the north and the Burhidihing, the Dhansiri, and the Kopili from south. The northern and southern bank tributaries of the Brahmaputra river differ considerably in their hydro-geomorphological characteristics owing to different geological, physiographic and climatic conditions. Whilst the northern tributaries are marked by frequent avulsions (mostly westward) slow meander migrations is more frequent in the southern tributaries which is a manifestation of different tectonic regimes of these tributaries [32].The north bank tributaries are generally of Himalyan origin fed by glaciers in their upper reaches,e.g the Pagladia,the Subansiri,the Jiabharali,the Manas etc. whereas the south bank tributaries are of different origin,most of which have their origin in khasi hills of Meghalaya,for e.g the Kulsi.The northern tributaries have steep channel gradient, shallow braided channels, coarse sandy beds and more sediment load as compared to that of the southern tributaries. The southern tributaries have flatter channel gradient, meandering channels and banks composed of alluvial soils.

1.5 Significance of this study

Environmental geochemistry of rivers represents complex interactions in the rock-water-air-life system giving rise to a wide range of chemical characteristics in the surface environment which consequently are of critical importance to human beings. Thus, knowledge of fluvial processes involved in the generation, transportation, and deposition of river sediments are of fundamental importance in the Earth system science [3]. Moreover, constraining the processes that control the geochemistry of floodplain deposits is of particular importance for chemical weathering studies (e.g., [7]) because "large rivers" flow through areas that are subject to continuous deposition and erosion of sediments [33, 34]. Weathering and sediment generation in river catchments and subsequent soil formation supports life on earth. Weathering processes supply large quantities of sediments from the river catchments to build up river floodplains and sustain vegetation and agriculture by providing nutrient-laden river water. Moreover, the sediments transported by river controls atmospheric carbon dioxide levels on geological timescales through silicate weathering, riverine transport and subsequent burial of organic carbon in oceanic sediment. Sediment data also helps in providing the historical record of geochemical conditions of the river basin, identifying sources and sinks of pollutants, estimating geochemical cycles and formulating transport model [35]. Fluvial data are the basic information that we need to plan and manage any water resource program and also for maintaining sustainable agriculture. More importantly in the field of hydrological modelling, data are critically important. The availability of a common database would be a great contribution to a country's development and planning.

Inspite of the important role of Asian rivers in contributing to the total sediment budget delivery to the oceans, very few of them have been investigated in details. The Ganges-Brahmaputra River System transports the world's highest annual sediment load at one billion tons [36, 37], and yet because of its remote location, research on sediment transport and deposition has been limited [38, 39]. In reviewing the literature on the studies in the Brahmaputra river we see that the earlier workers have emphasized on the grain size, clay mineralogy and geochemistry of estuarine and deltaic regions and the dissolved load of Brahmaputra river basin. Only limited studies of the sediment characteristics [40, 41, 42, 43, 44, 45] have been carried out in the Indian part of this river and its tributaries. The Brahmaputra River along with the Ganga plays an important role in the C-burial but only a few works have reported the dynamics of Corg during transport in the Ganga-Brahmaputra system and especially its fate during floodplain transit.

In order to have a proper understanding of large river basin, it is essential to study the small and medium size sub-basins present within it. During river transport the composition of the sediment might be affected by weathering reactions, mixing with sediments of compositionally different tributaries and deposition or resuspension of a given size fraction which results in evolution of sediment grain size feature [5]. The large Brahmaputra river system has several medium to small size tributary rivers within its basin. The water and sediment chemistry of tributaries significantly influences the composition of the mainstream. The tributaries of the Brahmaputra have received very little attention excepting, few studies.

We continue to depend on rivers for agriculture, drinking water, fisheries, hydro power, transportation, construction, industries and most of the day to day activities as they are the most easily accessible water resources on the Earth. Therefore, no doubt, nation's socioeconomic development largely depends on the state and condition of its river systems. Moreover, as the Ganga and Brahmaputra basins are so far less influenced by construction of reservoirs; these are ideal areas for the studies of natural sediment transport and yield to the oceans.

As part of my research work the suspended, bed load, overbank and floodplain sediments of the 750 km stretch of the Brahmaputra river (the part of the river falling within the geographical boundary of India) and 6 of the major tributaries (the Subansiri, the Jiabharali ,the Pagladia, the Burhidihing, the Dikhow and the Kopili) were selected for the present work and an attempt was made to characterise and evaluate the sediment for their textural, mineralogical and geochemical characteristics by carrying out a detailed and systematic study. Thus with this background, the following objectives have been framed keeping the above mentioned points in mind.

1.6 Objectives

1. To study the role of riverine control on selective deposition, differential transport and distribution of various grain sizes of the Brahmaputra River and its tributaries.

2. To study the role of floodplain storage in controlling the chemical weathering of sediments.

3. To study the distribution and characteristics of riverine carbon.

4. To study the control of tributaries in maintaining the nutrient and sediment budget of the river Brahmaputra.

Bibliography

[1] Marsh, W. M., and Grossa Jr, J. (2002). Environmental geography: science, land use, and earth systems. John Wiley and Sons.,New York, pp 412.

[2] Forstner, U., and Muller, G. (1974). Schwermetallanreicherungen in datierten Sedimentkernen aus dem Bodensee und aus dem Tegernsee.Tschermaks mineralogische und petrographische Mitteilungen,21(3-4), 145-163.

[3] Singh, M., Singh, I. B., and Muller, G. (2007). Sediment characteristics and transportation dynamics of the Ganga River.Geomorphology,86(1), 144-175.

[4] Wall, G. J., and Wilding, L. P. (1976). Mineralogy and related parameters of fluvial suspended sediments in northwestern Ohio.Journal of Environmental Quality,5(2), 168-173.

[5] Bouchez, J., Gaillardet, J., Lupker, M., Louvat, P., France-Lanord, C., Maurice, L., Armijos, E. and Moquet, J. S. (2012). Floodplains of large rivers: Weathering reactors or simple silos?. Chemical Geology,332, 166-184.

[6] Lupker, M., Blard, P.H., Lave, J., France-Lanord, C., Leanni, L., Puchol, N., Charreau, J. and Bourles, D. (2012). 10 Be-derived Himalayan denudation rates and sediment budgets in the Ganga basin.Earth and Planetary Science Letters,333, 146-156.

[7] Singh, P., and Rajamani, V. (2001). Geochemistry of the floodplain sediments of the Kaveri River, southern India.Journal of Sedimentary Research,71(1), 50-60.

[8] Tripathi, J. K., Ghazanfari, P., Rajamani, V., and Tandon, S. K. (2007). Geochemistry of sediments of the Ganges alluvial plains: evidence of large-scale sediment recycling.Quaternary International,159(1), 119-130.

[9] Bland, W. J., and Rolls, D. (2016).Weathering: an introduction to the scientific principles. Routledge.

[10] Meybeck, M. (1993). C, N, P and S in rivers: from sources to global inputs. InInteractions of C, N, P and S Biogeochemical cycles and global change(pp. 163-193). Springer Berlin Heidelberg.

[11] Gaillardet, J., Dupre, B., and Allegre, C. J. (1999). Geochemistry of large river suspended sediments: silicate weathering or recycling tracer?.Geochimica et Cosmochimica Acta,63 (23), 4037-4051.

[12] Gaillardet, J., Dupre, B., Louvat, P., and Allegre, C. J. (1999). Global silicate weathering and CO 2 consumption rates deduced from the chemistry of large rivers.Chemical geology,159 (1), 3-30.

[13] Galy, V., France-Lanord, C., Beyssac, O., Faure, P., Kudrass, H., and Palhol, F. (2007). Efficient organic carbon burial in the Bengal fan sustained by the Himalayan erosional system.Nature,450 (7168), 407-410.

[14] Ashworth, P. J., and Lewin, J. (2012). How do big rivers come to be different?.Earth-Science Reviews,114 (1), 84-107.

[15] Sinha, R., and Friend, P. F. (1994). River systems and their sediment flux, Indo-Gangetic plains, Northern Bihar, India. Sedimentology,41(4), 825-845.

[16] Hovius, N. (1998). Controls on sediment supply by large rivers.,in: K.W. Shanley, P.J. McCabe (Eds.), Relative Role of Eustasy, Climate and Tectonism in Continental Rocks, Soc. Econ. Paleontol. Mineral. Spec. Publ., vol. 59. 3-16 Tulsa.

[17] Tandon, S. K., and Sinha, R. (2007). Geology of large river systems.Large rivers: geomorphology and management, 7-28.

[18] Raymo, M. E., and Ruddiman, W. F. (1992). Tectonic forcing of late Cenozoic climate.Nature,359(6391), 117-122.

[19] Derry, L. A., and France-Lanord, C. (1996). Neogene Himalayan weathering history and river87Sr86Sr: Impact on the marine Sr record.Earth and Planetary Science Letters,142(1), 59-74.

[20] Najman, Y. (2006). The detrital record of orogenesis: A review of approaches and techniques used in the Himalayan sedimentary basins.Earth-Science Reviews,74(1), 1-72.

[21] Chakrapani, G. J., Saini, R. K., and Yadav, S. K. (2009). Chemical weathering rates in the Alaknanda-Bhagirathi river basins in Himalayas, India.Journal of Asian Earth Sciences,34(3), 347-362.

[22] Tripathi, J. K., Bock, B., and Rajamani, V. (2013). Nd and Sr isotope characteristics of Quaternary Indo-Gangetic plain sediments: Source distinctiveness in different geographic regions and its geological significance. Chemical Geology, 344, 12-22.

[23] Morgan, J. P., and McINTIRE, W. G. (1959). Quaternary geology of the Bengal basin, East Pakistan and India.Geological Society of America Bulletin,70 (3), 319-342.

[24] Coleman, J. M. (1969). Brahmaputra River: channel processes and sedimentation.Sedimentary Geology, 3 (2-3), 129-239.

[25] Curray, J. R., and Moore, D. G. (1971). Growth of the Bengal deep-sea fan and denudation in the Himalayas.Geological Society of America Bulletin,82 (3), 563-572.

[26] Montgomerie, T. G. (1868). Report of a Route-Survey Made by Pundit, from Nepal to Lhasa, and Thence through the Upper Valley of the Brahmaputra to its Source.The Journal of the Royal Geographical Society of London,38, 129-219.

[27] Zeitler, P.K., Meltzer, A.S., Koons, P.O., Craw, D., Hallet, B., Chamberlain, C.P., Kidd, W.S., Park, S.K., Seeber, L., Bishop, M. and Shroder, J.

(2001). Erosion, Himalayan geodynamics, and the geomorphology of metamorphism.GSA Today,11(1), 4-9.

[28] Hay, W. W. (1998). Detrital sediment fluxes from continents to oceans.Chemical geology,145(3), 287-323.

[29] Islam, M. R., Begum, S. F., Yamaguchi, Y., and Ogawa, K. (1999). The Ganges and Brahmaputra rivers in Bangladesh: basin denudation and sedimentation.Hydrological Processes,13(17), 2907-2923.

[30] Guan Z., and Chen C. (1981) Hydrographical features of the Yarlung Zangbo river. In Geological and Ecological Studies of Qinghai-Xizang Plateau, pp. 1693-1703. Science Press, Beijing, Gordon and Breach. New York.

[31] Hu M., Stallard R. F., and Edmond J.(1982) Major ion chemistry of some large Chinese Rivers. Nature 298, 550-553.

[32] Lahiri, S. K., and Sinha, R. (2012). Tectonic controls on the morphodynamics of the Brahmaputra River system in the upper Assam valley, India.Geomorphology,169, 74-85.

[33] Allison, M. A., Kuehl, S. A., Martin, T. C., and Hassan, A. (1998). Importance of flood-plain sedimentation for river sediment budgets and terrigenous input to the oceans: Insights from the Brahmaputra-Jamuna River. Geology, 26(2), 175-178.

[34] Bourgoin, L. M., Bonnet, M. P., Martinez, J. M., Kosuth, P., Cochonneau, G., Moreira-Turcq, P., and Seyler, P. (2007). Temporal dynamics of water and sediment exchanges between the Curuaoodplain and the Amazon River, Brazil. Journal of Hydrology, 335(1), 140-156.

[35] Horowitz, A. J. (1985).A primer on trace metal-sediment chemistry(p. 67). US Government Printing Office.

[36] Milliman, J. D., and Meade, R. H. (1983). World-wide delivery of river sediment to the oceans.The Journal of Geology, 1-21.

[37] Milliman, J. D., and Syvitski, J. P. (1992). Geomorphic/tectonic control of sediment discharge to the ocean: the importance of small mountainous rivers.The Journal of Geology, 525-544.

[38] Barua, D. K., Kuehl, S. A., Miller, R. L., and Moore, W. S. (1994). Suspended sediment distribution and residual transport in the coastal ocean off the Ganges-Brahmaputra river mouth. Marine Geology, 120(1), 41-61.

[39] Goodbred, S. L., and Kuehl, S. A. (1999). Holocene and modern sediment budgets for the Ganges-Brahmaputra river system: Evidence for highstand dispersal to flood-plain, shelf, and deep-sea depocenters. Geology, 27(6), 559-562.

[40] Subramanian, V. (1980): A geochemical model for Phosphate mineralization in marine environment. Geological Survey of India Special Publications, 44, 308-313.

[41] Goswami, D. C. (1985). Brahmaputra River, Assam, India: Physiography, basin denudation, and channel aggradation.Water Resources Research,21(7), 959-978.

[42] Singh, S. K., and France-Lanord, C. (2002). Tracing the distribution of erosion in the Brahmaputra watershed from isotopic compositions of stream sediments.Earth and Planetary Science Letters,202(3), 645-662.

[43] Singh, S. K., Kumar, A., and France-Lanord, C. (2006). Sr and 87 Sr/86 Sr in waters and sediments of the Brahmaputra river system: Silicate weathering, CO 2 consumption and Sr flux.Chemical Geology,234(3), 308-320.

[44] Garzanti, E., Vezzoli, G., Ando, S., France-Lanord, C., Singh, S. K., and Foster, G. (2004). Sand petrology and focused erosion in collision orogens: the Brahmaputra case.Earth and Planetary Science Letters,220(1), 157-174.

[45] Garzanti, E., Ando, S., France-Lanord, C., Vezzoli, G., Censi, P., Galy, V., and Najman, Y. (2010). Mineralogical and chemical variability of fluvial sediments: 1. Bedload sand (Ganga-Brahmaputra, Bangladesh).Earth and Planetary Science Letters,299(3), 368-381.

Chapter 2

Literature Review

2.1 General Introduction

Rivers are the major component of the global water cycle [1] and also the primary agents of weathering and erosion which determines the transfer and redistribution of materials on the Earth's surface. The slow geologic erosion is a constructive process, which has created vast tracts of fertile soils of alluvial flood plains. These soils, with built-in soil fertility renewal mechanisms, have supported ancient civilisations (e.g., in the valleys of the Nile, Euphrates, Indus, Yangtze) and thriving cultures for millennia [2]. Erosion, transportation, and deposition processes of sediments are essentially controlled by topography and climate of the region. The sediments are delivered to the oceans by rivers from the continents which represent the records of the Earth's geological history [3]. They supply approximately 90% of the terrigenous materials to the ocean and are, in a way, veins of continents draining ca. 35000 km3 water [4]. Thus the knowledge of fluvial processes involved in the generation, transportation, and deposition of river sediments are of fundamental importance in the Earth system science [3].

2.1.1 The role of river systems in the earth system

The rivers by the geologic process of erosion and deposition have created vast tracts of fertile soils of alluvial flood plains. These soils, with built-in soil fertility renewal mechanisms, have supported ancient civilisations (e.g., in the valleys of the Nile, Euphrates, Indus, Yangtze) and thriving cultures for millennia [2]. Several tropical rivers have sustained human civilisations for more than 5000 years and have provided fertile floodplains for agriculture. Moreover the rivers supply approximately 90% of the terrigenous materials to the ocean. Thus rivers are, in a way, veins of continents draining ca. 35000 km^3 water [4], 15.5 billion tonnes sediment [5] and 3.5 billion tonnes total dissolved solids [6] every year to the world oceans out of which nearly 70% of the global river load (20×10^{15} gyr^{-1}) [6, 7] to the ocean is contributed by the south-east Asian rivers [8]. In broader perspective of geological evolution ,disappearance or disintegration of rivers ,shifting of their courses ,capture of one river by another and steady decline of discharge resulting in drying up are all normal responses to several geological processes acting on the earth's crust. These include tectonic activities (resulting from both orogenic and epeirogenic causes) sea-level changes, climatic factors and human intervention. Tropical rivers form an important component of the continental drainage systems and several of them have been classified as large river systems in the world [9, 10, 11, 12].

Continental-scale rivers, draining large areas from high-relief orogens to passive margins, flow through vast foreland basins and lowland areas. In these relatively flat regions, river sediments are continuously deposited and re-involved into riverine transport through a variety of geomorphological processes, resulting in continuous exchanges of sediments between the channel and its floodplain (e.g. [13, 14, 15]). The transient storage of solid particles in these alluvial plains results in presumably long sediment transfer times (i.e. the average time needed for a grain to be transported from the entry to the outlet of the river reach) [16]. The transfer time of river sediments in large river floodplains remains largely unknown, even if U-series disequilibria provide a first set of constraints that range from a few kyr for suspended load in the Mackenzie, Amazon and Ganges systems [17, 18, 19, 20], to several 100s of kyr for coarse sediments in the Gangetic plain [21]. These studies also suggest that the floodplain transfer time is longer than the residence time of sediment in the soils of the actively eroding orogens.

River borne material can reach the coastal zone and oceans, or be stored in continental sinks, as hill slopes, lakes and floodplains, or in endorheic basins that characterize the internal regions, not currently connected to open oceans, of 18.8 million km^2 of the continental area [22]. The transfer of river material at the Earth's surface is a

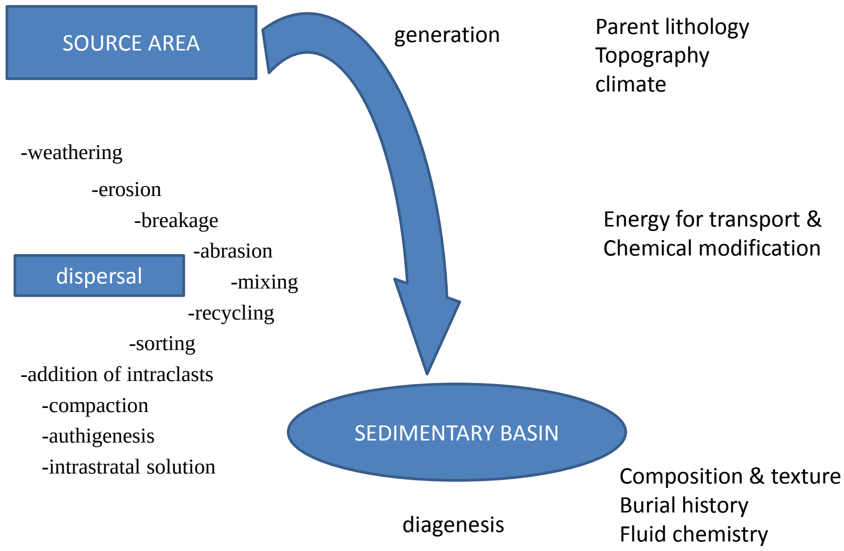

Figure 2.1: Main steps in sediment evolution and principal processes that modify the composition of clastic sediments along the pathway from source area to sedimentary basin (Adopted from [49]).

key component of the hydrological balance, the carbon balance at the decadal to centennial scale, the sediment balance, the nutrient balance (P, N, Si) and of the biodiversity of surface waters. It also controls the coastal zone functioning to a great extent [23, 24, 25]. These global natural riverine transfers have been established by various workers [26, 27, 28, 29, 30, 31, 5, 32, 33].

2.2 Clastic sediments and their influence on rivers

On a global scale the average composition of sediment evolves with time [34]. The present-day mass of global sediments is $\sim 2.7 \times 10^{24}$ g [35, 36]. Of these, $\sim$ 72.6% are situated within the confines of the present-day continents (orogenic belts 51.9% and platforms 20.7%), 12.9% at passive margin basins, 5.5% at active margin basins, and the sediments covering the ocean floor account for $\sim$ 8.3% of the total [37, 36, 38]. Broadly speaking, clastic sediments are made up of two types of material. Detrital grains, the dominant component of coarse clastic sediments, are the residues of weathered (crystalline or detrital) parent rocks, whereas fine-grained sediments may be essentially composed of clay minerals formed by weathering of unstable minerals. As shown in Fig. 2.1, specifically the nature and extent of source rock weathering, physical sorting during transport [39, 40] and environment of deposition and diagenesis exert significant control on sediment geochemistry [34, 41, 42]. Fluvial sediments are composite weathering products of all the lithologies in the drainage basin of the rivers [43, 44]. Sediment is an integral part of any river system and it plays a major role in the hydrological, geo-morphological and ecological functioning of river systems. Any changes in the sediment quantity and geochemistry can influence many inter-related natural and anthropogenic systems. Thus, estimating the sediment budgets and quality of "large rivers" is essential for reconstructing sediment redistributions, rearrangement of drainages due to tectonic or climatic changes, global geochemical cycles, and sediment fluxes into the oceans as well as weathering rates and burial of organic carbon in floodplains [31, 45, 46, 47, 48].

2.3 Role of Weathering in geochemical cycle of sediments

Weathering causes the depletion of unstable minerals like feldspars and mafic minerals (e.g., pyroxene, amphibole, biotite), whereas comparatively stable minerals like quartz and zircon, as well as clay minerals, are enriched in the detrital spectrum. The rate of change from primary minerals to secondary minerals depends on the availability of reactive mineral surfaces, the rate at which pore solutions are flushed by more dilute rain-driven waters [50] and stability of minerals to weathering [51]. On smaller scales, the relative importance of parent rock type (its structure, texture and mineralogy), slope and hydrodynamics of the region is highly variable. These, local variables determine the nature of different secondary minerals and their paragenesis. These variables in turn also control the mobilities of different elements during rock weathering [52].

The chemical weathering rates on continents are regulated by many factors, including the source rock type, climate regime, tectonic and topographic settings, vegetation, soil development, and human activities [53, 54, 55, 56, 57, 58, 45, 46, 59]. Climate, as represented by temperature and precipitation, has been identified as

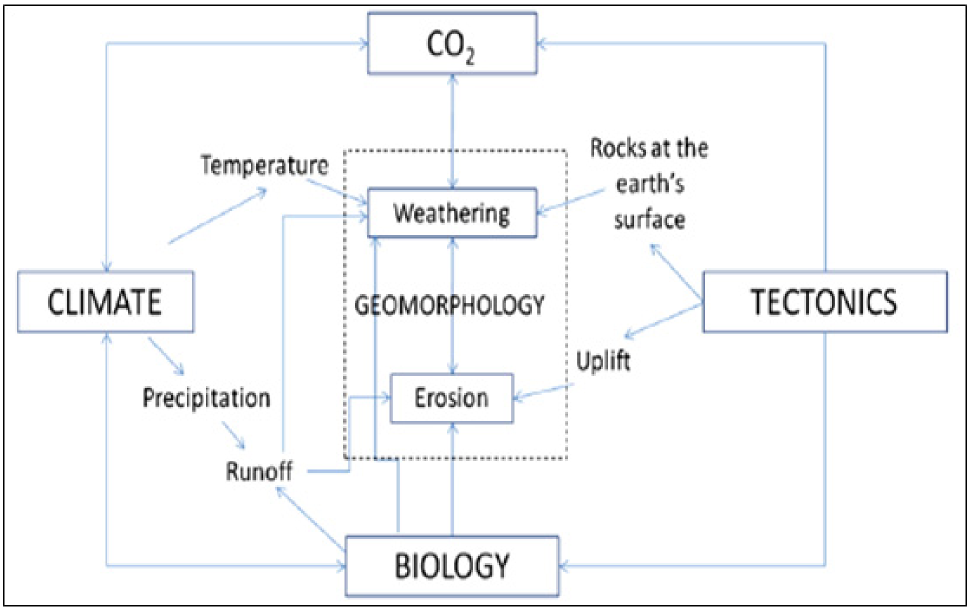

Figure 2.2: Schematic diagram of the broad linkages between weathering, climate, tectonics, biology, geomorphology and the carbon cycle [70].

a critical factor influencing silicate weathering rates. The role of temperature is particularly interesting because of the potential negative feedback between climate and silicate weathering rates. White and colleagues [58, 60] concluded from the analysis of field data that the weathering of Si and silicate-derived Na are primarily controlled by climatic factors. Similarly, others have determined that chemical denudation rates were correlated with runoff, a proxy for precipitation [61, 62, 63, 64]. In contrast, other studies have concluded that the exposure of fresh mineral surfaces by erosion is the most important factor determining rates of chemical weathering [65, 66, 67, 59]. Indeed, [68] and [69] found that chemical denudation was strongly correlated to erosion rate. The potential influence of erosion on chemical weathering rates is intriguing because it provides a link between tectonic and atmospheric processes (Figure 2.2).

The authors of [71] suggested that chemical weathering is more pronounce in tectonically active regions which increases the dissolved load of the river. However, this fact was countered by a negative correlation between sediment yields in major river systems of the world and weathering intensity [72]. This observation and that of [58] seem to suggest that physical erosion may not have any critical influence on chemical weathering rates. So the role of tectonics is still not established.

On the broader perspective and over geological scale, the basin tectonics at source and sink exert the overall control on sediment chemistry [73, 74, 75, 76, 77]. Many studies argued that basin relief is also strongly coupled with both mechanical and chemical denudation rates, especially for those tectonic active areas, such as the Himalaya region [78, 43, 79]. Finally, biological factors also affect weathering rates. Directly, microorganisms, plants and animals enhance (and sometimes retard) the rate of chemical weathering through altering soil acidity and pCO_2, whilst indirectly such communities act to reduce erosion, with knock-on effects on weathering. The climatic, tectonic and biological factors outlined above in Fig. 2.2 (in very simple terms) do not act independently of one another, and there are many important inter-linkages (some of which are shown in Fig. 2.3). Thus, for example, climatic, tectonic and biological factors all play a role in influencing erosion rates, whilst biological and climatic factors interact in conditioning temperature, acidity and moisture regimes in soils. These interlinkages make it very difficult to isolate the impact of any one controlling factor on weathering rates [70].

2.3.1 Weathering and Carbon cycle

The authors of [80] linked climatic and geochemical processes by proposing that the weathering of Ca- and Mg-bearing silicate minerals sequesters atmospheric CO_2 through the ultimate precipitation of calcite and dolomite. This process is governed by the rate of carbonic acid dissolution reactions, as originally proposed by [81].

$$2CO_2 + 3H_2O + Ca\ Al_2Si_2O_8 = Ca^{+2} + 2HCO_3^- + Al_2Si_2O_5(OH_4) \tag{2.1}$$

Since then, a concerted effort has been made to understand the fundamental controls on chemical weathering (e.g., [82, 58, 62, 83]). These investigations have been stimulated by conceptual and numerical models that propose links and feedbacks between atmospheric processes, weathering, tectonic processes, and erosion (e.g., [84, 71, 78, 85]). Although chemical weathering may influence atmospheric carbon dioxide levels, the links also work the other way through the nexus of feedbacks within the linked climate-biological-tectonic system shown in Fig. 2.2. Increases in atmospheric CO_2 would raise global temperatures through greenhouse effects; the increase in temperature, in turn, should enhance silicate weathering rates and lead to a decrease in atmospheric CO_2, thus bringing temperatures back down [86, 84]. Decreasing CO_2 levels will lead to climatic cooling which should in turn lead to decreased chemical weathering. On the other hand, increasing rates of CO_2 fertilisation cause a change in terrestrial biomass productivity, which in turn should enhance weathering rates directly and indirectly [87, 88, 89]. These sorts of negative feedback processes [86, 90] illustrate how weathering acts as a brake on fluctuations in carbon cycling. The ”thermostat” hypothesis originally posed by [86], that the temperature dependence of the weathering of aluminosilicate rocks acts as a negative feedback on pCO_2, is intuitively elegant and has gained much consensus [84, 91, 85]. The hypothesis is based on two fundamental laws of nature. Thermodynamically, the saturation vapor pressure of water increases rapidly with increasing temperature (Clausius-Clapeyron relationship) as is observed in environmental measurements [92], leading to higher precipitation and runoff. Kinetically, reaction rates also increase almost exponentially with increasing temperature (Arrhenius law); this has also been demonstrated in laboratory dissolution experiments [93, 94]. Any temperature increase is negated by CO_2 uptake due to accelerated aluminosilicate weathering. The abrupt and rapid increase in the 87Sr/86Sr ratio in sea water since 40 Ma, broadly coincident with a period of convergent tectonics, uplift and erosion in the Himalayas, provides perhaps the best evidence for orogenic control on depletion of atmospheric CO_2 due to the increased rates of weathering of crustal lithologies. For valid model simulations of the evolution of atmospheric pCO_2, an understanding of the relationship between lithology, relief, temperature and weathering rates is required.

Interactions between atmosphere, ocean and continent determine both the shape and climate of the Earth's surface through a sequence of complex processes. Ancient deposits can be further affected by reworking by glacial, fluvial, marine and aeolian activity [95, 96]. Of all these geological agents, rivers are the most important supplier of these weathered and eroded continental materials to the ocean system. They are the main conveyors of elements from the continents to the ocean, carrying both mineral and organic species as dissolved and particulate phases. Their role in the long-term climate regulation has long been highlighted and debated, especially through the transport of dissolved cations derived from silicate weathering ([45, 97]

and ref. therein).

2.4 Factors controlling the water and sediment geochemistry of world rivers

The chemistry of river water and sediment is a cumulative reflection of catchment geology, rainfall, weathering processes and anthropogenic interventions [98, 99]. River geochemistry integrates the contribution of several sources: atmospheric input + chemical weathering ± biospheric effect ± ion-exchange effect [100]. These factors will also be responsible for the chemistry of loose sediments being transported by the river [101]. River geochemistry is an integrative function of catchment solute inputs and biogeochemical cycling, and so is an excellent tool with which to quantify and understand weathering rates, provided inputs of solutes from non-silicate sources, biological cycling and human activity can be successfully de-convolved [102]. Climate and topography in the source area are the main controlling factors of processes like weathering and erosion, which determine the detrital spectrum supplied to first-order tributaries at the beginning of the dispersal system connecting source and basin. In general the nature of the bedrock exerts a dominant control on dissolved fluvial fluxes [65, 103]. Vegetation, which plays an important role as principal modulator of the output from the source area into first-order tributaries [104], is also largely controlled by climate and topography. Organic matter plays an important role in the transport of metals since it is able to bind trace metals and the suspended particles which are covered with organic films are found to have large contents of trace metals because of increased adsorptive characteristics [105]. In addition to the presence of organic matter, grainsize variation, mineralogy etc. also affect the trace metal transport in a river system.

While modern weathering rates are often derived from river solute fluxes (e.g. [54, 45, 83], their solid counterparts have received far less attention (e.g. [46, 106, 107]) probably because of the difficulty of integrating the variability of detrital sediments over space and time [108, 109, 110, 111]. Sediment records are however one of the rare archives that can be reliably used to trace past erosion fluxes at regional scales. Recognition of sediments both as carrier as well as potential source of nutrients as well as contaminants in aquatic systems has stimulated increasing interest in fluvial transport of sediments [112]. Knowledge of the distribution of sediment sources and sinks within a catchment is also essential for recommending controls. Information on sediment chemistry may also be of value in elucidating the processes operating within the upstream drainage basin. Clay mineralogy has, for example, been successfully used to distinguish sediment contributions from individual tributary basins, or from field and channel sources [113].

Compositional and textural characteristics of the initial detritus are modified by abrasion and sorting during transport, when sediments are carried away from their source area. While sediment is in transit, chemical alteration acts as important sediment modifier during transport and temporary storage of the sediment in alluvial systems [114]. The mineralogical and grain size changes produce geochemically diverse type of sediments. These geochemically different sediments are useful in understanding provenance composition, weathering conditions (climate and tectonics of the provenance), and sequestration and release of nutrient and toxic elements in the present day environmental condition. River sediments experiences mineralogical maturation with increasing deposition time [114]. Mixing of detritus from multiple sources may further modify the initial sediment characteristics, especially when dispersal pathways are complex and involve recycling of previously deposited sediments. The complexity of these interdependent modifications imposes certain limits on our capability to infer the characteristics of source areas from the properties of their products, just like "...we can not tell all we want to know of a sand grain's origin from its composition alone, any more than we can deduce political history from human physiology" [115].

Floodplain-river interaction is a major control of the chemical composition of river sediments [116]. Floodplains regulates water levels by temporarily storing water during discharge peaks, sequesters large amounts of sediments and associated pollutants [117]. The sediment delivery or conveyance processes operating within the channel system of a river basin are spatially and temporally complex [118, 119], providing many opportunities for short- and longer-term storage of fine-grained sediment, both within the channel and on the floodplains bordering the channel. Existing studies have shown that typically between 10 and 60% of the sediment

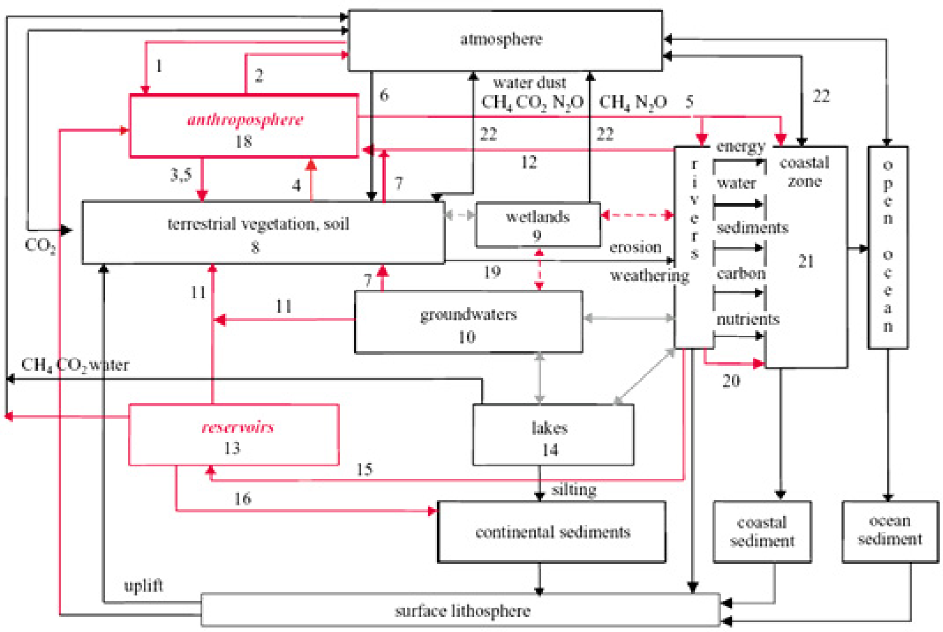

Figure 2.3: Continental aquatic systems in the present day earth system [70]: Black, natural fluxes and pathways of material; red, major impacts of human activities: 1, N fixation; 2, water consumption; 3, fertilization; 4, food and fibre consumption; 5, waste release; 6, atmospheric pollutants fallout; 7, water abstraction; 8, land use (deforestation, cropping, urbanization); 9, draining; 10, salinization, contamination, depletion; 11, irrigation; 12, diversion; 13, evaporation, regulation, eutrophication; 14, eutrophication; 15, damming, water storage, diversion; 16, silting; 17, mining; 18, industrial transformation; 19, enhanced soil erosion; 20, xenobiotic fluxes; 21, changes of inputs to coastal zone; 22, changes in greenhouse gas emissions.

delivered to the main channel system may be deposited and stored within the channel or on the floodplains and, therefore, fail to reach the catchment outlet (e.g. [120, 121, 122, 123, 124, 14, 125, 126]). The amount of sediment deposition increases with increasing inundation frequency, sediment supply, water depth, decreasing flow velocity and decreasing distance to the river channel [117]. During river transport the composition of the sediments might be affected by weathering reactions , mixing with sediments of compositionally different tributaries and deposition and resuspension of a given size fraction which results in evolution of sediment grain size feature [16].

In the last few decades, geochemical studies of rivers have received worldwide attention, primarily with a view to 1) define a world average river water and sediment composition and their fluxes, 2) to determine various factors and processes controlling water and sediment chemistry, 3) to estimate the weathering and erosion rates of river basins to understand their impact on global climate, biogeochemical cycling of elements in the continent-river-ocean system, and 4) to establish a global geochemical budget [26, 27, 6, 28, 127, 128, 8, 45]. The geochemical studies of major world rivers has been initiated by various workers, for Amazon [129, 9, 8, 34, 130, 131, 132], Mackenzie [133], Chinese rivers [134, 135], Mekong [136], Congo [132] and Ganges-Brahmaputra river system [137, 138, 139, 140, 141, 108, 142, 116] and these studies show a spectrum of variations in natural concentrations of various chemical species in their water and sediments, the variations are simply a reflection of different geological and climatic features of different basin.

In most of the studies of alluvial system, chemistry of channel bed and suspended load sediments have been used to evaluate the provenance characteristics [143, 144, 145]. Neither of them represents closely the composition of source rocks [40]. This is because of the strong physical sorting of sediments during transport and deposition leading to concentration of quartz and feldspar with some heavy minerals in the coarse fraction (bed sediments)and of secondary ,lighter and more weatherable mineral sin the suspended load. This mineral sorting results in chemical differences between the two types of sediment load and consequently their deviation from source rock composition. On the other hand, floodplain sediments which have textures intermediate between bed and suspended load could have chemistry more close approximating their source rocks if source rock weathering did not remove soluble cations from the rocks. Particularly the use of immobile major and trace elements which are thought to be carried in the particulate load, such as Al, Fe, Ti, Th, Sc, Co, Zr and the rare earth elements (REEs), have been found to be useful indicators of the source [34].

2.5 The Himalayan rivers

Himalayan rivers have received more attention because of younger age of sediments, its recent upliftment and Cenozoic climate change [78, 146, 147, 47, 148]. Global tectonic movement during the Cenozoic, in particular the uplift of the Himalayan-

Tibetan Plateau and its environmental effect, have been widely highlighted in earth system science and global change research since [149] proposed the "tectonic uplift-weathering" hypothesis. The Tibetan uplift fostered the Asian monsoon climate and major river systems. Chemical weathering in these river basins plays a key role in earth surface processes and geochemical cycles in supergene environments, including the global carbon cycle and the chemical composition of the oceans [84, 78, 150, 151, 62]. The foreland basin of the Himalaya was formed due to India-Asia collision during the earliest Eocene (∼50Ma) [152, 153] and was filled with sediments brought by the Indus-Ganges-Brahmaputra river systems to make the Indo-gangetic alluvial plains [154]. Tectonic-weathering-climate hypothesis considers Himalayan uplift as a major cause of Cenozoic cooling due to uptake of CO_2 through silicate weathering. In India, many studies to understand nature and rate of weathering, provenance, silicate and carbonate erosion rate and their impact on climate, dissolved and material flux of rivers to the oceans are available for various river basins [139, 140, 141, 150, 155, 156, 157, 158, 159, 160, 161, 162, 43, 44, 163, 164, 165, 166].

2.6 Studies on the Brahmaputra

The Brahmaputra is one of the most sediment charged large rivers of the world, which is widely documented in sediment flux studies [167, 168, 8]. In total, the Brahmaputra carries over 73 million tons of dissolved material annually, which accounts for approximately 4% of the total dissolved flux to the world's oceans [169]. In spite of a much smaller catchment area than the Indus and the Ganga, the Brahmaputra has a significantly larger sediment discharge (suspended load 540-1157 million tons/yr), surpassed only by the Huanghe and the Amazon [170, 171]. During monsoon months, June through September, the daily rate of sediment discharges at Pandu averages 2.0 million metric tons, whereas average annual suspended load is 402 million tons [172]. The Brahmaputra also has the highest downstream gradient of the three rivers, which is a result of it having occupied its present channel for only 200 years [173]. As a braided stream, the river is characterised by many channels, shoals, and islands, which is one characteristic of a river with a high sediment load [167]. Sediments eroded from the banks mostly through slumping during

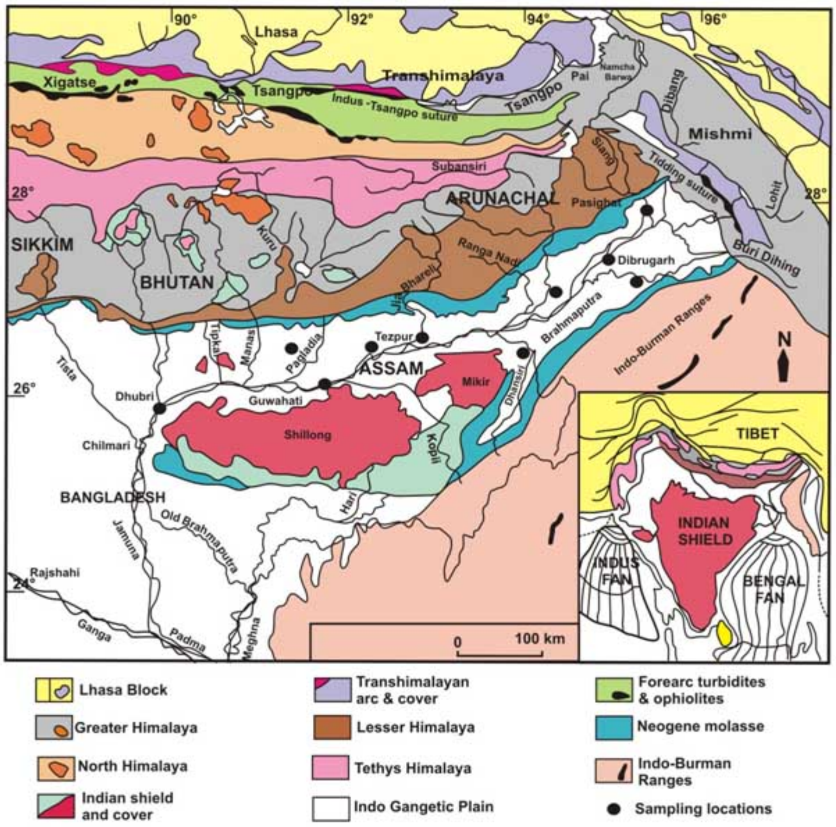

Figure 2.4: Figure showing geographical locations and features in the Brahmaputra basin. Source: modified from [179].

falling stages [167, 172] are deposited in the channel belt and are manifested as the overall increase in sand bar area with high valley slope. The authors of [159] compared the Himalayan erosion rates with the suspended sediment loads of the rivers, and determined that the eastern portion of the Himalayan Range is eroding faster than the western portion, which contributes to the Brahmaputra having a higher suspended load than the Ganges. The higher erosion in the eastern region is likely caused by higher precipitation in the eastern region [174, 159]. Given the high runoff and lithology of the Eastern Himalaya, both physical and chemical erosion rates for the Brahmaputra Basin are higher than those for the Ganga, and much higher than the world average [140, 139, 175, 158, 159, 43, 166, 169]. Total erosion in the Brahmaputra is about 1.5 to 2 times higher than that of the Ganga [159]. These high rates of chemical weathering result in the consumption of $\sim 6 \times 10^5$ mol km^{-2}yr^{-1} CO_2 due to the weathering of silicate minerals [169]. In contrast, to the Ganga only limited studies have been reported for the Brahmaputra water and sediment geochemistry [176, 150, 177, 158] despite the fact that (i) it drains the eastern Himalaya, Transhimalaya, Mishmi complex and the Burmese ranges, characterised by quite different geology and lithology, (ii) it has significantly higher runoff and chemical erosion than the Ganga [159, 169] and (iii) its sediment and dissolved f luxes are higher than those of the Ganga. Major efforts to investigate weathering and erosion of the Brahmaputra system have been initiated only recently [166, 169, 178, 179, 79]. Limited studies have been carried out to understand the geological evolution, stratigraphy, geomorphology, sedimentology, geochemistry and fluvial processes of the Brahmaputra basin [159, 166, 180, 181, 172].

The Brahmaputra has been best studied geomorphologically, in three different locations. The authors of [172] has described the Brahmaputra in Assam studying its physiography, basin denudation, and channel aggradation [167], the entire reach in Bangladesh and studied the channel processes and sedimentation and [182] along a 200 km reach, also in Bangladesh studied the channel pattern and migration. He observed that the Brahmaputra is 60-70 ft deep in most stretches; however, narrow points along the river can be as deep as 150 ft. All those studies indicate the dynamic nature of the river by highlighting the changing hydraulic, hydrologic and sediment transport conditions in large floods and also the effect of the seasonal flow regime.

Petrographic and mineralogical information on the Ganga and Brahmaputra rivers in Bangladesh has been reported by [9, 183, 184]. Only Bengal Fan turbidites have been accurately studied both petrographically and mineralogically [185, 186]. The authors of [166] and [169] investigated the sources of the clastic sediment and dissolved matter in the Brahmaputra Basin. The Brahmaputra has been studied for its large sediment flux [167, 182, 187, 188, 189, 190, 180] and highly dynamic hydrologic regime [172, 191, 192, 193, 194, 195]. Notwithstanding the huge detrital volumes involved, only a few studies have been done to study the composition of sediments carried by the Brahmaputra and its tributaries (e,g. [166, 179, 196]) (The features and geographical locations shown in Figure 2.4).

The high water discharge and low residence time of the sediments in the Brahmaputra Basin indicate that weathering in the basin is transport limited [57] and alteration of the composition of the sediment is low. This is supported by the low proportion of clay in the sediment and the composition of this clay [169].

As the waters of the Brahmaputra river system including many of its tributaries are undersaturated in calcite [169], the Sr/Ca in waters reflects the ratio of their release. The dominant mineral housing Ca and Sr in the silicates of the Himalaya and the Transhimalaya is calcic plagioclase. It has been shown that the abundance of dissolved Na to this river is dominated by dissolution of evaporites [169] and hence the elemental ratios of sample having high concentration of Na should represent that of the evaporite end member. The authors of [180] did a comprehensive chemical and isotope study of its waters and sediments to determine the chemical erosion patterns among its various sub-basins and provide an assessment of the sources supplying dissolved Sr to the Brahmaputra river system and a data set for comparison with the Ganga waters.

Bedloads of the Brahmaputra mainstream have CIA ranging from 58 to 64 [166]. These lower CIA values indicate that they are less weathered. The lower CIA of the Brahmaputra can arise due to the presence of Transhimalayan Plutonic rocks. Weathering indices are similar in Brahmaputra bedload (CIA 55 $\pm$ 5) and Himalayan source rocks (CIA 50-65; [106, 169, 197]), suggesting relatively limited silicate weathering (CIAUCC=47; [180, 198]). The clay content of Brahmaputra mainstream, from Dibrugarh to Guwahati, is only 1.7 to 3 wt% of total sediments. Provenance-related differences in chemical composition are dimmed by overwhelming hydrodynamic effects in the Brahmaputra river sediments [196]. Brahmaputra bedload tends to be richer in Na, Sr, Cr, Co, and Ni, reflecting more abundant plagioclase, amphibole and Cr-spinel,whereas Ganga bedload is richer in Ca, reflecting significant carbonate. Weathering indices are similar in Ganga-Brahmaputra bedload (CIA 55$\pm$5) and Himalayan source rocks (CIA 50-65; [106, 169, 197]), suggesting relatively limited silicate weathering (CIAUCC 47; [190, 3]). Plagioclase is largely preserved (PIA 55$\pm$4 in Brahmaputra sand), but alkali and alkaline-earth metals are systematically depleted relative to UCC in all Ganga-Brahmaputra sediments.

The authors of [179] documented composition of sand-sized detritus carried by the Tsangpo-Siang-Brahmaputra River and its tributaries and suggested that the Namche Barwa area, representing only $\sim$ 4% of total basin area, contributes 35; 6% of the total Brahmaputra sediment flux; Tibet, with an area of $\sim$ 1/3, contributes only 5%.The mineralogy of sediments of the Brahmaputra River System [179] show that (1) there is a marginal decrease in the plagioclase/feldspars (P/F) ratio from the mountain streams to the Assam plains, (2) there is no indication of selective dissolution of plagioclase over the more resistive K-feldspar, (3) clinopyroxenes and amphiboles show similar extent of alteration, and (4) quartz/feldspar (Q/F) ratio, P/F ratio, and hornblende-dominated dense-mineral assemblages remain constant. All these observations infer minimal chemical weathering of the Brahmaputra sediments.

The authors of [184] studied the mineralogy of the Ganges and Brahmaputra Rivers and observed that Ganges and Brahmaputra rivers have distinctive mineralogies which result from geologically distinct source areas. The Brahmaputra drains the Tibetan Plateau of China and is dominated by upland tributaries originating in the Himalayas. The Brahmaputra flows through various rock types including Precambrian metamorphics (high-grade schists, gneisses, quartzites, metamorphosed limestones), felsic intrusives, and Paleozoic-Mesozoic sandstones, shales and limestones [199]. Another mineralogical difference includes slightly lower amphibole contents in the Ganges than the Brahmaputra [199, 183]. Carbonates (mostly dolomite) may also be used to distinguish Ganges from Brahmaputra alluvium [199] Illite is ubiquitous in both the Ganges and Brahmaputra rivers, indicating erosion from relatively unweathered granitic or metamorphic terrain of the Himalayas. However, the Ganges has high smectite (56%, 41%; [140], [200] respectively) while the Brahmaputra has low smectite (5% average of three samples; [140]). In addition, the Brahmaputra has higher abundances of kaolinite than the Ganges (18% vs. 4%, respectively, [140]). The authors of [196] studied that the Brahmaputra sands and reported that the sands are richer in feldspar, lack carbonate grains, and include minor volcanic, metavolcanic, metabasite, and ultramafic lithic grains. Plagioclase ($\sim$ 40% albite, $\sim$ 60% Ca-plagioclase) prevails over K-feldspar and biotite over muscovite. Rich to very-rich amphibole-epidote-garnet suites include opaques, clinopyroxene, titanite, sillimanite, rutile, apatite, ypersthene,tourmaline, zircon, kyanite, staurolite, chloritoid, allanite,monazite, and rare Cr-spinel, enstatite, olivine, and xenotime.

Only a few studies have been done to study the C-dynamics in the Brahmaputra river system. The authors of [169] studied the water chemistry (major ion composition of waters, and δC13 of its DIC (dissolved inorganic carbon) for source apportionment of the solutes in the Brahmaputra River and its tributaries from silicates and carbonates and also determined the CO_2 consumption rates. This study suggested that the Eastern Syntaxis basin of the Brahmaputra is one of most intensely chemically eroding regions of the globe; and that runoff and physical erosion are the controlling factors of chemical erosion in the eastern Himalaya. The authors of [79] studied the role of the eastern syntaxis on chemical weathering fluxes in the Brahmaputra River and examined spatial patterns of CO_2 consumption by silicate weathering in different portions of this basin. They found that the TDS flux from the eastern syntaxis is greater than 526 tons $km^{-2}yr^{-1}$ and CO_2 consumption by silicate weathering is 15.2×10^5 mol $km^{-2}yr^{-1}$ which is more than twice the Brahmaputra average and forty times greater than the CO_2 consumption rates for the Tibetan portion of the drainage. This represents more than 15% of the Brahmaputra total from only 4% of the total basin drainage area. Thus the calculations support previous studies that show that the eastern syntaxis has a significant impact on the chemical fluxes in the Brahmaputra [169] and dominates sediment fluxes [166]. The authors of [201] recorded the sedimentary Corg from the Himalayan range to the delta to study the transport of Corg in the Ganga-Brahmaputra system and especially its fate during floodplain transit.

Bibliography

[1] Garrels, R. M., Lerman, A., and Mackenzie, F. T. (1976). Controls of atmospheric O_2 and CO_2: past, present, and future: geochemical models of the earth's surface environment, focusing on O_2 and CO_2 cycles, suggest that a dynamic steady-state system exists, maintained over time by effective feedback mechanisms. American Scientist, 306-315.

[2] Lal, R. (2003). Soil erosion and the global carbon budget.Environment International,29(4), 437-450.

[3] Singh, M., Singh, I. B., and Muller, G. (2007). Sediment characteristics and transportation dynamics of the Ganga River.Geomorphology,86(1), 144-175.

[4] Milliman, J. D. (1991). Flux and fate of fluvial sediment and water in coastal seas.Ocean margin processes in global change, 69-89.

[5] Milliman, J. D., and Syvitski, J. P. (1992). Geomorphic/tectonic control of sediment discharge to the ocean: the importance of small mountainous rivers.The Journal of Geology, 525-544.

[6] Meybeck, M. (1976). Total mineral dissolved transport by world major rivers/Transport en sels dissous des plus grands fleuves mondiaux.Hydrological Sciences Journal,21(2), 265-284.

[7] Meybeck, M. (1977). Dissolved and suspended matter carried by rivers : composition, time and space variations and world balance. In:Interactions between sediments and fresh waters, H. L. Golterman ed. - Junk et Pudok, Amsterdam, 25-32.

[8] Milliman, J. D., and Meade, R. H. (1983). World-wide delivery of river sediment to the oceans.The Journal of Geology, 1-21.

[9] Potter, P. E. (1978). Petrology and chemistry of modern big river sands.The Journal of Geology, 423-449.

[10] Hovius, N. (1998). Controls on sediment supply by large rivers.,in: K.W. Shanley, P.J. McCabe (Eds.), Relative Role of Eustasy, Climate and Tectonism in Continental Rocks, Soc. Econ. Paleontol. Mineral. Spec. Publ., vol. 59. 3-16 Tulsa.

[11] Latrubesse, E. M., Stevaux, J. C., and Sinha, R. (2005). Tropical rivers.Geomorphology,70(3), 187-206.

[12] Gupta, A. (Ed.). (2008).Large rivers: geomorphology and management. John Wiley and Sons.

[13] Meade, R. H., Dunne, T., Richey, J. E., Santos, U. D. M., and Salati, E. (1985). Storage and remobilization of suspended sediment in the lower Amazon River of Brazil.Science,228 (4698), 488-490.

[14] Allison, M. A., Kuehl, S. A., Martin, T. C., and Hassan, A. (1998). Importance of flood-plain sedimentation for river sediment budgets and terrigenous input to the oceans: Insights from the Brahmaputra-Jamuna River. Geology, 26 (2), 175-178.

[15] Dunne, T., Mertes, L. A., Meade, R. H., Richey, J. E., and Forsberg, B. R. (1998). Exchanges of sediment between the flood plain and channel of the Amazon River in Brazil.Geological Society of America Bulletin,110(4), 450-467.

[16] Bouchez, J., Gaillardet, J., Lupker, M., Louvat, P., France-Lanord, C., Maurice, L., Armijos, E. and Moquet, J.S. (2012). Floodplains of large rivers: Weathering reactors or simple silos?Chemical Geology,332, 166-184.

[17] Vigier, N., Bourdon, B., Turner, S., and Allegre, C. J. (2001). Erosion timescales derived from U-decay series measurements in rivers.Earth and Planetary Science Letters,193(3), 549-563.

[18] Dosseto, A., Bourdon, B., Gaillardet, J., Allegre, C. J., and Filizola, N. (2006). Time scale and conditions of weathering under tropical climate: Study of the Amazon basin with U-series.Geochimica et Cosmochimica Acta,70(1), 71-89.

[19] Dosseto, A., Bourdon, B., Gaillardet, J., Maurice-Bourgoin, L., and Allegre, C. J. (2006). Weathering and transport of sediments in the Bolivian Andes: Time constraints from uranium-series isotopes.Earth and Planetary Science Letters,248(3), 759-771.

[20] Granet, M., et al. (2010), "U-series disequilibria in suspended river sediments and implication for sediment transfer time in alluvial plains: the case of the Himalayan rivers."Geochimica et Cosmochimica Acta74.10: 2851-2865.

[21] Granet, M., Chabaux, F., Stille, P., France-Lanord, C., and Pelt, E. (2007). Time-scales of sedimentary transfer and weathering processes from U-series nuclides: clues from the Himalayan rivers.Earth and Planetary Science Letters,261(3), 389-406.

[22] Vorosmarty, C. J., Meybeck, M., Fekete, B., Sharma, K., Green, P., and Syvitski, J. P. (2003). Anthropogenic sediment retention: major global impact from registered river impoundments.Global and planetary change,39(1), 169-190.

[23] Milliman, J. D., Yun-Shan, Q., Mei-e, R., and Saito, Y. (1987). Man's influence on the erosion and transport of sediment by Asian rivers: the Yellow River (Huanghe) example.The Journal of Geology, 751-762.

[24] Martin, J. M., and Windom, H. L. (1991). Present and future roles of ocean margins in regulating marine biogeochemical cycles of trace elements.Ocean margin processes in global change, 45-67.

[25] Caddy, J. F., and Bakun, A. (1994). A tentative classification of coastal marine ecosystems based on dominant processes of nutrient supply.Ocean and coastal management,23(3), 201-211.

[26] Livingstone, D. A.(1963). Chemical Composition of Rivers and Lakes, in Data of Geochemistry, US Geol. Survey Prof. Paper, 440 , 64.

[27] Garrels, R. M., and Mackenzie, F. T. (1971). Evolution of sedimentary rocks. W.W. Norton, New York, 397 pp.

[28] Martin, J. M., and Meybeck, M. (1979). Elemental mass-balance of material carried by major world rivers.Marine chemistry,7(3), 173-206.

[29] Meybeck, M. (1979). Concentrations des eaux fluviales en elements majeurs et apports en solution aux oceans.Rev. Geol. Dyn. Geogr. Phys,21(3), 215-246.

[30] Meybeck, M. (1982). Carbon, nitrogen, and phosphorus transport by world rivers.Am. J. Sci,282(4), 401-450.

[31] Meybeck, M. (1993). C, N, P and S in rivers: from sources to global inputs. In-Interactions of C, N, P and S Biogeochemical cycles and global change.Springer Berlin Heidelberg, 163-193 pp.

[32] Ludwig, W., Amiotte Suchet, P., and Probst, J. L. (1996). River discharges of carbon to the world's oceans: determining local inputs of alkalinity and of dissolved and particulate organic carbon.Sciences de la terre et des planetes (Comptes rendus de l'Academie des sciences),323, 1007-1014

[33] Ludwig, W., and Probst, J. L. (1998). River sediment discharge to the oceans; present-day controls and global budgets.American Journal of Science, 298(4), 265-295

[34] Taylor S. R. and McLennan S.M. (1985). The continental crust: its composition and evolution. Blackwell Scientific Publication, Carlton, 312.

[35] Hay, W. W., Wold, C. N., Soding, E., and Floegel, S. (2001). Evolution of sediment fluxes and ocean salinity. InGeologic modeling and simulation(pp. 153-167). Springer US.

[36] Ronov, A. B. (1982). The Earth's sedimentary shell (quantitative patterns of its structure, compositions, and evolution) The 20th VI Vernadskiy Lecture, March 12, 1978.International geology review,24(11), 1313-1363.

[37] Gregor, C. B. (1985). The mass-age distribution of Phanerozoic sediments.Geological Society, London, Memoirs,10(1), 284-289.

[38] Veizer, J., and Jansen, S. L. (1985). Basement and sedimentary recycling-2: Time dimension to global tectonics.The Journal of Geology, 625-643.

[39] Sawyer, E. W. (1986). The influence of source rock type, chemical weathering and sorting on the geochemistry of clastic sediments from the Quetico metasedimentary belt, Superior Province, Canada.Chemical Geology,55(1-2), 77-95.

[40] Nesbitt, H. W., and Young, G. M. (1996). Petrogenesis of sediments in the absence of chemical weathering: effects of abrasion and sorting on bulk composition and mineralogy. Sedimentology, 43(2), 341-358.

[41] Milliken, K. L., and Mack, L. E. (1990). Subsurface dissolution of heavy minerals, Frio Formation sandstones of the ancestral Rio Grande Province, South Texas.Sedimentary Geology,68(3), 187-199.

[42] McCann, T. (1998). Sandstone composition and provenance of the Rotliegend of the NE German Basin. Sedimentary Geology, 116(3-4), 177-198.

[43] Dalai, T. K., Krishnaswami, S. and Sarin, M. M. (2002). Major ion chemistry in the headwaters of the Yamuna river system: Chemical weathering, its temperature dependence and CO2 consumption in the Himalaya. Geochim. Cosmochim. Acta 66, 3397-3416.

[44] Dalai, T. K., Krishnaswami, S., and Sarin, M. M. (2002). Barium in the Yamuna River System in the Himalaya: Sources, fluxes, and its behavior during weathering and transport.Geochemistry, Geophysics, Geosystems, 3(12), 1-23.

[45] Gaillardet, J., Dupre, B., and Allegre, C. J. (1999). Geochemistry of large river suspended sediments: silicate weathering or recycling tracer?Geochimica et Cosmochimica Acta,63(23), 4037-4051.

[46] Gaillardet, J., Dupre, B., Louvat, P., and Allegre, C. J. (1999). Global silicate weathering and CO 2 consumption rates deduced from the chemistry of large rivers.Chemical geology,159(1), 3-30.

[47] Galy, V., France-Lanord, C., Beyssac, O., Faure, P., Kudrass, H., and Palhol, F. (2007). Efficient organic carbon burial in the Bengal fan sustained by the Himalayan erosional system.Nature,450 (7168), 407-410.

[48] Ashworth, P. J., and Lewin, J. (2012). How do big rivers come to be different?.Earth-Science Reviews,114(1), 84-107.

[49] Weltje, G. J., and von Eynatten, H. (2004). Quantitative provenance analysis of sediments: review and outlook.Sedimentary Geology,171(1), 1-11.

[50] Polynov, B. B. (1937).The cycle of weathering. Translated from Russian by Alexander Muir. Thomas Murby and Co., London.

[51] Goldich, S. S. (1938). A study in rock-weathering.The Journal of Geology, 17-58.

[52] Harris, R. C., and Adams, J. A. S., 1966. Geochemical and mineralogical studies on the weathering of granitic rocks. American Journal of Science, 264, 146-173.

[53] Gibbs, R. J. (1970). Mechanisms controlling world water chemistry.Science,170(3962), 1088-1090.

[54] Meybeck, M. (1987). Global chemical weathering of surficial rocks estimated from river dissolved loads.American Journal of Science,287(5), 401-428.

[55] Grantham, J. H. and Michael A. V. (1988)."The influence of climate and topography on rock-fragment abundance in modern fluvial sands of the southern Blue Ridge Mountains, North Carolina."Journal of Sedimentary Research58.2

[56] Berner, R. A. (1992). Weathering, plants, and the long-term carbon cycle.Geochimica et Cosmochimica Acta,56(8), 3225-3231.

[57] Stallard, R. F. (1995). Tectonic, environmental, and human aspects of weathering and erosion: a global review from a steady-state perspective.Annual Review of Earth and Planetary Sciences,23, 11-40.

[58] White, A. F., and Blum, A. E. (1995). Effects of climate on chemical weathering in watersheds.Geochimica et Cosmochimica Acta,59(9), 1729-1747.

[59] Oliva, P., Viers, J., and Dupre, B. (2003). Chemical weathering in granitic environments.Chemical Geology,202(3), 225-256.

[60] White, A. F., Blum, A. E., Bullen, T. D., Vivit, D. V., Schulz, M., and Fitzpatrick, J. (1999). The effect of temperature on experimental and natural chemical weathering rates of granitoid rocks.Geochimica et Cosmochimica Acta,63(19), 3277-3291.

[61] Dunne, T. (1978). Rates of chemical denudation of silicate rocks in Kenya,Nature, 274, 244-246.

[62] Kump, L. R., Brantley, S. L., and Arthur, M. A. (2000). Chemical weathering, atmospheric CO2, and climate.Annual Review of Earth and Planetary Sciences,28(1), 611-667.

[63] West, A. J., Bickle, M. J., Collins, R., and Brasington, J. (2002). Small-catchment perspective on Himalayan weathering fluxes.Geology,30(4), 355-358.

[64] France-Lanord, C., Evans, M., Hurtrez, J. E., and Riotte, J. (2003). Annual dissolved fluxes from Central Nepal rivers: budget of chemical erosion in the Himalayas.Comptes Rendus Geoscience,335(16), 1131-1140.

[65] Stallard, R. F., and Edmond, J. M. (1983). Geochemistry of the Amazon: 2. The influence of geology and weathering environment on the dissolved load.Journal of Geophysical Research: Oceans, 88(C14), 9671-9688.

[66] Edmond, J. M., Palmer, M. R., Measures, C. I., Brown, E. T., and Huh, Y. (1996). Fluvial geochemistry of the eastern slope of the northeastern Andes and its foredeep in the drainage of the Orinoco in Colombia and Venezuela.Geochimica et Cosmochimica Acta,60 (16), 2949-2974.

[67] Huh, Y., and Edmond, J. M. (1999). The fluvial geochemistry of the rivers of Eastern Siberia: III. Tributaries of the Lena and Anabar draining the basement terrain of the Siberian Craton and the Trans-Baikal Highlands.Geochimica et Cosmochimica Acta,63(7), 967-987.

[68] Riebe, C. S., Kirchner, J. W., Granger, D. E., and Finkel, R. C. (2001). Minimal climatic control on erosion rates in the Sierra Nevada, California.Geology,29(5), 447-450.

[69] Millot, R., Gaillardet, J., Dupre, B., and Allegre, C. J. (2002). The global control of silicate weathering rates and the coupling with physical erosion: new insights from rivers of the Canadian Shield.Earth and Planetary Science Letters,196(1), 83-98.

[70] Goudie, A. S., and Viles, H. A. (2012). Weathering and the global carbon cycle: Geomorphological perspectives.Earth-Science Reviews,113(1), 59-71.

[71] Raymo, M. E., Ruddiman, W. F., and Froelich, P. N. (1988). Influence of late Cenozoic mountain building on ocean geochemical cycles. Geology 16 (7): 649.

[72] McLennan, S. M. (1993). Weathering and global denudation.The Journal of Geology, 295-303.

[73] Dickinson, W. R., and Suczek, C. A. (1979). Plate tectonics and sandstone compositions.Aapg Bulletin, 63(12), 2164-2182.

[74] Bhatia, M. R. (1983). Plate tectonics and geochemical composition of sandstones.The Journal of Geology, 611-627.

[75] Bhatia, M. R., and Crook, K. A. (1986). Trace element characteristics of graywackes and tectonic setting discrimination of sedimentary basins.Contributions to mineralogy and petrology,92(2), 181-193.

[76] Roser, B. P., and Korsch, R. J. (1988). Provenance signatures of sandstone-mudstone suites determined using discriminant function analysis of major-element data.Chemical geology,67(1), 119-139.

[77] Feng, R., and Kerrich, R. (1990). Geochemistry of fine-grained clastic sediments in the Archean Abitibi greenstone belt, Canada: implications for provenance and tectonic setting.Geochimica et Cosmochimica Acta,54(4), 1061-1081.

[78] Raymo, M. E., and Ruddiman, W. F. (1992). Tectonic forcing of late Cenozoic climate.Nature,359(6391), 117-122.

[79] Hren, M. T., Chamberlain, C. P., Hilley, G. E., Blisniuk, P. M., and Bookhagen, B. (2007). Major ion chemistry of the Yarlung Tsangpo-Brahmaputra river: chemical weathering, erosion, and CO_2 consumption in the southern Tibetan

plateau and eastern syntaxis of the Himalaya.Geochimica et Cosmochimica Acta,71(12), 2907-2935.

[80] Urey, H. C. (1952). On the early chemical history of the Earth and the origin of life. Proc. Nat. Acad. Sci. U.S.A. 38, 351-363.

[81] Ebelmen, J. J. (1845). Sur les produits de la dmposition des esps minles de la famille des silicates. InAnnales des Mines, 7(3), 66.

[82] Berner, R. A. (1978). Rate control of mineral dissolution under earth surface conditions.American Journal of Science,278(9), 1235-1252.

[83] West, A. J., Galy, A., and Bickle, M. (2005). Tectonic and climatic controls on silicate weathering.Earth and Planetary Science Letters,235(1), 211-228.

[84] Berner R. A., Lasaga A. C., and Garrels R. M. (1983). The carbonate- silica geochemical cycle and its effect on atmospheric carbon dioxide and climate. Amer. J. Sci. 283, 641-683.

[85] Berner, R. A. (1994). GEOCARB II: A revised model of atmospheric CO [sub 2] over phanerozoic time.American Journal of Science; (United States), 294(1).

[86] Walker, J. C. G., Hays, P. B., and Kasting, J. F. (1981). A negative feedback mechanism for the long-term stabilization of the earth's surface temperature. J. Geophys. Res. 89:9776-9782

[87] Broecker, W. S., and Sanyal, A. (1998). Does atmospheric CO2 police the rate of chemical weathering?.Global Biogeochemical Cycles,12(3), 403-408.

[88] Banwart, S. A., Berg, A., and Beerling, D. J. (2009). Process-based modeling of silicate mineral weathering responses to increasing atmospheric CO2 and climate change.Global Biogeochemical Cycles,23(4).

[89] Le Hir, G., Donnadieu, Y., Godderis, Y., Meyer-Berthaud, B., Ramstein, G., and Blakey, R. C. (2011). The climate change caused by the land plant invasion in the Devonian.Earth and Planetary Science Letters,310(3), 203-212.

[90] Li, G., Ji, J., Chen, J., and Kemp, D. B. (2009). Evolution of the Cenozoic carbon cycle: the roles of tectonics and CO2 fertilization.Global Biogeochemical Cycles,23(1).

[91] Bemer R. A. (1991). Model for atmospheric CO2 over Phanerozoic time. Amer. J. Sci. 291, 339-376.

[92] Webster, P. J. (1994). The role of hydrological processes in ocean-atmosphere interactions.Reviews of Geophysics,32(4), 427-476.

[93] Lasaga, A. C. (1984). Chemical kinetics of water-rock interactions.Journal of geophysical research: solid earth,89(B6), 4009-4025.

[94] Lasaga, A. C., Soler, J. M., Ganor, J., Burch, T. E., and Nagy, K. L. (1994). Chemical weathering rate laws and global geochemical cycles.Geochimica et Cosmochimica Acta,58(10), 2361-2386.

[95] McLennan, S. M. (1982). On the geochemical evolution of sedimentary rocks.Chemical Geology,37(3), 335-350.

[96] Cox, R., and Lowe, D. R. (1995). A conceptual review of regional-scale controls on the composition of clastic sediment and the co-evolution of continental blocks and their sedimentary cover.Journal of Sedimentary Research,65(1).

[97] Ruddiman, W. F. (Ed.). (2013).Tectonic uplift and climate change. Springer Science and Business Media.

[98] Billen, G., Lancelot, C., Meybeck, M., Mantoura, R. F. C., Martin, J. M., and Wollast, R. (1991). N, P and Si retention along the aquatic continuum from land to ocean. InOcean Margin Processes in Global Change, 1 John Wiley and Sons.19-44.

[99] Hedges, J. I., Clark, W. A., Quay, P. D., Richey, J. E., Devol, A.H. and Santos, U. de M. (1986). Compositions and fluxes of particulate organic material in the Amazon River. Limnol. Qceanogr., 31: 717-738.

[100] Dupre, B., Dessert, C., Oliva, P., Godderis, Y., Viers, J., Frans, L., Millot, R. and Gaillardet, J. (2003). Rivers, chemical weathering and Earth's climate.Comptes Rendus Geoscience,335(16), 1141-1160.

[101] Gupta, L. P., and Subramanian, V. (1998). Geochemical factors controlling the chemical nature of water and sediments in the Gomti River, India.Environmental Geology,36(1-2), 102-108.

[102] Frings, P. J., Clymans, W., Fontorbe, G., Gray, W., Chakrapani, G., Conley, D. J., and De La Rocha, C. (2015). Silicate weathering in the Ganges alluvial plain.Earth and Planetary Science Letters,427, 136-148

[103] Edmond, J. M., Palmer, M. R., Measures, C. I., Grant, B., and Stallard, R. F. (1995). The fluvial geochemistry and denudation rate of the Guayana Shield in Venezuela, Colombia, and Brazil.Geochimica et Cosmochimica Acta,59(16), 3301-3325.

[104] Weltje, G. J., Meijer, X. D., and de Boer, P. L. (1998). Stratigraphic inversion of siliciclastic basin fills: a note on the distinction between supply signals resulting from tectonic and climatic forcing. Basin Res. 10, 129-153.

[105] Hunter, K. A., and Liss, P. S. (1982). Organic matter and the surface charge of suspended particles in estuarine waters. Limnol. Oceanogr. 27 (2), 322-335.

[106] France-Lanord, C., and Derry, L. A. (1997). Organic carbon burial forcing of the carbon cycle from Himalayan erosion.Nature,390(6655), 65-67.

[107] Gislason, S. R., Oelkers, E. H., and Snorrason, A. (2006). Role of river-suspended material in the global carbon cycle.Geology,34(1), 49-52

[108] Lupker, M., France-Lanord, C., Lave, J., Bouchez, J., Galy, V., Metivier, F., Gaillardet, J., Lartiges, B. and Mugnier, J.L. (2011). A Rouse-based method to integrate the chemical composition of river sediments: Application to the Ganga basin.Journal of Geophysical Research: Earth Surface,116(F4).

[109] Bouchez, J., Beyssac, O., Galy, V., Gaillardet, J., France-Lanord, C., Maurice, L., and Moreira-Turcq, P. (2010). Oxidation of petrogenic organic carbon in the Amazon floodplain as a source of atmospheric CO2. Geology, 38(3), 255-258.

[110] Bouchez, J., Gaillardet, J., France-Lanord, C., Maurice, L., and Dutra Maia, P. (2011). Grain size control of river suspended sediment geochemistry: Clues

from Amazon River depth profiles. Geochemistry, Geophysics, Geosystems, 12(3).

[111] Bouchez, J., Metivier, F., Lupker, M., Maurice, L., Perez, M., Gaillardet, J., and France-Lanord, C. (2011). Prediction of depth-integrated fluxes of suspended sediment in the Amazon River: Particle aggregation as a complicating factor. Hydrological processes, 25(5), 778-794.

[112] Forstner, U., and Muller, G. (1974). Schwermetallanreicherungen in datierten Sedimentkernen aus dem Bodensee und aus dem Tegernsee.Tschermaks mineralogische und petrographische Mitteilungen,21(3-4), 145-163.

[113] Wall, G. J., and Wilding, L. P. (1976). Mineralogy and related parameters of fluvial suspended sediments in northwestern Ohio.Journal of Environmental Quality,5(2), 168-173.

[114] Johnsson, M. J., and Meade, R. H. (1990). Chemical weathering of fluvial sediments during alluvial storage: The Macuapanim Island point bar, Solimoes River, Brazil.Journal of Sedimentary Research,60(6).

[115] Siever, R. (1988). Sand, W. H. Freeman and Co. USA.

[116] Lupker, M., France-Lanord, C., Galy, V., Lave, J., Gaillardet, J., Gajurel, A.P., Guilmette, C., Rahman, M., Singh, S.K. and Sinha, R. (2012). Predominant floodplain over mountain weathering of Himalayan sediments (Ganga basin).Geochimica et Cosmochimica Acta,84, 410-432.

[117] Walling, D. E., Owens, P. N. and Leeks, G. J. L. (1998). 'The role of channel and floodplain storage in the suspended sediment budget of the River Ouse, Yorkshire, UK', Geomorphology, 22, 225-242.

[118] Walling, D. E. (1983). The sediment delivery problem. Journal of hydrology, 65(1-3), 209-237.

[119] Trimble, S. W. (1995). Catchment sediment budgets and change. In: Gurnell, A.M., Petts, G.E. (Eds.), Changing RiverChannels. Wiley, Chichester, pp. 201-215

[120] Trimble, S.W. (1983). A sediment budget for Coon Creek, the Driftless Area, Wisconsin, 1853-1977. Am. J. Sci. 283, 454-474.

[121] Phillips, J.D. (1991). Fluvial sediment budgets in the North Carolina Piedmont. Geomorph. 4, 231-241.

[122] Walling, D. E., and Quine, T. A. (1993). Using Chernobyl-derived fallout radionuclides to investigate the role of downstream conveyance losses in the suspended sediment budget of the River Severn, United Kingdom. Phys. Geog. 14, 239-253.

[123] Campo, S. H., and Desloges, J. R. (1994). Sediment yield conditioned by glaciation in a rural agricultural basin of southern Ontario, Canada. Phys. Geog. 15, 495-515.

[124] Mertes, L. K. (1994). Rates of flood-plain sedimentation on the central Amazon River. Geology 22, 171-174

[125] Goodbred, S.L., and Kuehl, S.A. (1998). Floodplain processes in the Bengal Basin and storage of Ganges-Brahmaputra river sediment: an accretion study using 137Cs and 210Pb geochronologies. Sed. Geol. 121, 239-258.

[126] Walling, D. E., Owens, P. N., Carter, J., Leeks, G. J. L., Lewis, S., Meharg, A. A., and Wright, J. (2003). Storage of sediment-associated nutrients and contaminants in river channel and floodplain systems. Applied Geochemistry, 18(2), 195-220.

[127] Subramanian, V. (1979). Chemical and suspended sediments characteristics of the rivers of India. Journal of Hydrology, 44, 37-55.

[128] Subramanian, V. (1987). Heavy metals distribution in the sediments of Ganges and Brahmaputra river sediments. Environmental Geology and Water Sciences, 9, 93 -103.

[129] Gibbs, R. J. (1972). Water chemistry of the Amazon River.Geochimica et Cosmochimica Acta,36(9), 1061-1066.

[130] Stallard, R. F., and Edmond, J. M. (1987). Geochemistry of the Amazon: 3. Weathering chemistry and limits to dissolved inputs.Journal of Geophysical Research: Oceans,92(C8), 8293-8302.

[131] Goldstein, S. J., and Jacobsen, S. B. (1988). Rare earth elements in river waters.Earth and Planetary Science Letters,89(1), 35-47.

[132] Dupre, B., Gaillardet, J., Rousseau, D., and Allegre, C. J. (1996). Major and trace elements of river-borne material: the Congo Basin.Geochimica et Cosmochimica Acta,60(8), 1301-1321.

[133] Reeder, S. W., Hitchon, B., and Levinson, A. A. (1972). Hydro-geochemistry of the surface waters of the Mackenzie River drainage basin, Canada-I. Factors controlling inorganic composition. Geochim. Cosmochim. Acta 36: 825-865.

[134] Zhang, J., Huang, W. W., Liu, M. G., and Zhou, Q. (1990). Drainage basin weathering and major element transport of two large Chinese rivers (Huanghe and Changjiang).Journal of Geophysical Research: Oceans,95(C8), 13277-13288.

[135] Chen, J. S., and Xia, X. H. (2000). Progress in research on river water chemistry in China.Chinese Geographical Science,10(1), 7-12.

[136] Carbonnel, J. P., and Meybech, M. (1975). Quality variations of the Mekong river at Pnom-Penh, Cambodia and chemical transport in the Mekong basin. Journal of Hydrology, 27 (3/4), 249-265.

[137] Raymahashay, B. C. (1970). Characteristics of stream erosion in the Himalayan region of India. Proc Symp Hydrogeochem Biochem 1:82-89

[138] Abbas, N., and Subramanian, V. (1984). Erosion and sediment transport in the Ganges river basin (India).Journal of hydrology,69(1), 173-182.

[139] Sarin, M. M., and Krishnaswami, S. (1984). Major ion chemistry of the Ganga-Brahmaputra river systems, India.Nature, 1984, 312, 538-541.

[140] Sarin, M. M., Krishnaswami, S., Dilli, K., Somayajulu, B. L. K., and Moore, W. S. (1989). Major ion chemistry of the Ganga-Brahmaputra river system:

Weathering processes and fluxes to the Bay of Bengal.Geochimica et cosmochimica acta,53(5), 997-1009.

[141] Sarin, M. M., Krishnaswami, S., Trivedi, J. R., and Sharma, K. K. (1992). Major ion chemistry of the Ganga source waters: weathering in the high altitude Himalaya.Proceedings of the Indian Academy of Sciences-Earth and Planetary Sciences,101(1), 89-98.

[142] Lupker, M., Blard, P. H., Lave, J., France-Lanord, C., Leanni, L., Puchol, N., Charreau, J. and Bourles, D. (2012). 10 Be-derived Himalayan denudation rates and sediment budgets in the Ganga basin.Earth and Planetary Science Letters,333, 146-156.

[143] Cullers, R. (1988). Mineralogical and chemical changes of soil and stream sediment formed by intense weathering of the Danburg granite, Georgia, USA.Lithos,21(4), 301-314.

[144] Cullers, R. L., Basu, A., and Suttner, L. J. (1988). Geochemical signature of provenance in sand-size material in soils and stream sediments near the Tobacco Root batholith, Montana, USA.Chemical Geology,70(4), 335-348.

[145] Nesbitt, H. W., Young, G. M., McLennan, S. M., and Keays, R. R. (1996). Effects of chemical weathering and sorting on the petrogenesis of siliciclastic sediments, with implications for provenance studies.The Journal of Geology, 525-542.

[146] Derry, L. A., and France-Lanord, C. (1996). Neogene Himalayan weathering history and river 87Sr 86Sr: Impact on the marine Sr record.Earth and Planetary Science Letters,142(1), 59-74.

[147] Najman, Y. (2006). The detrital record of orogenesis: A review of approaches and techniques used in the Himalayan sedimentary basins.Earth-Science Reviews,74(1), 1-72.

[148] Chakrapani, G. J., Saini, R. K., and Yadav, S. K. (2009). Chemical weathering rates in the Alaknanda-Bhagirathi river basins in Himalayas, India.Journal of Asian Earth Sciences,34(3), 347-362.

[149] Raymo, M. E., D. Hodell, and E. Jansen (1992), Response of deep ocean circulation to initiation of Northern Hemisphere glaciation (3-2 MA), Paleoceanography, 7, 645-672.

[150] Krishnaswami, S., Trivedi, J. R., Sarin, M. M., Ramesh, R., and Sharma, K. K. (1992). Strontium isotopes and rubidium in the Ganga-Brahmaputra river system: Weathering in the Himalaya, fluxes to the Bay of Bengal and contributions to the evolution of oceanic 87 Sr/86 Sr.Earth and Planetary Science Letters,109(1), 243-253.

[151] Suchet, P. A., and Probst, J. L. (1993). Modelling of atmospheric CO 2 consumption by chemical weathering of rocks: application to the Garonne, Congo and Amazon basins.Chemical Geology,107(3), 205-210.

[152] Dewey, J. F., and Bird, J. M. (1970). Plate tectonics and geosynclines.Tectonophysics,10(5-6), 625-638.

[153] Rowley, D. B. (1996). Age of initiation of collision between India and Asia: A review of stratigraphic data.Earth and Planetary Science Letters,145(1), 1-13.

[154] Tripathi, J. K., Ghazanfari, P., Rajamani, V., and Tandon, S. K. (2007). Geochemistry of sediments of the Ganges alluvial plains: evidence of large-scale sediment recycling.Quaternary International,159(1), 119-130.

[155] Pande, K., Sarin, M. M., Trivedi, J. R., Krishnaswami, S., and Sharma, K. K. (1994). The Indus river system (India-Pakistan): Major-ion chemistry, uranium and strontium isotopes.Chemical Geology,116(3-4), 245-259.

[156] Ahmad, T., Khanna, P. P., Chakrapani, G. J., and Balakrishnan, S. (1998). Geochemical characteristics of water and sediment of the Indus river, Trans-Himalaya, India: constraints on weathering and erosion.Journal of Asian Earth Sciences,16(2), 333-346.

[157] Singh, S. K., Trivedi, J. R., Pande, K., Ramesh, R., and Krishnaswami, S. (1998). Chemical and strontium, oxygen, and carbon isotopic compositions of carbonates from the Lesser Himalaya: Implications to the strontium iso-

tope composition of the source waters of the Ganga, Ghaghara, and the Indus rivers.Geochimica et Cosmochimica Acta,62(5), 743-755.

[158] Galy, A., and France-Lanord, C. (1999). Weathering processes in the Ganges-Brahmaputra basin and the riverine alkalinity budget.Chemical Geology,159(1), 31-60.

[159] Galy, A., and France-Lanord, C. (2001). Higher erosion rates in the Himalaya: Geochemical constraints on riverine fluxes.Geology,29(1), 23-26.

[160] Ramesh, R., Ramanathan, A. L., Ramesh, S., Purvaja, R., and Subramanian, V. (2000). Distribution of rare earth elements and heavy metals in the surficial sediments of the Himalayan river system.Geochemical Journal,34(4), 295-319.

[161] Dalai, T. K., Singh, S. K., Trivedi, J. R. and Krishnaswami, S. (2002) Dissolved rhenium in the Yamuna River System and the Ganga in the Himalaya: Role of black shale weathering on the budgets of Re, Os, and U in rivers and CO2 in the atmosphere. Geochim. Cosmochim. Acta 66, 29-43.

[162] Dalai, T. K., Krishnaswami, S. and Kumar, A. (2003) Sr and 87Sr/86Sr in the Yamuna River System in the Himalaya: Sources, fluxes and controls on radiogenic Sr isotopic composition. Geochim. Cosmochim. Acta 67, 2931-2948

[163] Di-Giovanni, C., Disnar, J. R. and Macaire, J. J. (2002) Estimation of the annual yield of organic carbon released from carbonates and shales by chemical weathering. Global Planet. Change 32, 195-210.

[164] Jacobson, A. D., Blum, J. D., and Walter, L. M. (2002). Reconciling the elemental and Sr isotope composition of Himalayan weathering fluxes: insights from the carbonate geochemistry of stream waters.Geochimica et Cosmochimica Acta,66(19), 3417-3429.

[165] Stummeyer, J., Marchig, V., and Knabe, W. (2002). The composition of suspended matter from Ganges-Brahmaputra sediment dispersal system during low sediment transport season.Chemical Geology,185(1), 125-147.

[166] Singh, S. K., and France-Lanord, C. (2002). Tracing the distribution of erosion in the Brahmaputra watershed from isotopic compositions of stream sediments.Earth and Planetary Science Letters,202(3), 645-662.

[167] Coleman, J. M. (1969). Brahmaputra River: channel processes and sedimentation.Sedimentary Geology, 3(2-3), 129-239.

[168] Holeman, J. N. (1968). The sediment yield of major rivers of the world.Water Resources Research,4(4), 737-747.

[169] Singh, S. K., Sarin, M. M., and France-Lanord, C. (2005). Chemical erosion in the eastern Himalaya: major ion composition of the Brahmaputra and δ 13C of dissolved inorganic carbon.Geochimica et Cosmochimica Acta,69(14), 3573-3588.

[170] Hay, W. W. (1998). Detrital sediment fluxes from continents to oceans.Chemical geology,145(3), 287-323.

[171] Islam, M. R., Begum, S. F., Yamaguchi, Y., and Ogawa, K. (1999). The Ganges and Brahmaputra rivers in Bangladesh: basin denudation and sedimentation.Hydrological Processes,13(17), 2907-2923.

[172] Goswami, D. C. (1985). Brahmaputra River, Assam, India: Physiography, basin denudation, and channel aggradation.Water Resources Research,21(7), 959-978.

[173] Barua, D. K., Kuehl, S. A., Miller, R. L., and Moore, W. S. (1994). Suspended sediment distribution and residual transport in the coastal ocean off the Ganges-Brahmaputra river mouth. Marine Geology, 120(1), 41-61.

[174] Fluteau, F., Ramstein, G., and Besse, J. (1999). Simulating the evolution of the Asian and African monsoons during the past 30 Myr using an atmospheric general circulation model.Journal of Geophysical Research: Atmospheres,104(D10), 11995-12018.

[175] Harris, N., Bickle, M., Chapman, H., Fairchild, I., and Bunbury, J. (1998). The significance of Himalayan rivers for silicate weathering rates: evidence from the Bhote Kosi tributary.Chemical Geology,144(3), 205-220.

[176] Palmer, M. R., and Edmond, J. M. (1989). The strontium isotope budget of the modern ocean.Earth and Planetary Science Letters,92(1), 11-26.

[177] Dekov, V. M., Araujo, F., Van Grieken, R., and Subramanian, V. (1998). Chemical composition of sediments and suspended matter from the Cauvery and Brahmaputra rivers (India).Science of the total environment,212(2), 89-105.

[178] Singh, S. K., Dalai, T. K., and Krishnaswami, S. (2003). 238 U series isotopes and 232 Th in carbonates and black shales from the Lesser Himalaya: implications to dissolved uranium abundances in Ganga-Indus source waters.Journal of environmental radioactivity,67(1), 69-90.

[179] Garzanti, E., Vezzoli, G., Ando, S., France-Lanord, C., Singh, S. K., and Foster, G. (2004). Sand petrology and focused erosion in collision orogens: the Brahmaputra case.Earth and Planetary Science Letters,220(1), 157-174.

[180] Singh, S. K., Kumar, A., and France-Lanord, C. (2006). Sr and 87 Sr/86 Sr in waters and sediments of the Brahmaputra river system: Silicate weathering, CO 2 consumption and Sr flux.Chemical Geology,234(3), 308-320.

[181] Dutta, P., and Konwar, M. (2013). Morphological aspects of Floodplain Wetlands with Reference to the upper Brahmaputra River Valley.International Journal of Scientific and Research Publications, 230.

[182] Bristow, C. S. 1987. Brahmaputra River: Channel migration and deposition. In: Ethridge, EG., Flores, R.M. and Harvey, M., (eds). Recent Developments ill Fluvial Sedimentology, The Society of Economic Palaeontologists and Mineralogists, 39, 63-72

[183] Datta, D. K., and Subramanian, V. (1997). Texture and mineralogy of sediments from the Ganges-Brahmaputra-Meghna river system in the Bengal Basin, Bangladesh and their environmental implications. Environmental Geology,30 (3-4), 181-188.

[184] Heroy, D. C., Kuehl, S. A., and Goodbred, S. L. (2003). Mineralogy of the Ganges and Brahmaputra Rivers: implications for river switching and Late Quaternary climate change.Sedimentary Geology,155(3), 343-359.

[185] Thompson, R. W. (1974). Mineralogy of sands from the Bengal and Nicobar fans, Sites 218 and 211, eastern Indian Ocean. In: Von der Borsch C C, Sclater J C, and others Initial Reports of the Deep Sea Drilling Project, Volume 22. U.S. Government Printing Office, Washington DC, 711-713

[186] Yokohama K., Amano K., Taira A., and Saito Y. (1990). Mineralogy of silts from the Bengal Fan, in: J.R. Cochran, D.A.V. Stow (Eds.),et al., Proc. ODP Program, Sci. Res., 116, 59-73.

[187] Curray, J. R. (1994). Sediment volume and mass beneath the Bay of Bengal.Earth and Planetary Science Letters,125(1-4), 371-383.

[188] Goodbred, S. L., and Kuehl, S. A. (2000). Enormous Ganges-Brahmaputra sediment discharge during strengthened early Holocene monsoon.Geology,28(12), 1083-1086.

[189] Goodbred, S. L., and Kuehl, S. A. (2000). The significance of large sediment supply, active tectonism, and eustasy on margin sequence development: Late Quaternary stratigraphy and evolution of the Ganges-Brahmaputra delta.Sedimentary Geology,133(3), 227-248.

[190] Singh, S. K. (2006). Spatial variability in erosion in the Brahmaputra basin: causes and impacts.Current Science,90(9), 1272-1275.

[191] Sarma, J. N., and Phukan, M. K. (2004). Origin and some geomorphological changes of Majuli Island of the Brahmaputra River in Assam, India.Geomorphology,60 (1), 1-19.

[192] Sarma, J. N., and Phukan, M. K. (2006). Bank erosion and bankline migration of the Brahmaputra River in Assam during the twentieth century.Journal-Geological Society of India,68(6), 1023.

[193] Kotoky, P., Bezbaruah, D., Baruah, J., Borah, G. C., and Sarma, J. N. (2006). Characterization of clay minerals in the Brahmaputra river sediments, Assam, India.CURRENT SCIENCE-BANGALORE-,91(9), 1247.

[194] Sarma, J. N. (2005). Fluvial process and morphology of the Brahmaputra River in Assam, India.Geomorphology,70(3), 226-256.

[195] Lahiri, S. K., and Sinha, R. (2012). Tectonic controls on the morphodynamics of the Brahmaputra River system in the upper Assam valley, India.Geomorphology,169, 74-85.

[196] Garzanti, E., Ando, S., France-Lanord, C., Vezzoli, G., Censi, P., Galy, V., and Najman, Y. (2010). Mineralogical and chemical variability of fluvial sediments: 1. Bedload sand (Ganga-Brahmaputra, Bangladesh).Earth and Planetary Science Letters,299(3), 368-381.

[197] Singh, S. K., Rai, S. K., and Krishnaswami, S. (2008). Sr and Nd isotopes in river sediments from the Ganga Basin: Sediment provenance and spatial variability in physical erosion.Journal of Geophysical Research: Earth Surface,113(F3).

[198] Singh, P. (2009). Major, trace and REE geochemistry of the Ganga River sediments: influence of provenance and sedimentary processes.Chemical Geology,266(3), 242-255.

[199] Huizing, H. G. J. (1971). A reconnaissance study of the mineralogy of sand fractions from East Pakistan sediments and soils.Geoderma,6(2), 109-133.

[200] Chakrapani, G. J., Subramanian, V., Gibbs, R. J., and Jha, P. K. (1995). Size characteristics and mineralogy of suspended sediments of the Ganges River, India.Environmental Geology,25(3), 192-196.

[201] Galy, V., France-Lanord, C., and Lartiges, B. (2008). Loading and fate of particulate organic carbon from the Himalaya to the Ganga-Brahmaputra delta.Geochimica et Cosmochimica Acta,72(7), 1767-1787.

Chapter 3

Materials and Methods

The chapter explains the scientific methods adopted in the present thesis which are combinations of experimentations, observations and logical arguments for achieving systematic interrelation of the facts. The structure of a research method mainly depends on the nature of sample and the objective of analysis. The research methodology adopted in this research work is categorised into five groups which are further elaborated in this chapter.

1. Sample collection.
2. Sample processing.
3. Particle size analysis.
4. Mineralogical analysis.
5. Geochemical analysis.

In this research work sediments of the river Brahmaputra and six of its tributaries (Subansiri, Jiabharali, Pagladia , Burhidihing, Dikhow and Kopili) were studied for their textures, mineralogy and geochemistry.

3.1 Sample collection

Figure 3.1 shows sampling sites of this study for all the rivers. To study the geochemical variations across the rivers, four sites were selected: channel, overbank, floodplain and suspended sediments (Figure 3.2).

3.1.1 For suspended sediment

Sampling for this study was done in monsoon, 2013 (the monsoon season in Assam is from June to August) for suspended load. For suspended sediments 25L of water sample from each sampling station was collected in polypropylene bottles, during monsoon season (August 2013). Suspended sediments were collected by the filtration of bulk water samples using 0.45μm Millipore membrane filter for bulk suspended sediment (63μm − 0.45μm) using vacuum pressure pump in the lab.

3.1.2 For overbank, floodplain and channel sediments

Sediment samples collected from the subsurface of a river's active channel were classified as bedload/channel sediments, whereas sediment samples collected from the top of sandbars or from an overbank were classified as bank sediments. The floodplains of the study were characterised by subdued microtopography, with the local relief rarely exceeding 1 m (at a distance approximately 100 m from the main channel). Distinct natural levees were generally absent from the flood plains.

Sediments samples (floodplain, overbank and channel sediments) were collected by channel sampling method, after removing the upper few centimetres layer, approximately 2 kg of sediment from selected locations. The collected sediment samples were then packed and sealed in polyethylene bags and transferred to the laboratory.

3.2 Sample processing for mineralogical and geochemical analysis

The sample processing required for mineralogical and geochemical analysis was common for both channel, overbank and suspended sediments as described here. The sediment samples were collected and brought to the laboratory where they were thoroughly sundried. The dried samples were mixed according to coning and quartering method as suggested by [1, 2] and divided in two parts. One half of this was stored and another half was used for the analysis purpose. After coning and

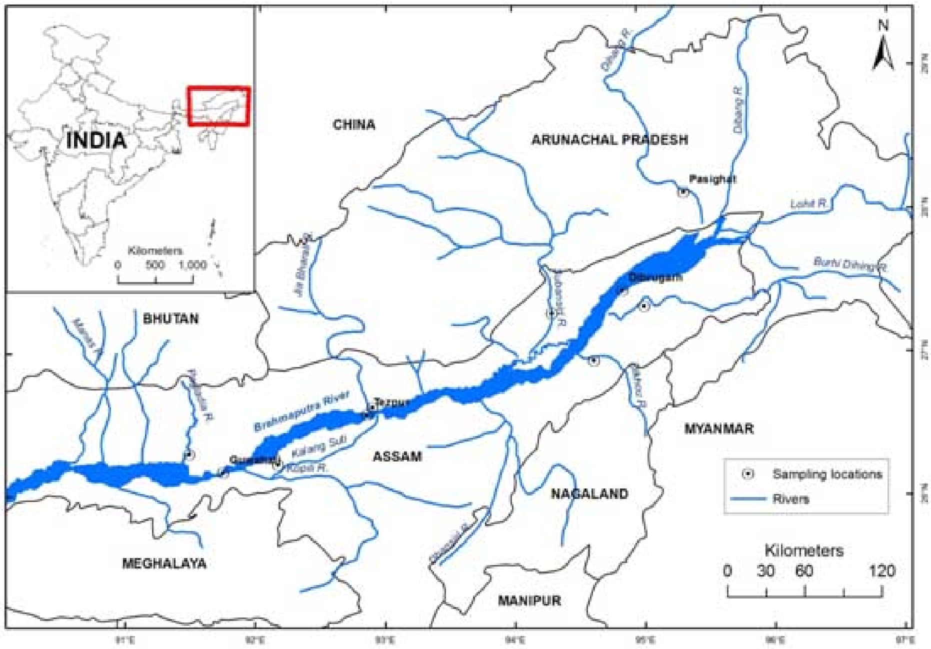

Figure 3.1: The Brahmaputra Basin in India with the sampling locations.

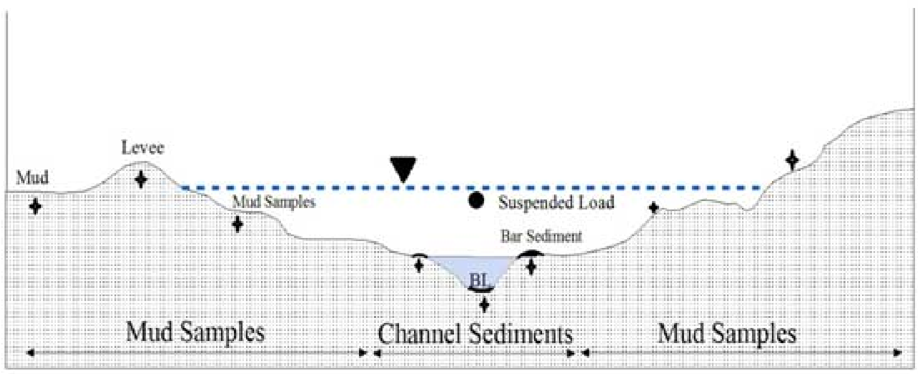

Figure 3.2: Locations of various sediment samples collected across the river.

quartering method, about 100 g of the sample was taken and crushed in hardened steel mortar to 60 mesh size. This crushed sample was placed on a butter sheet and homogenised thoroughly for about 20 minutes and about 50 g of the homogenised powder was collected after coning and quartering and ground to 200 mesh size in an agate mortar. This 200 mesh size sample powder was stored in plastic vial and the same was used for geochemical as well as for mineralogical analysis. Once the sample was ground to 200 mesh size, the steel mortar, pestle, agate mortar and the sieves were washed with soap solution, dried with the help of air blower and cleaned with acetone before proceeding to next sample, thereby limiting the inter-sample contamination. The clay was separated from the sediments by "Atterberg Cylinder Method" based on Stoke's law [3].

3.3 Grain size distribution

Grain size distribution of clastic sediment samples constitutes basic data in sedimentology that helps in providing insights regarding hydrodynamics of flows and about depositional conditions. Relation between sedimentary processes and textural responses is a powerful tool for interpreting the depositional environments. The grain size analysis of the sediment samples was performed to observe the coarser distribution through dry sieving and finer distribution through siltation method.

Grain size analysis is done for sizes and amount of particles present in a soil or sediment sample [4]. The grain size distribution of the sediment is a function of the size range of available material, its accessibility for weathering, erosion and transportation, and the energy input into the sediments [5]. The sediments can be classified on the basis of grain size, or the diameter of individual grain of sediments. This classification is based on Φ logarithmic scale (which is Krumbein's modification of the Wentworth scale)

$$\Phi = -\log_2 \frac{D}{D_0} \tag{3.1}$$

where Φ is the Krumbein phi scale, D is the diameter of the particle and D_0 is a reference diameter. If the samples were having a great proportion of clay and clumps then the deflocculation of the sample was done by pretreatment with HCl and H_2O_2 as mentioned below.

Particle size analysis requires dissolution of material into elementary particles that involves destruction of aggregates by removing carbonate, organic matter and clay clumps or aggregates. The deflocculation was done by pretreatment (modified after [1]) with HCl and H_2O_2 to remove the carbonate and organic content. Pretreatment varies according to type and characteristics of soil and sediment and hence modifications are done according to their properties.

3.3.1 Carbonate leaching and organic matter removal

This method is adopted and modified after [1, 2]. 100 g of dry sediment sample was weighed in centrifuge tubes (500 ml). To this 1.3 N HCl (250 ml) was added and left overnight to remove the carbonate content. The sample was centrifuged at 7000 rpm (modified after [6]) for 15 min if effervescence disappears. Supernatant was discarded and the same was centrifuged with milliQ to wash out the traces of HCl. To this 250 ml of H_2O_2 (30%) was added in next step to remove the organic matter. The samples are kept in 500 ml beaker and 30% w/v H_2O_2 was added. Beakers were shaken well and covered with watch glasses so that sample may not come out with effervescence. The beakers were then kept on a water bath at 60° C with covers for about 30 min and then left until the reaction stopped and allowed to cool [1]. The samples were filtered and washed with MilliQ water. The dried samples were then ready for both dry sieving and pipette analysis.

3.3.2 Pipette method

The pipette method was used to extract finer fractions of sediment sample [7]. After removing carbonates and organic matter, 50 ml 10% calgon (sodium hexametaphosphate) was added to the sample. The suspension was mixed for 30 min on a horizontal shaker and then sonicated for 15 min to deflocculate the clay particles. The suspension was then passed through a 0.063 mm sieve and the finer fraction was collected in a 1000 ml measuring cylinder. The volume was made up with MilliQ water.

The solution was mixed thoroughly with stirrer in vertical manner and left for 20 seconds. A 20 ml pipette was marked at 5, 10 and 20 cm and used to extract the suspension. After 20 seconds 20 ml solution was extracted from 20 cm in a

Diameter in micrometers finer than	Withdrawal depth (cm)	Elapsed time for withdrawal of sample at 25° C
62.5	20	20 s
44.2	20	1 m 41 s
	Restir	
31.2	10	1 m 41 s
15.6	10	6 m 45 s
	Restir	
7.8	10	27 m 1 s
3.9	5	54 m 2 s
1.95	5	3 hr 36 m

Table 3.1: Pipette withdrawal times calculated from Stoke's Law

previously weighed 50 ml beaker. The suspension was extracted at different time intervals (Table 3.1) for different size fractions and dried in an incubator at 50° C. The dry weight of these samples was used for calculation of weight percent of each size fraction.

3.3.3 Dry sieving

The samples greater than 0.063 mm were sieved through a set of American Standard Test Sieve Series (ASTM) sieves having pore size of 0.5 mm, 0.35 mm, 0.25 mm, 0.171 mm, 0.125 mm, 0.088 mm, 0.063 mm screens which were placed with coarsest at the top and finest at the bottom held by a pan. The sample was dropped into the topmost sieve having largest screen openings. The column was typically placed in a mechanical shaker. After 15 minute shaking the material on each sieve was separated and weighed. These weights were used for grain size calculations by using Gradistat 8.0 programme [8].

3.3.4 Grain size parameters

Statistical parameters were calculated using the method of [4] as follows:

1. **Mean grain diameter in Φ units**: Mean grain diameter, the most widely used distribution parameter, is regarded by most authors [4, 10] as an indicator of the average energy of the transport and as sedimentation agent.

Graphic mean

$$M_Z = \frac{\phi(16 + 50 + 84)}{3} \tag{3.2}$$

2. **Standard deviation (Sorting)**: This is a measure of the standard deviation which is the spread of the grain size distribution with respect to the mean [4]. Sorting is the most useful grain size data since it gives an indication of the effectiveness of the depositional medium in separating grains of different classes. Hydraulic sorting is done through the selective sedimentation of the material, which is in movement.

Inclusive graphic standard deviation (Sorting)

$$\frac{\phi(84 - 16)}{4} + \frac{\phi(95 - 5)}{6.6} \tag{3.3}$$

$< \phi0.35$ Very well sorted

$\phi0.35$ to $\phi0.5$ Well sorted

$\phi0.50$ to $\phi0.71$ Moderately well sorted

$\phi0.71$ to $\phi1.0$ Moderately sorted

$\phi1.0$ to $\phi2.0$ Poorly sorted

$\phi2.0$ to $\phi4.0$ Very poorly sorted

$> \phi4.0$ Extremely poorly sorted

3. **Skewness**: This is a reflection of the depositional process [4]. It is simply a measure of the symmetry of the distribution. Skewness is useful in environmental diagnosis because it is directly related to the fine and coarse tails of the size distribution, and hence suggestive of energy of deposition.

Inclusive graphic skewness

$$S_K = \frac{\phi16 + \phi84 - 2\phi50}{2(\phi84 - \phi16)} + \frac{\phi5 + \phi95 - 2\phi50}{2(\phi95 - \phi5)} \tag{3.4}$$

$\phi1.0$ to $\phi0.3$ Very fine skewed

$\phi0.3$ to $\phi0.1$ Fine skewed

$\phi0.1$ to $\phi - 0.1$ Near symmetrical

$\phi - 0.1$ to $\phi - 0.3$ Coarse skewed

$\phi - 0.3$ to $\phi - 1.0$ Very coarse sorted

4. **Graphic kurtosis**:

$$K_G = \frac{\phi 95 - \phi 5}{2.44(\phi 75 - \phi 25)} \tag{3.5}$$

$< \phi 0.67$ Very Platykurtic

$\phi 0.90$ to $\phi 1.11$ Mesokurtic

$\phi 1.11$ to $\phi 1.50$ Leptokurtic

$\phi 1.50$ to $\phi 3.0$ Very leptokurtic

$> \phi 3.0$ Extremely leptokurtic

$\phi 0.67$ to $\phi 0.90$ Platykurtic

3.4 Mineralogical analysis

The bulk mineralogy of channel, overbank, floodplain, clay and suspended sediment samples were done using X-Ray Diffractometer (Philips EXPERT) at Jawaharlal Nehru University (JNU), New Delhi. Sediment samples were ground to 200 mesh size and were used for the mineralogical studies to decipher the mineral assemblages. The minerals in the samples were identified using X-ray diffractogram of the samples with specified d spacing and 2θ values by comparing it with the values given in reference database [11, 12].

For clay mineralogical analysis, slides were prepared by drop on slide technique [13]. The samples were untreated, glycolated, heated at 400° C and 550° C and run on Philips X-ray Diffractometer using CuK- radiation and Ni-filter. The accelerating voltage was kept at 45 kV along with tube current of 40 mA. The scanning was done at 1 degree 2θ per minute for sediments and 0.5 degree 2θ per minute for clay mineralogy.

S. No.	Mineral Name	d spacing values
1	Biotite	10.1, 4.59, 3.37, 3.16, 2.92, 2.66, 2.52, 2.45, 2.28
2	Calcite	3.03, 2.834, 2.495, 2.945
3	Chlorite	14.4, 7.15, 4.79, 4.63, 3.59, 2.87, 2.68, 2.61, 2.55, 2.475, 2.39, 2.29
4	Dolomite	4.03, 3.69, 2.88, 2.67, 2.54, 2.40, 2.192
5	Goethite	4.98, 4.18, 3.38, 2.69, 2.58, 2.52, 4.9, 2.452
6	Hematite	3.66, 2.69, 2.51, 2.285
7	Hornblende	8.96, 8.4, 4.5, 3.26, 3.1, 2.939, 2.789, 2.697, 2.587, 2.537, 2.325
8	Illite	10.0, 5.0, 3.3
9	Kaolinite	7.16, 4.18, 3.57, 2.56
10	Microcline	6.46, 4.21, 3.98, 3.83, 3.71, 3.57, 3.48, 3.366, 3.29, 3.244, 3.025, 2.964, 2.902, 2.759, 2.62, 2.572, 2.531
11	Muscovite	9.95, 4.97, 4.47, 4.3, 4.11, 3.95, 3.882, 3.731, 3.489, 3.342, 3.32, 3.199, 2.987, 2.859, 2.789, 2.596, 2.566, 2.384
12	Montmorillonite	
13	Orthoclase/ Plagioclase	6.44, 5.86, 4.25, 3.8, 3.49, 3.33, 3.18, 3, 2.93, 2.83, 2.65, 2.53, 2.47, 2.39, 2.29
14	Oligoclase/ Alkali feldspar	6.43, 4.69, 4.02, 3.88, 3.74, 3.68, 3.63, 3.46, 3.41, 3.36, 3.26, 3.2, 3.17, 3.12, 3.01, 2.94, 2.91, 2.65, 2.52
15	Quartz	4.26, 3.343, 2.458, 2.282
16	Vermicullite	14.4, 7.2, 3.59

Table 3.2: Showing the d spacing values by XRD for mineral identification

3.5 Geochemical analysis

3.5.1 Sample dissolution

The elements constituting the sample need to be brought in the solution form for the determination of their nature and abundance using Inductively Coupled Plasma - Atomic Emission Spectrophotometre (ICP-AES). The sample processing and dissolution procedures were kept the same as far as possible for both, standards and sample solutions for any particular set of analysis. During the major and trace element analysis, the international rock standards (IRS) e.g.- BHVO, GSP etc. and in house rock standards digested with the set of samples were used to check the precision for a given set of analysis. The different digestion methods are discussed and explained here.

3.5.2 Preparation of B-solution by acid digestion

Majority of the major and trace elements were analysed using B-solution prepared by the acid digestion method, which is a modified procedure of [14]. In this method of solution preparation, 0.5 g of sample powder ($\sim$ 200 mesh size) was taken in a clean teflon crucible and to this 10 ml of concentrated HF, 5 ml of concentrated HNO_3 and 1 ml $HClO_4$ were added and heated to a temperature of about $85 - 90°$ C with the lid on the crucible for about 5-6 hours on an electric hot plate. After 5-6 hours, the lid was removed and the solution was evaporated to dryness. In the second step, 5 ml of concentrated HF, 10 ml of concentrated HNO_3 were added and again evaporated to dryness. In the third step, 10 ml of concentrated HNO_3 was added to remove the traces of HF and the solution was dried completely. Finally 25 ml of 2 N HCl was added and heated to about 100° C to bring the digested sample into the solution. After regular swirling, the solution was transferred to a 100 ml volumetric flask and the volume was made up with Millipore ultra clean water. By this method a 200 times diluted sample solution (200X) was prepared for the determination of trace elements such as V, Ni, Cr, Co, Ba, Cu, Zn, Sr. An aliquot of this solution was diluted 20 times more to obtain 4000 times diluted solution (4000X) and was used for major element analyses.

3.5.3 Preparation of A-solution for determination of silica (SiO_2)

In this method, 10 ml of 15% NaOH solution was taken in a clean Ni crucible and dried under infrared lamp. A sample weight of 0.05 g was taken in the same Ni crucible and fused under low flame over a Maker burner. After the fusion time of 20-30 minutes, the crucible was allowed to cool and triple distilled water was added to 3/4 of the crucible. The crucible was then kept overnight before transferring to 500 ml beaker containing about 300 ml of triple distilled water and 10 ml of concentrated HCl (12 N). While pouring the alkaline solution from Ni crucible care was taken to make sure that the solution did not touch the walls of the glass beaker and it was poured directly into the dilute acid solution in the beaker. If the solution was cloudy then it was heated on a hot plate and then allowed to cool. The solution was then transferred to a 1 litre volumetric flask and volume was made up with distilled water. About 100 ml of the solution was transferred to plastic bottles after rinsing the same with the solution several times. This 100 ml of the sample solution A was stored for SiO_2 determination, within one or two days.

Reagents: The following reagents were prepared for SiO_2 determination. Ammonium Molybdate Solution (7.5%): Ammonium Molybdate was prepared by dissolving 7.5 g of reagent grade $(NH_4)_6Mo_7O_{24}.4H_2O$ in 75 ml of distilled water in a 100 ml volumetric flask. To this 10 ml of 1 : 1 H_2SO_4 was added and mixed thoroughly and made up to 100 ml volume. The solution was then stored in a plastic bottle. Tartaric acid solution (8%): Tartaric acid solution was prepared by dissolving 40 g of reagent grade tartaric acid in distilled water and diluted to 500 ml in a volumetric flask. Reducing solution: 0.5 g of reagent grade anhydrous sodium sulphite was dissolved in 10 ml of water. 0.15 g of 1-amino-2-naphthol-4-sulphonic acid was added to 90 ml distilled water and stirred until it was totally dissolved. This solution was added to the first solution, mixed thoroughly and stored in a plastic bottle in a cool, dark place.

All the solutions were kept at room temperature. 10 ml each of sample solution-A of unknown samples, standards and blank were pipetted out into a 100 ml volumetric flask. To this 1 ml of ammonium molybdate solution was added and the contents stirred during addition. After mixing thoroughly, these solutions were allowed to stand for 10 minutes. Then 5 ml of tartaric acid solution was added to each flask and mixed by shaking the flask continuously. Immediately after this, 1 ml of reducing solution was added again swirling the flasks continuously and the whole solution was diluted to 100 ml in a volumetric flask. After 30 minutes the absorbance of each solution was determined at 650 nm after calibrating the spectrophotometer with blank solution-A and international standard RGM-1 and in-house standard solutions of 22-7, 22-22 and 21-6. Once the absorbance of the solution was determined by spectrophotometer (make: Bausch and Lomb), the known values of standards were plotted against the observed absorbance value to get a linear graph. Using the linear graph the silica value of unknown samples was directly obtained by plotting the respective absorbance value of the unknown samples.

3.5.4 Microwave digestion method

The Microwave digestion procedure was followed after [15]. In this method, 0.2 g of sample (∼200 mesh) was accurately weighed in teflon crucibles meant for microwave digestion system. After this 5 ml of MilliQ water, 2 ml of aqua regia and 3 ml of HF was added to the sample and the solution was digested for 45 minutes at 200° C in CEM MARS (Microwave Accelerated Reaction System-5). After cooling down to room temperature, 10 ml of 4% of boric acid was added and the digestion process was repeated for extra 15 min at 200° C. After cooling, the solution was made up to 100 ml in standard flasks with exactly 40 ml of boric acid solution used for rinsing and the rest with MilliQ water. The solution was then transferred into polypropylene bottles and shaken vigorously for 15-20 minutes on an automatic shaker. The solution was then ready for analysis on ICP-AES.

3.5.5 Determination of Loss on Ignition (LOI)

LOI was determined as suggested by [16]. The analysis was performed to account for the loss of water from hydrates and volatiles like carbon dioxide from carbonates. It is important for an accurate estimation of geochemical composition of samples. For this, 1 g of each of the sample of 200 mesh size was taken on a pre-weighed silica crucible of 50 ml volume and kept in muffle furnace for 12 hours at 105° C temperatures for removal of moisture content and this was the dry weight of the sample. The organic matter was combusted in the first step at a temperature of 550° C. The sample was kept in furnace for 4 hours. In the second step this sample was again kept for combustion in muffle furnace at 950° C for 2 hours. Carbon dioxide evolved from carbonates, leaving oxides. The calculation for organic matter and LOI are as follows

$$\text{LOI550} = \frac{\text{DW105} - \text{DW550}}{\text{DW105}} \times 100$$

(DW105 = Dry weight of the sample after heating at 105° C; DW550 = Dry weight after heating to 550° C)

$$\text{LOI950} = \frac{\text{DW550} - \text{DW950}}{\text{DW105}} \times 100$$

(DW550 = Dry weight after combustion at 550° C; DW950 = Dry weight after heating at 950° C)

3.5.6 Determination of organic carbon (OC)

Two types of carbon are present in sediments: organic carbon (OC) and inorganic carbon (IC). Organic carbon binds with hydrogen or oxygen to form organic compounds. Collectively, the two forms of carbon are referred to as total carbon (TC) and the relationship between them is expressed as:

$$\text{OC} = \text{TC} - \text{IC}$$

Organic carbon (OC) was determined by treating an aliquot of dried sample with sufficient phosphoric acid (1:1) to remove inorganic carbon prior to instrument analysis. Each sample boat was treated with phosphoric acid drop by drop until the sample stopped bubbling and the sample was completely moist with acid. The sample was placed into an oven set at 50° C for 24 hours and then transferred to an oven set at 105° C. Once the sample was dry, the boat was loaded onto the carbon analyser and analysed in the laboratory using a TOC Analyser (Multi NC 2100S, HT 1300, Analytik Zena, Germany)-solid module in Tezpur University, Tezpur. The sample was introduced in the combustion tube, which was filled with an oxidation catalyst and heated to 6800° C. In the samples, carbon was first converted to CO_2 by the combustion furnace for OC and TC analysis or by the IC sparger for IC analysis.

Carrier gas flows to the combustion tube and carries the sample combustion products from the combustion tube to an electronic dehumidifier, where the gas is cooled and dehydrated. The gas then carries the sample combustion products through a halogen scrubber to remove chlorine and other halogens. A carrier gas then sweeps the derived CO_2 through a non-dispersive infrared (NDIR) detector. Sensitive to the absorption frequency of CO_2, the NDIR generates a non-linear signal that is proportional to the instantaneous concentration of CO_2 in carrier gas. That signal is then plotted versus the sample analysis time. The peak area is proportional to the TC concentration of the sample. Calibration curve equation that mathematically expresses the relationship between the peak area and the TC concentration can be generated by analysing various concentrations of a TC standard solution. The TC concentration in a sample can be determined by analysing the sample to obtain the peak area and then using the peak area in the calibration curve equation. The resulting area is then compared to the stored calibration data of a sample with concentration in parts per million. Carbon Analyser was calibrated prior to the analysis of samples. Different amounts of high purity calcium carbonate standard (99.95% purity, carbon content of 12.0%) were used to calibrate the instrument. The approximate amounts of calcium carbonate used for the six-point calibration were: 0.01 g, 0.05 g, 0.10 g, 0.25 g and 0.50 g. An empty carbon-free combustion boat was analysed as a blank for the calibration curve.

3.5.7 ICP-AES analysis

The interpretation based on parameters analysed in samples depends on precision and accuracy with which the concentrations of the elements are determined. The sensitivity of instruments used is crucial to the data quality. The use of ICP-AES for determination of major and trace elements is well acknowledged [17, 18]. The high temperature in ICP-AES gives excellent analytical signals for most of the elements except alkali metals. Most of the analytical difficulties encountered in the ICP-AES by many laboratories the world over, are not caused by lack of sensitivity or a restricted choice of emission lines. Instead, the problem lies in not optimising the operating parameters of the instrument for both sequential (monochromator) and simultaneous (polychromator) mode of analysis. Many of the operating parameters such as observation height above the coil (torch height), sample gas flow, coolant gas flow pressures, selection of appropriate wavelength and PMT voltage in the case of monochromator analysis have to be optimised before any given set of analysis. Observation height refers to which part of the plasma is used for generating the light signal. For example, certain refractory elements such as Zr, Ti etc will require a higher temperature portion of the plasma, which means an increase in torch height, is required for the analyses of these elements. On the other hand for the analysis of Na which is readily ionisable element, cooler portion of the plasma is needed which means a reduction in the torch height and a considerable increase in the auxiliary and coolant gas flow supplies to the plasma is required.

Another important aspect of major and trace element determination by the sequential ICP (monochromator) analysis is the selection of a suitable wavelength with minimal spectral interference. Although an element has several sensitive wavelengths, we selected relatively sensitive wavelengths devoid of spectral interference from other elements in the analyte solution. During the initial period of data generation, the spectral interference problem was checked using the top 4-5 sensitive emission lines and the most suitable wavelength was found out. The above exercises, to find out the optimum instrument settings and wavelength selection in the monochromator ICP analysis were done mainly by keeping an eye on the optimum peak/background (P/B) ratio, for any particular element of interest. Higher the P/B ratio for any particular element, the better it is in terms of quality of the data. This is particularly important for trace element analysis, because a higher P/B ratio means that spurt in the detection limit, which means even at very low levels, good quality data can be obtained. Proper nebulisation without any pulsation in the aerosol spray produced was checked by looking at the Radiative Standard Deviation (RSD) % of the counts for 10 ppm Cu before calibration of the instrument for analysis. The precision and accuracy of the analysis for major and trace elements was monitored using United States Geological Survey (USGS) rock standards as well as in-house standards, and are better than 5% and 2%, respectively.

S	Wavelength (nm)	% Error
Si	288.158	1.5
Ti	336.121	1.78
Al	396.152	0.65
Fe	259.940	1.52
Mn	257.610	1.78
Mg	285.213	0.18
Ca	317.933	1.10
Na	588.995	0.56
K	766.5	1.3
P	213.620	6.02
Zr	339.198	10.6
Ni	231.604	6.72
Cr	267.716	2.25
Ba	455.403	1.98
Sr	407.771	3.95
Cu	324.754	1.0
Zn	213.856	4.5
V	292.402	3.5
Co	228.616	5.0

Table 3.3: Commonly used wavelengths for major and trace elements analysis on ICP-AES

3.5.8 Elemental analysis by X-ray fluorescence (XRF)

X-ray fluorescence spectrometry was used to determine both major and trace element chemistry of sediment samples. It is a rapid method for precise analysis of elements. XRF is based upon the excitation of sample by X-rays. A primary X-ray beam excites secondary X-ray (X-ray fluorescence) which has wavelength characteristic of the elements present in the sample. The intensity of secondary X-rays is used to determine the concentrations of the elements present in the sample in reference to calibration standards, with appropriate corrections being made for instrumental errors. Depending on the spacing between the atoms of the crystal lattice (diffractive device) and its angle in relation to the sample and detector, specific wavelengths directed at the detector can be controlled. The angle can be changed in order to measure elements sequentially, or multiple crystals and detectors may be arrayed around a sample for simultaneous analysis. The higher resolution of Wavelength Dispersive (WD)-XRF provides advantages in reduced spectral overlaps, so that complex samples can be more accurately characterised. The major and trace elements data of sediment samples were verified by using WD-XRF (PANalytical, Axios) to monitor the accuracy of the analysis.

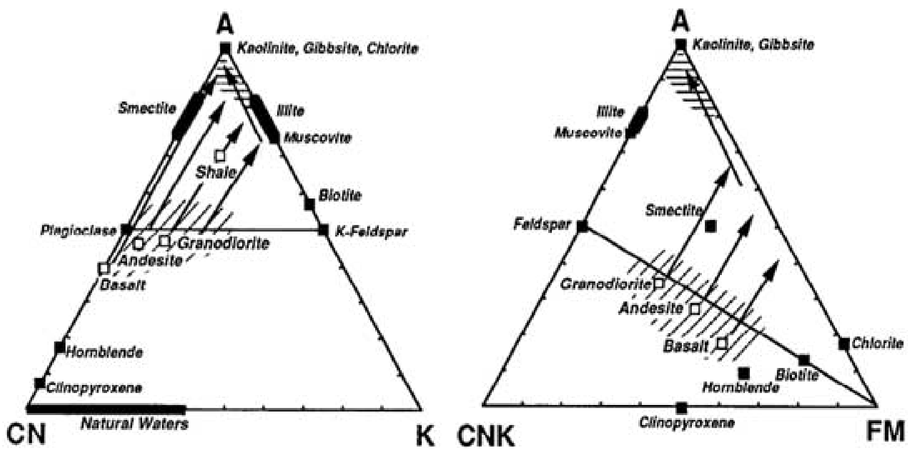

Figure 3.3: The A-CN-K and A-CNK-FM diagram: where A = Al_2O_3, C = CaO (in silicate fraction only, corrected for phosphates carbonates) N = Na_2O, K = K_2O, F = FeO and M = MgO.

3.5.9 Calculation of chemical index of alteration

The authors of [19] suggested a parameter called chemical index of alteration (CIA) to be calculated from the chemical data of rocks and sediments. The CIA is helpful in interpreting the weathering pattern of rocks and sediments. The parameter is an index of weathering status of sample that takes Al as a reference which is least mobile of all the phases as compared to other elements like Ca, Na and K. For the calculations, the molar proportions of the oxides of Al, Ca, Na and K were taken from the chemical. The index is defined as

$$\mathrm{CIA} = \frac{\mathrm{Al_2O_3}}{\mathrm{Al_2O_3} + \mathrm{CaO}^* + \mathrm{Na_2O} + \mathrm{K_2O}} \times 100 \tag{3.6}$$

CaO^* represents the CaO in the silicate fraction only. For the determination of CIA of the sediments where Ca is present as carbonates, the CaO has been determined by leaching the samples with cold diluted 1.3 N HCl in 1:10 ratio [20, 21] and corrected for P_2O_5. The other elements were recalculated to 100% accordingly and have been used for the calculation of CIA. For fresh rock and slightly weathered samples, the CaO^* values were taken as equal to CaO minus Ca for apatite. For better representation of CIA, the molar proportions of $Al_2O_3, CaO^*{+}Na_2O$ and K_2O were plotted on a triangular plot [19, 22] which is known as the A-CN-K diagram and the A-CNK-FM in the triangle (Figure 3.3) represents ($Al_2O_3, CaO^* + Na_2O +$ K_2O, FeO+MgO). The A-CN-K and A-CNK-FM diagrams are used to interpret the weathering trends of aluminosilicate minerals usually found on the earth's crust.

In case of A-CN-K diagram, some typical rock types and natural waters are plotted and the arrows indicate the general trends for increasing degrees of weathering. Trends shown by geochemical data from weathering profile match the theoretical trends predicted from thermodynamic and kinetic data [23]. Here, in this study, A-CN-K and A-CNK-FM diagrams have been used to evaluate mineralogical changes and degree of weathering using major element data of the channel, overbank, floodplain and suspended sediments of the Brahmaputra river and its tributaries.

Bibliography

[1] Jackson, M. L. (1956). Soil Chemical Analysis Advanced Course. Published by Author: JACKSON. ML Madison, 991.

[2] Jackson, M. L. (1958). Soil Chemical Analysis, Prentice - Hall, Inc., Englewood Cliffs.

[3] Griffiths, J. C. (1967). Scientific method in analysis of sediments. McGraw-Hill, New York. 508.

[4] Fredlund, M. D., Fredlund, D. G., and Wilson, G. W. (2000). An equation to represent grain-size distribution. Canadian Geotechnical Journal, 37 (4), 817-827.

[5] Pandey, S. K., Singh, A. K., and Hasnain, S. I. (2002). Grain-size distribution, morphoscopy and elemental chemistry of suspended sediments of Pindari Glacier, Kumaon Himalaya, India. Hydrological Sciences Journal, 47 (2), 213-226.

[6] Tessier, A., and Campbell, P. G. C. (1987). Partitioning of trace metals in sediments: relationships with bioavailability. In Ecological Effects of in Situ Sediment Contaminants. Springer Netherlands, 43-52.

[7] Galehouse, J. S. (1971). Sedimentation analysis, in Carver, R. E., ed., Procedures in sedimentary petrology, 69.

[8] Blott, S. J., and Pye, K. (2001). GRADISTAT: a grain size distribution and statistics package for the analysis of unconsolidated sediments. Earth surface processes and Landforms, 26 (11), 1237-1248.

[9] Folk, R. L., and Ward, W. C. (1957). Brazos River bar: a study in the significance of grain size parameters.Journal of Sedimentary Research,27(1).

[10] Passega, R. (1964). Grain size representation by CM patterns as a geological tool.Journal of Sedimentary Research,34 (4).

[11] Griffin, W. L. (1971). Mineral reactions at a peridotite-gneiss contact, Jotunheimen, Norway. Mineral. Mag., 38, 435-445.

[12] Lindholm, R. C. (1987). A practical approach to sedimentology. London: Allen and Unwin.

[13] Gibbs, R. J. (1968). Clay Mineral Mounting Techniques for X-ray Diffraction Analysis: A DISCUSSION: NOTES. Journal of Sedimentary Research, 38 (1).

[14] Shapiro, L. M., and Brannock, W. W. (1962).Rapid analysis of silicate, carbonate and phosphate rocks(No. 1144). US Government Printing Office.

[15] Pruseth, K. L., Yadav, S., Mehta, P., Pandey, D., and Tripathi, J. K. (2005). Problems in microwave digestion of high-Si and high-Al rocks. Current Science, 89 (10), 1668-1671.

[16] Maxwell, A. J. (1968). Rock and Mineral Analysis. In: P. J. Elving and I. A. Koltoff (eds.) Chemical Analysis (Vol. 27). Interscience Publishers, New York, 559p.

[17] Fassel, V. A. (1978). Quantitative elemental analysis by plasma emission spectroscopy. Science, 202 (4364), 183-191.

[18] Floyd, M. A. Fassel, V. A., and D'Silva, A. P. (1980). Computer-controlled scanning monochromator for the determination of 50 elements in geochemical and environmental samples by inductively coupled plasma-atomic emission spectrometry. Analytical Chemistry, 52 (13), 2168-2172.

[19] Nesbitt, H. W., and Young, G. M. (1984). Prediction of some weathering trends of plutonic and volcanic rocks based on thermodynamic and kinetic considerations. Geochimica et Cosmochimica Acta, 48 (7), 1523-1534.

[20] Gale, J. G., and Hoare, P. G. (1991). The physical composition and analysis of regolith materials. In Quaternary Sediments: Petrographic Methods for the Study of Unlithified Rocks. Belhaven Press New York, 87-94.

[21] Tripathi, J. K., and Rajamani, V. (1999). Geochemistry of the loessic sediments on Delhi ridge, eastern Thar desert, Rajasthan: implications for exogenic processes. Chemical Geology, 155 (3), 265-278.

[22] Nesbitt, H. W., Young, G. M. (1989). Formation and diagenesis of weathering profiles.The Journal of Geology,97(2), 129-147.

[23] McLennan, S. M. (1995). Sediments and soils: chemistry and abundances.Rock Physics Phase Relations: A Handbook of Physical Constants, 8-19.

Chapter 4

Study Area

4.1 The Brahmaputra River

The Brahmaputra River originates in a glacier in the Kailash Mountain in the Transhimalaya and flows with a very gentle slope eastward for ~1200 km in Tibet as Yarlung Tsangpo or Tsangpo. The Tsangpo takes a U-turn after Pai around Namche Barwa, the Eastern Syntaxis, where it makes the deepest gorge of the world and turns south to enter India (Arunachal Pradesh), where it is known as the Siang or Dihang. This part of the river with the deepest gorge has a very steep slope (~30 m/km) causing very turbulent and rapid flow and intense physical erosion [1, 2]. Immediately after Pasighat, the Siang River turns in SW direction and enters the Assam Plain, where it is called the Brahmaputra and flows in WSW direction as a wide and deep braided river. The Brahmaputra acquires a width of ~20 km and depth of ~35 m at some locations in the Assam Plain (Figure 4.1). The Brahmaputra turns south near Dhubri at the Indo-Bangladesh border and flows as the river Jamuna until it meets the Ganga at Arichaghat. The Brahmaputra River receives many tributaries along its course. In Tibet, the Tsangpo receives the Lhasa He (Zangbo), Doilung, and Nyang Qu [3, 4] in addition to tributaries from the northern slope of the Himalaya. After Pai, the river Parlung Zangbo [3] merges with it. The slope of this tributary is very high and comparable to that of the Siang in this section. In the Assam plain the Brahmaputra receives the Dibang and the Lohit from the east and the Subansiri, the Ranganadi, the Jia Bhareli, the Puthimari, the Manas, and the Tipkai from the north and the Burhidihing, the Dhansiri, and the Kopili from south (Figure 4.2). The Tista is another northern tributary of the Brahmaputra which merges with it in Bangladesh (Figure 4.2).

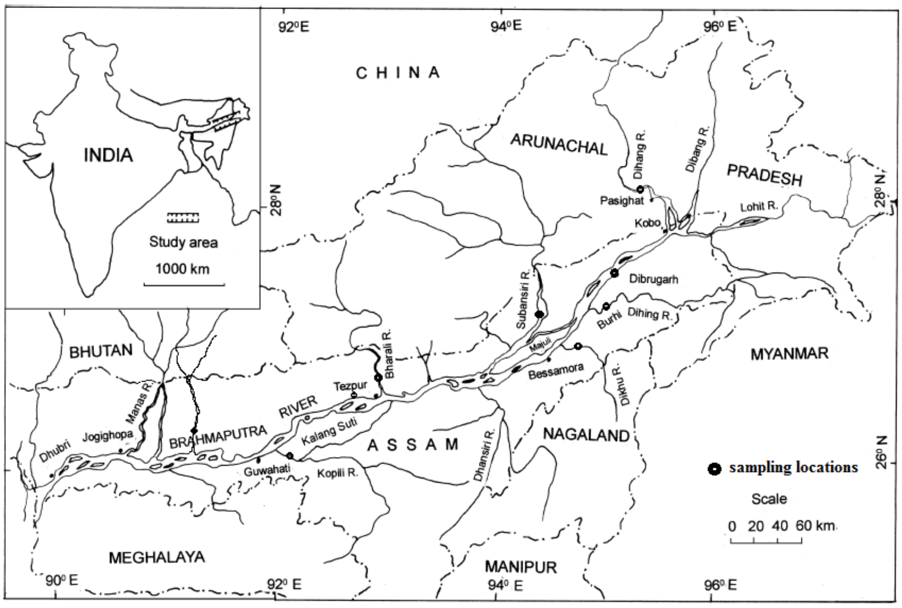

Figure 4.1: Figure showing the map of the study area.

4.1.1 Geology

The Brahmaputra drains a wide spectrum of metamorphic, magmatic -intrusive and effusive. and sedimentary rocks aged from Precambrian to Quaternary [5].The drainage basin of the Brahmaputra System can be divided into six geologically and climatically different subbasins (Figure 4.2, [6]) which are discussed below.

1. Tibet: In upper reaches the Tsangpo drains turbidites and ophiolites of the Indus-Tsangpo Suture Zone. The tributaries from the northern slope of the Himalaya drain the Tethyan Sedimentary Sequences and the gneiss zone. The tributaries from Tibetan Plateau, the Doilung, Zangbo, and Nyang Qu predominantly drain Trans himalayan gabbroic to granodioritic batholiths. The basins of these tributaries also contain evaporite deposits [4, 7, 8, 2].

2. The Eastern Syntaxis: The rocks near the Eastern Syntaxis are highly metamorphosed. At its core, gneisses of the Indian Plate have been exhumed from below the Transhimalayan Plutonic Belt (TPB; [9]). In this zone the calc-alkaline plutons of the TPB are surrounded by quartzites, phyllites, and marbles [9]. Discrete lenses

Basin Extent	
Longitude	88°11′ to 96°57′ E
Latitude	24°44′ to 30°3′ N
Length of Brahmaputra River (km)	916 (in India)
Catchment Area (square km)	194413
Average Water Resource Potential (MCM)	537240
Utilisable Surface Water Resource (MCM)	24000
Live Storage Capacity of Completed Projects (MCM)	1710
Live Storage Capacity of Projects Under Construction (MCM)	690
Total Live Storage Capacity of Projects (MCM)	2400
No. of Hydrological Observation Stations (CWC)	108
No. of Flood Forecasting Stations (CWC)	27

Table 4.1: Salient Features of the Brahmaputra Basin [10].

of etabasites and serpentinites occur in these areas, which indicate the continuation of the Indus- Tsangpo Suture in the eastern section [9]. These are drained by the Dibang, Parlung Tsangpo, and Lohit.

3. The Mishmi Hills: The two eastern tributaries, the Lohit and the Dibang, flow through the Mishmi Hills composed of calc-alkaline diorite-tonalite-granodiorite complexes and tholeiitic metavolcanic rocks [11]. It represents the eastern continuation of the TPB. The iding Suture present in this area marks the boundary between the TPB and the Himalaya in this section.

4. The Himalaya: The geology of the eastern Himalaya, through which the northern tributaries of the Brahmaputra System in Assam Plain, such as the Subansiri, Renganadi, Jia Bhareli, Puthimari, and Manas, flow is similar to those of its central and western sections, which form the Ganga basin. It comprises of the Higher and the Lesser Himalaya and the Siwaliks [12, 13]. In general, the proportion of the Lesser Himalaya increases from east to west in this watershed [1, 14]. The Higher Himlayan rocks consist mainly of schists and marbles with amphiboles at some locations. In Bhutan and Sikkim, the Manas and the Tista drain through metamorphic rocks of the Higher Himalaya. The Lesser Himalaya in the Brahmaputra System drainage

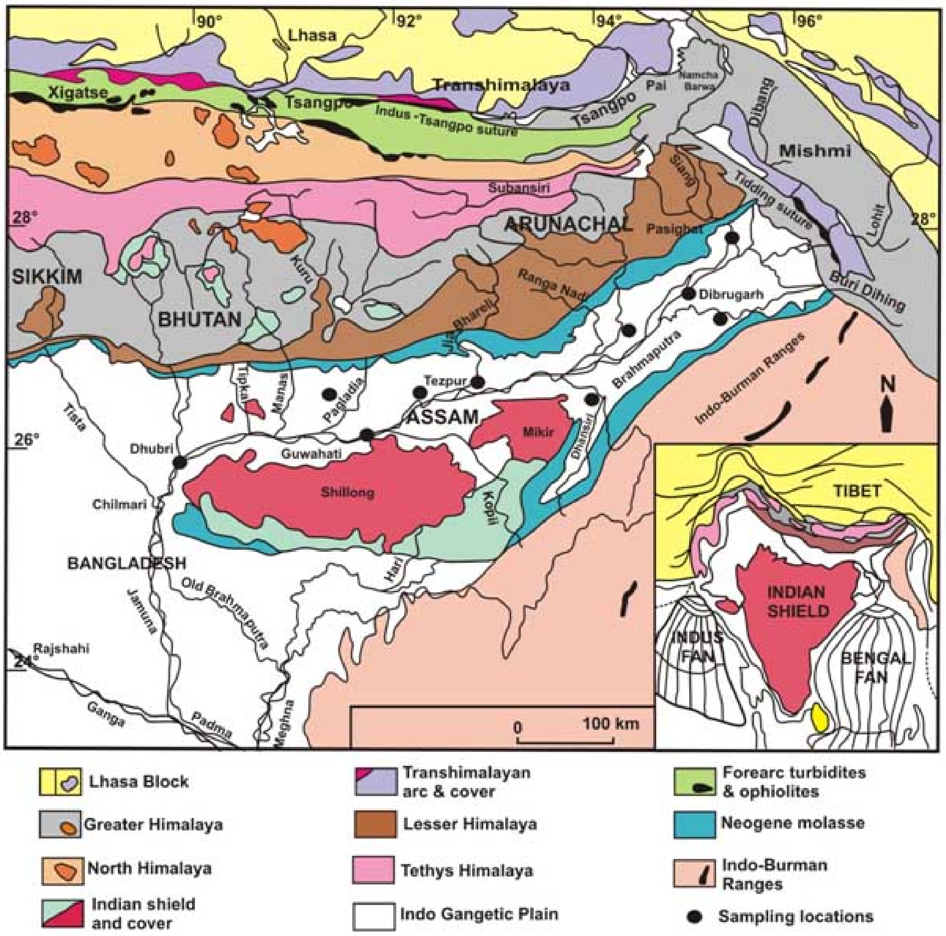

Figure 4.2: Geology of the Brahmaputra basin. Source: modified from [15].

is composed mainly of quartzites and schists. Precambrian limestones, dolostones, shales, and quartzites along with orthogneiss bodies and dolerite sills are exposed in the Lesser Himalaya. The Siwalik is discontinuous in the eastern section of the Himalaya. It includes a thick section of Neogene molasses. Continuing uplift and deformation are evident in this section by the presence of tilted gravel terraces and steep fault scarps [16]. Apart from these rocks of the Himalaya the basalts of the Abor volcanic are present in the Himalayan drainage of the Siang [17]. The northern tributaries of the Brahmaputra in the Assam plain drain through the southern slope of the Himalaya. Only a few of them, the Subansiri, have their drainage in the Tethys Himalaya [11].

5. Indo-Burmese Ranges: These ranges are made of pelagic sediments overlain by thick turbidites associated with ophiolites. The Dhansiri and the Kopili also drain the Indian basement of the Shillong Plateau and the Mikir Hills [11].

6. The Brahmaputra plain is a narrow and elongated foredeep (or rift valley) be-

tween the rigid massifs of Meghalaya and Karbi plateau (an extended part of the peninsular Gondwanaland) and the fold-mountains of Tertiary origin born out of the Tethyan geosyncline [18].The oldest (Precambrian) rocks are exposed in the Shillong Plateau and Mikir Hills, which are made up of high-grade metamorphites, gneiss, schists and granites overlain by metasediments. On the northern side, the alluvial plain of Assam abutts against Siwalik ridges of the Himalayas, which are in turn overlain by highly tectonized Paleozoic sediments. On the eastern side of Assam Valley, the alluvial deposits abut directly against metasediments, which are successively followed eastward by gneisses, high grade schists, some sediments, low grade schists, ultrabasic rock and diorite, granodiorite complex of Mishimi Massif. On the southeastern side of the alluvial plain the Tertiary rock sequences occur in Patkai and Naga Hills and consists of dark grey shales, sandstones and shales with coal seams, thin conglomerates, ferruginous sandstones and mottled clays, soft sandstones, clays and conglomerates, thick pebble beds, thin clays and sand. The Quaternary sediments, overlying unconformably the Tertiary deposits, are described as Older Alluvium or High Level Terraces, consist of indurated yellowish or reddish clays with sand, shingle, gravel and boulder deposits. The Recent sediments in the Brahmaputra valley were deposited as alluvial fan and floodplain sediments of the Brahmaputra and its several tributaries [19, 20] (Table 4.2).

4.1.2 Hydrology

The Brahmaputra Rive flows for approx. 3000 km to its confluence with the Ganges, after which the mixed waters of the two rivers empty into the Bay of Bengal. The Brahmaputra basin covers approx. 1600000 km^2 and includes 24 major tributaries, the majority of which originate in the Himalayas. The Brahmaputra is the fourth largest river in the world in terms of average flow discharge at its mouth with a flow of 19830 m^3s^{-1} [21], whereas the river ranks 22nd in terms of drainage area. Hence, discharge per unit drainage area in the Brahmaputra is amongst the highest in the world. At Pandu flow in the Brahmaputra yields 0.0306 $m^3s^{-1}km^{-2}$ which show that discharge increases progressively towards downstream. The Brahmaputra receives a large proportion of its discharge from its tributaries. The contributions of discharge of the major rivers in percentage are: Dihang (31.63), Lohit (7.90), Dibang (6.64),

Table 4.2: The geological formations in the Brahmaputra basin covering Assam are summarised into the following stratigraphic sequences.

Quaternary	Recent	Unclassified	Newer alluvium	Clay sand silt and Shingle
		Unconformity		
	Pleistocene	Unclassified	Older alluvium	Clay, coarse sand, shingle, gravel and boulder deposits
		Unconformity		
Tertiary	Pliocene	Dihing group	Dihing formation	Pebble bed, sandy clay, clay, conglomerate, grit and sandstone
		Unconformity		
	Miocene to Piocene	Dupi Tila group	Dupi Tila formation (Surma valley: 33000m) and Namsang formation (upper Assam: 800m)	Sandstone, mottled clay, grit and conglomerate with coal beds at places
		Unconformity		
	Miocene	Tipam group	Girujan formation (1800 m)	Mottled clay, sandy shales and subordinate gritty sandstone
			Tipam sandstone formation	Bluish grey to greenish, coarse to gritty, false bedded ferruginous sandtone, clay, shale conglomerate
		Surma group	Boka bill formation (900m to 1800m)	Shale, sandy shale, siltstone, mudstone and lenticular, coarse, ferruginous sandstone.
			Bhuban formation (1400m to 2400m)	Alterations of sandstone, sandy shale and thin conglomerate.
		Unconformity		
	Oligocene	Barail group	Renji formation (600m to 1000m)	Massive bedded sandstone (= tikak prabat formation (in upper Assam)
			Jenum formation (1000m to 3300m)	Shale, sandy shale and carbonaceous shale (=baragolai formation in upper Assam)
			Laisong formation (2000m to 2500 m)	Well bedded compact, flaggy sandstone and subordinate shale (=nagaon formation in upper Assam)
		Unconformity		
Eocene		Geosynclinals	Shelf	
	Disang group (not divided)	Splintery, dark grey shale and thin sandstone interbeds	Jaintia Kopili group	shale, sandstone Sylhet limestone member (fossiliferous) Sylhet sandstone member
		Unconformity		
Precambrian	Shilling group	(not classified)	Quartzite, phyllite and schist	
Archaean	Archaean group	(not classified)	Complex metamorphic group of gneisses and schists, metasediments later intruded by basic rocks	

State	Drainage area (square km)
Arunachal Pradesh	81424
Assam	70634
West Bengal	12585
Meghalaya	11667
Nagaland	10803
Sikkim	7300
Total	194413

Table 4.3: Drainage area of the Brahmaputra Basin in India [10].

Subansiri (7.92), Jiabharali (4.90), Manas (5.48), Sonkosh (2.81) and Burhidihing (1.87).

The major source of water in the Brahmaputra is rainfall, though meltwater and groundwater contributions are also important. In the Tsangpo in Tibet, for example, meltwater, groundwater and rainfall contributions are roughly the same [3]. The runoff in the Tsangpo drainage is 300 mm yr^{-1} which increases by more than order of magnitude, to 5000 mm yr^{-1}, for the Siang in Arunachal Pradesh. Runoff in the Himalayan drainage for the northern tributaries in the Assam Plain is 1000-2000 mm yr^{-1} and for the eastern tributaries it is 3000 mm yr^{-1}. The southern drainage is exposed to heavy rainfall and the runoff in this region is 4000 mm yr^{-1}. The major contributor to the Brahmaputra discharge is rainfall during SW monsoon (July to September). The monthly water discharge pattern of the Brahmaputra at Bahadurabad reflects the monsoon with significant temporal variation.It varies from $\sim$ 3300 m^3s^{-1} in February to $\sim$ 59000 m^3s^{-1} in July. The discharge in February is the lowest owing to paucity of rain and less melt water contribution. This trend is almost similar to that at The Brahmaputra System drains a total area of $\sim 630,000$ km^2. Of the total drainage, about one third is in Tibet with an average elevation of $\sim$ 5000 m. The Tibetan drainage contributes $\sim$ 10% of the water discharge of the Brahmaputra at its mouth. The Brahmaputra drains total area of 200,000 km^2 in the plains of Assam and the Bangladesh and its Himalayan tributaries occupy an area of 120,000 km^2 in the Himalaya. The two eastern tributaries, the

Rivers	Catchment area (square km)	Length (km)	Average annual discharge (m^3s^{-1})	Sediment yield (ton $km^{-2}yr^{-1}$)
Northern tributaries				
Subansiri	28000	442	755771	959
Jiabharali	11716	247	349487	4721
Pagladia	1674	197	15201	1883
Southern tributaries				
Burhidihing	8730	360	1411539	1129
Dikhow	3610	200	41892	252
Kopili	13556	297	90046	230
Dhansiri	10242	352	68746	379

Table 4.4: Hydrological characteristics of the tributaries of Brahmaputra rivers [22].

Lohit and the Dibang flowing through the Mishmi Hills have drainage area 50,000 km^2.

4.1.3 Sediment load

The Brahmaputra is one of the most sediment charged large rivers of the world. It is second only to the Yellow River in China in the amount of sediment transported per unit drainage area. During monsoon months, June through September, the daily rate of sediment discharges at Pandu averages 2.0 million metric tons, whereas average annual suspended load is 402 million tons [21].

4.1.4 Geography and Climate

Assam extends from 82°42′ E to 96° E longitude and 24°8′ N and 28°2′ N latitude covering an area of 78,438 sq. km. The Brahmaputra Valley of Assam trends almost east-west and its width varies from 40 to 100 km and is underlain by recent alluvium, consisting of clay, silt and gravels. The valley and its adjoining highlands constitute an extremely unstable seismic region (the Himalaya Ranges in the North are uplifting at a rate of order of 1m/century and the whole region is subjected to frequent seismic movements and periodic earthquakes).The major north-bank tributaries, such as the Subansiri, Jia Brarali, Manas, Sonkosh, exhibit partially braiding character at present but they were meandering rivers prior to the great earthquake of 1950. All of the southbank tributaries and smaller tributaries of the north bank are meandering rivers. The characteristic features of the Brahmaputra floodplain are anabranches, locally known as Suti or Sota. The longest of these is the Kalang Suti (165 km) and the others include Burhi Suti, Kherkatiya Suti, Disai Suti, Miri Suti, Dhaniya Suti, Lakshi Suti, Hajo Sota and Baralia Suti. Many palaeochannels exist, some of which can be traced uninterrupted for more than 50 km Most of these originate from neotectonic effects and result in river piracy in the headwaters. Presently some misfit streams are found to occupy the palaeochannels [23]. Natural levees occur as wedges all along the banks. West of Dibrugarh the average thickness and extension of the levee sediments towards the floodplain are 2.0 m and 1.0 km, respectively. Several large shallow water bodies or swamps are located in between the levee and the floodplain, some of them were formed from the sagging of ground during earthquakes. The floodplain also possessed abundant oxbow lakes and meander scars. Point bars occur at the convex side of meander bends with a greater extension toward downstream. Natural levees, channel bars, sediment/side bars and point bar islands are also characteristic features. Several deferred tributaries emerge near to the convex side of the lobes and flow parallel to the main river for some distance because of an aggraded alluvial ridge before joining the main river [24].

The Brahmaputra valley or the state of Assam including the adjoining regions, such as Arunachal Pradesh, Nagaland, Meghalaya, Mizoram, Tripura and Manipur, have a typical climatic personality, incomparable with any other part of India. The area in general forms an integral part of the south east Asiatic monsoon land, but its peculiar, high land guarded orography plays a dominant role in creating local weather phenomenon and climatic individuality. According to Koppen climate classification, this region, excluding the high mountain barriers, falls under 'Cwg' or typical Cwg type. Being a part of the sub-tropical belt, obviously its climate is akin to the South-East Asiatic monsoon. The local physical conditions, of course, modify the general characteristics of South-East monsoon to a certain extent. The major climatic controls of the Brahmaputra valley are: (a) orography; (b) presence

Zone	Average rainfall (mm)	Humidity (%)	Maximum Temperature (° C)	Minimum Temperature (° C)
NBPZ	1000	80	37	5
UBVZ	> 2000	> 80	37	5
CBVZ	1600	< 80	38	8
LBVZ	1700	80	31	10

Table 4.5: Climatic characteristics of the four zones of the Brahmaputra basin.

of alternating pressure calls of North west and Bay of Bengal; (c) predominance of tropical maritime humid air masses; (d) the roving periodic and occasional western disturbances; and (e) the local mountain and valley winds. The minor factors or controls are: (i) sub-tropical location; and (ii) occasional development of local depression, reduction of thermal difference by the extensive forest etc., deviate from the normal Gangetic type of humid mesothermal climate. The whole Brahmaputra basin is broadly delineated into the four macroclimatic zones: (a) North Bank Plain (NBPZ); (b) Upper Brahmaputra Valley (UBVZ); (c) Central Brahmaputra Valley (CBVZ) and (d) Lower Brahmaputra Valley (LBVZ). Each of these zones has been further divided into different belts.

During the period of summer from March to August low pressure develops in western India as well as over the Bay of Bengal. These cells are the dominating factors so far as incursion of the moist tropical air mass is concerned. The Bay of Bengal cell has its influence zone all over the Brahmaputra valley and its surroundings. Causally, a weak low also forms in the upper air layers, causing strong attractions to the tropical moist air masses. Similarly, with the shift of the thermal zone to the south, northwest India as well as southern Bengal develop high pressure cells and come under the continental cool stable air masses from Tibet or central Siberia, causing severe cold over the northern Gangetic plains, including the mountain and sub-mountain periphery of the northern Brahmaputra valley. However, the southern tongue of this high pressure cell does not extend beyond the hills, for which the severity of winter is much less than in the Gangetic plains in the west. The meteorologist refers to the extension of the easterly jet stream and upper air westerlies to the extreme northeast

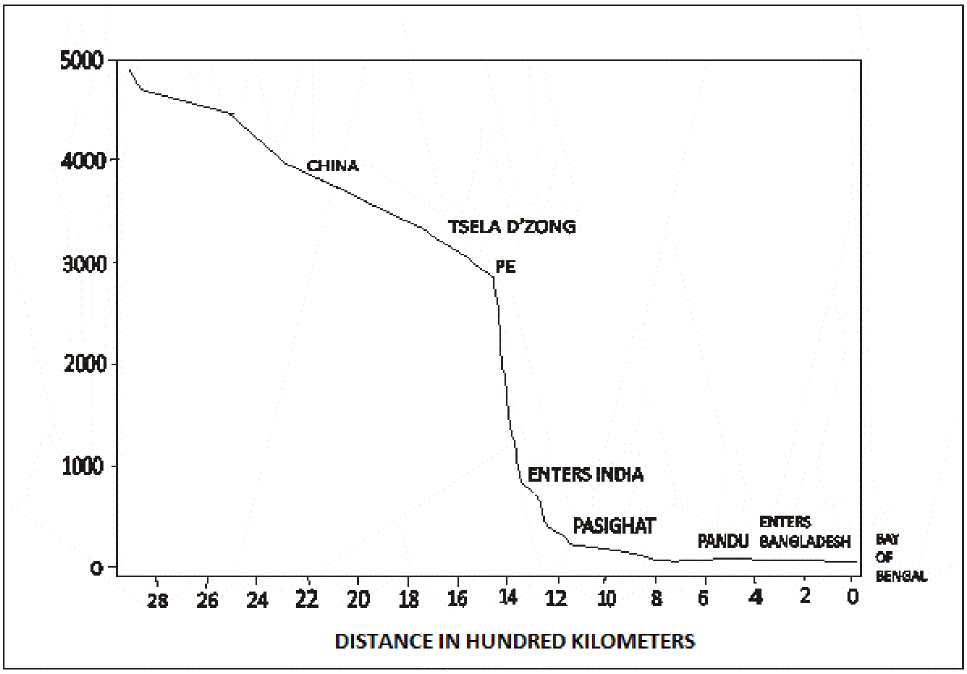

Figure 4.3: Longitudinal profile of the Brahmaputra river (after [21]).

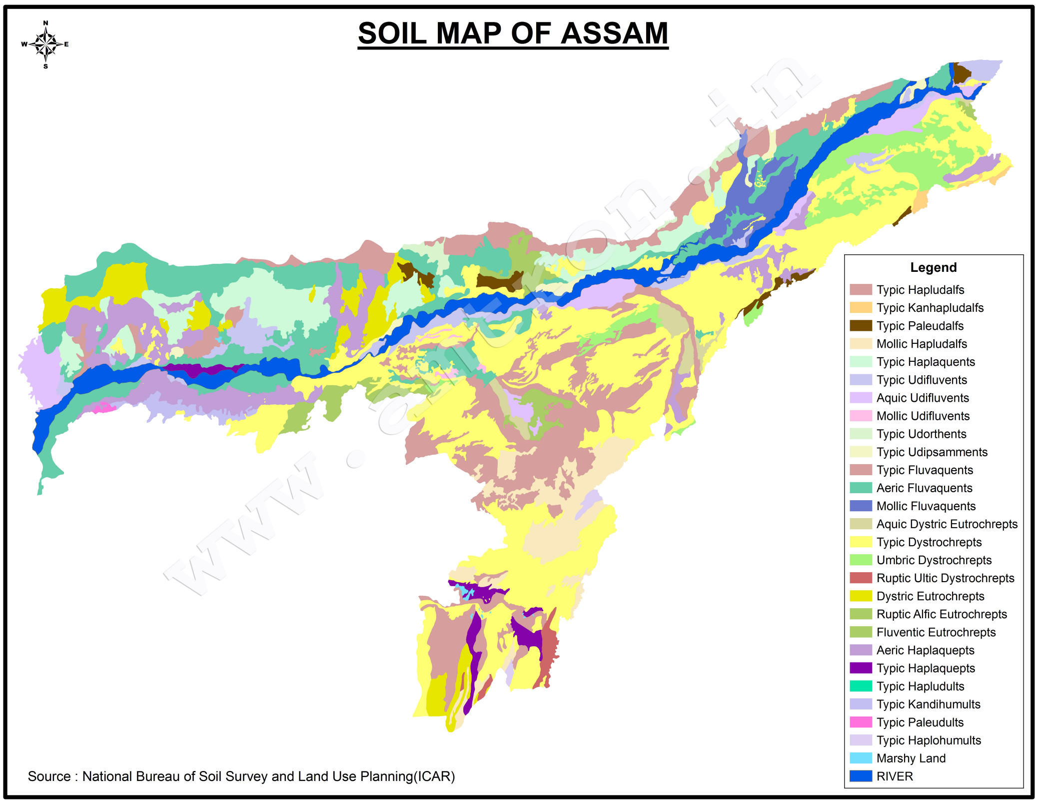

Figure 4.4: Figure showing soil map of Assam.

Seasons		Winter		PM		Monsoon					RM		Winter
Major stations	Climatic variables	Jan	Feb	Mar	Apr	May	June	July	Aug	Sep	Oct	Nov	Dec
Dibru-garh	Temp (°C)	13.33	16	19.83	22.22	24.83	26.28	26.67	27	26.68	24.33	19.83	14.22
	Rainfall (cm)	3.78	6.2	16.51	24.1	30.71	49.96	53.64	45.11	35.18	15.21	3.35	1.6
	Humidity (%)	94	88	79	82	86	90	90	90	89	95	95	94
Sib-sagar	Temp (°C)	13.17	15.67	19.39	22.22	25.11	27.17	27.56	27.59	26.83	24.28	19.17	14.11
	Rainfall (cm)	3.07	5.13	11.18	25.7	30.63	38.42	45.69	41.58	30.05	13.13	3.1	1.47
	Humidity (%)	96	91	84	84	87	88	90	89	90	91	92	97
Tezpur	Temp (°C)	14	16.33	20.61	23.17	25.22	26.94	27.33	27.5	27.44	24.72	20.22	15.17
	Rainfall (cm)	1.47	2.74	4.88	15.27	27.05	30.84	34.77	33.07	20.98	10.41	2.29	0.64
	Humidity (%)	91	84	74	77	84	87	89	90	89	85	84	91
Guwa-hati	Temp (°C)	14.17	16.44	20.83	24	25.83	27.44	28.11	28.11	27.56	25.06	20	15.28
	Rainfall (cm)	0.97	2.97	5.05	14.5	23.6	31.24	31.19	26.06	16.74	7.06	1.4	0.41
	Humidity (%)	91	82	73	76	82	85	86	86	85	86	89	92
Dhubri	Temp (°C)	14.56	16.67	21.39	24.39	25.44	26.5	27.5	27.56	27	25.11	20.79	16.27
	Rainfall (cm)	0.97	1.88	4.22	13.77	40.11	61.23	43.66	33.76	35.61	12.45	1.02	0.18
	Humidity (%)	87	79	69	74	85	82	88	88	88	85	82	86

Table 4.6: Temperature , humidity and rainfall at diff locations in the Brahmaputra valley [25]. PM and RM refer to pre-monsoon and retreating monsoon respectively.

Assam. The jet streams often pull down the western disturbances to the north of the valley and develop longer rainy days during the later part of the winter season. Owing to prolonged sunny weather during January and February or early March, rapid evaporation takes place over the entire valley. Rising temperatures often help the growth of local pressure centres in the valley. The supply of moisture and rising temperature stimulate growth of thunderstorms and hail storms, followed by heavy showers. The temperature in the valley gradually rises from 13° C in late January to 28° C in April. The rising temperature, coupled with upper air low, develops surface depression and stormy weather follows. In the case in which the western depression reaches the valley, it develops prolonged stormy and cloudy weather in the basin. The presence of enormous evaporated water augments the growth of thermodynamic local storms. June and July are the rainiest months. Rainfall is mostly associated with storms. These two months usually record the highest amount of rainfall. The humidity in the air increases beyond 90% and the temperature remains as high as 27° C or more The melting snow over the eastern Himalayan region, coupled with enormous rain water, in capacitates the river channels and swelling waters spread over the flood plains causing devastating floods.

4.1.5 Soil type

Soils of the valley are of varied types and their characteristics reflect the influence of both the parent material (geology) and the peculiar climate and vegetation of the region (Figure 4.4).

However, at present these soils are classified according to the Soil Taxonomy (Soil Survey Staff [26]). The major groups of alluvium-derived soils are Entisols, Inceptisols and Alfisols [27, 28, 29, 30, 31].

The flood plain soils, the channel soils, and low lying soils of upland have characteristic gleyed colours associated with wetness [32, 33, 30, 31].

The chemical processes associated with reduction and mobilisation of iron and manganese (gleying) under saturated conditions responsible for lowering of chroma of soil colour and their subsequent oxidation and precipitation under oxidised conditions results in higher chroma of soil colour.

The flood plain is mostly made up of sandy silty loam to clay loam, light grey to dark grey in colour with moderate to high permeability mostly developed under Kolong and Kopili river influences. Soil samples for soil nutrient analysis obtained from the farm field sites and analysed at RCSD laboratory reveals that the soil is acidic in nature with a pH 4 to 4.5. The soils of the area are characterized by low organic matter (below 0.5% by wt), low to medium presence of Nitrate nitrogen 9-18 lbs/ acre, very low presence of ammoniacal Nitrogen $<$ 100 lbs/acre, Phosphate $<$ 20 lbs/acre. Secondary elements such as Sulphate (SO_4) lbs $<$ 500 lbs are low in presence.

4.2 Tributaries and their characteristics

The south flowing tributaries of the Brahmaputra for most of their length drain the steep slopes of the Himalayas where rainfall is very high (of the order of 460 cm annually). Consequently, they not only carry heavy run-off,particu1arly where slopes are denuded of forests, but also a very large volume of detritus, the result of excessive soil erosion. The enormous mass of debris thus brought down form sandbanks and even islands in the lower valley. The soil is very friable, resulting not only in considerable tortuosity of the streams, but also frequent shifting of inner courses. North and south bank tributari.es are quite conspicuously different. Most of the northern bank tributaries (e.g. Subansiri, Jiabharali, Aie, Manas) are comparatively larger in size, have bigger catchments, are with steeper slopes and shallow braided channels, have coarse sandy bed and carry heavy silt discharge. They are also generally prone to. having flash floods resulting in enormous sediment load. On the other hand the south bank tributaries (e.g. Disang, Dikhou, Janji, Dhansiri) have flatter gradients, deep meandering channels, the banks and beds of non-alluvial soil and a comparatively low silt discharge. The Manas is the largest Himalayan tributary of Brahmaputra followed by Subansiri, Jia-Bharali, Burhi-Dihing, Beki, Aie and Dhansiri.

The major tributaries of the Brahmaputra river system (Subansiri, Jiabharali and Pagladia in the north bank and Burhidihing , Dikhow and Kopili in the south bank) from where samplings were done are discussed below.

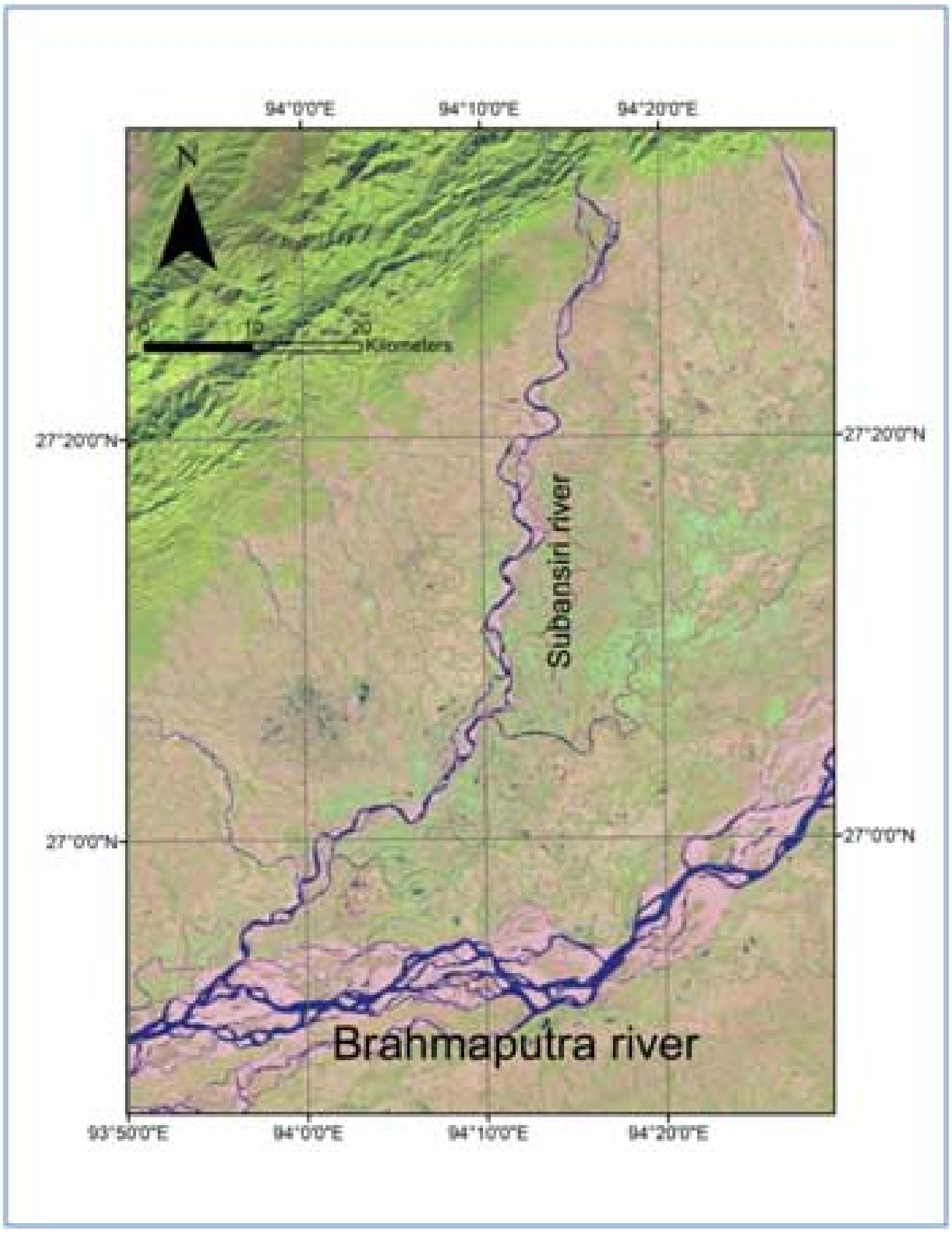

Figure 4.5: Map of the Subansiri Basin.

4.2.1 Subansiri river basin

The Subansiri is a perennially snowfed Trans-Himalayan river originating from the western part of the Mount Porom ∼5059 msl in the Tibetan Himalaya, formed by the association of the Lokong Chu (Char Chu), Chayal Chu and Tsdri Chu in Tibet. After flowing for 190 km through Tibet, it traverses the Himalayas and passes through the Miri Hills of India for 200 km and enters into the plains of Assam through a gorge near Gerukamukh joining the Brahmaputra river in Lakhimpur. In upper reaches, the river is locally known as 'Tsarichu' [34]. In the Subansiri basin two main tectonic features are seen, namely the Main central Thrust (MCT) and the Main Boundary Thrust (MBT). MBT lies about 9 km north of the Lower Subansiri dam site presently under construction. The rock units are aligned as NE-SW trending zone with folded and local window structures. Towards the north of Chamoli quartzite, chinka formations are present. The rock structure of Subansiri basin is fine grained to pebbly, weathered, highly jointed to massive sandstone, medium to coarse grained, soft weathered to shared, massive to moderately jointed sandstone with stringers of carbonaceous material. The Subansiri is the largest tributary of the Brahmaputra. Its total length is 442 km and it drains a basin of 37,000 km^2 as measured from SRTM (Shuttle Radar Topographic Mission) [35, 36]. Its maximum observed discharge was 18,799 m^3s^{-1}, and its minimum 131m^3s^{-1}. It contributes 7.92% of the Brahmaputra's total flow. The Kamala, Ghagar and Sampara are its major tributaries in India. Valley soils are well developed from colluvial material brought down from the upslopes and are sandy loam in texture [35].

4.2.2 Jiabharali river basin

The Jiabharali River which is also known as Kameng in its upper reaches originates in the upper Himalayan ranges at an elevation of ∼5400 m. The river has a total length of ∼242 km. It debouches from Himalaya through a dissected piedmont plain and is restricted within a narrow valley. The river flows on gravel bed upto Ghoramari along straight, braided channel and then follows a straight sinuous braided path up to the confluence with Brahmaputra. During the course from source to mouth, Kameng is joined by several major tributaries namely Bichom, Digien,

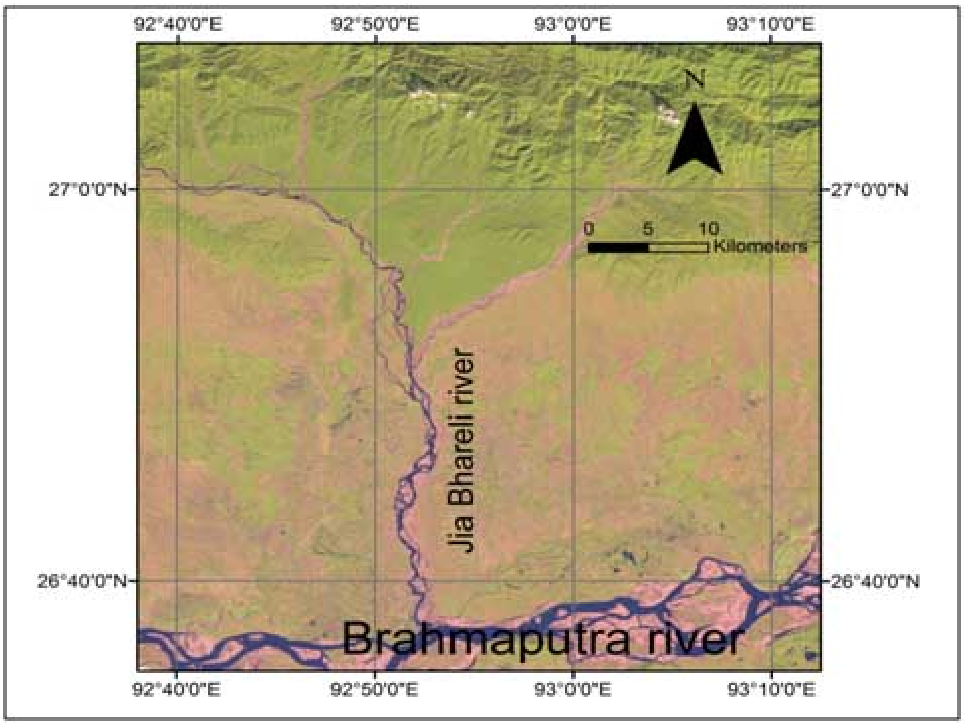

Figure 4.6: Map of the Jiabharali Basin.

Tenga, Pachuk, Pakke, Sesa Nadi, Tipi Nadi, Diju Nadi, Nameri Nadi, Upper Dikrai Nadi, Khari Dikrai Nadi. Bor Dikrai, Nam Sonai, Darikati, Mansari, Jorasar are major tributaries on the right bank in the alluvial part. The Jiabharali has a total catchment area of 11,280 sq km and is bounded by longitudes $92°00' - 93°25'$ E and latitudes $26°39' - 28°00'$ N [37]. Geologically the Jiabharali basin is characterized by a wide spectrum of lithostratigraphic units ranging from Quaternary Alluvium in the south to Precambrian crystallines in the north. The catchment area covers the outer hills or Sub-Himalaya (Siwalik), Lesser Himalaya and Higher Himalaya. Jiabharali basin is constituted of four major geological units (Table 4.7). The Quaternary sediments constitute the alluvial part. The Sub-Himalayan zone consists of Siwalik rocks constituted of indurated sandstone and shale at the bottommost part followed upwards by monotonous soft, massive sandstone along with siltstone, clay and gravel, while the Lesser Himalayan zone comprises of two litho-units, viz. Gondwana Group and Bomdila Group. The Gondwana Group, constituted of shale/slate, sandstone and siltstone with coaly material, is thrusted over the Siwaliks along the Main Boundary Thrust (MBT). Towards the north of the Gondwanas lie the Bomdila Group constituted primarily of gneissic rocks belonging to the Precambrian

Quaternary sediments	
Younger Alluvium	Holocene to Recent
Older Alluvium	Middle to Upper Pleistocene
HFT	
Siwalik Group (Neogene Clastics)	
Kimin Formation	Mio-Pliocene
Subansiri Formation	Mio-Pliocene
Tipi Thrust	
Dafla Formation	Mio-Pliocene
MBT	
Gondwana Group	
Bharali Formation	Permo-Carboniferous
Bichom Formation	Permo-Carboniferous
Miri Formation	Lower Paleozoic
Intrusive contact	
Biotite Granite	
Intrusive contact	
Dirang Formation	
Unconformity	
Bomdila Group	
Bomdila/Ziro/Daporijo Gneiss	Paleo-Proterozoic
Chiliepam (Dedza) Formation	
Tenga Formation	
Khetabari	
MBT	
Sela Group	Paleo-Proterozoic

Table 4.7: Generalised lithostratigraphy of the Jiabharali basin (after Geological Survey of India, 2010, [11]).

age [38]. Further northwest of the catchment Higher Himalayan crystalline rocks of Sela Group appear along the MCT. Dirang Formation is in between the Bomdila Group of rock and Sela Group [37].

4.2.3 Pagladia river basin

Pagladia is an important tributary on the north bank of the Brahmaputra valley. It originates from the southern slopes in the Bhutan Hills of Himalayan range at an altitude of 3000 m above msl in the form of two streams Pagla and Dia that meet near Chowki and passes through undivided Nalbari district (presently Bagsa and Nalbari) and finally connect with the Brahmaputra river near Sotemari of Nalbari District. The basin lies between 91°18′ N to 91°42′ N latitude and 26°14′ E to 27°0′

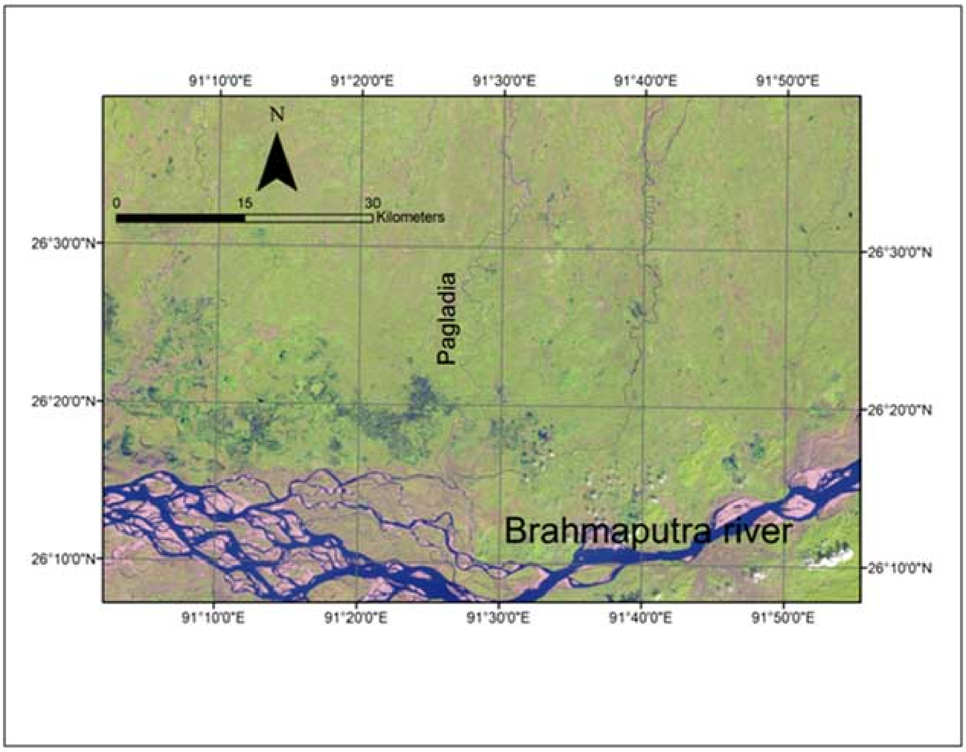

Figure 4.7: Map of the Pagladia River Basin.

E long longitude [39]. The catchment area of the basin is 1507 km^2 of which 1084 is in India and remaining 423 km^2 is in Bhutan and is 196.8 km in length of which 19 km is in Bhutan and 177.8 is in India. The major tributaries are Mutunga, Dimla, Nona and Chowlkhowa [40]. The Pagladiya basin has been developed by the actively migrating nature of the stream and resulted in a basin consisting of complex channel migration pattern. Apart from tectonic activity, erratic flash floods and heavy sediment load also contribute towards active channel migration. Physiographically, it is characterised by the different land forms resulting from a) denudation structural hill and b) alluvial plain. The low mounds/hillocks are covered by a thick lateritic mantle and these are occupied by evergreen mixed forests. The alluvial plains comprise of Older and Newer alluvium. The Older alluvium occupies the piedmont zone towards the north of the district bordering Bhutan. The narrow zone at the Himalayan foothill is known as the Bhabar zone and it supports grow of dense forests. To the south of the Bhabar zone and parallel to it, the flat Terai zone lays where the ground remains damp and sometimes, spring oozes out. The Terai zone is covered by tall grass. The Newer alluvium includes sand, gravel, pebble with silt and clay.

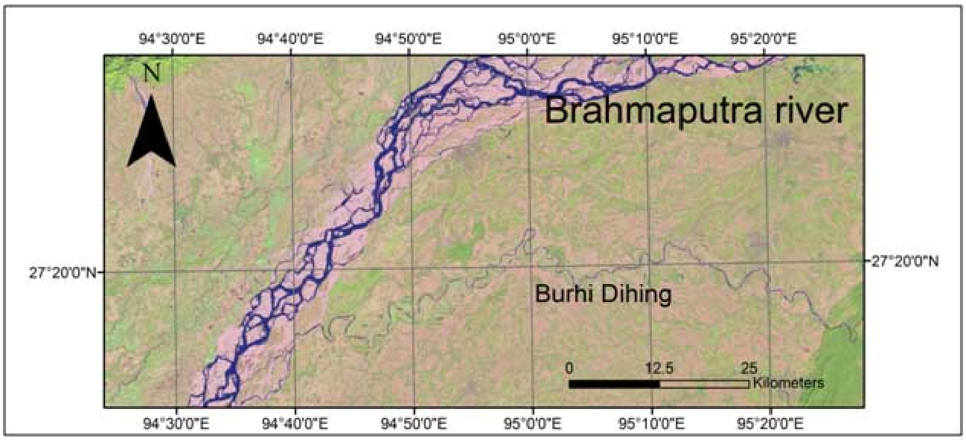

Figure 4.8: Map of the Burhidihing River Basin.

4.2.4 Burhidihing river basin

The Burhidihing is the largest south-bank tributary of the Brahmaputra in Assam. It originates as Namphuk which rises in the Patkai Range at the Indo-Myanmar border and flows through the Patkai Range for about 115 km before coming out into a piedmont alluvial plain where it changes its name for the Burhidihing. After flowing for about 70 km through the alluvial plain from east towards west, the river again passes through the outcrops of Tertiary sedimentary rocks exposed on a low hill range in between 95°25′ E to 95°31′ E for about 19 km. Thereafter it again flows through the alluvial plains of Assam for 128 km and falls in the Brahmaputra at Dihingmukh. The river drains a basin of about 6000 km^2 and its width varies from 300 m to 400 m in the plains. The Burhidihing is a meandering river of sinuosity 1.6; hence shifting of the banks of the river takes place along its meander bends within the alluvial plain by erosion in one part and deposition in the other. There are local variations of geology and constituent bank materials along the course of the river. Important tributaries are Namphuk, Namchik, Megantion, Khaikhe, Tirap, Digboi, Tingrai, and Sessa.

The Burhidihing drain the outer part of the northern Indo-Burman Ranges, the accretionary prism, which includes the Cretaceous-Eocene pelagic sediments overlain by thick Eocene-Oligocene turbidites associated with ophiolitic allochthons, emplaced onto the eastern India shelf during mid-Tertiary oblique collision with southeast Asia. It enters the alluvial plains passing through the outcrops of tertiary sedimentary rocks exposed in a low hill range. Thereafter it again flows through the alluvial plains of Assam and meets the Brahmaputra at Dihingmukh.

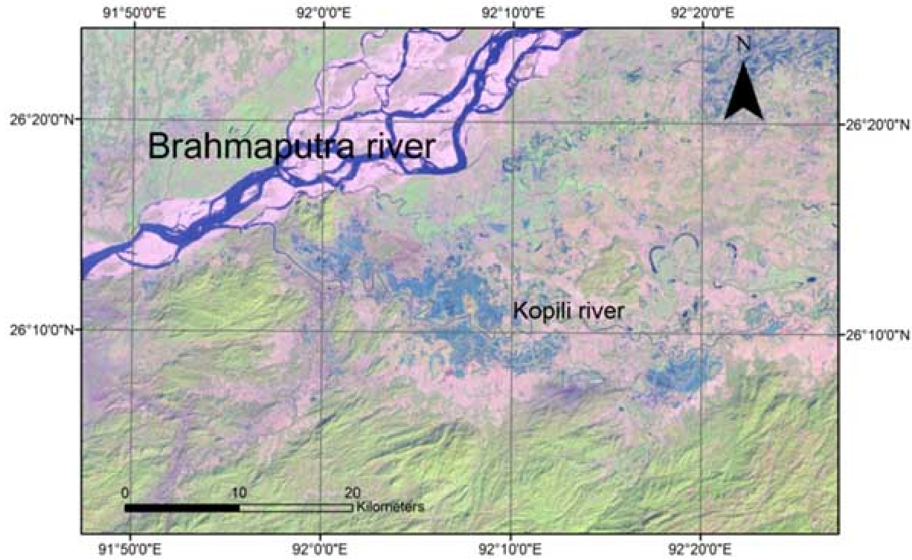

Figure 4.9: Map of the Kopili River Basin.

4.2.5 Kopili river basin

The Kopili finds its origin in the Jaintia Hills (Meghalaya) in the Borail Range at an elevation of 1,630 m. Its total length is 297 km and it drains a basin of 15868 km^2. Its major tributaries are the Diyung, Jamuna, Borpani and Kiling. The Kalang along with Kopili contributes 1.47% of the total flow of the Brahmaputra. Kharkor, Myntriang, Dinar, Longsom, Amring, Umrong, Longku and Langkri are its major tributaries in its upper reaches. The total catchment of Kopili River is about 16,421 km^2.

The unconsolidated alluvium of Quaternary age comprise of younger and older alluvium consisting of sand of various textures with minor amount of silt and clay and is found in the area between Kolong and Brahmaputra, while the older alluvium is found in the channels of Kolong and Kopili river and to the south. The Archean group of rocks comprise of biotite- hornblende gneiss granulites, schist intruded by granites and pegmatites exhibit NE-SW trend with moderate dip towards NW. As

Group	Formation	Lithology
Recent	Alluvium	Loose sand, pebbles and borders sandstones and gneissic rocks, clay and silt.
	Unconformity	
Dihing group (Plio-Pleistocene)	Dihing formation	Boulder of sandstone, gneisses, schist and basic rocks set in sandy and clay matrix, bluish grey medium to coarse gritty sandstone with sandy clay lenses.
	Namsang Formation	Bluish to green, loose, unconsolidated sand beds with pebbles of quartzite and lignite fragments, carbonised and silicified wood.
	Unconformity	
	Girujan Formation	Mottled, gret, bluish clays with greenish sandstone beds and chert nodules
Tipam group (Mio-Pliocene)	Tipam Formation	Bluish to green, medium to coarse, friable to well indurated sandstone intercalated with mottled clay, grit and conglomerate beds.
	Tiakak parbat Formation	White to grey, sandy clay-shale, intercalated with brown, argillious sandstone and coal seams in the basal part.
Barail Group (Oligocene)	Baragolai Formation	Grey to brownish red, thickly bedded, micaceous to argillaceous sandstone with pellets. Carbonaceous shale and coal stringers/lenses..
	Nagaon Formation	Grey hard flaggy thin bedded sandstone with intercalation of dark grey splintery shale and sandy shale.

Table 4.8: Stratigraphic succession of the outcrops of the tertiary rocks in the hilly area and alluvial plains in the Burhidihing basin. (after [41]).

Age	Formation	Lithology
Quaternary	Younger and older alluvium	Fine to coarse sand, gravel pebble embedded in sand.
Archean	Shillong Group	Gneiss intruded by acidic granite and basic intrusive.

Table 4.9: The stratigraphic succession of the the Kopili basin between the Mikir Hills and the Shillong Plateau.

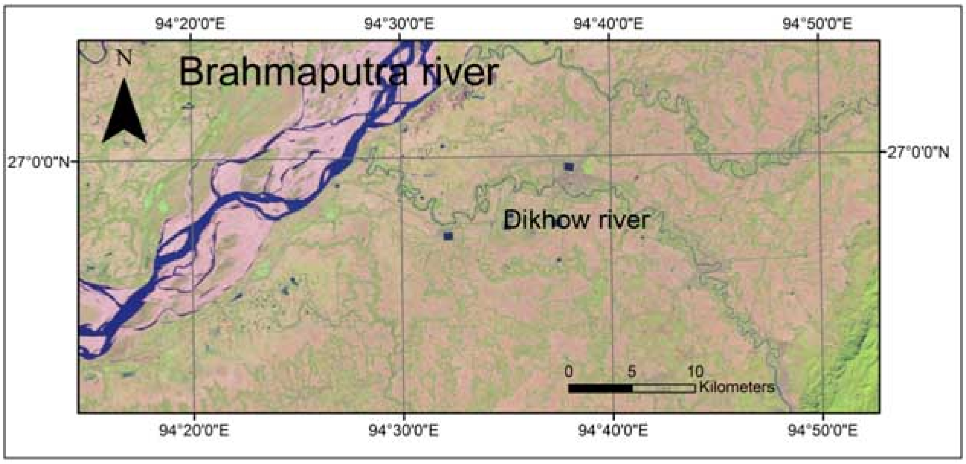

Figure 4.10: Map of the Dikhow River Basin.

per CGWB records, the granite basement is encountered at a depth of 95m at Jagiroad, 239 m at Dharamtul and 254 m at Rajagaon towards Brahmaputra, i.e., the slope of the basin dips from south to north.

4.2.6 Dikhow river basin

Dikhow, a major south bank tributary of Brahmaputra has its origin in the Naga Hills and flows through the central part of the Sibsagar district. The river has a length of 200 km from its source to mouth at a place called dikhowmukh. Including both plains and hills its basin covers an area of 4372 sq km. The river enters the plain of Assam at Naginimara. While meandering through the plains, the river leaves more than fifteen abandoned channels at different places. Many of these are ox-bow lakes [39]. The Yangmun and the Namdang are major tributaries of the Dikhow.

The Dikhow basin bounds from the Naga Hills to the south to the Brahmaputra in the north, the Dikhow flowing across the mountainous topography of the state of

Group	Formation	Lithology
Recent	Alluvium	Loose sand, pebbles and boulders of sandstones and gneissic rocks, clay and silt.
	Unconformity	
Dihing group (Plio-Pleistocene)	Dihing formation	Boulder of sandstone, gneisses, schist and basic rocks set in sandy and clay matrix, bluish grey medium to coarse gritty sandstone with sandy clay lenses.
	Namsang Formation	Bluish to green, loose, unconsolidated sand beds with pebbles of quartzite and lignite fragments, carbonised and silicified wood.
	Unconformity	
Tipam group (Mio-Pliocene)	Girujan Formation	Mottled, grey, blueish clays with greenish sandstone beds and chert nodules.
	Tipam Formation	Blueish to green, medium to coarse, friable to well indurated sandstone intercalated with mottled clay, grit and conglomerate beds.
Brail Group (Oligocene)	Tiakak parbat Formation	White to grey, sandy clay-shale, intercalated with brown, argillious sandstone and coal seams in the basal part.
	Baragolai Formation	Grey to brownish red, thickly bedded, micaceous to argillaceous sandstone with pellets. Carbonaceous shale and coal stringers/lenses.
	Nagaon Formation	Grey hard flaggy thin bedded sandstone with intercalation of dark grey splintery shale and sandy shale.
	Unconformity	
Disang Group (Eocene-Lr Oligocene)	Disang Formation	Dark grey to black splintery shale interbedded with fine to medium, grey, flaggy to massive sandtone siltstone.
	Unconformity	
Metamorphic (Precambrian)		Quartz-mica schist, quartzites, slate.

Table 4.10: Showing stratigraphic succession of the Dikhow basin.

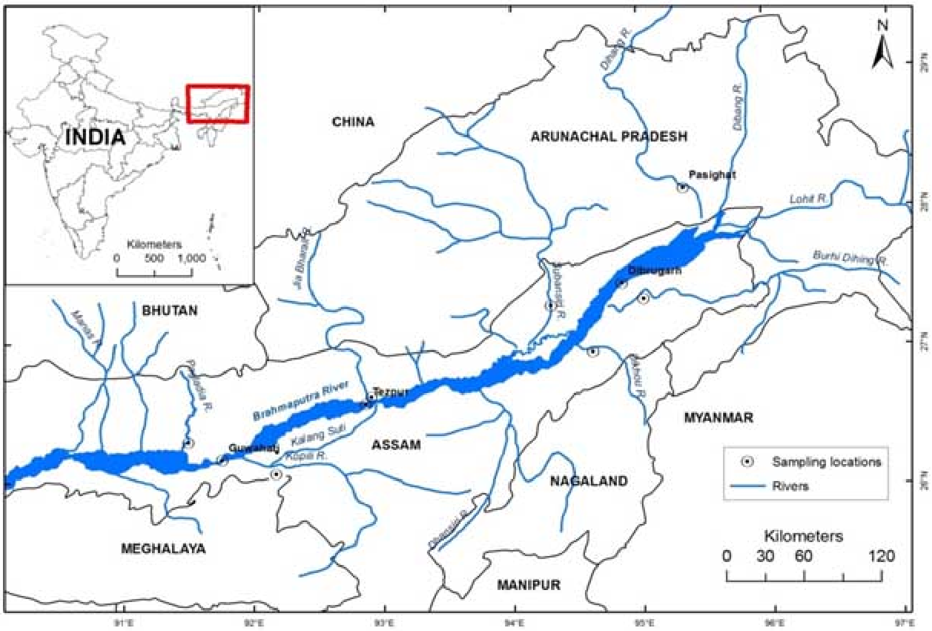

Figure 4.11: Map of the Brahmaputra Basin with the sampling locations.

Nagaland which includes the Cretaceous-Eocene pelagic sediments overlain by thick Eocene-Oligocene turbidites associated with ophiolitic allochthons, emplaced onto the eastern India shelf during mid-Tertiary oblique collision with southeast Asia. The river enters the plain of Assam at Naginimara. While meandering through the plains, the river leaves more than fifteen abandoned channels at different places.The continuity of this floodplain is broken by isolated hillocks of Archaean origin. The hillocks of Negheriting of Golaghat district belong to this type [18].

4.3 Sampling locations

Table 4.11 and 4.12 show the sampling sites of this study for all the rivers with the sampling coordinates and sample codes. The suspended sediments were sampled in high discharge periods (monsoon) and channel, overbank and floodplain samples were collected in post-monsoon season. Figure 4.11 shows the map of all the sampling locations.

Location	Sample	Latitude	Longitude	Sampling date
Pasighat	PSG SS	28°5′57.88” N	95°16′16.79” E	10/08/2013
	PSG CH, BNK, FP	28°5′57.60” N	95°16′16.78” E	25/10/2013
Dibrugarh	DIB SS	27°27′57.29” N	94°51′48.17” E	10/08/2013
	DIB CH, BNK, FP	27°27′57.34” N	94°51′48.17” E	27/10/2013
Tezpur	TEZ SS	26°36′14.51” N	92°51′23.73” E	10/08/2013
	TEZ CH, BNK, FP	26°36′14.47” N	92°51′23.75” E	4/11/2013
Guwahati	GHY SS	26°11′41.00” N	91°44′36.72” E	6/08/2013
	GHY CH, BNK, FP	26°11′41.05” N	91°44′36.75” E	6/11/2013
Dhubri	DBR SS	25°59′21.69” N	90°3′18.89” E	7/08/2013
	DBR CH, BNK, FP	25°59′21.72” N	90°3′18.92” E	4/12/2013

Table 4.11: Sampling locations in the Brahmaputra river with sample codes and coordinates and sampling dates. SS: Suspended, CH: Channel, BNK: Overbank, FP: Floodplain.

Location	Sample	Latitude	Longitude	Sampling date
Pagladia	PGL SS	26°4′39.15” N	91°53′53.23” E	6/08/2013
	PGL CH, BNK, FP	26°4′39.15” N	91°53′53.23” E	5/10/2013
Jiabharali	JBR SS	26°39′15.12” N	92°53′53.11” E	6/08/2013
	JBR CH, BNK, FP	26°39′15.14” N	92°53′57.12” E	27/10/2013
Subansiri	SBN SS	25°51′77.82” N	94°28′38.09” E	4/08/2013
	SBN CH, BNK, FP	25°51′77.78” N	94°28′38.08” E	4/11/2013
Dikhow	DK SS	26°13′13.04” N	91°6′67.04” E	6/08/2013
	DK CH, BNK, FP	26°13′13.15” N	91°6′67.16” E	6/11/2013
Kopili	KPL SS	26°15′07.13” N	92°10′04.13” E	6/08/2013
	KPL CH, BNK, FP	26°15′08.12” N	92°10′05.13” E	6/11/2013
Burhidihing	BHD SS	27°32′42.12” N	95°13′32.06” E	6/08/2013
	BHD CH, BNK, FP	27°32′42.10” N	95°13′32.11” E	5/12/2013

Table 4.12: Sampling locations in the tributaries with the sample codes ,dates and coordinates. SS: Suspended, CH: Channel, BNK: Overbank, FP: Floodplain.

Bibliography

[1] Singh, S. K., and France-Lanord, C. (2002). Tracing the distribution of erosion in the Brahmaputra watershed from isotopic compositions of stream sediments.Earth and Planetary Science Letters,202(3), 645-662.

[2] Singh, S. K., Sarin, M. M., and France-Lanord, C. (2005). Chemical erosion in the eastern Himalaya: major ion composition of the Brahmaputra and δ 13 C of dissolved inorganic carbon.Geochimica et Cosmochimica Acta,69(14), 3573-3588.

[3] Guan Z. and Chen C. (1981) Hydrographical features of the Yarlung Zangbo River. In Geological and Ecological studies of QinghaiXizang Plateau. Gordon and Brach Science Publishers, New York, 1693-1703.

[4] Ming-Hui, H., Stallard, R. F., and Edmond, J. M. (1982). Major ion chemistry of some large Chinese rivers.Nature,298(5874), 550-553.

[5] Wadia, D. N. (1975) Geology of India. New Delhi: Tata-McGraw Hill Publ. Co.

[6] Singh, A. K. (2006). Chemistry of arsenic in groundwater of Ganges-Brahmaputra river basin.Current Science,91(5), 599-606.

[7] Pande, K., Sarin, M. M., Trivedi, J. R., Krishnaswami, S. and Sharma, K. K. (1994) The Indus river system (India-Pakistan): major-ion chemistry, uralium and strontium isotopes, Chem. Geol. 116, 245-259.

[8] Pascoe, E. H. (1963) A Manual of the Geology of India and Burma, Vol. 3, Government of India Press, Calcutta, pp. 2073-2079.

[9] Burg, J. P., Nievergelt, P., Oberli, F., Seward, D., Davy, P., Maurin, J. C., ... and Meier, M. (1998). The Namche Barwa syntaxis: evidence for exhumation

related to compressional crustal folding.Journal of Asian Earth Sciences,16(2), 239-252.

[10] Singh, V., Sharma, N., and Ojha, C. S. P. (Eds.). (2013).The Brahmaputra basin water resources(Vol. 47). Springer Science Business Media.

[11] Kumar, G. 1997. Geology of Arunachal Pradesh. Special Publication Geological Society of India, 53, 217.

[12] Thakur, V. C. (1986) Tectonic zonation and regional framework of eastern Himalaya. Memoires, Sciences de la Terre, 47, 347-360.

[13] Gansser, A. (1964). Geology of the Himalayas, 289 pp.Interscience, New York.

[14] Robinson D. M., DeCelles P. G., Patchett P. J., and Garzione C. N. (2001). The kinematic evolution of the Nepalese Himalaya interpreted from Nd isotopes. Earth Planet. Sci. Lett. 192, 507-521.

[15] Garzanti, E., Vezzoli, G., Ando, S., France-Lanord, C., Singh, S. K., and Foster, G. (2004). Sand petrology and focused erosion in collision orogens: the Brahmaputra case.Earth and Planetary Science Letters,220(1), 157-174.

[16] Nakata, T. (1989). Active faults of the Himalaya of India and Nepal.Geological Society of America Special Papers,232, 243-264.

[17] Jain, A. K. and Thakur, V. C. (1978). Abor volcanics of the Arunachal Himalaya, J. Geol. Soc. India, V. 19, 335-349.

[18] Taher, M. (1986). Physiographic Frame work of North-East India: A diagnostic Survey in Spatial Pattern.North East Geographer,Vol.IX, 1 and 2.

[19] Evans, P. (1932). Tertiary succession in Assam.Trans. Min. Geol. Inst. India,27(3), 155-260.

[20] Mathur, L. P., and Evans, P. (1964). Oil in India, Int. Geol. Congr.22nd Session, New Delhi,58.

[21] Goswami, D. C. (1985). Brahmaputra River, Assam, India: Physiography, basin denudation, and channel aggradation.Water Resources Research, 21(7), 959-978.

[22] Bora, A. K. (2004). Fluvial geomorphology. InThe Brahmaputra Basin Water Resources(pp. 88-112). Springer Netherlands.

[23] Sarma, J. N. (1993, November). A study on palaeochannels from satellite imagery in a part of Upper Assam. InProc. of Nat. Symp. on Remote sensing Applications for resource Management with special emphasis on NE region, held at Guwahati,pp. 74-83.

[24] Gregory, K. J., and Walling, D.E. (1973). Drainage Basin Form and Process. Edward Arnold, London, 456pp.

[25] Barthakur, M. (2004). Weather and climate. InThe Brahmaputra Basin Water Resources. Springer Netherlands, pp. 17-23.

[26] Taxonomy, S. (1975). Soil Survey Staff.Soil Conservation Service, USDA, Agricultural Handbook, 436.

[27] Chakravarty, D. N., Sehgal, J. L., and Dev, G. (1981). Soil taxonomy of some alluvium derived soils of Assam (India).Journal of the Indian Society of Soil Science (India).

[28] Karmakar, R. M. (1985).Genesis and classification of soils of Northern Brahmaputra valley of Assam.

[29] Das, K. N., Bora, N., Bordoloi, P. K., and Sharma, P. K. (1997). Soils of rain shadow belt of central Brahmaputra valley of Assam (India)-their characterization and classification.INTERNATIONAL JOURNAL OF TROPICAL AGRICULTURE,15, 149-158.

[30] Dey, J. K., and Sehgal, J. L. (1997). Characteristics and classification of some alluvium derived paddy and associated non-paddy soils of Assam. Agropedology (India).

[31] Bhattacharyya, T., Dubey, P. N., Das, T. K., Baruah, U., Gangopadhyay, S. K., and Kumar, D. (1998). Soil formation as influenced by geomorphic processes in the Brahmaputra flood plains of Assam.Journal of the Indian Society of Soil Science,46(4), 647-651.

[32] Chakravarty, D. N., Sehgal, J. L., and Dev, G. (1978). Influence of climate and topography on the pedogenesis of alluvium-derived soils in Assam: geographical settings, morphology and physico-chemical properties [India].Indian Journal of Agricultural Chemistry (India).

[33] Bhattacharyya. D. and Sindhu, P. S. (1984). Morphology and physiochemical characteristics of some soils of Assam. J.Res.Assam agric. Univ. 5:20-29.

[34] Das, B. K., Dutta, B., Kar, S., Boruah, P., and Kar, D. (2013). Icthyofauna of Subansiri River in Assam and Arunachal Pradesh, India.International Journal of Current Research,5(11), 3314-3317.

[35] Gogoi, C., and Goswami, D. C. (2013). A study on bank erosion and bank line migration pattern of the Subansiri river in Assam using remote sensing and GIS technology.The International Journal of Engineering and Science (IJES),2, 1-6.

[36] Goswami, U., Sarma, J. N., and Patgiri, A. D. (1999). River channel changes of the Subansiri in Assam, India.Geomorphology,30(3), 227-244.

[37] Duarah, B. P., and Phukan, S. (2011). Seismic hazard assessment in the Jia Bhareli river catchment in eastern Himalaya from SRTM-derived basin parameters, India.Natural hazards,59(1), 367-381.

[38] Srinivasan, V. (2003). Stratigraphy and structure of Siwaliks in Arunachal Pradesh: A reappraisal through remote sensing technique. J. of Geological Soc. of India, 62, 139-151.

[39] Sarma, J. N. (2008). Asamar Nad-Nadi, 2nd ed. Kiran Prakashan, Dhemaji.

[40] Das, B. K. 1990. Studies on certain Ultra Surface structures And Ecobiology of Rheophilic Fish; Unpublished Ph. D. thesis, Gauhati University.

[41] Jhanwar, M. L. Shrivastava, R. N., Rajesham, T., Datta, D. R. Shrivastava, S. K., Rath, P. K. and Misra, H. (1999). Geology of the Dibang valley. In Geological studies of the Eastern Himalaya 178-189 (Ed. P.K. Verma), Pilgrims Book Pvt. Ltd. Delhi.

Chapter 5

Textural Characteristics of the Sediments of the Brahmaputra river and its Tributaries

5.1 Introduction

Sediments are mechanically and/or chemically weathered rocks; they are loose, unconsolidated materials. Compositional and textural characteristics of the initial detritus are modified by abrasion and sorting during transport, when sediments are carried away from their source area [1]. River sediments originate from the erosion of near surface, exposed igneous, metamorphic or sedimentary rocks. Some of these are easily eroded, whereas others, especially the igneous and metamorphic rocks, are affected by streams only when altered in the surface [2]. The river sediments are transported and deposited in floodplains depending on the grain size of the material taken in the alluvia (material available from various sources),on the one hand, and on environment energy (current velocity) on the other [3].

5.1.1 Textural Classification of Sediments

Composition and texture are the bases for classification of sediments and sedimentary rocks. Composition refers to the mineralogy of grains derived from other rocks

Scale	Size Range	Size Range	Aggregate Name	Other
< -8	> 256 mm	> 10.1 in	Boulder	
-6 to 8	64-256 mm	2.5-10.1 in	Cobble	
-5 to 6	32-64 mm	1.26-10.1 in	Very core gravel	Pebble
-4 to 5	16-32 mm	0.63-1.26 in	Core gravel	Pebble
-3 to 4	8-16 mm	0.31-0.63 in	Medium gravel	Pebble
-2 to 3	4-8 mm	0.157-0.31 in	Fine gravel	Pebble
-1 to 2	2-4 mm	0.079-0.157 in	Very fine gravel	Granule
0 to 1	1-2 mm	0.039-0.079 in	Very coarse sand	
1 to 0	0.5-1 mm	0.020-0.039 in	Coarse sand	
2 to 1	0.25-0.5 mm	0.010-0.020 in	Medium sand	
3 to 2	125-250 μm	0.0049-0.010 in	Fine sand	
4 to 3	62.5-125 μm	0.0025-0.0049 in	Very fine sand	
8 to 4	3.90625-62.5 μm	0.00015-0.0025 in	Silt	Mud
> 8	< 3.90625 μm	< 0.00015 in	Clay	Mud
> 10	< 1 μm	< 0.000039 in	Colloid	Mud

Table 5.1: Sediment classification based on grain size.

or to the types of grains formed at the depositional site and the mineralogy of matrix and chemical cements.

5.1.2 Grain Size Analysis

Grain size is a fundamental property of sediment particles, and influences their entrainment, transport and deposition. Therefore, grain size analysis provides important clues to the sediment provenance, transport history and depositional conditions (e.g. [4, 5, 6, 7]). Moreover it is a descriptive measure of sediment and is also commonly related to other properties (e.g. Permeability), which have major economic implications [8, 9, 10]. Hence, grain size analysis is an important aspect of sedimentological studies [11, 12].

A relation between sedimentary processes and textural responses helps in interpreting the nature of depositional environments [13]. The grain size distribution of the sediment is a function of the source material, extent and nature of weathering, erosion and transportation, and stream energy [14]. The sediments can be classified on the basis of particle size, or the diameter of individual grain of sediments. This classification is based on Φ logarithmic scale (which is Krumbein's modification of the Wentworth scale)

$$\Phi = -\log_2 \frac{D}{D_0} \tag{5.1}$$

where Φ is the Krumbein phi scale, D is the diameter of the particle and D_0 is a reference diameter. Grain size analysis discloses the texture and composition of grains in a given sample. Standard methods for grain-size analysis are based on sedimentation rates for the fine fractions and sieving for the coarse fractions [15].

Changes in statistics (mean, sorting, and skewness) describing grain-size distributions have long been used to deduce about sediment transport. The mean grain size, sorting, and skewness of a sedimentary deposit are dependent on the sediment grain size distribution of its source and the sedimentary processes of i) winnowing (erosion), ii) selective deposition of the grain size distribution in transport, and iii) total deposition of the sediment in transport [16].

Attributes of particle frequency distributions (grain size, grain volume, or settling velocity), in particular curve shapes and textural parameters, have for many decades been investigated for potential information about transport behaviour and size-sorting processes of sediments in numerous environments (e.g. [4, 17, 18, 19, 20, 13, 21, 22, 23, 24, 25, 26, 27, 28, 29]). In some cases, transport pathways are inferred from size-sorting effects observed in spatial distribution patterns of particular grain-size parameters such as mean size, sorting, skewness etc. (e.g. [30, 31]). In other cases, they are reconstructed by visual comparison of grain-size distribution curves of sediments collected along known or inferred hydrodynamic energy gradients (e.g. [23, 32]). In yet others, they are reconstructed by a mathematically derived sediment trend analyses using a variety of textural or curve shape parameters (e.g. [27, 33, 34]).

The aim of this study is to understand the grain size characteristics of the sediments of the Brahmaputra River and its tributaries. In this study we have tried to, if possible, determine the geologic significance of such parameters as skewness and

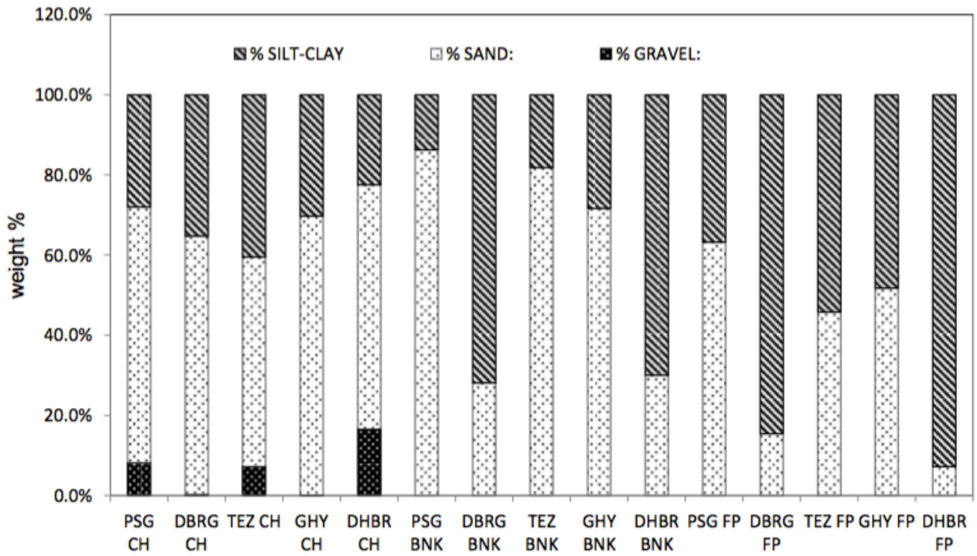

Figure 5.1: Displaying bar diagram representing the textural characteristics of bed-load, overbank and floodplain sediments of the Brahmaputra.

kurtosis by taking representative samples from 6 tributaries of Brahmaputra (3 north banks and 3 south banks). For the grain size analysis, data obtained by dry sieving and pipette method were analysed using GRADISTAT software (version 8) [7].

5.2 Results and Discussion

5.2.1 Textural properties of sediments

Rivers originating from the Himalaya orogenic belt region were characterised by the predominance of fine sand and very fine sand. The south bank tributaries bring much coarser sediments than the Himalayan rivers and were characterised by the high content of coarse- and medium-grained sand than the Himalayan rivers. The authors of [16] also argued that grain size characteristics of sediment are controlled more by the nature of the source area than by the transportation process or depositional environment.Thus, the Brahmaputra and its tributaries have their sediment textural characteristics determined by their geologically distinct drainage regions.

The grainsize distribution of the bedload, overbank and floodplain sediments along the Brahmaputra has been presented by the textural diagram in Figure 5.1 and 5.2.

Sampling locations	Samples	% Gravel	% Sand	% Slit-clay	Sample type	Textural group
Pasighat	Channel	8.2	63.8	28.0	Unimodel, very poorly sorted	Gravelly muddy sand
	Bank	0.0	86.3	13.7	Bimodal, moderately sorted	Muddy sand
	Floodplain	0.0	63.2	36.8	Trimodal, poorly sorted	Sandy mud
Dibrugarh	Channel	0.3	64.4	35.3	Unimodal, poorly sorted	Slightly gravelly muddy sand
	Bank	0.0	28.1	71.9	Bimodal, poorly sorted	Sandy mud
	Floodplain	0.0	15.4	84.6	Unimodal, poorly sorted	Mud
Tezpur	Channel	7.3	52.3	40.5	Trimodal, very poorly sorted	Gravelly muddy sand
	Bank	0.0	81.8	18.2	Unimodal, poorly sorted	Sandy mud
	Floodplain	0.0	45.8	54.2	Unimodal, poorly sorted	Mud
Guwahati	Channel	0.1	69.6	30.3	Unimodal, poorly sorted	Slightly gravelly muddy sand
	Bank	0.0	71.7	28.3	Unimodal, poorly sorted	Muddy sand
	Floodplain	0.0	51.8	48.2	Unimodal, poorly sorted	Mud
Dhubri	Channel	16.6	60.9	22.5	Bimodal, very poorly sorted	Gravelly muddy sand
	Bank	0.0	30.0	70.0	Unimodal, poorly sorted	Sandy mud
	Floodplain	0.0	7.2	92.8	Bimodal, poorly sorted	Mud

Table 5.2: % sand-silt-clay and Textural characteristics of bedload, overbank and floodplain sediments of the Brahmaputra river.

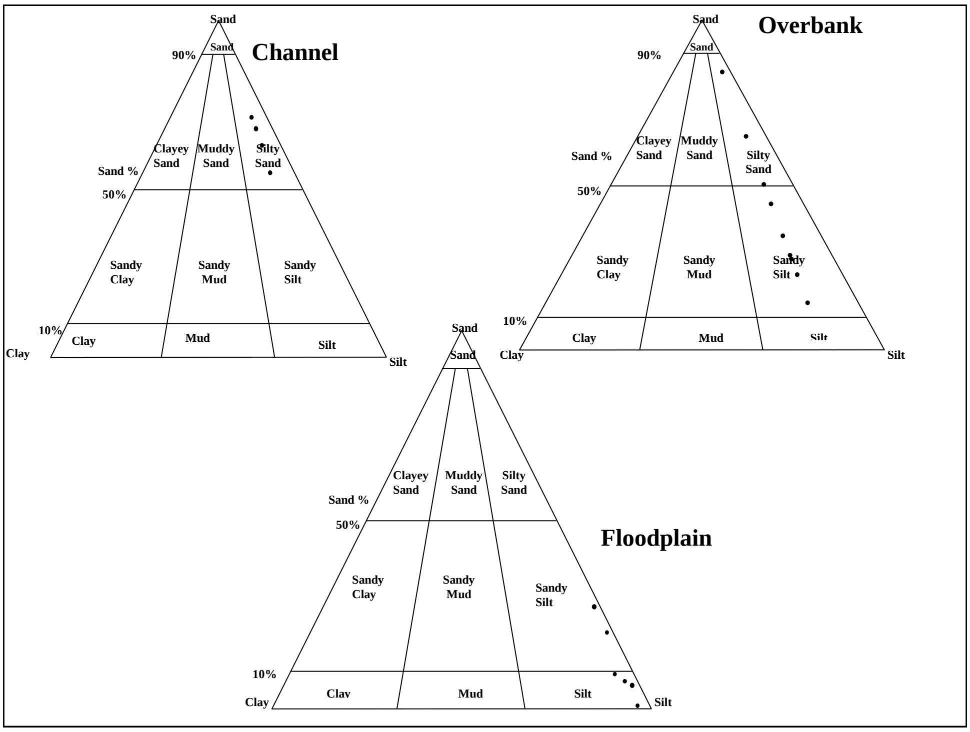

Figure 5.2: Sand-silt-clay diagram of the Brahmaputra river.

From Figure 5.1 and 5.2 we can surmise that the percentage silt-clay increased from bedload to bank to floodplain sediments. This may be due to the deposition of the finer fraction during floods and further weathering of the deposited sediments over time. But no clear downward increase of the % silt and clay (i.e. downward fining) was observed in the longitudinal profile of the river. Contribution from the tributaries may play a significant role in downstream changes in textural characteristics of the Brahmaputra River sediments.

The % silt clay in bedload was found to be almost same in all the tributaires except Subansiri (dominated by fine and very fine sand fraction-characteristic of rivers originating from the Trans-Himalaya orogenic belt region). Jiabharali (originating in the Higher Himalayas) bedload is characterised by coarse, medium and fine sand. Pagladia (originating in the Siwaliks, consisting of reworked fluvial-derived sediments) bedload is dominated by fine sand and coarse silt. Bedload in all the south bank tributaries are dominated by fine sand and coarse silt and show similar textural characteristics. The above variations clearly indicate the importance of source area in textural characteristics of the river sediments.

Figure 5.3 shows that the percentage silt-clay increases from bedload to bank to

Rivers	Samples	% Gravel	% Sand	% Slit-clay
South bank tributaries				
Burhidihing	Channel	0.0	65.6	34.4
	Bank	0.0	78.7	21.3
	Floodplain	0.0	25.2	74.8
Dikhow	Channel	0.0	100.0	0.0
	Bank	0.0	62.3	37.7
	Floodplain	0.0	37.8	62.2
Kopili	Channel	0.0	67.4	32.6
	Bank	0.0	70.0	30.0
	Floodplain	0.0	15.0	85.0
North bank tributaries				
Subansiri	Channel	0.0	98.5	1.5
	Bank	0.0	46.8	53.2
	Floodplain	0.0	47.8	52.3
Jiabharali	Channel	0.1	65.4	34.5
	Bank	0.0	47.6	52.4
	Floodplain	0.0	60.5	39.5
Pagladia	Channel	0.3	67.1	32.6
	Bank	0.0	11.7	88.3
	Floodplain	0.0	46.4	53.6

Table 5.3: % sand-silt-clay of the tributaries.

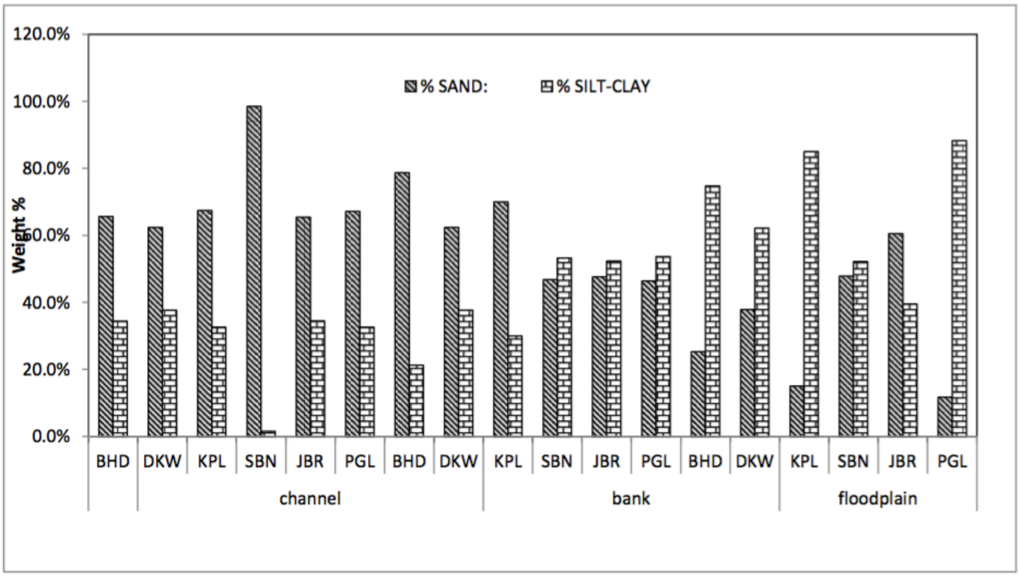

Figure 5.3: % sand-silt-clay of the channel, bank and floodplain sediments of the tributaries.

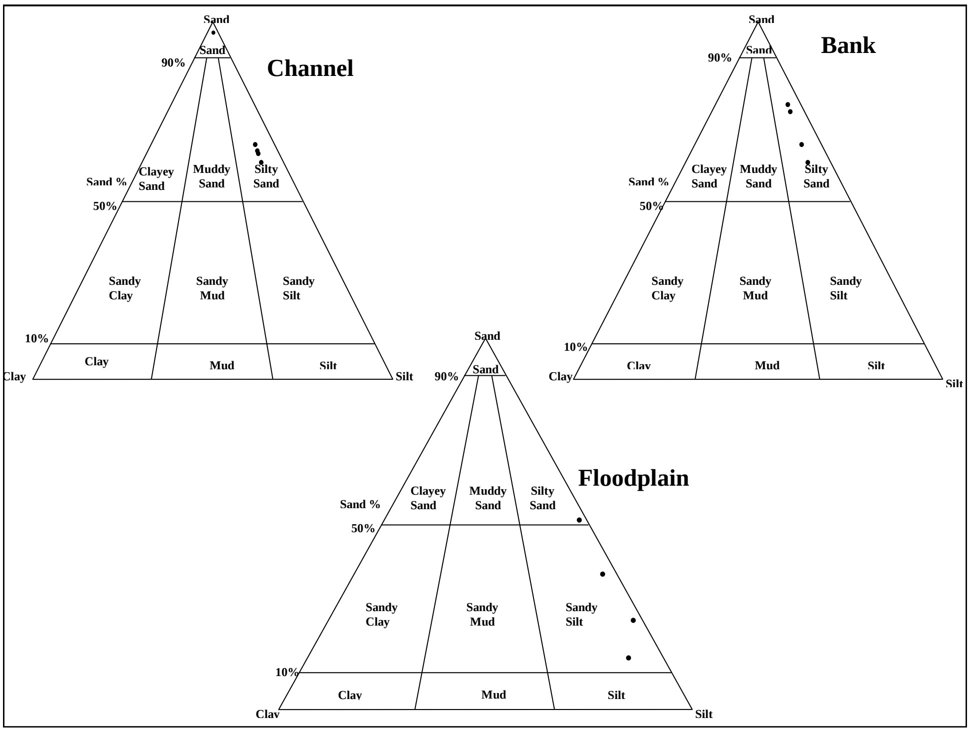

Figure 5.4: Sand-silt-clay diagram of the south bank tributaries.

Locations	Samples	Sample type	Textural group	Sediment class
South bank tributaries				
Burhidihing	Channel	Bimodal, very poorly sorted	Muddy sand	Very coarse silty, very fine sand
	Bank	Bimodal, poorly sorted	Muddy sand	Very coarse silty, very fine sand
	Floodplain	Trimodal, poorly sorted	Sandy mud	Very fine sandy, very coarse silt
Dikhow	Channel	Unimodal, well sorted	Muddy sand	Well sorted medium sand
	Bank	Unimodal, poorly sorted	Muddy sand	Fine silty, very fine sand
	Floodplain	Unimodal, poorly sorted	Sandy mud	Very fine sandy, very coarse silt
Kopili	Channel	Bimodal, poorly sorted	Muddy sand	Medium silty, very fine sand
	Bank	Bimodal, poorly sorted	Muddy sand	Fine silty, very fine sand
	Floodplain	Unimodal, poorly sorted	Sandy mud	Very fine sandy, very coarse silt
North bank tributaries				
Subansiri	Channel	Bimodal, moderately well sorted	Sand	Moderately well sorted, very fine sand
	Bank	Unimodal, poorly sorted	Sandy mud	Very fine sandy, coarse silt
	Floodplain	Trimodal, very poorly sorted	Sandy mud	Fine sandy medium silt
Jiabharali	Channel	Bimodal, very poorly sorted	Slightly gravelly muddy sand	Slightly very fine gravelly coarse silty coarse sand
	Bank	Bimodal, poorly sorted	Sandy mud	Very fine sandy, coarse silt
	Floodplain	Bimodal, poorly sorted	Muddy sand	Very coarse silty, fine sand
Pagladia	Channel	Trimodal, poorly sorted	Slightly gravelly muddy sand	Slightly very fine gravelly very coarse silty very fine sand
	Bank	Bimodal, very poorly sorted	Sandy mud	Very fine sandy, very coarse silt
	Floodplain	Trimodal, poorly sorted	Sandy mud	Very fine sandy medium silt

Table 5.4: % sand-silt-clay of the tributaries.

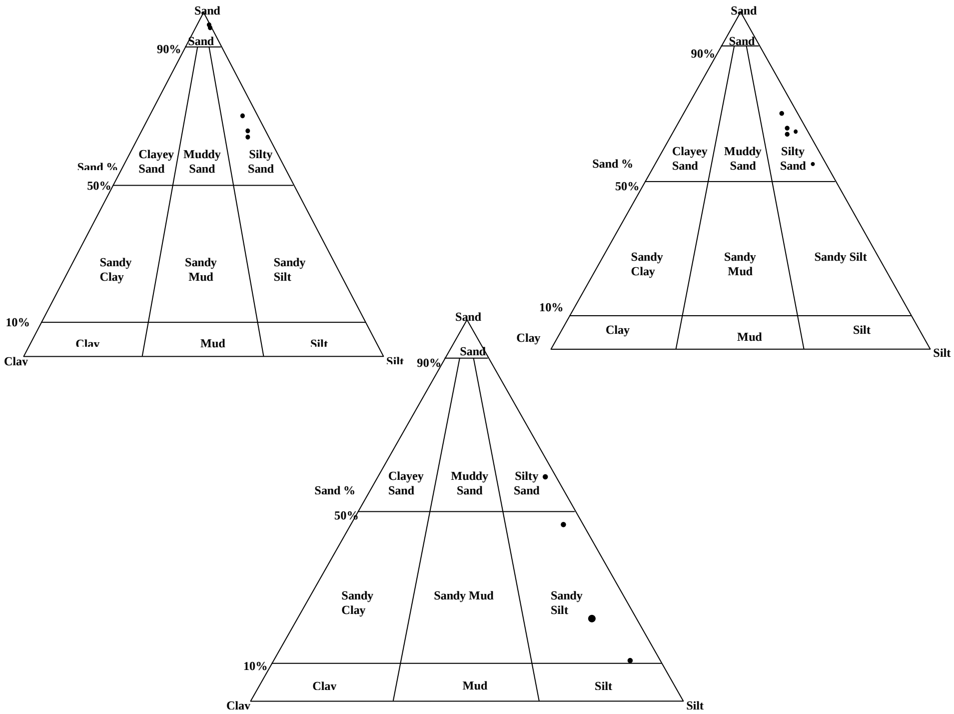

Figure 5.5: Sand-silt-clay diagram of the north bank tributaries.

floodplain sediments. This may be due to the deposition of the finer fraction during floods and further weathering of the deposited sediments over time.

5.2.2 Grain size parameters

Table 5.5 displays these grain size parameters of the bedload , bank and floodplain sediments of the Brahmaputra River, which are discussed in following sections.

The variation of the mean grain diameter of sediments along the Brahmaputra river and its tributaries

The reduction of the mean grain diameter of bed load particles according to the transport distance, a widely used concept in sedimentology [35, 36, 37, 38] is not valid along the course of the Brahmaputra. This may be due to the countless sources, mainly tributary rivers, which introduce into the system particles whose sizes frequently differ from those in the Brahmaputra's riverbed upstream the point of confluence. The mean size range variation of the channel remains small (fine to very fine sand; ϕ=2.274 to ϕ= 3.971) throughout the course except a small decrease at Dibrugarh (coarse silt; ϕ=4.120 to ϕ= 4.213). Even in the floodplain the mean size range variation is small (medium to fine silt; ϕ=5.065 to ϕ= 6.335) unlike the

Locations	Samples	Mean	Sorting	Skewness	Kurtosis	Description			
		(ϕ)	(σ)	(S_K)	(K_G)	Mean	Sorting	Skewness	Kurtosis
Pasighat	Channel	3.183-3.198	2.454-2.534	0.075-0.082	1.197-1.201	Very fine sand	Very poorly sorted	Symmetrical	Leptokurtic
	Bank	3.426-5.317	0.893-1.539	0.121-0.371	0.682-2.890	Very fine sand-coarse silt	Moderately sorted	Very fine skewed	Platykurtic
	Flood-plain	5.065-5.021	0.763-1.602	0.18-0.173	1.116-1.121	Coarse silt	Moderately sorted	Fine skewed	Leptokurtic
Dibrugarh	Channel	4.120-4.213	1.603-1.694	0.584-0.602	0.922-0.967	Very coarse silt	Poorly sorted	Very fine skewed	Mesokurtic
	Bank	5.633-5.761	1.483-1.532	-0.056-(-0.032)	0.832-0.867	Coarse silt	Poorly sorted	Symmetrical	Platykurtic
	Flood-plain	5.834-5.856	0.983-1.345	0.078-0.081	0.912-0.996	Medium silt	Moderately sorted	Symmetrical	Mesokurtic
Tezpur	Channel	3.347-3.365	2.843-2.898	0.017-0.023	0.871-0.883	Very fine sand	Very poorly sorted	Symmetrical	Platykurtic
	Bank	3.967-4.866	1.516-1.733	0.489-0.497	0.732-0.786	Very coarse silt	Poorly sorted	Very fine skewed	Platykurtic
	Flood-plain	6.013-6.213	0.863-1.024	0.186-0.214	1.112-1.116	Medium silt	Moderately sorted	Fine skewed	Mesokurtic
Guwahati	Channel	3.971-4.012	1.550-1.662	0.601-0.689	1.100-1.121	Very fine sand	Poorly sorted	Very fine skewed	Mesokurtic
	Bank	4.631-5.239	1.543-1.925	-0.163-(-0.01)	0.760-0.960	Very coarse silt	Poorly sorted	Very fine skewed to coarse skewed	Platykurtic to mesokurtic
	Flood-plain	6.335-6.246	0.765-1.431	0.068-0.078	1.022-1.018	Medium silt	Moderately sorted	Symmetrical	Mesokurtic
Dhubri	Channel	2.274-2.296	2.732-2.788	0.021-0.034	0.733-0.786	Fine sand	Very poorly sorted	Symmetrical	Platykurtic
	Bank	5.032-5.290	1.546-1.828	0.045-0.132	0.687-0.849	Coarse silt	Poorly sorted	Fine skewed to symmetrical	Platykurtic
	Flood-plain	5.828-6.201	0.689-1.513	0.179-0.201	0.819-0.864	Coarse silt	Moderately sorted	Fine skewed	Platykurtic

Table 5.5: Summary of the ranges and average values for the [4] grain size parameters in channel, bank and floodplain sediments of the Brahmaputra river.

Locations	Samples	Mean	Sorting	Skewness	Kurtosis	Description			
		(ϕ)	(σ)	(S_K)	(K_G)	Mean	Sorting	Skewness	Kurtosis
Burhi-Dihing	Channel	3.716-3.731	2.128-2.154	0.138-0.152	1.060-1.247	Very fine sand	Very poorly sorted	Fine skewed	Leptokurtic
	Bank	3.188-3.240	1.819-1.953	0.112-0.128	1.164-1.184	Very fine sand	Poorly sorted	Fine skewed	Leptokurtic
	Flood-plain	4.841-5.080	1.549-2.071	0.363-0.603	0.787-1.053	Coarse silt	Poorly sorted	Very fine skewed	Mesokurtic
Dikhow	Channel	2.018-2.176	0.439-0.657	0.071-0.112	0.883-0.983	Fine sand	Well sorted	Symmetrical	Mesokurtic
	Bank	4.201-4.404	1.321-1.345	0.662-0.821	0.895-0.934	Very coarse silt	Poorly sorted	Very fine skewed	Platykurtic
	Flood-plain	5.054-5.213	1.667-1.532	0.523-0.623	0.916-0.998	Coarse silt	Poorly sorted	Very fine skewed	Mesokurtic
Kopili	Channel	4.157-4.123	1.431-1.690	0.320-0.365	1.212-1.493	Very coarse silt	Poorly sorted	Very fine skewed	Leptokurtic
	Bank	4.081-4.121	1.580-1.690	0.319-0.327	1.345-1.518	Very coarse silt	Poorly sorted	Very fine skewed	Very leptokurtic
	Flood-plain	5.388-5.879	1.800-2.871	0.578-0.643	1.208-1.341	Coarse silt	Poorly sorted	Very fine skewed	Leptokurtic
Subansiri	Channel	2.909-2.932	0.507-0.510	-0.496	0.616-0.630	Fine sand	Moderately well sorted	Very coarse skewed	Very platykurtic
	Bank	4.664-4.678	1.842-1.896	0.247-0.253	0.876-0.897	Very coarse silt	Poorly sorted	Fine skewed	Platykurtic
	Flood-plain	4.632-4.645	2.084-2.098	0.403-0.412	0.729-0.732	Very coarse silt	Very poorly sorted	Very fine skewed	Platykurtic
Jia-Bharali	Channel	3.221-3.423	2.619-2.513	0.097-0.089	0.667-0.678	Very fine sand	Very poorly sorted	Symmetrical	Very platykurtic
	Bank	4.617-4.612	1.862-1.892	0.254-0.345	0.865-0.897	Very coarse silt	Poorly sorted	Fine skewed	Platykurtic
	Flood-plain	4.105-4.101	1.870-1.888	0.669-0.674	1.017-1.112	Very coarse silt	Poorly sorted	Very fine skewed	Mesokurtic
Pagladia	Channel	3.656-3.989	1.427-1.911	0.326-0.599	0.846-2.080	Very fine sand	Poorly sorted	Very fine skewed	Platykurtic
	Bank	4.477-4.482	2.014-2.008	0.134-0.146	0.772-0.786	Very coarse silt	Very poorly sorted	Fine skewed	Platykurtic
	Flood-plain	6.296-6.121	1.803-1.823	-0.091	0.693-0.702	Medium silt	Poorly sorted	Symmetrical	Platykurtic

Table 5.6: Summary of the ranges and average values for the [4] grain size parameters in channel, bank and floodplain sediments of the tributaries.

overbank sediment which showed a wide range of variation in mean grain diameter (very fine sand to medium silt; ϕ=3.347 to ϕ= 5.761).

The mean grain size values in the bedload of the south bank tributaries are slightly more than north bank tributaries. The mean grain size decreases from bedload to overbank to floodplain sediments.

Variations in sorting degree and skewness values

In specialised literature [35, 37] fluvial deposits are regarded as poorly sorted deposits and their skewness is usually positive since the material is introduced through deposits of solid suspensions. Analyses of standard deviation and skewness values along the course of the of Brahmaputra reveals that in many channel sediment samples standard deviation values indicate a poor to very poor sorting, normal for a fluvial environment, and that skewness is symmetrical to slightly positive. In the vicinity of the banks standard deviation has lower values due to the disappearance of coarser elements, but sorting still remains in the "very poor" domain. The bank sediments however numerous standard deviation values which place them in the poorly to moderate sorting categories and skewness values (positive to negative skewness to symmetry categories). Sorting values decreases from bank (poorly sorted) to floodplain sediments (moderately sorted), due to the higher percentage of finer particles in their composition.

In the tributaries the sediments are poorly sorted except Subansiri (well-sorted, with the predominance of fine and very fine sands and negative skewness suggesting high environment energy of deposition). The south bank tributaries showed more positive skewness than the north bank tributaries (except Pagladia which showed positive skewness) indicating the excess of fine material in the composition of sediments of these rivers.

Variations in kurtosis

The author of [39] suggested that the extreme high or low values of kurtosis imply that part of sediment achieved its sorting elsewhere in high-energy environment. Variation in the kurtosis values is a reflection of the flow characteristic of the depositing medium [40, 41], and the dominance of finer size of platykurtic nature of sediments reflects the maturity of the sand.The channel sediments in the Brahmaputra were mostly platykurtic and mesokurtic. The channel sediments in the north bank tributaries were platykurtic whereas the south bank tributaries were leptokurtic suggesting their different origins.

5.3 Conclusion

In this study we found that the Brahmaputra River tributaries play a significant role in downstream changes in textural characteristics of the Brahmaputra River sediment. Analyses of standard deviation and skewness values along the course of the of Brahmaputra reveals that in many channel sediment samples standard deviation values indicate a poor to very poor sorting, normal for a fluvial environment, and that skewness is symmetrical to slightly positive. In the vicinity of the banks standard deviation has lower values due to the disappearance of coarser elements, but sorting still remains in the ”very poor” domain. The bank sediments however numerous standard deviation values which place them in the poorly to moderate sorting categories and skewness values (positive to negative skewness to symmetry categories). Rivers originating from the Himalaya orogenic belt region are characterised by the predominance of fine sand and very fine sand whereas the south bank tributaries bring much coarser sediments than the Himalayan rivers and are characterised by the high content of coarse- and medium-grained sand. Percentage silt-clay increases from bedload to bank to floodplain sediments. This may be due to the deposition of the finer fraction during floods and further weathering of the deposited sediments over time. The textural parameters clearly indicate the importance of source area in textural characteristics of river sediments.

Bibliography

[1] Johnsson, M. J., and Meade, R. H. (1990). Chemical weathering of fluvial sediments during alluvial storage: The Macuapanim Island point bar, Solimoes River, Brazil.Journal of Sedimentary Research,60(6).

[2] Joshua, E. O., and Oyebanjo, O. A. (2010). Grain-size and heavy mineral analysis of River Osun sediments.Australian Journal of Basic and Applied Sciences,4(3), 498-501.

[3] Opreanu, G., Oaie, G., and PauN, F. (2007). The dynamic significance of the grain size of sediments transported and deposited by the Danube.Geo-Eco-Marina Coastal Zone Processes and Management. Environmental Legislation,13, 111-119.

[4] Folk, R. L., and Ward, W. C. (1957). Brazos River bar: a study in the significance of grain size parameters.Journal of Sedimentary Research,27(1).

[5] Friedman, G. M. (1979). Differences in size distributions of populations of particles among sands of various origins: addendum to IAS Presidential Address.Sedimentology, 26(6), 859-862.

[6] Lindholm R. (1987). A Practical Approach to Sedimentology. Allen and Unwin, London.

[7] Blott, S. J., and Pye, K. (2001). GRADISTAT: a grain size distribution and statistics package for the analysis of unconsolidated sediments.Earth surface processes and Landforms,26 (11), 1237-1248.

[8] McManus, J. (1988). Grain size determination and interpretation.Techniques in sedimentology,408, 63-85.

[9] Tucker, M. E. (1991). Sedimentary Petrology: Blackwell Science.

[10] Pell, S. D., Chivas, A. R., and Williams, I. S. (2000). The Simpson, Strzelecki and Tirari Deserts: development and sand provenance.Sedimentary Geology,130 (1), 107-130.

[11] Pye, K. and Tsoar, H. (1990). Aeolian sand and sand dunes. London: Unwin Hyman.

[12] El-Sayed, M. I. (1999). Sedimentological characteristics and morphology of the aeolian sand dunes in the eastern part of the UAE, a case study from Ar Rub'Al Khali.Sedimentary Geology,123 (3), 219-238.

[13] Visher, G. S. (1969). Grain size distributions and depositional processes.Journal of Sedimentary Research, 39 (3).

[14] Pandey, S. K., Singh, A. K., and Hasnain, S. I. (2002). Grain-size distribution, morphoscopy and elemental chemistry of suspended sediments of Pindari Glacier, Kumaon Himalaya, India.Hydrological sciences journal,47 (2), 213-226.

[15] Gee, G. W., and Bauder, J. W. (1986). Particle-size analysis.Methods of soil analysis: Part 1: Physical and mineralogical methods, (methodsofsoilan1), 383-411.

[16] McLaren, P. (1981). An interpretation of trends in grain size measures.Journal of Sedimentary Research,51 (2).

[17] Mason, C. C., and Folk, R. L. (1958). Differentiation of beach, dune, and aeolian flat environments by size analysis, Mustang Island, Texas.Journal of Sedimentary Research,28 (2).

[18] Friedman, G. M. (1961). Distinction between dune, beach, and river sands from their textural characteristics.Journal of Sedimentary Research,31 (4), 514-529.

[19] Spencer, D. W. (1963). The interpretation of grain size distribution curves of clastic sediments.Journal of Sedimentary Research,33 (1).

[20] Tanner, W. F. (1964). Modification of sediment size distributions.Journal of Sedimentary Research,34 (1).

[21] Van Andel, T. H. (1973). Texture and dispersal of sediments in the Panama Basin.The Journal of Geology,81 (4), 434-457.

[22] Reed, W. E., Le Fever, R., and Moir, G. J. (1975). Depositional environment interpretation from settling-velocity (Psi) distributions.Geological Society of America Bulletin,86 (9), 1321-1328.

[23] Bein, A., and Sass, E. (1978). Analysis of log-probability plots of recent Atlantic sediments and its analogy with simulated mixtures.Sedimentology,25 (4), 575-581.

[24] Taira, A., and Scholle, P. A. (1979). Discrimination of depositional environments using settling tube data.Journal of Sedimentary Research,49 (3), 787-799.

[25] Clark, M. W. (1981). Quantitative shape analysis: a review.Mathematical Geology,13 (4), 303-320.

[26] Sly, P. G., Thomas, R. L., Pelletier, B. R. (1983). Interpretation of moment measures derived from water-lain sediments.Sedimentology,30 (2), 219-233.

[27] McLaren, P., and Bowles, D. (1985). The effects of sediment transport on grain-size distributions.Journal of Sedimentary Research,55 (4).

[28] Flemming, B. W. (1988). Process and pattern of sediment mixing in a microtidal coastal lagoon along the west coast of South Africa.Tide-influenced sedimentary environments and facies. D Reidel, Dordrecht, 275-288.

[29] SyvitskiJ. P. M. (ed.) (1991). Principles, Methods, and Application of Particle Size Analysis. Cambridge, New York, Port Chester, Melbourne, Sydney: Cambridge University Press.

[30] Flemming, B. W. (1988). Process and pattern of sediment mixing in a microtidal coastal lagoon along the west coast of South Africa.Tide-influenced sedimentary environments and facies. D Reidel, Dordrecht, 275-288.

[31] Flemming, B. W., and Ziegler, K. (1995). High-resolution grain size distribution patterns and textural trends in the backbarrier environment of Spiekeroog Island (southern North Sea).Senckenbergiana maritima,26 (1), 1-24.

[32] Bartholoma, A., and Flemming, B. W. (2007). Progressive grain-size sorting along an intertidal energy gradient.Sedimentary Geology,202 (3), 464-472.

[33] Hartmann, D., and Bowman, D. (1993). Efficiency of the Log-Hyperbolic Distribution: A Case Study: Pattern of Sediment Sorting in a Small Tidal-Inlet: Het Zwin, The Netherlands.Journal of coastal research, 1044-1053.

[34] Le Roux, J. P. (1994). An alternative approach to the identification of net sediment transport paths based on grain-size trends.Sedimentary Geology,94 (1-2), 97-107.

[35] Parker, G. (1991). Selective sorting and abrasion of river gravel. I: Theory.Journal of Hydraulic Engineering,117 (2), 131-147.

[36] Paola, C., Parker, G., Seal, R., Sinha, S. K., Southard, J. B., and Wilcock, P. R. (1992). Downstream fining by selective deposition in a laboratory flume.SCIENCE-NEW YORK THEN WASHINGTON-,258, 1757-1757.

[37] Pizzuto, J. E. (1995). Downstream fining in a network of gravel-bedded rivers.Water Resources Research,31 (3), 753-759.

[38] Gasparini, N. M., Tucker, G. E., and Bras, R. L. (1999). Downstream fining through selective particle sorting in an equilibrium drainage network.Geology,27 (12), 1079-1082.

[39] Friedman, G. M. (1962). On sorting, sorting coefficients, and the lognormality of the grain-size distribution of sandstones.The Journal of Geology,70 (6), 737-753.

[40] Ray, A. K., Tripathy, S. C., Patra, S., and Sarma, V. V. (2006). Assessment of Godavari estuarine mangrove ecosystem through trace metal studies. Environ Int 32:219-223.

[41] Baruah, J., Kotoky, P. and Sarma, J. N. (1997). Textural and geochemical study on river sediments: a case study on the Jhanji River, Assam. J. Indian Assoc. Sedimento., 16:195-206.

Chapter 6

Mineralogy of the sediments of the Brahmaputra river and its Tributaries

6.1 Introduction

Minerals in ancient time were categorised as any natural substance which is inorganic in nature and later in twentieth century these were defined as a chemical compound that is normally crystalline and formed by geological process. In geology, mineral means the basic building blocks from that the entire earth crust has formed. The minerals, in natural environment decompose chemically releasing soluble materials and synthesise new minerals either by minor chemical alterations or by complete chemical breakdown of original mineral [1]. In addition to their utility in determining sediment provenance (e.g., [2, 3]), mineralogical studies are also valuable in understanding past weathering regimes induced by changing climatic conditions (e.g., [4, 5]). Clay mineralogy studies of the Bengal Fan have been prompted by recent interest in Cenozoic climate change, providing researchers with long-term records of Neogene climate and Himalayan uplift [6, 4, 7]. The chemical weathering in a basin can also be gauged from the change in mineralogy and chemical composition of sediments along the river course. Sediment composition can be modified by a number of processes occurring during erosion, transport, recycling, and diagenesis [8].

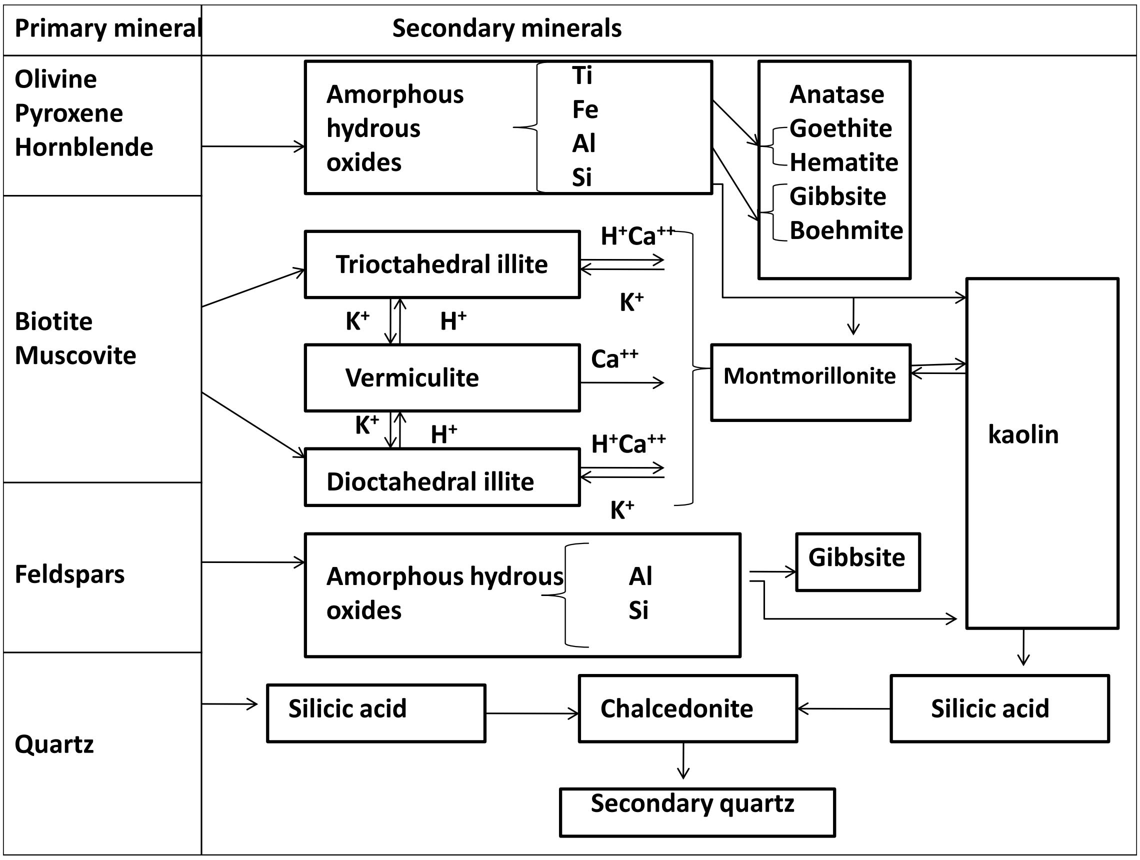

Figure 6.1: Weathering of primary rock-forming minerals (after [9]).

This chapter deals with mineralogy of Brahmaputra River and its tributaries and attempts to use clay mineralogy to elucidate weathering conditions in the river basins. The Brahmaputra and its tributaries have distinctive mineralogies which result from geologically distinct source areas. It drains the Tibetan Plateau of China and is dominated by upland tributaries originating in the Himalayas. The Brahmaputra flows through various rock types including Precambrian metamorphics (high-grade schists, gneisses, quartzites, metamorphosed limestones), felsic intrusives, and Paleozoic-Mesozoic sandstones, shales and limestones [10].The Brahmaputra is dominated by upland tributaries originating in the Himalayas. Five locations along the Brahmaputra were sampled (channel, overbank and floodplain) before and after the confluence of the major tributaries (Burhidihing, Dikhow, Kopili, Subansiri, Jiabharali and Pagladia) from the Himalaya and the Indian shield draining the Assam plains were sampled. The bulk mineralogy of channel and overbank and floodplain

Locations	Channel	Overbank	Floodplain
Pasighat	Qtz, ortho, oligo, musco, horn, micro, chl	Qtz, ortho, oligo, micro, horn, musco, chl, bio, cal, dol	Qtz, ortho, bio, musco, horn, chl
Dibrugarh	Qtz, ortho, oligo, musco, horn, micro, chl	Otz, ortho, oligo, musco, horn, micro, chl, bio, cal, dol	Qtz, musco, plagio, ortho, horn, chl, cal
Tezpur	Qtz, ortho, plagio, bio, chl	Qtz, ortho, plagio, musco, chl, horn, cal, dol	Qtz, ortho, bio, musco, horn, chl
Guwahati	Qtz, ortho, plagio, musco, chl	Qtz, ortho, plagio, musco, chl, horn, cal, dol	Qtz, ortho, bio, musco, horn, chl
Dhubri	Qtz, ortho, plagio, musco, chl	Qtz, ortho, musco, chl	Qtz, ortho, bio, musco, horn, chl

Table 6.1: Mineralogy of channel ,overbank and floodplain sediments of the Brahmaputra. Qtz ≡ Quartz, ortho ≡ orthoclase, plagio ≡ plagioclase, Musco ≡ Muscovite, bio ≡ biotite, horn ≡ hornblende, chl ≡ Chlorite, dol ≡ Dolomite, cal ≡ Calcite, micro ≡ microcline, apa ≡ apatite, oligo ≡ oligoclase.

sediment were done using X-Ray Diffractometer (Philips EXPERT) at JNU, New Delhi. Sediment samples ground to 200 mesh size and were used for the mineralogical studies to decipher the mineral assemblages. The minerals in the samples were identified using X-ray diffractogram of the samples with specified d spacing and 2θ values by comparing it with the values given in reference database [11, 12]. For clay mineralogical analysis, slides were prepared by drop on slide technique [13]. The samples were untreated, glycolated, heated at 400° C and 550° C and run on Philips X-ray Diffractometer using CuK- radiation and Ni-filter. The accelerating voltage kept 45 kV along with tube current of 40 mA. The scanning was done at 1 degree 2θ per minute for sediments and 0.5 degrees 2θ per minute for clay mineralogy.

6.2 Results and Discussion

6.2.1 Mineralogical compositions of the sediments in the Brahmaputra river

1. Mineral abundance both in channel and overbank sediments was found to be:

$$\text{Quartz} > \text{feldspar} > \text{mica} > \text{amphibole}$$

Rivers	Channel	Bank	Floodplain	
			Old	New
Dikhow	Qtz, ortho, plagio, micro, chl, musco	Qtz, ortho, plagio, micro, chl, musco	Qtz, micro, chl	Qtz, micro, chl
Kopili	Qtz, plagio=ortho, musco, chl	Qtz, ortho, oligo, horn, micro, musco, chl, kya	Qtz, micro, chl	Qtz, micro, chl
Burhi-Dihing	Qtz, ortho, musco, chl	Qtz, ortho, musco, chl	Qtz, ortho, bio, chl	Qtz, ortho, bio, chl=musco
Jia-Bharali	Qtz, ortho, plagio, musco, micro, chl	Qtz, ortho, plagio, bio, musco, horn, chl	Qtz, musco, ortho= plagio, horn, chl	Qtz, ortho, musco, chl, horn
Subansiri	Qtz, ortho, oligo, musco, chl	Qtz, ortho, plagio, bio, musco, chl= horn, dol	Qtz, ortho, musco, chl	Qtz, ortho, musco, chl
Pagladia	Qtz, albite=oligo, micro, musco=chl	Qtz, ortho-plagio, bio, musco, chl	Qtz, ortho, musco, chl	Qtz, ortho, musco, chl

Table 6.2: Mineralogy of channel ,overbank and floodplain sediments of the tributaries. Qtz ≡ Quartz, ortho ≡ orthoclase, plagio ≡ plagioclase, Musco ≡ Muscovite, bio ≡ biotite, horn ≡ hornblende, chl ≡ Chlorite, dol ≡ Dolomite, cal ≡ Calcite, micro ≡ microcline, apa ≡ apatite, oligo ≡ oligoclase.

Brahmaputra sediments reflect higher abundance of plagioclase, amphibole and apatite than Ganga sediments as reported by [8]. The plagioclase seemed to be is largely preserved in the Brahmaputra channel from upstream (Pasighat) to downstream Dhubri (Figure 6.2). There is thus no indication of selective destruction of plagioclase with respect to the more stable K-feldspar which indicates that the sediments are transported by physical erosion. Dolomite and calcite (carried not only by the Tsangpo draining arid Tibet but also by major Himalayan and Mishmi rivers including the Siang, Dibang, Lohit, and Manas) are lacking in Brahmaputra channel indicating complete dissolution. Brahmaputra overbank sediments contain some dolomite and very little calcite in the upstream locations which are lacking in the downstream locations due to dissolution of calcite. Chlorite inspite of its low stability is present in sediments in all locations indicating less alteration of minerals during transport. More abundance of muscovite than biotite at downstream locations indicates strong hydrolysis in the catchment as biotite is more weatherable than muscovite [16].

Rivers	This study			Singh et al 2005 [14]	Kotoky et al 2006 [15]
	Bank	New fp	Old fp		
Dikhow	Chl $\gg$ smec, kao	Chl > ill > smec			
Kopili	Kao $\gg$ chl > smec	Kao $\gg$ ill > mont, chl	Kao $\gg$ ill > mont, chl	Mont, ill, chl	
Burhidihing	Kao > chl > smec	Chl = kao > ill	ill > chl > kao		
Jiabharali	ill > chl $\gg$ smec/mont	ill > chl > smec/mont	ill > chl > smec/mont		
Subansiri	ill > chl > smec/mont	chl > ill > smec/mont	kao > ill > smec/mont	vermi, ill, mont	
Pagladia	ill $\gg$ chl	ill $\gg$ chl > smec	ill > chl > smec		
Pasighat	ill > chl	ill > chl $\gg$ kao > mon/smec			kao, ill, chl
Dibrugarh	ill > chl, smec	ill > chl $\gg$ kao > mon/smec	ill > chl $\gg$ kao > mon/smec	vermi, ill, chl	kao, ill, chl
Tezpur	ill > chl > kao > smec	ill > chl $\gg$ kao > smec	ill > chl $\gg$ kao > mon/smec	vermi, ill, chl	kao, ill, chl
Guwahati	ill > chl > kao > smec	ill > chl $\gg$ kao > smec	ill > chl > kao > mon/smec	vermi, ill, chl	kao, ill, chl
Dhubri	ill > chl > kao > smec	ill > chl $\gg$ kao > smec	ill > chl $\gg$ kao > mon/smec		kao, ill, chl

Table 6.3: Clay Mineralogy of floodplain sediments of Brahmaputra and its tributaries. Ill ≡ illite, chl ≡ Chlorite, kao ≡ kaolinite, smec ≡ smectite, mont ≡ monmorillonite, vermi ≡ vermiculite.

2. Floodplain mineralogy:

$$\text{quartz} > \text{mica} > \text{feldspar} > \text{amphibole}$$

The floodplain soils were not much weathered as seen from the mineralogy results in Table 6.2 which indicates the younger age of the floodplain and tectonic activities in the basin. The floodplain sediments contain very little dolomite. Muscovite prevails over biotite and chlorite as a result of some insitu weathering after deposition in the floodplains.

3. Clay mineralogy in the sediments:

Presence of different types of clays indicates the physico-chemical conditions operating within the system. Weathering of alkali feldspar under acidic condition produces

Sample	Smectite (%)	Illite (%)	Kaolinite (%)	Chlorite (%)
Pasighat	9.12	50.36	0.00	40.53
Pasighat	8.47	50.19	0.00	41.34
Dibrugarh	6.57	49.29	15.55	28.59
Dibrugarh	8.77	50.78	12.48	27.97
Tezpur	7.43	58.38	10.79	23.40
Guwahati	7.87	55.67	18.80	18.80
Dhubri	7.32	57.10	22.70	12.99
Subansiri	7.76	42.04	0.00	50.19
Pagladia	2.23	80.78	0.00	16.99
Jiabharali	3.24	73.60	0.00	23.16
Dikhow	4.08	43.14	18.10	34.67
Kopili	5.18	29.83	64.99	0.00
Burhidihing	9.39	40.78	27.42	22.42

Table 6.4: Relative abundance of clay minerals in sediments of the Brahmaputra and the tributaries.

mainly the kaolinite group without any exchangeable cations, whereas illite and chlorite are developed by alteration of mica, alkali feldspars, biotite, etc. under alkaline conditions.

The Brahmaputra is characterised by the presence of significant amount of illite and chlorite(50% and 32% respectively in our study) indicating erosion from relatively unweathered granitic or metamorphic terrain of the Himalayas. The authors of [17] also reported that illite and chlorite are higher in Brahmaputra than the Ganges (60% vs 42% and 17% vs 7% respectively), which results from the dominance of Himalayan tributaries in the Brahmaputra. This is also supported by high illite and chlorite concentration found in the Himalayan tributaries (Table 6.4).

In addition, Brahmaputra has higher abundances of kaolinite(also reported by [15]) than the Ganges (18% vs 4% respectively; [17]) which may be due to contribution from the south bank tributaries. The authors of [18] highlighted the decrease in chlorite content with an increase of kaolinite downstream of a river which can also

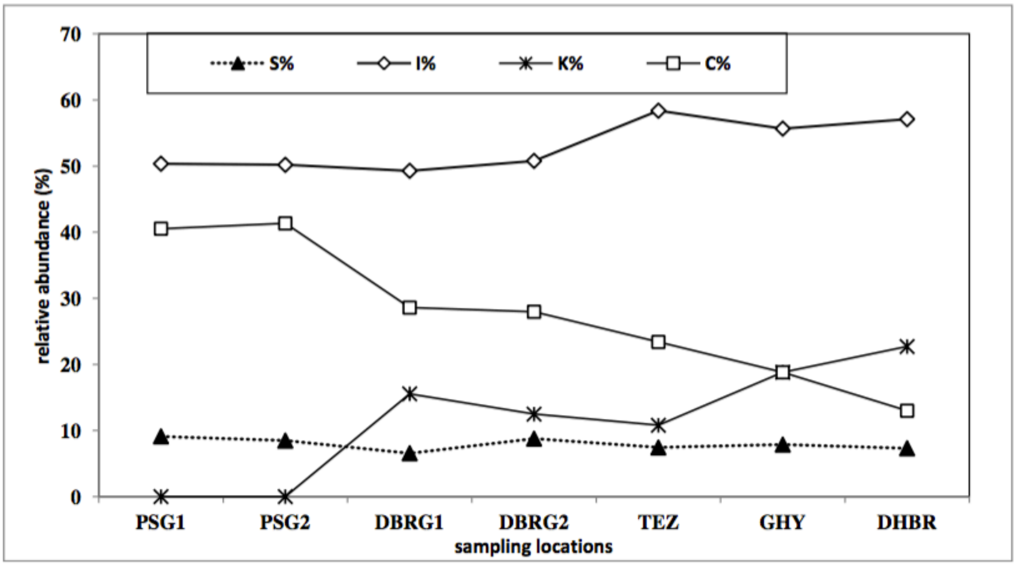

Figure 6.2: Downstream variation in abundances of clay minerals in overbank sediments along Brahmaputra(S-smectite ; I-illite; K-kaolinite; C-chlorite). PSG ≡ Pasighat, DBRG ≡ Dibrugarh, SBR ≡ Subansiri, TEZ ≡ Tezpur, GHY ≡ Guwahati, DHBR ≡ Dhubri.

be observed in our study (Figure 6.2)

6.2.2 Mineralogy of the sediments in the tributaries

Though the mineralogy of the sediments in all the tributaries were found to be same yet the north bank tributaries contains more micaceous minerals (biotite, muscovite) than the south bank tributaries. This may be due to the dominance of phyllites and micaceous minerals in the source rocks of the north bank tributaries.There are traces of dolomite in Subansiri sands not present in Jiabharali and Pagladia which may be derived from its trans-Himalayan source. Biotite is absent in the south bank tributaries which may be indication of its source or hydrolysis of biotite due to intense weathering. Muscovite prevails over biotite and chlorite in the floodplain sediments which may be due to insitu weathering.

Abundance of clay minerals in the tributaries

North bank tributaries: ill $\gg$ chl > smec

South bank tributaries: kao $\gg$ chl > ill > smec

In the southern tributaries, where the clay content is higher indicating chemical weathering is high (also confirmed from CIA results in chapter 7). Strong mechanical abrasion in the along the river course makes physical weathering more efficient in formation of micaceous clay minerals [19] in the north bank tributaries than in the south bank tributaries. In the southern tributaries, where the kaolinite clay content is higher which is due to the high chemical weathering in the river basins (Flatter gradient and relax tectonic settings as compared to the Himalayan rivers).

6.3 Conclusions

Clay minerals may be used as a good indicator of the source area, weathering intensity and maturity of both sedimentary rocks and modern marine and fluvial sediments [20]. It is therefore essential to understand the clay mineral component of the associated sediments of the river basin, as it has an intimate relationship with the engineering properties of the bank sediments, which, in turn, are related with the extent and nature of erosion mechanisms involved.

In our study, presence of hornblende, plagioclase, chlorite and orthoclase in downstream locations indicate the lesser intensity of chemical weathering in the mainstream. The authors of [21] found that the amount of kaolinite increases as the sediments are transported from their source to the ocean, while smectite and vermiculite decrease and illite remains stable. This is also observed in our results as Kaonilite increases from Pasighat to Dhubri. Illite and chlorite are higher in Brahmaputra than the Ganges (60% vs 42% and 17% vs 7% respectively), which results from the dominance of Himalayan tributaries in the Brahmaputra [22].

Brahmaputra has higher abundances of kaolinite than the Ganges (18% vs 4% respectively; [17]) which may be due to contribution from the south bank tributaries which may lead to unstable banks along with the negligible amount of clay in the overbank sediments (around 5%).

Himalayan tributaries contain more micaceous minerals (with dominant biotite) south bank tributaries. This may be due to contribution from Higher and Lesser Himalaya metamorphic rock fragments and phyllites. This explains the abundance of illite and chlorite in the clays of these rivers. More Illite in the north bank tributaries is indicated with high sediment fluxes and periods of physical weathering and

Himalayan uplift, whereas more smectite in the south bank tributaries is associated with more chemical weathering.

Bibliography

[1] Brady, N., and Weil, R. R. (2002). The nature and properties of soils. 13 Edic.Prentince Hall. New Jersey. USA. 598p.

[2] Johnson, N. M., Stix, J., Tauxe, L., Cerveny, P. F., and Tahirkheli, R. A. (1985). Paleomagnetic chronology, fluvial processes, and tectonic implications of the Siwalik deposits near Chinji Village, Pakistan.The Journal of Geology,93 (1), 27-40.

[3] Uddin, A., and Lundberg, N. (1998). Unroofing history of the eastern Himalaya and the Indo-Burman Ranges: Heavy-mineral study of Cenozoic sediments from the Bengal Basin, Bangladesh.Journal of Sedimentary Research,68 (3).

[4] Debrabant, P., Fagel, N., Chamley, H., Bout, V., and Caulet, J. P. (1993). Neogene to Quaternary clay mineral fluxes in the Central Indian basin.Palaeogeography, palaeoclimatology, palaeoecology,103 (3-4), 117-131.

[5] Derry, L. A., and France-Lanord, C. (1996). Neogene Himalayan weathering history and river87Sr86Sr: Impact on the marine Sr record.Earth and Planetary Science Letters,142 (1-2), 59-74.

[6] Brass, G. W., and Raman, C. V. (1990). Clay mineralogy of sediments from the Bengal Fan.Cochran JR, Stow DAV et al, 35-42.

[7] Galy, A., France-Lanord, C., and Derry, L. A. (1996). The Late Oligocene-Early Miocene Himalayan belt constraints deduced from isotopic compositions of Early Miocene turbidites in the Bengal Fan.Tectonophysics,260 (1), 109-118.

[8] Garzanti, E., Ando, S., France-Lanord, C., Censi, P., Vignola, P., Galy, V., and Lupker, M. (2011). Mineralogical and chemical variability of fluvial sediments

2. Suspended-load silt (Ganga-Brahmaputra, Bangladesh).Earth and Planetary Science Letters,302 (1), 107-120.

[9] Fieldes, M., and Swindale, L. D. (1954). Chemical weathering of silicates in soil formation.New Zealand Journal of Science and Technology B,36, 140-154.

[10] Huizing, H. G. J. (1971). A reconnaissance study of the mineralogy of sand fractions from East Pakistan sediments and soils. Geoderma, 6(2), 109-133.

[11] Griffin, G. M. (1971). Interpretation of X-ray diffraction data.Procedures in sedimentary petrology, 541-569.

[12] Lindholm, R. C. (1987). A practical approach to sedimentology. London: Allen and Unwin, 276.

[13] Gibbs, R. J. (1967). The geochemistry of the Amazon River system: Part I. The factors that control the salinity and the composition and concentration of the suspended solids.Geological Society of America Bulletin,78 (10), 1203-1232.

[14] Singh, S. K., Sarin, M. M., and France-Lanord, C. (2005). Chemical erosion in the eastern Himalaya: major ion composition of the Brahmaputra and δ 13C of dissolved inorganic carbon.Geochimica et Cosmochimica Acta,69(14), 3573-3588.

[15] Kotoky, P., Bezbaruah, D., Baruah, J., Borah, G. C., and Sarma, J. N. (2006). Characterization of clay minerals in the Brahmaputra river sediments, Assam, India.Current Science-Bangalore,91 (9), 1247.

[16] Goldich, S. S. (1938). A study in rock-weathering. The Journal of Geology, 17-58.

[17] Sarin, M. M., Krishnaswami, S., Dilli, K., Somayajulu, B. L. K., and Moore, W. S. (1989). Major ion chemistry of the Ganga-Brahmaputra river system: Weathering processes and fluxes to the Bay of Bengal.Geochimica et cosmochimica acta,53 (5), 997-1009.

[18] Irion, G. (1983). Clay mineralogy of the suspended load of the Amazon and of rivers in the Papua-New Guinea mainland. Transport of carbon and minerals in major world rivers, 2, 482-504.

[19] Faria, L. D. (1997). Controle e tipologia de mineralizacoes de grafita flake do nordeste de Minas Gerais e sul da Bahia: uma abordagem regional.Belo Horizonte, IGC-UFMG, Dissertacao de Mestrado.

[20] Guyot, J. L., Jouanneau, J. M., Soares, L., Boaventura, G. R., Maillet, N., and Lagane, C. (2007). Clay mineral composition of river sediments in the Amazon Basin. Catena,71 (2), 340-356.

[21] Martinelli, L. A., Victoria, R. L., Dematte, J. L. I., Richey, J. E., and Devol, A. H. (1993). Chemical and mineralogical composition of Amazon River floodplain sediments, Brazil.Applied Geochemistry,8 (4), 391-402.

[22] Heroy, D. C., Kuehl, S. A., and Goodbred, S. L. (2003). Mineralogy of the Ganges and Brahmaputra Rivers: implications for river switching and Late Quaternary climate change.Sedimentary Geology,155(3), 343-359.

Chapter 7

Geochemistry of the sediments of the Brahmaputra river and its Tributaries

7.1 Introduction

Fluvial sediments geochemistry is a function of lithology, morphology of the catchment, climate regime , weathering rates hydrology as well as biotic factors such as type of vegetation cover [1, 2, 3, 4, 5, 6, 7, 8, 9], the tectonic settings of the source area and environment of deposition and diagenesis [10, 11, 12, 13, 6, 14, 15, 16, 17, 18]. In addition sediment re working also affects the sediment chemistry ,particularly in ancient sediments [19, 20]. Some studies reported that during sediment transport some processes significantly homogenise the chemical composition of sediments [21, 22, 23]. More geochemical data from wide range of geological environments and diverse climatic regimes are needed to understand in detail the dynamics of surface processes in element distribution and migration in modern and older sediments.

Many studies have used the geochemistry of channel bed and suspended load sediments to evaluate the provenance characteristics of fluvial sediments (e.g. [24, 8]). But some studies claim that neither of these alone are useful in representing closely the source area rock composition [25, 8]. They have stated that this is because of the strong physical sorting of sediments during transport and deposition which lead to concentration of quartz and feldspar with some heavy minerals in the coarse fraction (bed sediments) and of secondary , lighter and more weatherable minerals in the suspended load. This mineral sorting results in chemical differences between the two types of sediment load and consequently their deviation from source rock composition. On the other hand, floodplain sediments which have textures intermediate between bed and suspended load could have chemistry more close approximating their source rocks if source rock weathering did not remove soluble cations from the rocks. Particularly the use of immobile major and trace elements which are thought to be carried in the particulate load, such as Al, Fe, Ti, Th, Sc, Co, Zr and the rare earth elements (REEs), have been found to be useful indicators of the source [10]. With this background we studied the geochemical characteristics (major and trace) of the entire spectrum of sediments deposited by the Brahmaputra River and its 6 of its tributaries (Burhidihing, Dikhow, Kopili, Subansiri, Jiabharali and Pagladia) draining the Assam plains. This study also provided some information on geochemical differentiation during transport and deposition.

7.2 Results and discussions

7.2.1 Sediment geochemistry

Geochemical composition (major and trace elements) of sediments of the Brahmaputra River and its tributaries are shown in Table 7.1, 7.2, 7.3 and 7.4.

Major Elements

Major element composition of river sediments was used to study the quantification of chemical and physical weathering, to ascertain inter-element relationships and rock classification, as well as for assessing geochemical processes operating on a river basin [26, 27]. The results obtained for the major elements determined by XRF in the sediment samples are shown in Table 7.1. SiO_2, Al_2O_3 and Fe_2O_3 were the dominant constituents of the sediments, whose concentrations were similar to those found in the UCC. CaO, Na_2O, K_2O and MgO are minor constituents, generally totalling $< 10\%$. K_2O was present in significant amounts, probably reflecting mica and illite in the sediments. There was increase in Al_2O_3, FeOt, TiO_2 and decease

Sample	BHD CH	DKW CH	KPL CH	BHD BNK	DKW BNK	KPL BNK	BHDNFP	BHD O FP	DKW NFP	DKW OFP	KPL NFP	KPL OFP	KPL MUD
SiO_2	72.67	73.81	74.9	64.72	67.84	79.30	67.85	59.21	65.67	68.09	78.12	83.67	72.97
TiO_2	0.49	0.62	1.0	0.73	0.60	0.77	0.88	0.99	0.98	1.02	1.02	0.53	0.90
Al_2O_3	9.34	9.55	12.0	11.67	11.88	9.08	13.47	14.64	14.59	15.23	12.15	6.43	13.09
FeO	3.95	5.12	4.8	5.56	6.49	3.55	6.14	6.91	6.70	6.66	4.83	2.33	4.43
MnO	0.09	0.11	0.1	0.10	0.15	0.05	0.13	0.13	0.09	0.10	0.06	0.04	0.07
MgO	2.03	1.52	0.9	2.47	1.80	0.68	2.39	2.58	1.90	1.80	0.94	0.44	1.00
CaO	1.24	0.68	0.3	1.03	0.72	0.26	0.94	0.85	0.31	0.28	0.33	0.21	0.32
Na_2O	1.46	1.07	0.7	1.15	1.30	0.53	0.80	1.00	0.98	0.61	0.43	0.48	0.13
K_2O	1.97	1.39	1.8	1.96	1.86	1.46	2.03	2.06	1.79	1.82	1.80	1.14	1.94
P_2O_5	0.09	0.09	0.1	0.14	0.13	0.11	0.14	0.16	0.13	0.14	0.14	0.08	0.13
LOI	4.37	3.54	4.87	5.76	5.81	3.74	4.19	7.31	6.47	5.83	3.01	5.72	5.36
Total	93.71	97.50	96.09	95.29	98.58	99.52	98.95	95.84	99.61	101.57	102.83	101.08	100.33
Mz	3.731	4.214	4.123	3.240	4.404	4.121	4.961	5.120	5.102	5.284	5.391	5.888	6.089
A%	**58.46**	**67.96**	**65.29**	**67.84**	**68.62**	**74.73**	**72.84**	**75.17**	**78.39**	**81.58**	**77.01**	79.75	**83.74**
CN%	**28.23**	**21.35**	**19.74**	**20.12**	**20.11**	**12.10**	**15.25**	**12.57**	**11.20**	**7.88**	**10.48**	7.36	**2.82**
K%	**13.31**	**10.68**	**14.97**	**12.04**	**11.27**	**13.17**	**11.92**	**12.26**	**10.41**	**10.53**	**12.52**	12.89	**13.44**
Ba	514.51	183.16	249.6	443.09	382.56	217.13	433.95	334.51	159.17	238.69	305.21	180.88	372.41
Co	16.42	15.01	20.7	22.54	27.44	19.65	27.06	31.29	29.12	28.44	18.57	9.28	14.14
Cr	190.21	312.70	100.3	233.94	188.50	71.80	307.60	273.56	269.67	285.42	100.71	42.18	75.15
Ni	135.76	114.80	46.8	157.97	156.12	37.94	167.49	173.64	143.25	135.65	44.65	28.19	38.88
Pb	20.47	20.74	23.5	22.88	19.64	22.96	25.50	25.16	20.94	28.21	30.30	22.45	32.99
Rb	89.03	66.69	100.6	91.74	81.89	84.97	89.86	100.66	87.31	77.56	93.46	69.61	88.79
Sr	145.62	114.78	82.0	126.54	140.26	71.14	133.08	114.59	94.62	102.04	87.79	60.90	88.80
V	82.31	105.68	138.4	102.30	71.67	101.02	124.50	140.63	138.60	140.47	140.86	78.59	127.17
Zn	74.39	68.24	66.5	81.55	72.05	48.82	79.56	110.61	96.68	86.52	61.55	29.13	47.37
Zr	189.83	380.20	1554.6	218.27	175.76	1008.00	334.93	236.07	331.47	394.01	1580.12	450.81	401.89
Cu	55.59	13.15	18.8	33.50	17.02	14.72	29.55	49.64	32.97	29.87	17.26	10.13	13.70

Table 7.1: Major and trace elements composition of sediments from the South bank tributaries from different locations along with their LOI (Loss on Ignition), CIA, Mean size (Mz) in phi. The major oxides and trace elements are in percentage and ppm respectively. CH ≡ channel; BNK ≡ bank; FP ≡ floodplain, NFP ≡ new floodplain, OFP ≡ old floodplain.

Sample	SBN CH	JBR CH	PGL CH	SBN BNK	JBR BNK	PGL BNK	SBN FP	JBR FP C	JBR FP B	JBR FP A	PGL FP
SiO_2	69.14	65.31	75.99	73.44	70.13	72.42	60.40	65.38	58.51	61.16	79.51
TiO_2	0.68	0.61	0.66	0.58	0.40	0.57	0.89	0.83	0.87	0.85	0.65
Al_2O_3	13.09	10.82	11.25	11.22	11.16	10.41	15.97	17.00	17.46	17.53	12.38
FeO	4.81	4.98	3.33	4.03	3.06	2.71	6.60	6.21	5.73	5.97	2.94
MnO	0.08	0.08	0.06	0.07	0.05	0.05	0.10	0.07	0.08	0.10	0.05
MgO	1.49	2.29	1.13	1.24	1.15	1.03	2.01	1.93	2.26	1.96	1.03
CaO	1.37	1.17	0.39	1.22	0.79	0.51	1.95	0.51	0.81	0.51	0.45
Na_2O	1.43	1.17	0.88	1.26	1.26	0.74	1.02	0.93	0.76	0.70	0.33
K_2O	2.42	2.44	2.21	2.28	2.71	2.06	2.81	3.81	3.79	3.69	2.22
P_2O_5	0.15	0.14	0.09	0.13	0.09	0.08	0.22	0.13	0.29	0.26	0.07
LOI	2.13	3.77	4.17	1.46	2.62	4.45	6.89	3.36	4.45	6.68	3.88
Total	96.79	92.77	100.17	96.93	93.41	95.02	98.87	100.16	94.99	99.41	103.51
Mz	2.90	3.22	3.65	4.66	4.61	4.47	4.63	4.01	4.10	4.40	6.29
A%	**55.46**	**60.75**	**68.33**	**63.82**	**63.73**	**72.30**	**71.37**	**70.91**	**72.55**	**74.29**	**77.97**
CN%	**27.33**	**22.01**	**15.91**	**22.22**	**20.23**	**12.90**	**15.00**	**12.12**	**10.40**	**8.79**	**6.92**
K%	**17.20**	**17.24**	**15.77**	**13.95**	**16.04**	**14.80**	**13.63**	**16.97**	**17.05**	**16.92**	**15.11**
Ba	407.01	555.59	433.30	400.05	484.21	406.48	495.29	652.59	621.49	637.67	492.74
Co	17.22	18.93	10.90	18.01	11.55	9.89	20.56	23.17	17.86	19.01	8.93
Cr	70.22	128.06	41.98	56.24	39.52	34.75	92.21	80.19	76.56	86.46	37.82
Ni	40.40	96.05	27.86	32.81	24.98	24.81	48.76	42.47	37.21	42.47	24.16
Pb	20.79	17.40	22.11	22.66	23.38	22.20	31.34	27.26	30.94	34.39	35.40
Rb	130.38	131.10	114.00	118.69	153.39	104.47	126.10	202.76	189.53	181.01	96.61
Sr	166.58	126.08	82.00	163.63	88.73	80.01	176.38	83.45	93.72	84.72	93.59
V	97.92	83.05	94.32	79.42	61.60	72.79	129.99	121.80	126.44	124.73	100.45
Zn	64.60	61.68	56.89	54.62	42.67	42.90	82.27	88.62	79.65	76.31	42.85
Zr	258.71	200.53	787.41	244.14	225.87	607.42	215.03	273.08	303.37	336.39	536.78
Cu	20.14	32.48	13.73	17.50	23.12	8.47	27.47	33.11	24.67	35.15	10.94

Table 7.2: Major and trace elements composition of sediments from the north bank tributaries from different locations along with their LOI (Loss on Ignition), CIA, Mean size (Mz) in phi. The major oxides and trace elements are in percentage and ppm respectively. CH ≡ channel; BNK ≡ bank; FP ≡ floodplain.

	CHANNEL						BANK						FLOODPLAIN							
Sample	PSG	DBRG	TEZ	GHY	NLB	DHBR	PSG	DBRG	TEZ	GHY	NLB	DHBR	PSG	DIBRUGARH FLOODPLAIN				TEZ	GHY	DHBR
														NFP	A	B	C			
SiO_2	60.17	60.01	62.99	69.48	68.72	66.94	55.87	56.74	57.35	68.38	69.23	64.56	59.34	56.32	59.57	61.97	62.01	62.67	67.01	78.61
TiO_2	1.01	0.81	0.85	0.53	0.59	0.67	0.92	0.84	0.82	0.59	0.57	0.70	1.19	0.84	0.88	0.97	0.97	0.66	0.76	0.51
Al_2O_3	11.41	11.83	13.07	10.31	11.27	11.30	12.11	12.52	13.20	11.04	10.75	11.97	14.77	13.32	14.17	14.84	15.16	10.91	16.20	10.4
FeO	6.88	6.61	7.27	3.96	4.17	4.48	7.21	7.36	7.36	4.21	4.14	4.89	6.17	7.49	6.77	7.05	7.07	5.36	5.54	2.95
MnO	0.12	0.10	0.12	0.06	0.08	0.07	0.12	0.11	0.13	0.08	0.08	0.07	0.13	0.11	0.09	0.11	0.10	0.08	0.08	0.07
MgO	4.11	4.04	4.44	1.68	2.07	2.27	4.55	4.81	4.02	2.11	2.07	2.55	3.31	4.55	3.77	3.23	3.23	2.49	1.93	1.3
CaO	5.99	4.65	4.63	2.65	2.61	2.51	5.26	4.95	4.56	2.51	2.45	2.58	1.30	5.12	3.23	2.79	2.80	2.75	0.96	1.36
Na_2O	2.37	1.93	2.06	1.84	1.84	1.84	2.33	2.21	1.83	1.78	1.69	1.75	0.71	2.23	1.64	1.63	1.55	1.66	0.69	0.69
K_2O	1.50	1.88	2.16	2.22	2.31	2.36	1.70	1.95	2.36	2.31	2.31	2.39	2.55	2.09	2.57	2.54	2.54	2.33	3.17	2
P_2O_5	0.30	0.19	0.25	0.19	0.15	0.20	0.25	0.22	0.26	0.15	0.13	0.19	0.48	0.21	0.18	0.18	0.18	0.24	0.17	0.12
LOI	3.00	2.96	2.35	2.31	1.75	2.04	5.18	3.66	3.61	4.35	3.28	2.52	7.35	4.14	4.57	4.07	4.12	10.52	4.16	4.45
Total	96.84	95.01	100.19	95.23	95.56	94.68	95.50	95.39	95.50	97.51	96.69	94.15	97.29	96.41	97.45	99.39	99.71	99.67	100.67	102.46
Mz	3.18	4.12	3.34	3.97	4.10	2.27	3.42	5.63	3.96	4.63	4.83	5.03	5.06	5.83	5.20	5.10	6.01	6.33	5.82	5.72
A%	**55.19**	**57.34**	**58.15**	**57.24**	**56.87**	**56.82**	**60.70**	**59.62**	**60.65**	**64.06**	**64.10**	**60.27**	**73.12**	**68.05**	**67.94**	**66.12**	**70.16**	**71.97**	**73.96**	**70.10**
CN%	**36.65**	**32.88**	**30.57**	**29.81**	**30.53**	**30.35**	**23.90**	**29.41**	**27.62**	**22.14**	**21.99**	**26.72**	**11.31**	**19.36**	**19.47**	**20.33**	**15.21**	**12.77**	**10.36**	**15.30**
K%	**8.16**	**9.78**	**11.27**	**12.95**	**12.60**	**12.83**	**15.40**	**10.97**	**11.72**	**13.80**	**13.91**	**13.00**	**15.57**	**12.59**	**12.59**	**13.56**	**14.63**	**15.25**	**15.67**	**14.59**
Ba	263.74	341.40	434.78	540.32	394.86	360.90	320.2	418.48	537.1	586.6	390.2	368.20	467.4	415.7	436.4	465.0	408.0	641.2	436.32	369.62
Co	28.38	39.93	30.25	22.71	16.56	24.79	27.62	31.58	23.72	34.06	21.45	27.94	37.00	44.08	35.23	35.92	34.21	17.46	8.27	31.579
Cr	176.37	158.67	171.06	56.93	69.16	82.59	180.5	181.41	163.0	81.26	62.51	90.54	67.66	148.4	151.4	158.2	90.13	77.41	41.59	103.37
Ni	107.61	98.62	108.73	42.30	44.15	48.29	106.9	110.02	101.1	48.80	43.60	55.01	44.67	99.89	97.30	101.3	69.44	44.78	23.99	62.741
Pb	16.72	15.91	18.78	21.95	19.80	19.71	15.10	14.92	22.52	21.24	19.74	19.53	20.62	18.43	22.90	22.34	21.14	31.95	31.69	19.446
Rb	64.35	75.18	81.95	100.77	111.33	110.52	59.39	69.20	79.57	161.7	113.1	113.54	145.9	116.1	108.3	113.5	117.3	135.4	79.33	116.44
Sr	302.52	272.43	279.16	245.13	226.53	224.94	296.8	283.12	271.3	123.4	223.5	227.83	208.5	226.8	211.4	215.8	195.5	131.4	150.64	229.33
V	142.87	120.68	129.30	70.72	108.65	88.33	120.1	103.06	126.3	97.33	75.56	93.92	108.2	121.8	136.5	133.4	92.86	116.1	86.44	100.55
Zn	84.99	80.36	91.39	102.14	52.42	79.53	69.18	74.42	84.24	90.77	58.73	83.23	92.14	92.90	91.81	97.05	241.3	79.93	25.15	88.509
Zr	265.41	204.71	190.71	254.22	267.66	309.00	251.7	185.97	155.6	260.4	242.4	275.10	228.6	215.3	225.8	212.4	199.5	246.6	253.29	237.26
Cu	53.61	51.11	61.25	29.30	13.03	19.36	50.30	61.42	65.68	27.37	17.62	25.20	24.21	53.25	47.00	60.12	38.91	27.94	3.33	29.862

Table 7.3: Major and trace elements composition of sediments from the Brahmaputra from different locations along with their LOI (Loss on Ignition), CIA, Mean size (Mz) in phi. The major oxides and trace elements are in percentage and ppm respectively.

	Brahmaputra					South bank tributaries			North bank tributaries		
	PSG	DIB	TEZ	GHY	DHBR	BHD	KPL	DKW	SBN	JBR	PGL
Al	15.56	14.76	18.20	16.55	16.66	15.81	14.81	19.13	15.76	18.51	17.11
Ca	2.40	3.42	2.24	2.41	2.33	1.06	1.86	0.72	1.38	4.81	0.56
Fe	6.11	7.43	7.59	7.59	7.19	7.77	7.74	8.12	6.62	9.78	6.08
Mg	2.52	3.69	2.88	3.24	2.95	2.91	3.37	1.91	1.75	5.53	1.42
Mn	0.12	0.12	0.14	0.13	0.12	0.13	0.12	0.11	0.12	0.17	0.10
P	0.12	0.15	0.29	0.20	0.20	0.18	0.19	0.25	0.64	0.37	0.16
Ti	0.71	0.82	0.85	0.84	0.76	0.86	0.84	0.99	0.75	1.00	0.79
K	3.46	2.39	3.37	2.88	2.92	2.36	2.77	2.62	2.92	3.05	3.00
Na	1.73	1.86	1.81	1.72	1.73	1.18	1.39	1.00	1.64	2.63	0.75
Co	5.34	6.57	6.15	6.62	6.26	6.89	6.5	7.23	5.62	6.05	3.85
Cr	47.65	70.03	55.76	65.87	67.83	95.57	83.23	95.39	47.49	82.92	36.64
V	42.12	54.67	47.76	50.74	49.95	51.44	48.88	65.8	42.85	75.32	32.62
Ba	222.71	231.65	220.11	883.99	218.81	202.95	279.2	148.98	197.86	232.08	180.82
Sr	72.18	78.17	68.06	68.44	65.66	43.15	50.56	47.42	61.71	73.45	58.32

Table 7.4: Major and trace elements composition of suspended sediments from the Brahmaputra and its tributaries from different locations. The major oxides and trace elements are in percentage and ppm respectively.

SAMPLE	SiO_2	TiO_2	Al_2O_3	FeO	MnO	MgO	CaO	Na_2O	K_2O	P_2O_5	LOI	Total	Ba	Cd	Cr	Ni	Pb	Rb	Sr	V	Zn	Zr	Cu
Brahmaputra clay																							
Dbrg	41.3	1.0	14.1	7.3	0.1	2.6	1.1	0.8	2.3	0.3	28.2	99.2	344.14	2.22	188.31	128.76	19.83	131.65	107.74	134.20	87.09	110.25	84.30
Ghy	33.7	1.1	15.0	9.3	0.1	2.3	0.7	0.6	2.4	0.3	34.4	99.9	346.75	2.76	194.58	151.48	21.68	146.76	87.23	140.07	122.91	98.21	98.62
Dhubri	40.5	1.0	13.8	7.2	0.1	2.5	1.1	0.8	2.3	0.3	30.5	100.2	338.15	2.58	184.33	130.52	20.05	131.26	107.78	127.77	89.12	110.84	87.94
Brahmaputra sand																							
Dbrg	61.1	0.8	13.8	6.1	0.1	3.8	1.2	1.7	3.5	0.1	7.1	99.3	530.42	4.99	131.20	82.38	22.31	168.11	175.09	89.73	266.06	87.98	197.53
Tez	61.6	0.8	13.9	6.1	0.1	3.8	1.2	1.7	3.5	0.1	6.2	99.3	509.22	4.60	130.08	79.65	22.12	167.85	174.65	94.03	268.62	88.63	197.21
Ghy	64.8	0.6	12.7	5.6	0.1	3.8	2.7	2.6	2.3	0.3	4.1	99.6	439.50	4.43	126.13	85.31	17.01	98.87	276.45	96.12	325.50	102.56	221.82
Dhubri	73.1	0.5	11.7	3.7	0.1	2.0	1.7	2.0	2.7	0.1	2.3	100.1	429.70	5.91	69.22	46.74	20.12	135.89	224.46	55.58	239.25	108.10	168.78
South bank tributaries clay																							
BHDNFP	30.6	1.1	14.7	10.6	0.1	1.8	0.2	0.3	2.1	0.2	38.1	99.9	265.99	1.46	276.01	257.40	18.98	130.63	74.43	148.22	135.76	107.07	55.97
KPLOLFP	42.7	1.3	18.8	8.7	0.0	0.9	0.1	0.3	2.4	0.2	24.2	99.8	190.92	2.70	151.62	83.15	21.84	166.83	80.16	150.83	103.91	150.61	39.71
DKW FP	43.1	1.4	20.6	8.0	0.1	1.4	0.1	0.5	3.0	0.3	21.1	99.8	217.86	3.87	263.81	140.00	23.37	167.37	137.00	187.44	100.97	171.54	50.95
South bank tributaries sand																							
BHDNFP	71.9	0.7	11.6	4.4	0.1	1.8	0.6	1.4	2.0	0.2	5.1	99.8	347.21	6.21	238.84	134.57	20.83	98.56	113.03	74.65	93.03	178.92	51.65
DKW FP	79.8	0.8	10.7	5.4	0.1	1.5	0.1	1.0	1.3	0.2	1.1	102.0	107.27	5.16	220.96	130.46	20.35	65.52	72.06	75.83	138.40	191.68	92.48
DKW OLFP	77.8	0.8	11.5	4.3	0.0	1.3	0.1	1.0	1.5	0.2	2.0	100.6	120.29	5.61	190.89	105.46	21.75	77.58	80.93	74.74	124.72	175.27	92.48
BHD OLFP	80.7	0.7	8.9	3.3	0.1	1.4	1.0	1.4	1.8	0.1	1.1	100.6	357.63	5.72	363.40	80.95	18.96	82.75	140.93	65.45	88.77	398.66	77.76
KPLOLFP	95.3	0.4	4.5	1.6	0.0	0.2	0.2	0.5	1.1	0.3	1.2	105.6	176.02	7.90	34.24	25.66	21.84	67.47	58.49	29.00	802.30	234.30	312.11
KPL MUD	98.6	0.4	4.5	1.4	0.0	0.2	0.2	0.5	1.1	0.1	1.0	108.1	172.81	7.99	27.99	21.84	21.85	68.38	59.25	26.34	149.66	202.50	131.82
North bank tributaries clay																							
JBR FP	33.2	1.2	18.6	12.6	0.2	2.4	0.1	0.3	3.9	0.5	26.0	99.2	736.75	1.63	152.05	80.09	28.15	232.90	32.02	146.10	159.58	58.28	95.37
SBNFP	33.7	1.2	19.0	12.7	0.2	2.4	0.1	0.3	3.9	0.5	26.0	100.1	755.70	0.81	154.81	82.46	27.82	234.05	32.41	159.32	158.53	57.70	93.94
PGLFP	35.3	1.3	19.4	13.1	0.1	3.1	0.1	0.3	4.3	0.5	23.0	100.7	705.86	2.09	156.07	81.01	22.95	290.21	34.70	165.75	190.53	65.37	74.14
North bank tributaries sand																							
JBR FP	78.6	0.5	10.5	3.0	0.0	1.0	0.4	1.4	2.7	0.2	2.0	100.4	428.25	6.38	48.07	33.82	20.65	173.74	76.84	39.72	337.71	207.34	255.31
SBNFP	82.8	0.3	10.0	2.2	0.0	0.8	0.4	1.6	2.5	0.1	1.0	101.7	417.67	7.96	33.72	32.06	24.57	143.05	69.58	22.72	217.30	107.97	122.35
PGLFP	78.6	0.4	10.5	2.9	0.0	1.0	0.4	1.4	2.7	0.2	1.0	99.4	434.67	6.10	48.39	33.39	20.60	174.70	76.11	47.74	337.89	207.09	253.33

Table 7.5: Major and trace elements composition of clay and sand fraction from the floodplain sediments of Brahmaputra and its tributaries from different locations. The major oxides and trace elements are in percentage and ppm respectively.

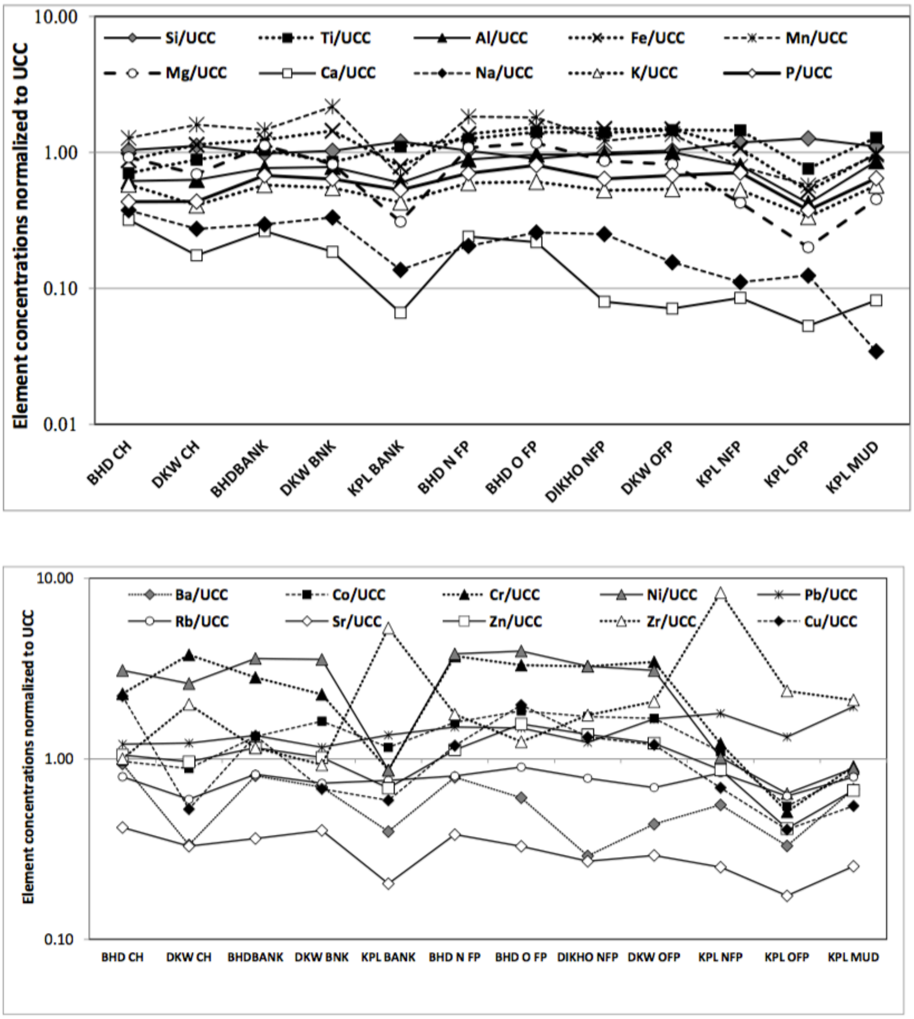

Figure 7.1: Major (upper panel) and trace (lower panel) element composition normalised with Upper Continental Crust (UCC) data of bulk sediments of the south bank tributaries (Burhidihing, Dikhow and Kopili).

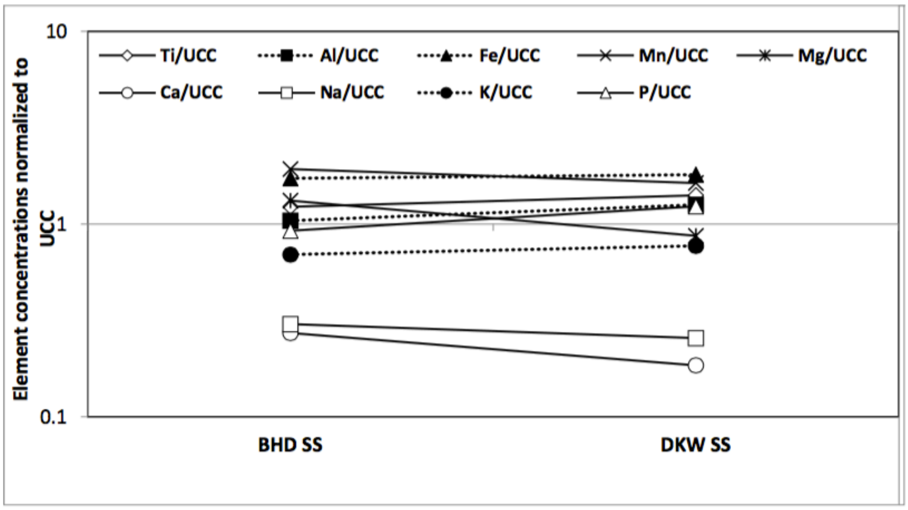

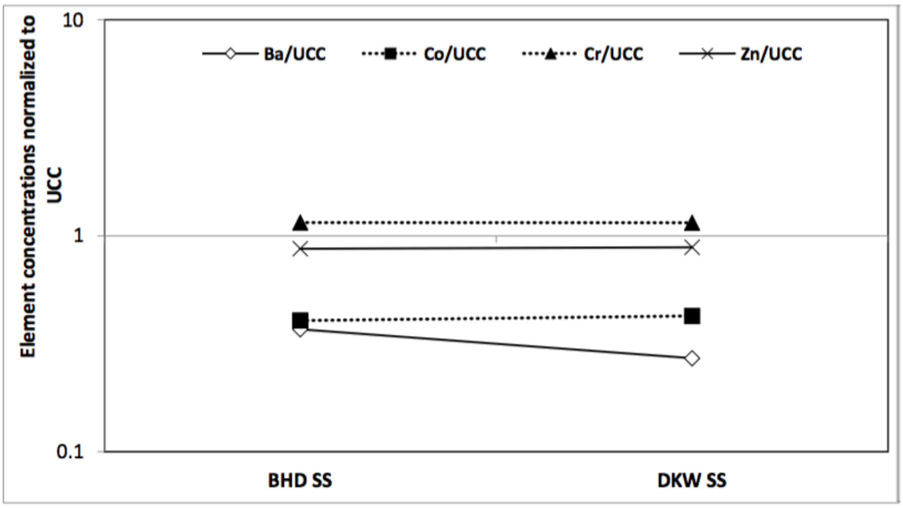

Figure 7.2: Major (upper panel) and trace (lower panel) element composition normalised with Upper Continental Crust (UCC) data of suspended sediments of the south bank tributaries (Burhidihing, Dikhow and Kopili).

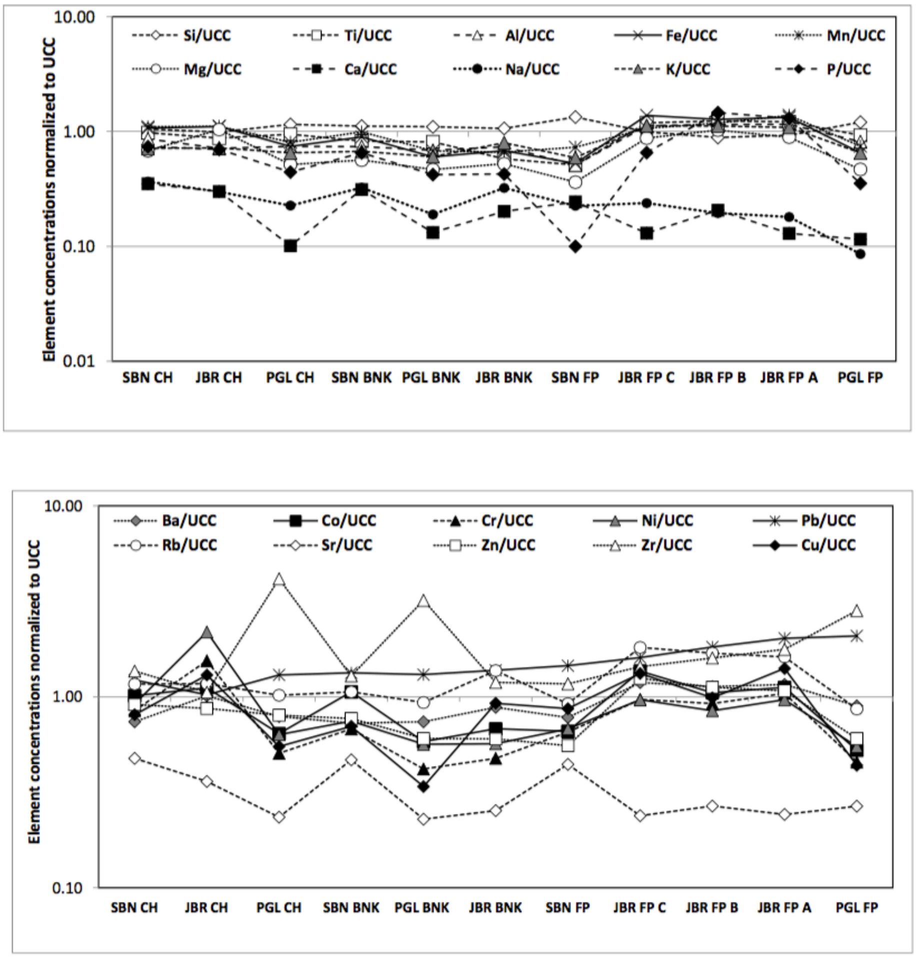

Figure 7.3: Major (upper panel) and trace (lower panel) element composition normalised with Upper Continental Crust (UCC) data of bulk sediments of the north bank tributaries (Jiabharali, Subansiri and Pagladia).

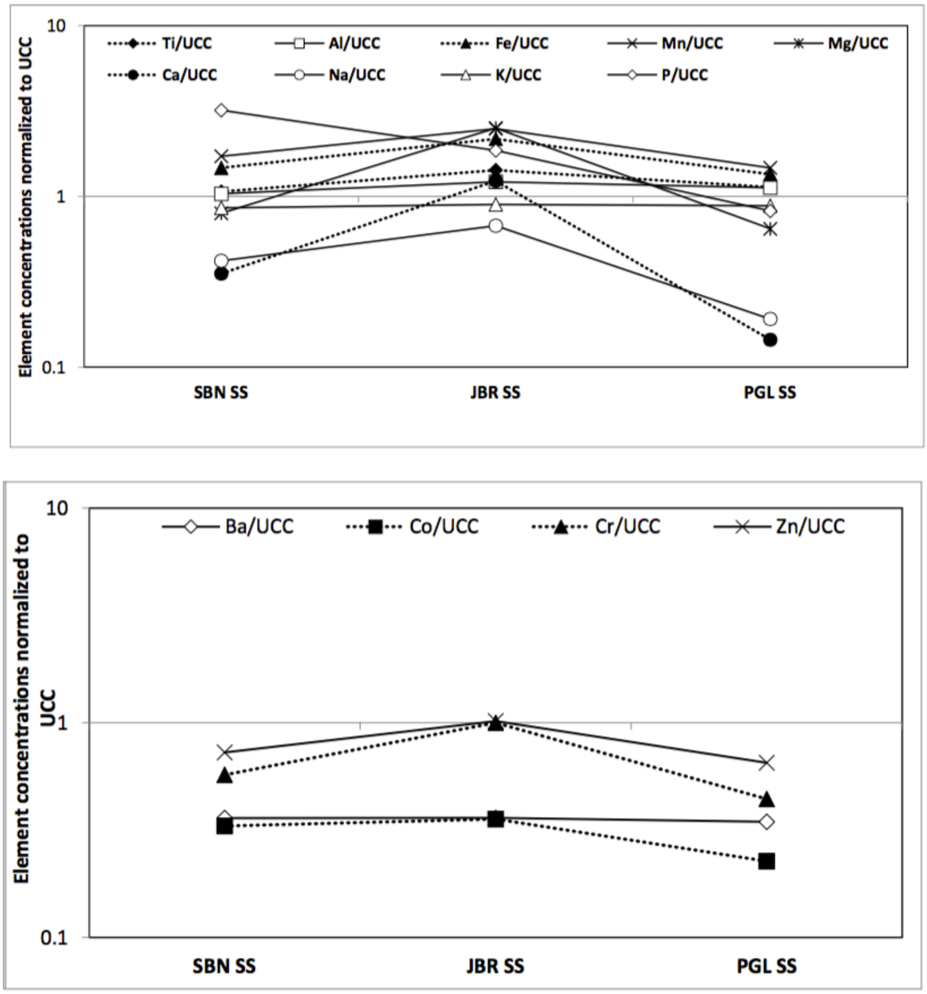

Figure 7.4: Major (upper panel) and trace (lower panel) element composition normalised with Upper Continental Crust (UCC) data of suspended sediments of the north bank tributaries (Jiabharali, Subansiri and Pagladia).

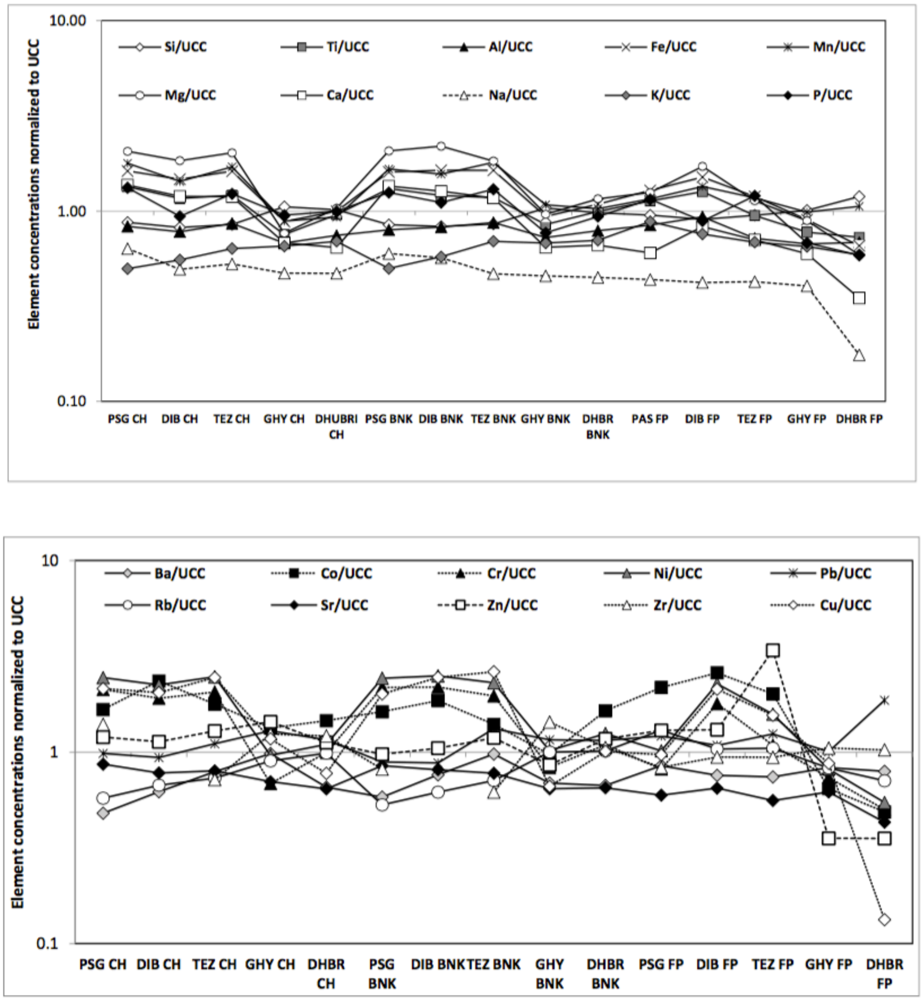

Figure 7.5: Major (upper panel) and trace (lower panel) element composition normalised with Upper Continental Crust (UCC) data of bulk sediments of the Brahmaputra from various locations.

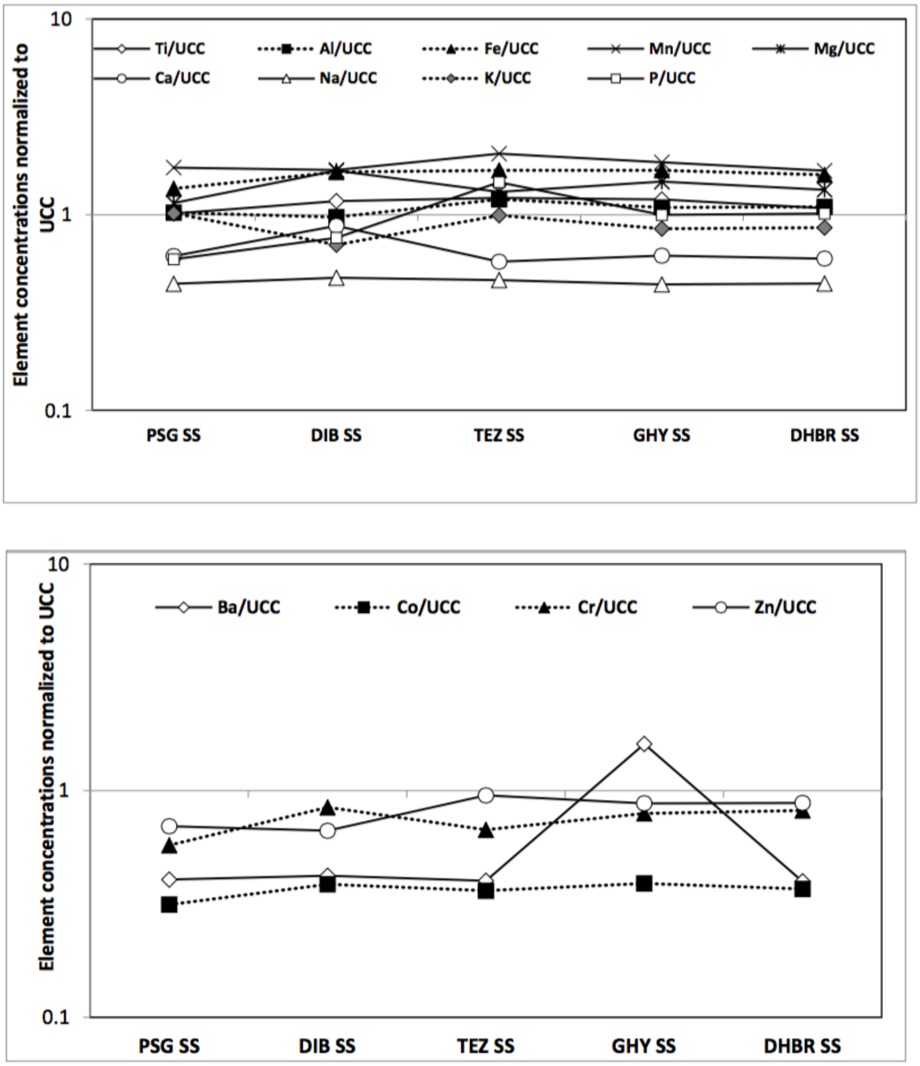

Figure 7.6: Major (upper panel) and trace (lower panel) element composition normalised with Upper Continental Crust (UCC) data of suspended sediments of the Brahmaputra from various locations.

in CaO, Na_2O from channel to floodplain sediments which may be due to higher mobility of Ca and Na compared to K and Mg during floodplain weathering (K showed slight enrichment in the floodplain sediments may be due to formation of illite clays). Suspended sediments have higher concentrations of major elements than channel and overbank sediments (Table 7.4). Upper Continental Crust normalised values were calculated to identify whether sediments were enriched or depleted in certain elements as compared to their sources (Upper Continental Crust). The sediments of Brahmaputra and its tributaries were normalised with respect to UCC and displayed in a multi-element diagram for elemental enrichment or depletion (Figure 7.1, 7.2, 7.3, 7.4, 7.5, 7.6). In the south bank tributaries, Si, Al, Ti, Fe and Mn is enriched in all the samples while Ca, Na, K, Mg are depleted in the floodplain samples (in Kopili overbank and floodplain all the major elements are depleted except Si). Even in suspended sediments of Kopili, most major elements were depleted. It was observed that all the major elements except Si were depleted in the north bank tributaries (more depletion observed in the Pagladia samples than Subansiri and Jiabharali). In Jiabharali floodplain all elements were found to be enriched except Ca and Mg. This may be due to associations with Fe and Al colloids. In Table 7.2 A, B, C indicate the weathering horizons; A -oldest horizon and C -youngest horizon. In the Brahmaputra, among the major elements, Si, Al, Ca, Mg, Na and K were observed to be depleted in most samples. More depletion was observed at downstream locations (Ca and Mg showed enrichment in samples taken from upstream locations).Ti, Fe, Mn and P were seen to be enriched in most samples. Depletion of elements were seen to be more in the samples taken from downstream locations (Guwahati, Nalbari and Dhubri). Only the mobile elements are depleted in the channel and overbank sediments indicating low chemical weathering in the source area.

Trace Elements

Ba, Cr , Ni, Sr, Zr and V were found to the dominant trace elements in the river sediments but their concentrations were higher in the south bank tributaries than in north bank tributaries and Brahmaputra (Table 7.1, 7.2, 7.3) suggesting a mafic rock-dominated source region. There was increased concentration of Ba, Sr, Zn, Zr and Cu in the sand fraction whereas Cr, Ni, V increased in the clay fraction. Zr showed excessive enrichment in the Kopili samples. Sediment sorting results in the enrichment of heavy minerals (zircon, monazite, magnetite, etc.) in coarse sediment fractions. Zr was enriched in all samples. Pagladia samples showed more depletion of all the trace elements than Subansiri and Jiabharali rivers. In Brahmaputra samples, most trace elements were depleted in downstream locations.

In the suspended sediments of the Brahmaputra river, the major and trace elements showed a conservative behaviour (unlike most rivers which show a downstream decrease or increase). This indicates that dilution effect from tributaries, redox cycling and associated with different phases related to biological activity within the river system do not control the variations in the major elements [28].

7.2.2 Weathering Geochemistry of Sediments

Chemical Index of Alteration (CIA), devised by Nesbitt and Young [29], quantifies the extent of chemical weathering undergone by the source rocks of the sediments and has been widely used in many provenance studies (e.g. [30, 31, 32, 33, 34, 35, 36]). Molar proportions of Al_2O_3 (A), CaO^* (C), Na_2O (N) and K_2O (K) are used to calculate Chemical index of alteration (CIA), where CaO^* represents the calcium in silicate fraction only. In the absence of CO_2data, correction for CaO in carbonate mineral is difficult. Therefore, in the samples where molecular proportion of CaO (after correction for apatite) is greater than molecular proportion of Na_2O, CaO is assumed to be equal to Na_2O [37, 21]. For primary minerals (non altered minerals), all feldspars have CIA value of 50 and the mafic minerals biotite, hornblende and pyroxenes have CIA values between of 50-55, 10-30, and 0-10, respectively. Feldspar and mica weathering to smectite and kaolinite result in a net loss of K and Na in weathering profiles, whereas Al is resistant and is enriched in weathering products [29]. This induces an increase of CIA values by about 100 (reflecting complete removal of alkali and alkaline earth elements from the parent rock) for kaolinite and 70-85 for smectite [38, 33, 39].

A-CN-K and A-CNK-FM ternary diagrams The influence of chemical weathering, diagenetic K-metasomatism as well as hydrodynamic sorting on the sedimentary rocks, can be visualized in the Al_2O_3-(CaO^*+Na_2O)-K_2O (Figure 7.7, A-CN-K) ternary diagram [30, 31, 33, 40]. The authors of [30] proposed ideal (predicted)

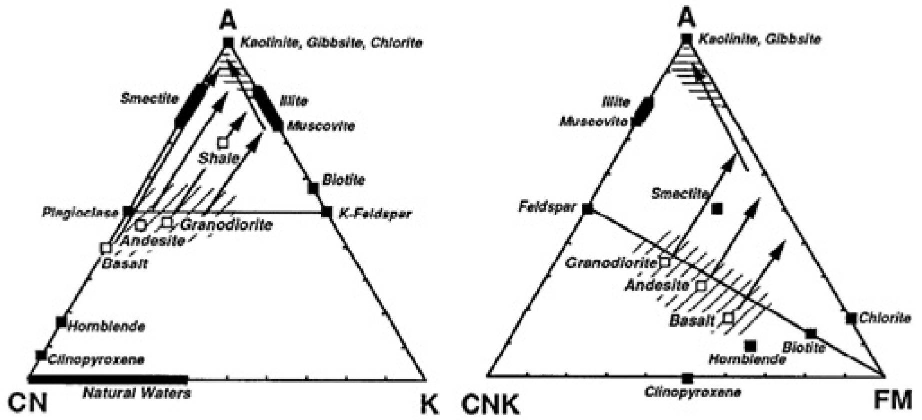

Figure 7.7: Ternary plots of A-CN-K and A-CNK-FM where, in mole fraction, A = Al_2O_3, C = CaO (silicate fraction only), N = Na_2O, K = K_2O, F = total Fe as FeO, and M = MgO (after [30, 38]). Plotted are simplified compositions of major minerals, typical rock types, and natural waters. Arrows indicate the general trends of weathering exhibited by various rock types.

weathering trends (Line 2 in Figure 7.7) of plutonic and volcanic rocks based on thermodynamic and kinetic considerations. The weathering trend first parallels the A-CN join because plagioclase is more susceptible to chemical weathering than K-feldspar and thus is preferentially destroyed [41, 38].

The ternary A-CN-K (Al_2O_3-CaO+Na_2O-K_2O) system is useful for evaluating the compositions of fresh plagioclase- and potassium-feldspar- rich rocks and examining their weathering trends, weathering products and clay minerals [30, 31].The A-CNK-FM (Al_2O_3-CaO+Na_2O+K_2O-FeO (total)+MgO) diagram introduced by [38] shows the chemical behaviour of MgO and Fe_2O_3 in the weathering profiles as these elements are potentially mobile in tropical environments [42].

Sediments were plotted on A-CN-K and A-CNK-FM ternary diagrams to know the weathering trend (Figure 7.8, 7.9, 7.10).

In the south bank tributaries all the samples plotted linearly parallel to A-CN line with floodplain samples closer to Al_2O_3 apex indicating leaching of mobile elements CaO and Na_2O and enrichment of Al_2O_3 , while K_2O remains constant. The samples are plotted away from the plagioclase-K-feldspar line indicating that they have undergone intense chemical weathering (CIA: 58-84). The mud samples plot closer to Illite.

In the north bank tributaries most of the samples plot parallel to A-CN line and

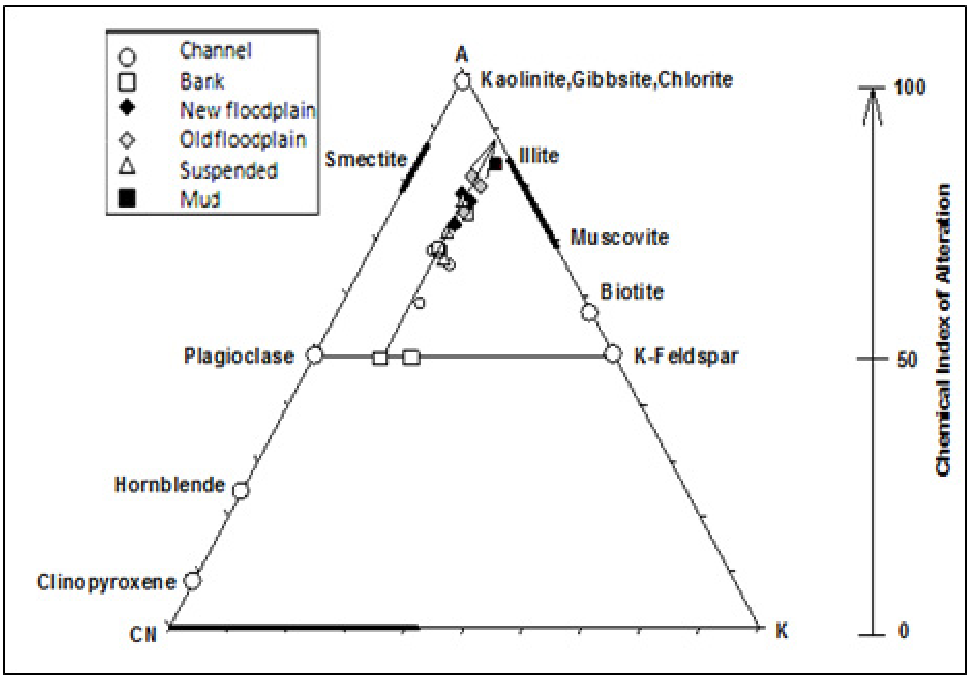

Figure 7.8: Ternary plot of A-CN-K of analyzed samples of South bank tributaries (Burhidihing, Dikhow and Kopili) of the Brahmaputra (after [30, 38]).Granite and Granodioritic composition were also included. Arrows indicate the general trends of weathering exhibited by the sediment samples. Most of the samples were in the intense weathered zone.

showed lesser weathering than the south bank tributaries (CIA:55-78) (fig 7.9). In the south bank tributaries all the samples plot away from the plagioclase-K-feldspar line indicating that they have undergone intense chemical weathering as compared to the north bank tributaries. This is due to the flatter gradient and more time for the sediments to weather due to the tectonically relax source area as compared to the north bank tributaries.

Brahmaputra samples showed very less chemical weathering (CIA:55-70). Despite little chemical weathering the source rocks in the provenance area provided load for physical erosion and deposition by the river.

In Figure 7.10, it was observed that Brahmaputra channel samples plot near to the granite-graniodiorite line (average upper continental crust composition) indicating very less chemical weathering in the source area (in the cold and dry Tibetan plains). Despite flowing through a length of 1600 km from the source into India, the sediments conserve the source rock signature which indicates high physical erosion due

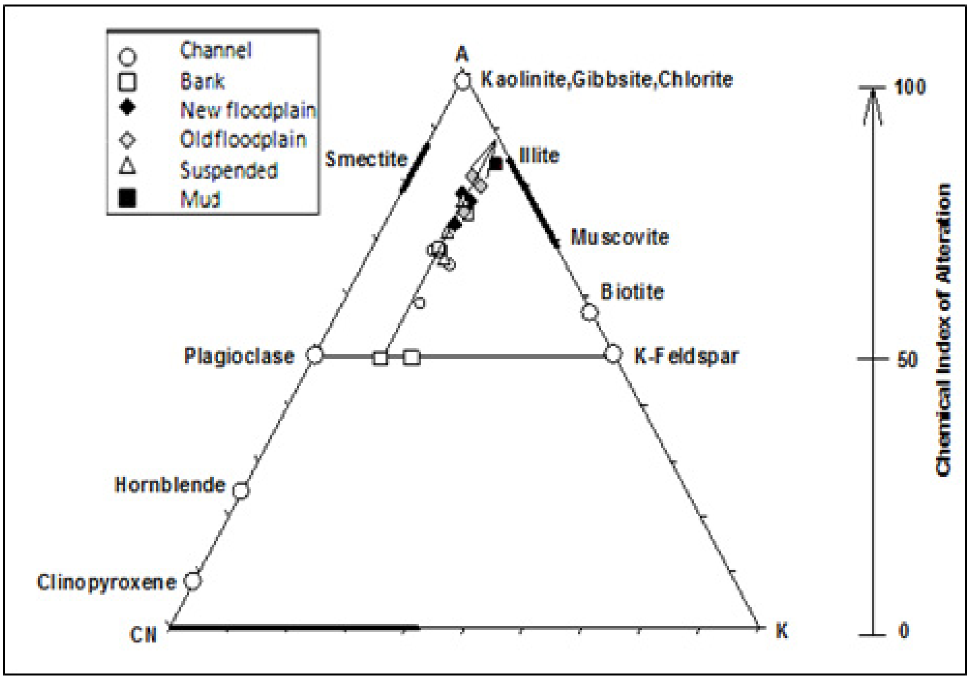

Figure 7.9: Ternary plot of analyzed samples of North bank tributaries (Jiabharali, Subansiri and Pagladia) of the Brahmaputra. Granite and Granodioritc composition were also included. Arrows indicate weathering trend.

to high hydraulic conductivity of the river and low chemical weathering during transport (also supported by the isotopic studies in [43]. The tributaries showed more chemical alteration and weathering compared to the Brahmaputra (Figure 7.9, 7.10).

7.3 Conclusions

In the Brahmaputra only the mobile elements are depleted in the channel and overbank sediments indicating low chemical weathering in the source area. In the suspended sediments, the major and trace elements show a conservative behaviour (unlike most rivers which show a downstream decrease).This indicates that dilution effect from tributaries, redox cycling and associated with different phases related to biological activity within the river system do not control the variations in the major elements [28].

The Brahmaputra samples plot near to the granite-graniodiorite line (average upper continental crust composition) indicating very less chemical weathering in the source

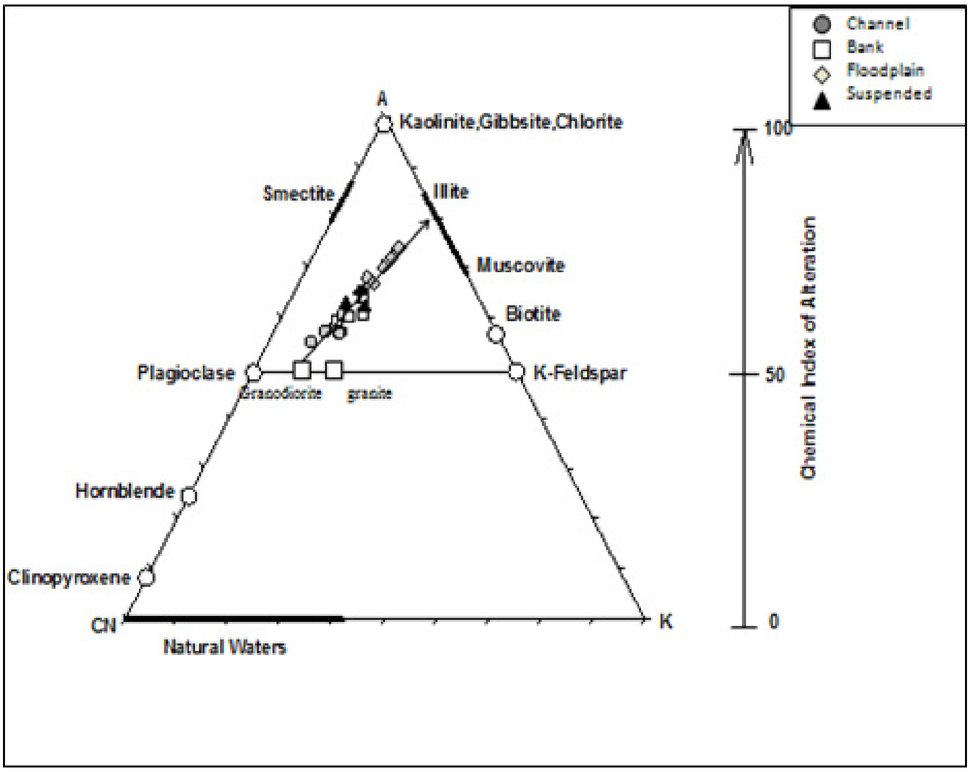

Figure 7.10: Ternary plot of A-CN-K after [30] of analyzed samples of the Brahmaputra.Granite and Granodioritc composition were also included. The dash arrow indicated the ideal weathering trend and the bold arrow indicated the weathering trend followed by the samples. These samples showed a linear trend that is inconsistent with simple weathering being the sole control of the composition (compare with Figure 7.7). For example, on the A-CN-K diagram the predicted weathering trend is shown for a hypothetical composition derived from extrapolating the sediment trend to an unweathered composition (dashed arrow). This may be due to mixing of a relatively weathered source with an unweathered source of differing primary composition or perhaps some influence from secondary sedimentary process that resulted in redistribution (gains or losses depending on composition) of Ca, Na, and/or K in the silicate fraction or addition of K from the illite rich clays [37].

area (in the cold and dry Tibetan plains).Despite flowing through a length of 1600 km from the source into India, the sediments conserve the source rock signature which indicates high physical erosion due to high hydraulic conductivity of the river and low chemical weathering during transport.(also supported by the isotopic studies in [43]).

The tributaries showed more chemical alteration and weathering compared to the Brahmaputra (Figure 7.5 and 7.6). In the South bank tributaries all the samples plot away from the plagioclase-K-feldspar line indicating that they have undergone intense chemical weathering as compared to the north bank tributaries. This is due to the flatter gradient and more time for the sediments to weather due to the tectonically relax source area as compared to the north bank tributaries.

In the north bank tributaries most of the samples plot parallel to A-CN line with the clay-fraction samples plot nearer to illite reference segment in the A-CN-K diagram reflecting predominance of illite in clay mineral assemblages in the river sediments. Generally, clay-fraction sediments have stronger correlations than bulk sediments for most major elements (Figure 7.8). Moderate to strong negative correlations between Al_2O_3 and SiO_2 and CaO in both bulk and clay fractions indicate mineralogical control on SiO_2 and CaO contents, because quartz- and anorthite-rich mineral associations often produce higher SiO_2 and CaO concentrations, respectively. Moderate negative correlations are also found in diagrams of Al_2O_3 versus K_2O and Na_2O in clay-fraction sediments, suggesting the leaching of the mobile elements K and Na_2O during the clay formation.

Bibliography

[1] Duddy, L. R. (1980). Redistribution and fractionation of rare-earth and other elements in a weathering profile.Chemical Geology,30 (4), 363-381.

[2] McLennan, S. M. (1989). Rare earth elements in sedimentary rocks; influence of provenance and sedimentary processes.Reviews in Mineralogy and Geochemistry,21 (1), 169-200.

[3] Cullers, R. L., and Stone, J. (1991). Chemical and mineralogical comparison of the Pennsylvanian Fountain Formation, Colorado, USA (an uplifted continental block) to sedimentary rocks from other tectonic environments.Lithos,27 (2), 115-131.

[4] Berner, R. A. (1992). Weathering, plants, and the long-term carbon cycle.Geochimica et Cosmochimica Acta,56 (8), 3225-3231.

[5] Stallard, R. F. (1992). 6 Tectonic Processes, Continental Freeboard, and the Rate-controlling Step for Continental Denudation.International Geophysics, 50, 93-121.

[6] Johnsson, M. J. (1993). The system controlling the composition of clastic sediments.Geological Society of America Special Papers,284, 1-20.

[7] White, A. F., and Blum, A. E. (1995). Effects of climate on chemical weathering in watersheds.Geochimica et Cosmochimica Acta,59 (9), 1729-1747.

[8] Nesbitt, H. W., and Young, G. M. (1996). Petrogenesis of sediments in the absence of chemical weathering: effects of abrasion and sorting on bulk composition and mineralogy. Sedimentology,43 (2), 341-358.

[9] Sawyer, E. W. (1986). The influence of source rock type, chemical weathering and sorting on the geochemistry of clastic sediments from the Quetico metasedimentary belt, Superior Province, Canada.Chemical Geology,55 (1-2), 77-95.

[10] Taylor, S. R., and McLennan, S. M. (1985). The continental crust: its composition and evolution. Blackwell Scientific Publication, Carlton, 312p.

[11] Milliken, K. L., and Mack, L. E. (1990). Subsurface dissolution of heavy minerals, Frio Formation sandstones of the ancestral Rio Grande Province, South Texas.Sedimentary Geology, 68(3), 187-199.

[12] Fralick, P. W., and Kronberg, B. I. (1997). Geochemical discrimination of clastic sedimentary rock sources.Sedimentary Geology,113 (1-2), 111-124.

[13] McCann, T. (1998). Sandstone composition and provenance of the Rotliegend of the NE German Basin.Sedimentary Geology,116 (3-4), 17.

[14] Dickinson, W. R., and Suczek, C. A. (1979). Plate tectonics and sandstone compositions.Aapg Bulletin,63 (12), 2164-2182.

[15] Bhatia, M. R. (1983). Plate tectonics and geochemical composition of sandstones.The Journal of Geology,91(6), 611-627.

[16] Bhatia, M. R., and Crook, K. A. (1986). Trace element characteristics of graywackes and tectonic setting discrimination of sedimentary basins.Contributions to mineralogy and petrology,92 (2), 181-193.

[17] Roser, B. P., and Korsch, R. J. (1988). Provenance signatures of sandstone-mudstone suites determined using discriminant function analysis of major-element data.Chemical geology, 67(1-2), 119-139.

[18] Feng, R., and Kerrich, R. (1990). Geochemistry of fine-grained clastic sediments in the Archean Abitibi greenstone belt, Canada: implications for provenance and tectonic setting.Geochimica et Cosmochimica Acta,54 (4), 1061-1081.

[19] McLennan, S. M. (1982). On the geochemical evolution of sedimentary rocks.Chemical Geology,37(3-4), 335-350.

[20] Cox, R., and Lowe, D. R. (1995). A conceptual review of regional-scale controls on the composition of clastic sediment and the co-evolution of continental blocks and their sedimentary cover.Journal of Sedimentary Research,65 (1).

[21] Tripathi, J. K., and Rajamani, V. (1999). Geochemistry of the loessic sediments on Delhi ridge, eastern Thar desert, Rajasthan: implications for exogenic processes.Chemical Geology,155 (3), 265-278.

[22] Tripathi, J. K., and Rajamani, V. (2007). Geochemistry and origin of ferruginous nodules in weathered granodioritic gneisses, Mysore Plateau, Southern India.Geochimica et Cosmochimica Acta,71(7), 1674-1688.

[23] Lupker, M., France-Lanord, C., Galy, V., Lave, J., Gaillardet, J., Gajurel, A. P., ... and Sinha, R. (2012). Predominant floodplain over mountain weathering of Himalayan sediments (Ganga basin).Geochimica et Cosmochimica Acta,84, 410-432.

[24] Cullers, R. (1988). Mineralogical and chemical changes of soil and stream sediment formed by intense weathering of the Danburg granite, Georgia, USA.Lithos,21 (4), 301-314.

[25] Stewart, A. D. (1993). The ratio of mechanical to chemical denudation in alluvial systems, derived from geochemical mass balance.Transactions of the Royal Society of Edinburgh: Earth Sciences,84 (01), 73-78.

[26] Rollinson, H. R. (1993). A terrane interpretation of the Archaean Limpopo Belt.Geological Magazine,130(06), 755-765.

[27] Singh, M., Sharma, M., and Tobschall, H. J. (2005). Weathering of the Ganga alluvial plain, northern India: implications from fluvial geochemistry of the Gomati River. Applied Geochemistry, 20(1), 1-21.

[28] Seyler, P. T., and Boaventura, G. R. (2001). Trace elements in the mainstream Amazon River.The Biochemistry of the Amazon Basin. Oxford University Press, Oxford, UK, 534.

[29] Nesbitt, H. W., and Young, G. M. (1982). Early Proterozoic climates and plate motions inferred from major element chemistry of lutites. Nature, 299, 715-717.

[30] Nesbitt, H. W., and Young, G. M. (1984). Prediction of some weathering trends of plutonic and volcanic rocks based on thermodynamic and kinetic considerations.Geochimica et Cosmochimica Acta,48(7), 1523-1534.

[31] Fedo, C. M., Nesbitt, H. W., and Young, G. M. (1995). Unraveling the effects of potassium metasomatism in sedimentary rocks and paleosols, with implications for paleoweathering conditions and provenance.Geology, 23(10), 921-924.

[32] Fedo, C. M., Eriksson, K. A., Krogstad, E. J. (1996). Geochemistry of shales from the Archean ($\sim$ 3.0 Ga) Buhwa Greenstone Belt, Zimbabwe: implications for provenance and source-area weathering.Geochimica et Cosmochimica Acta,60(10), 1751-1763.

[33] Nesbitt, H. W., Young, G. M., McLennan, S. M., and Keays, R. R. (1996). Effects of chemical weathering and sorting on the petrogenesis of siliciclastic sediments, with implications for provenance studies.The Journal of Geology,104(5), 525-542.

[34] Bock, B., McLennan, S. M., and Hanson, G. N. (1998). Geochemistry and provenance of the middle Ordovician Austin Glen member (Normanskill formation) and the Taconian orogeny in New England.Sedimentology,45(4), 635-655.

[35] Roddaz, M., Viers, J., Brusset, S., Baby, P., Boucayrand, C., and Herail, G. (2006). Controls on weathering and provenance in the Amazonian foreland basin: insights from major and trace element geochemistry of Neogene Amazonian sediments.Chemical Geology,226(1), 31-65.

[36] Schoenborn, W. A., and Fedo, C. M. (2011). Provenance and paleoweathering reconstruction of the Neoproterozoic Johnnie Formation, southeastern California.Chemical Geology,285(1), 231-255.

[37] McLennan, S. M., Hemming, S., McDaniel, D. K., and Hanson, G. N. (1993). Geochemical approaches to sedimentation, provenance, and tectonics.Geological Society of America Special Papers,284, 21-40.

[38] Nesbitt, H. W., and Young, G. M. (1989). Formation and diagenesis of weathering profiles.The Journal of Geology, 97(2), 129-147.

[39] Singh, M., Sharma, M., and Tobschall, H. J. (2005). Weathering of the Ganga alluvial plain, northern India: implications from fluvial geochemistry of the Gomati River. Applied Geochemistry, 20(1), 1-21.

[40] Jian, X., Guan, P., Zhang, W., and Feng, F. (2013). Geochemistry of Mesozoic and Cenozoic sediments in the northern Qaidam Basin, northeastern Tibetan Plateau: Implications for provenance and weathering. Chemical Geology, 360, 74-88.

[41] Grant, W. H. (1963).Weathering of Stone Mountain granite, in Ingersol, E., ed., Clays and Clay Minerals: Oxford, Pergamon. 65-73.

[42] Aristizabal, E., Roser, B., and Yokota, S. (2005). Tropical chemical weathering of hillslope deposits and bedrock source in the Aburrlley, northern Colombian Andes.Engineering Geology,81(4), 389-406.

[43] Singh, S. K., and France-Lanord, C. (2002). Tracing the distribution of erosion in the Brahmaputra watershed from isotopic compositions of stream sediments.Earth and Planetary Science Letters,202(3), 645-662.

Chapter 8

Total Suspended Matter and Particulate Flux

8.1 Total Suspended Matter and Particulate Flux

Rivers are the most important agents of continental erosion and play central role in sediment transfer from continents to oceans as shown in Table 8.1. Fluvial transport of materials to the world oceans has been studied for decades and is important in the context of geochemical cycling of elements. The world's rivers carry about 35000 km^3 water [1], 15.5 billion tons of sediment [2] and 3.5 billion tons of total dissolved solids [3] to the world oceans every year. Chemical and physical weathering result in dissolved and suspended flux carried by rivers, respectively. Continental erosion and transport of the eroded materials by rivers into the world oceans is of global significance. Many earth-related processes like crustal evolution, biogeochemical cycling, soil formation, etc., can be understood by studying both the nature and the amount of materials transferred by rivers to the oceans. Suggestions that chemical and physical denudation can disturb global geochemical cycle and thus global climate has further reiterated the need for a better understanding of fluvial processes in general and factors controlling denudation rates in particular. Though it is difficult to estimate the palaeoflux of the sediment to the oceans, [4] argue that the present day global sediment flux are at least 100% higher than 2,000 years ago when there

Transport Mechanism	Global Flux (billion tons/year)
Rivers: suspended and bed load	18
Bed load	2
Dissolved flux	5
Glaciers, sea ice, icebergs	2
Wind	0.7
Coastal erosion	0.4

Table 8.1: Global estimate of sediment flux from land to ocean [16].

was less human influence.

On a global scale, the Ganga- Brahmaputra river system ranks first in terms of sediment transport and fourth in terms of water discharge to the world oceans [5, 6]. The Ganga- Brahmaputra-Meghna (G-B-M) river system carries annually an estimated 1060 million tons of suspended solids, more than 1330 km^3 of water, and more than 173 million tons of total dissolved flux to the Bay of Bengal [2]. It is the largest sediment dispersal system in the world [7] and shows the highest rate of chemical denudation in the Bengal Basin on a global scale [8] and yet because of its remote location, research on sediment transport and accumulation has been limited [9, 10]. In the Brahmaputra basin ,seasonal overbank flooding [11] and high flood stages [12] result from annual monsoons, which have a primary impact on river flow and sediment discharge; 80% of the annual water discharge and 95% of the annual sediment load is debouched during the four summer monsoon months [13]. It is estimated that the bedload flux for the Ganges-Brahmaputra is only 10% of the suspended load flux, although the actual bedload flux remains undocumented [14, 15, 4].

However, the recent human activities like changing river courses and setting obstacles by constructing dams have had a significant impact on the natural erosion rates and sediments fluxes. Several workers estimated global sediment flux, few significant estimates have been shown in Table 8.2. Meade cautions that these estimates may not be the exact representative of the true flux into oceans. He argues that a significant amount of sediments could undergo deposition in the deltas. For instance,

Global sediment flux (billion tons/year)	Estimated by
18.3	Holeman (1986) [5]
20	Holland (1981) [17]
18	Milliman and Syvitski (1992) [4]

Table 8.2: Global sediment flux estimated by different workers.

in case of the Ganga and the Brahmaputra River, 55% of their combined annual sediment load (1.1 billion tons/year) is retained by their delta, with 36% reaching the continental shelf and 9% reaching the deep sea [16].
Factors controlling variations in river sediment loads include runoff, relief, geology, basin area and temperature [18]. Reservoir construction by humans exerts heavy influence. The authors of [19] estimated that large reservoirs trap 30% of the global sediment flux.
The authors of [20] compiled the various estimates of land-ocean sediment transfer by rivers worldwide. The estimates range from 12.6 to 24 billion tons/year with a commonly accepted value of around 15 billion tons/year. The major contributors of suspended sediments to the oceans in terms of their decreasing importance are the Amazon, the Huanghe (Yellow River), the Ganga and Brahmaputra and the Yangtze. Southern Asia, the large Pacific and Indian Ocean islands contribute a whopping 70% of the total world suspended sediment load. Unfortunately, monitoring mechanisms for the rivers draining these areas are poorly developed. This major drawback is a potential contributing factor to the high uncertainty levels in estimating the global sediment flux to the oceans.

8.1.1 Importance of qualitative and quantitative approach towards suspended load analysis

The total suspended matter is one of the important parameters in the river basin study. It is very important in calculating the particulate flux of the river. The qualitative and quantitative approaches in the analysis of suspended load transported by World Rivers allow us to:

1. Assess the continental crust recycling [21, 22].

2. Estimate the rates at which the continents are denudating [6, 23, 24, 20].

3. A sincere step towards long term climate moderation is evident from the recent attention paid to the study of transport of suspended sediments by rivers in relation to silicate weathering [25, 26, 27].

4. Characterise the major parameters exercising a control over these denudation rates [28], and

5. Assess anthropogenic influences, by the virtue of large surface areas offered by the sediments for the sorption of metal pollutants arising out of human activities [29, 30].

In this background, the Brahmaputra mainstream as well as the Himalayan tributaries of the Brahmaputra River that join from the north (the Subansiri, the Jia Bharali and the Pagladia) and south bank tributaries (the Burhi dihing, the Dikhow and the Kopili) were studied in terms sediment chemistry and associated particulate flux, and individual elemental contribution from each tributary into the Brahmaputra basin. The suspended sediment concentrations are used to assess the suspended load of the mainstream and the tributaries. Total suspended matter was sampled as discussed in Chapter 3. Sediment discharge estimates are calculated to determine each tributary's contribution to the suspended load of the entire river system. The instantaneous suspended sediment loads during the monsoon season are used to estimate the annual suspended sediment load for the system. To calculate the particulate flux of any river at any point on the river, the total suspended matter (TSM) in mg/l or g/l is multiplied by discharge value of that particular river at that particular point.
Calculations of suspended sediment load were determined by:

$$L_s = Q_t C_j \tag{8.1}$$

where L_s is suspended sediment load (kgs^{-1}) or particulate flux (tonnes/yr) , Q_t is discharge at time interval i (m^3s^{-1}), and C_j is suspended sediment concentration at time interval i ($mg\ l^{-1}$). Sediment yield was determined by dividing the load by the basin area at each site. Thus, we see that the sediment transport is a function of total suspended matter and river discharge. The annual average discharge data provided by source [31, 32, 33] are used here.

Particulate Fluxes of Individual Element

Based on suspended sediment geochemistry data shown in Table 8.5, the fluxes of each element is computed.. Four pieces of information was needed for the actual calculation of elemental fluxes: (1) discharge (m^3s^{-1})); (2) suspended sediment concentration (mg l^{-1}); (3) suspended sediment-associated trace element concentration (mg l^{-1}); and (4) filtered water-associated (dissolved) trace element concentration (mg l^{-1}) [34, 35]. The flux of each major and trace element was calculated using the following formula:

$$\text{Flux (tonnes per year)} = Q(\text{m}^3\text{s}^{-1})\text{conc.}(\text{mgl}^{-1})(0.0864)(365.24) \qquad (8.2)$$

Where Q= discharge, conc. = suspended sediment concentration, dissolved constituent concentration. The flux is reported in tonnes per year. The suspended sediment-associated major and trace element fluxes were estimated using the same formula after recalculation of the concentration from mass mass^{-1} units to mass volume^{-1} units as follows:

$$\text{Element Conc.}(\text{mgl}^{-1}) = \text{Element conc.}(\mu\text{gg}^{-1})\text{TSS conc.}(\text{gl}^{-1})\frac{1}{1000} \qquad (8.3)$$

where TSS conc. = total suspended sediment concentration. (NASQAN programme)

8.2 Results and Discussion

Total Suspended Matter and Particulate Flux The particulate flux of the Brahmaputra and the tributaries i.e. Subansiri, Jiabharali, Pagladia, Burhidihing and Kopili (Discharge data for Dikhow could not be found) during monsoon, 2013 are shown in Table 8.3. Particulate flux of monsoon 2013 was compared with earlier works done by [36, 5, 12, 6] in the Bangladesh part of the Brahmaputra in Table 8.4. The high intensity of monsoonal rains,easily erodible tertairy rocks of the Himalayan ranges,steep slopes,high incidence of landslides and high seismicity in the baisn have rendered the river a high sediment laden one [37]. Besides the natural sources ,

Sample ID	TSM (mg/l)	TDS (mg/l)	Discharge (m^3s^{-1})	Flux (10^6 tonnes/yr)	Total basin area (10^5 km^2)	Discharge per unit area (cumecs/km^2) $\times 10^3$	Sediment yield (tonnes/ yr/km^2)
PSG	623	62.5	6338	0.125	2.46	2.58	0.507
DBRG	663	47	10235	0.214	2.98	3.43	0.719
TEZ	396	63.5	12456	0.156	3.07	4.06	0.507
GHY	511	63.5	18094	0.291	4.05	4.47	0.720
DHBR	575	44	21231	0.385	6.36	3.34	0.606
BHD	371	60	444	0.005	0.08	5.55	0.649
KPL	52	80	887	0.001	0.16	5.54	0.090
DKW	nm	60	nm	nm	nm	-	nm
SBN	547	66.7	1711	0.029	0.33	5.18	0.894
PGL	542	60	1734	0.030	0.01	0.05	3.115
JBR	555	60	824	0.014	0.12	6.87	1.201

Table 8.3: Hydrological features and particulate flux of the Brahmaputra River and its tributaries (Monsoon). Nm ≡ not measured.

Main river channel (in Bangladesh)	Instantaneous load (g/s)	Annual load (tonnes/yr)	
Ganges	2.36×10^7	2.62×10^8	Rice, 2007
Brahmaputra	3.50×10^7	3.87×10^8	Rice, 2007
Brahmaputra		8×10^8	Holeman, 1968
Brahmaputra		6.17×10^8	Coleman, 1969
Brahmaputra		11.57×10^8	Milliman and Meade, 1983
Brahmaputra (in Assam, India)			
Pasighat	0.4×10^7	1.24×10^8	In study
Dibrugarh	0.7×10^7	2.14×10^8	In study
Tezpur	0.5×10^7	1.6×10^8	In study
Guwahati	0.9×10^7	2.9×10^8	In study
Tributaries			
Burhi Dihing	0.017×10^7	5.19×10^8	In study
Kopili	0.005×10^7	1.45×10^8	In study
Subansiri	0.09×10^7	0.094×10^8	In study
Pagladia	0.051×10^7	0.05×10^8	In study
Jiabharali	0.046×10^7	0.046×10^8	In study

Table 8.4: Calculations of annual suspended sediment loads.

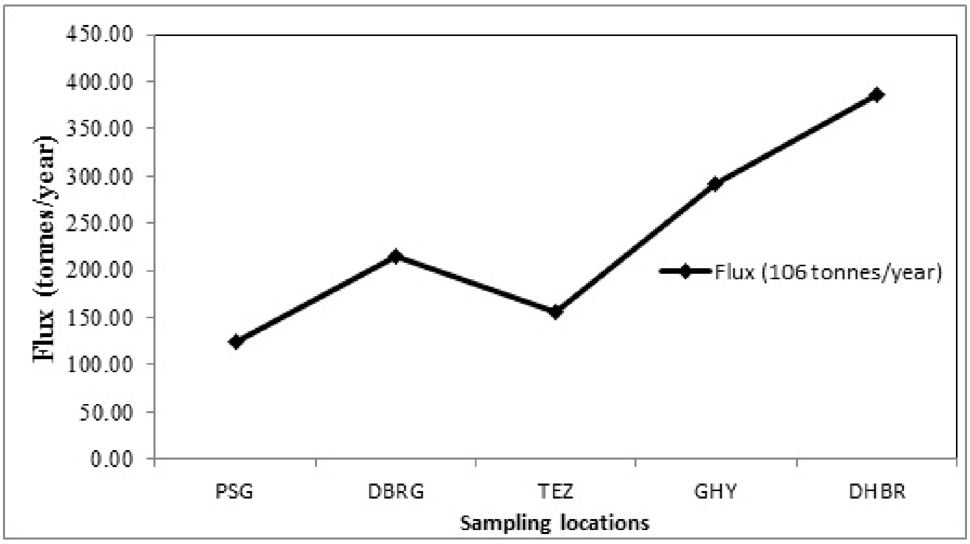

Figure 8.1: Total particulate flux during monsoon along the Brahmaputra river.

some human activities also contribute to the high sediment loads e.g. Jhuming , the shifting cultivation practiced in the mountanious areas in Arunachal Pradesh and southern Assam ranges.Heavy bank erosion by the Brahmapura river takes place at differnt reaches owing to excessive sedimnet load , erodible nature of the bank material , formaition of char island and consequent development banks [38]. In the Brahmaputra river load increased downstream and was probably due to tributary contribution and high bank erosion. Bank material of the Brahmaputra are mostly composed of dominant fine sand and silt with clay being less than 5% as found in our study.

The authors of [39] determined total suspended matter as 348 mg/l in Guwahati during monsoon,1977. In this study we measured a total suspended matter of 511 mg/l in Guwahati during monsoon, 2013. Based on this comparison we can surmise that there is an increase in the sediment flux of the Brahmaputra. Increase in sediment flux can be attributed to human activities in the catchment.

The authors of [40] reported that sediment load was more variable than water discharge in the Brahmaputra during 1971-79.

Particulate Fluxes of Individual Element

The suspended flux of the Brahmaputra and its tributaries were compared with suspended sediment average composition of world rivers reported by [41] and has been shown in Table 8.5. Figure 8.2 and 8.3 show suspended sediment global average concentration normalised plot of the Brahmaputra and its tributaries.

Element	unit	World average concentration of suspended sediments	PSG	DBRG	TEZ	GHY	DHBR	BHD	KPL	DKW	SBN	JBR	PGL
Al	%	8.72	8.2	7.8	9.6	8.8	8.8	8.4	7.8	10.1	8.3	9.8	9.1
Ca	%	2.59	1.7	2.4	1.6	1.7	1.7	0.8	1.3	0.5	1.0	3.4	0.4
Fe	%	5.81	4.8	5.8	5.9	5.9	5.6	6.0	6.0	6.3	5.1	7.6	4.7
K	%	1.69	2.9	2.0	2.8	2.4	2.4	2.0	2.3	2.2	2.4	2.5	2.5
Mg	%	1.26	1.5	2.2	1.7	2.0	1.8	1.8	2.0	1.2	1.1	3.3	0.9
Mn	%	0.16	0.1	0.1	0.1	0.1	0.1	0.1	0.1	0.1	0.1	0.1	0.1
Na	%	0.71	1.3	1.4	1.3	1.3	1.3	0.9	1.0	0.7	1.2	2.0	0.6
P	%	0.20	0.1	0.1	0.1	0.1	0.1	0.1	0.1	0.1	0.3	0.2	0.1
Si	%	25.4	29.2	29.7	26.9	28.2	27.9	28.6	25.9	26.8	28.8	23.2	30.6
Ti	%	0.44	0.4	0.5	0.5	0.5	0.5	0.5	0.5	0.6	0.4	0.6	0.5
Ba	μg/g	522	199.5	207.5	197.1	791.8	196.0	181.8	250.1	133.4	177.2	207.9	162.0
Co	μg/g	22.5	4.2	5.2	4.8	5.2	4.9	5.4	5.1	5.7	4.4	4.8	3.0
Cr	μg/g	130	32.6	47.9	38.2	45.1	46.4	65.4	56.9	65.3	32.5	56.7	25.1
Sr	μg/g	187	61.0	66.1	57.6	57.9	55.5	36.5	42.8	40.1	52.2	62.1	49.3
V	μg/g	129	23.6	30.6	26.8	28.4	28.0	28.8	27.4	36.9	24.0	42.2	18.3
Zn	μg/g	208	39.7	37.9	54.3	50.2	50.3	49.7	40.9	50.5	41.5	58.0	37.1

Table 8.5: The chemical composition of the suspended sediments and world average concentration of suspended sediments (world average concentration of suspended sediments from [41]).

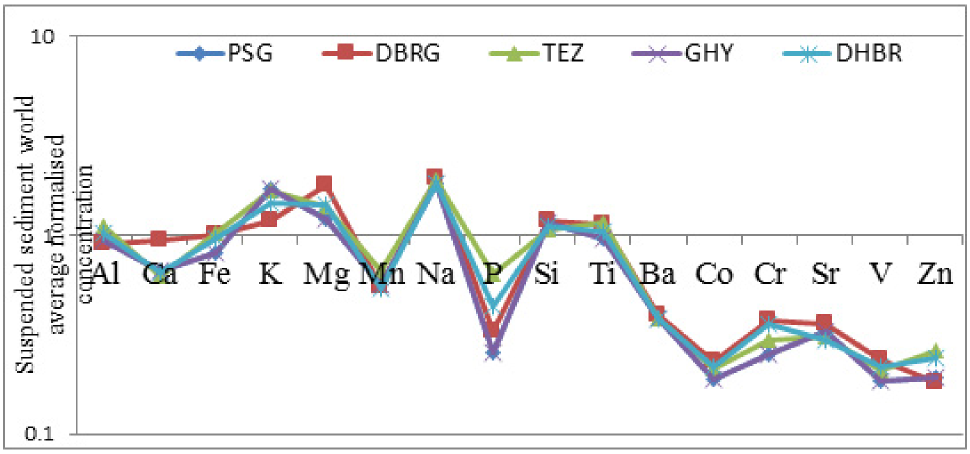

Figure 8.2: Suspended sediment global average concentration normalised plot of the Brahmaputra river.

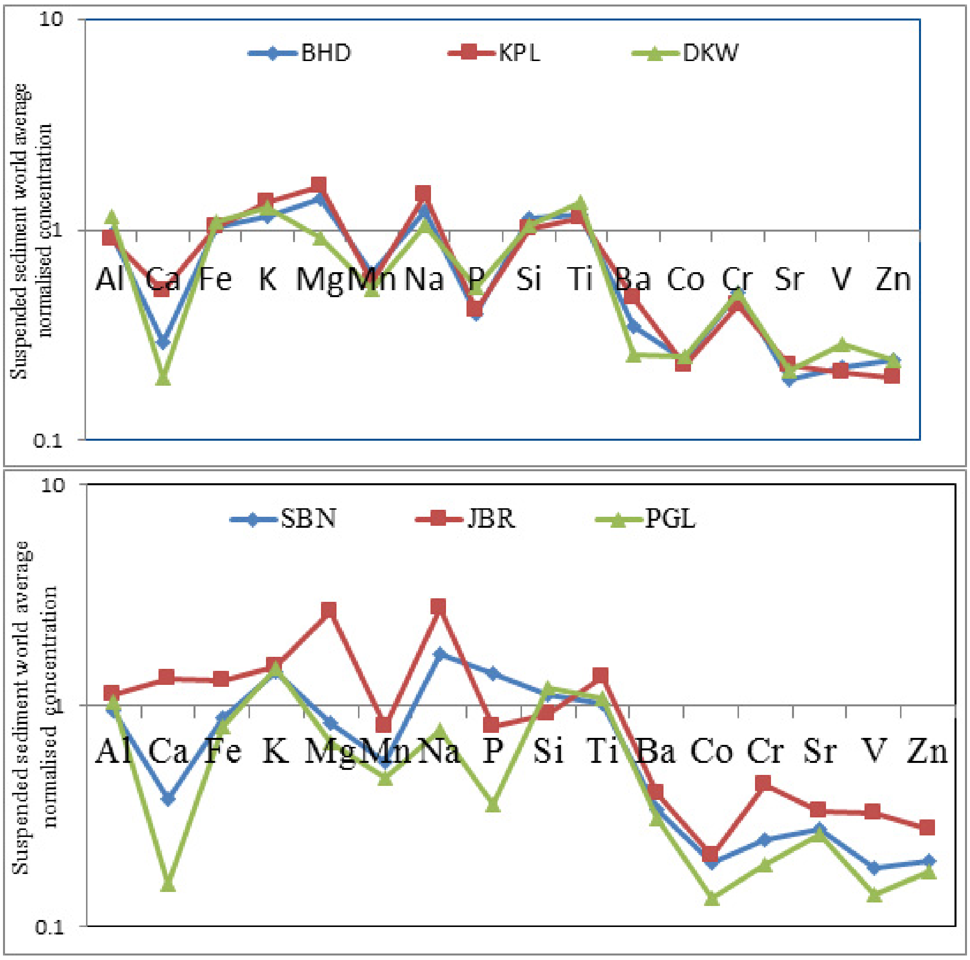

Figure 8.3: The upper and lower panels show the suspended sediment global average concentration normalised plot of the southern and northern Himalayan tributaries respectively.

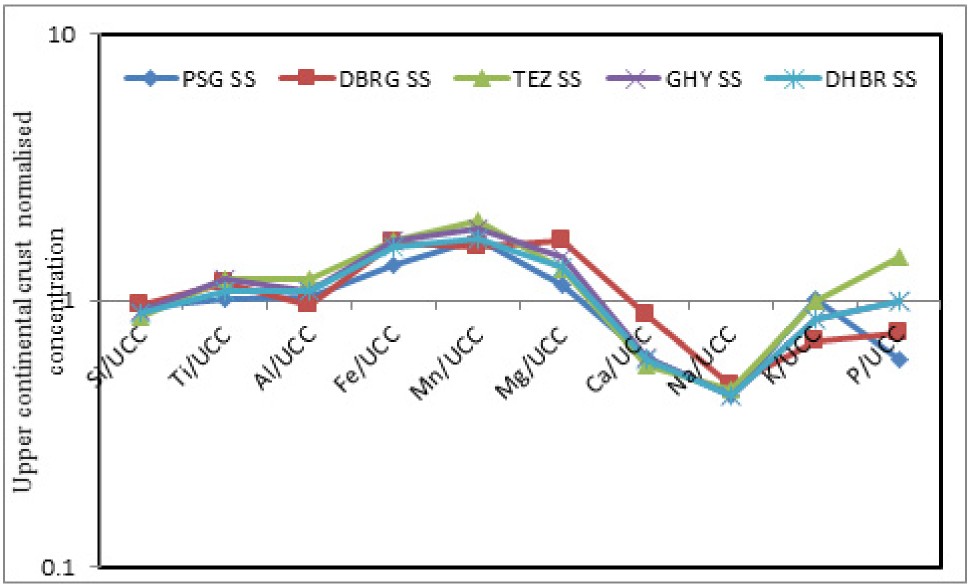

Figure 8.4: Upper continental crust concentration normalised plot of the Brahmaputra river.

From Figure 8.2 we can infer that aluminium, potassium, iron, magnesium, sodium, silicon and titanium are enriched in the Brahmaputra River sample compared to the world average concentration. Manganese and phosphorus are generally depleted in the river. Aluminium, potassium and sodium were found to be enriched may be due to clay minerals in the suspended sediments. Calcium is depleted in the Brahmaputra River unlike the Ganga River where calcium is enriched compared to World Rivers. All the analysed trace elements are depleted than that of the world average concentration.

The south bank tributaries show enrichment in aluminium, iron, potassium, magnesium sodium, manganese, silicon and titanium. All the analysed trace elements are depleted than the world average concentration. Unlike the north bank tributaries, the south bank tributaries showed a similar trend in major and trace elements.

Aluminium, potassium, silicon and titanium were found to be enriched in the north bank tributaries. In the Pagladia, all major elements except aluminium, potassium, titanium and silicon are depleted to the world average concentration (this may be due to its source in the Siwaliks which is made up of recycled sediments). In the Jiabharali all major elements are enriched except manganese and phosphorus. All the analysed trace elements are depleted than the world average concentration. Chemical composition of suspended sediments of the northern Himalayan tributaries

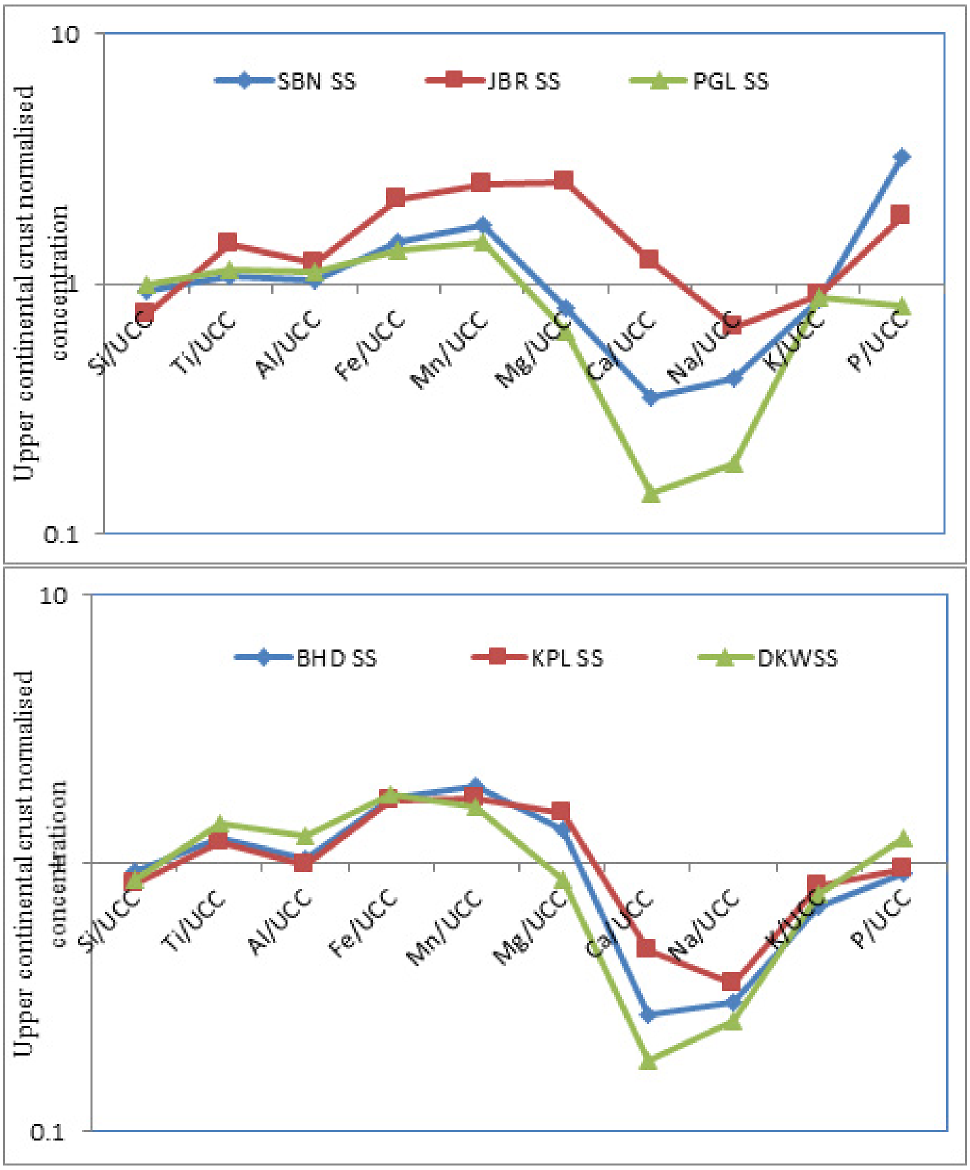

Figure 8.5: The upper and lower panels show the suspended sediment global average concentration normalised plot of the Southern and northern Himalayan tributaries respectively

Flux (tonnes/ yr)x 106	PSG	DBRG	TEZ	GHY	BHD	KPL	SBN	JBR	PGL
Si	36.4	63.6	41.9	82.13	1.49	0.37	8.5	3.35	4.92
Al	10.3	16.7	15	25.54	0.43	0.11	2.46	1.41	1.45
Ca	2.1	5.2	2.5	5.02	0.04	0.02	0.29	0.5	0.06
Fe	5.9	12.4	9.2	17.2	0.31	0.09	1.52	1.1	0.76
Mg	1.9	4.8	2.7	5.7	0.09	0.03	0.31	0.48	0.14
Mn	0.1	0.2	0.2	0.29	0.01	0	0.03	0.02	0.01
P	0.1	0.1	0.2	0.25	0	0	0.08	0.02	0.01
Ti	0.5	1.1	0.8	1.46	0.03	0.01	0.13	0.09	0.08
K	3.6	4.2	4.4	6.97	0.1	0.03	0.71	0.37	0.4
Na	1.6	2.9	2.1	3.71	0.05	0.01	0.36	0.28	0.09
Co	0.001	0.001	0.001	0.002	0.00003	7.00E-06	0.0001	0.0001	0
Cr	0.004	0.01	0.006	0.013	0.00034	8.00E-05	0.001	0.0008	0.0004
V	0.003	0.007	0.004	0.008	0.00015	4.00E-05	0.0007	0.0006	0.0003
Zn	0.005	0.008	0.008	0.015	0.00026	6.00E-05	0.0012	0.0008	0.0006
Ba	0.025	0.044	0.031	0.231	0.00094	4.00E-04	0.0052	0.003	0.0026
Sr	0.008	0.014	0.009	0.017	0.00019	6.00E-05	0.0015	0.0009	0.0008

Table 8.6: Elemental flux of the rivers in tonnes/yr $\times 10^6$.

of the Ganga River was also compared with the upper continental crust (UCC) value of [21]. Figure 8.4 and 8.5 show UCC normalised plot of suspended sediment of the Brahmaputra, the southern tributaries and northern Himalayan tributaries, respectively.. All major elements show enrichment except calcium and sodium in the Brahmaputra river sediments. In the south bank tributaries all major elements are enriched except calcium, sodium and potassium. In north bank tributaries almost all elements (major) were enriched. This suggest that the suspended sediments were transported through physical erosion and have undergone less chemical weathering.

It can be observed from Table 8.6 and Figure 8.6 that the elemental flux of the Himalayan tributaries (the Subansiri, the Jiabharali and the Pagladia) was more than that of the southern tributaries (the Burhi dihing, the Dikhow and the Kopili). Out of all the rivers the Subansiri River contributes the maximum elemental load to the mainstream. With the dam under construction in this river, the effect on suspended flux on the Brahmaputra needs to be further investigated after the completion of the dam.

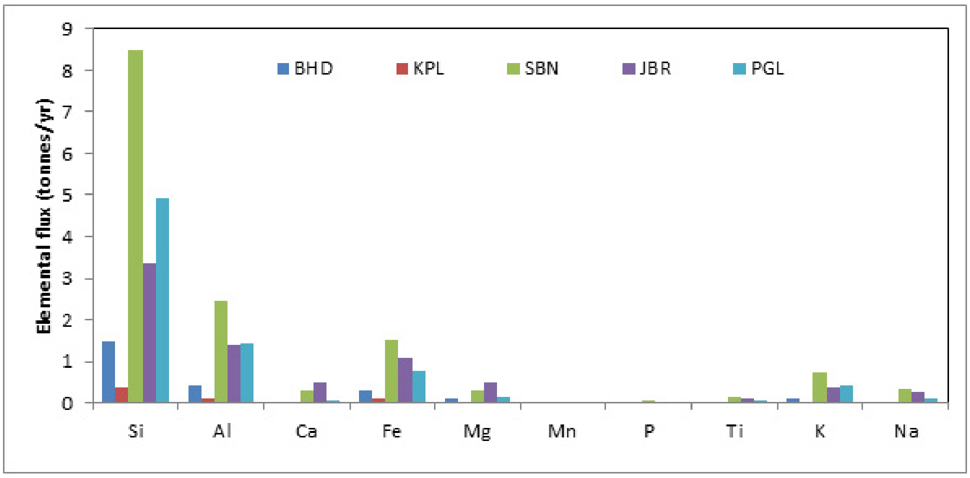

Figure 8.6: Elemental flux of the rivers in tonnes/yr $\times 10^6$.

8.3 Conclusion

Chemical composition of suspended sediments of the Brahmaputra river and its tributaries was compared with suspended sediment average composition of world rivers reported by [41] (Table 8.5). The heavy metals were depleted compared to the world average which suggests the unpolluted state of these rivers. In the Brahmaputra river load increased downstream and was probably due to (a) increased drainage area and tributary contribution and/or (b) high bank erosion and sediment remobilisation. In the Brahmaputra river load increased downstream and was probably due to tributary contribution and high bank erosion. Bank material of the Brahmaputra are mostly composed of dominant fine sand and silt with clay being less than 5% as found in our study. It was observed that the elemental and particulate flux for north bank tributaries was more than the south bank tributaries - flux in the Subansiri River was found to be highest among the tributaries. The high rate of the sediment yield in the Himalayan tributaries is probably due to the fact that the drainage basin of these rivers is characterised by erodible sedimentary rocks. With the dam under construction in the Subansiri River, the effect on suspended flux on the Brahmaputra needs to be further investigated after the completion of the dam. The suspended sediments have undergone very little chemical weathering in all the rivers and physical erosion seemed to be the dominant factor contributing to the suspended load.

Bibliography

[1] Milliman, J. D. (1991). Flux and fate of fluvial sediment and water in coastal seas.Ocean margin processes in global change, 69-89.

[2] Milliman, J. D., Rutkowski, C. M., and Meybeck, M. (1995).River discharge to the sea: a global river index (GLORI). School of Marine Science, Virginia Institute of Marine Science, College of William and Mary.

[3] Meybeck, M. (1976). TOTAL MINERAL DISSOLVED TRANSPORT BY WORLD MAJOR RIVERS/Transport en sels dissous des plus grands fleuves mondiaux.Hydrological Sciences Journal,21 (2), 265-284.

[4] Milliman, J. D., and Syvitski, J. P. (1992). Geomorphic/tectonic control of sediment discharge to the ocean: the importance of small mountainous rivers.The Journal of Geology,100 (5), 525-544.

[5] Holeman, J. N. (1968). The sediment yield of major rivers of the world.Water Resources Research,4 (4), 737-747.

[6] Milliman, J. D., and Meade, R. H. (1983). World-wide delivery of river sediment to the oceans.The Journal of Geology,91 (1), 1-21.

[7] Kuehl, S. A., Hariu, T. M., and Moore, W. S. (1989). Shelf sedimentation off the Ganges-Brahmaputra river system: Evidence for sediment bypassing to the Bengal fan.Geology,17 (12), 1132-1135.

[8] Datta, D. K., and Subramanian, V. (1997). Nature of solute loads in the rivers of the Bengal drainage basin, Bangladesh.Journal of Hydrology,198 (1), 196-208.

[9] Barua, D. K., Kuehl, S. A., Miller, R. L., and Moore, W. S. (1994). Suspended sediment distribution and residual transport in the coastal ocean off the Ganges-Brahmaputra river mouth.Marine Geology,120 (1-2), 41-61.

[10] Goodbred, S. L., and Kuehl, S. A. (1999). Holocene and modern sediment budgets for the Ganges-Brahmaputra river system: Evidence for highstand dispersal to flood-plain, shelf, and deep-sea depocenters.Geology,27 (6), 559-562.

[11] Allison, M. A., Kuehl, S. A., Martin, T. C., and Hassan, A. (1998). Importance of flood-plain sedimentation for river sediment budgets and terrigenous input to the oceans: Insights from the Brahmaputra-Jamuna River.Geology,26 (2), 175-178.

[12] Coleman, J. M. (1969). Brahmaputra River: channel processes and sedimentation.Sedimentary Geology,3 (2-3), 129-239.

[13] Goodbred, S. L. (2003). Response of the Ganges dispersal system to climate change: a source-to-sink view since the last interstade.Sedimentary Geology,162 (1), 83-104.

[14] Galy, A., and France-Lanord, C. (2001). Higher erosion rates in the Himalaya: Geochemical constraints on riverine fluxes.Geology,29 (1), 23-26.

[15] Lane, E. W., and Borland, W. M. (1951). Estimating bed load.Eos, Transactions American Geophysical Union,32 (1), 121-123.

[16] Syvitski, J. P. (2003). Supply and flux of sediment along hydrological pathways: research for the 21st century.Global and Planetary Change, 39 (1), 1-11.

[17] Holland, H. D. (1981). River transport to the oceans.The Sea. The Ocean Lithosphere,7, 763-800.

[18] Chakrapani, G. J. (2005). Factors controlling variations in river sediment loads.Current Science,88 (4), 569-575.

[19] Vorosmarty, C. J., Sharma, K. P., Fekete, B. M., Copeland, A. H., Holden, J., Marble, J., and Lough, J. A. (1997). The storage and aging of continental runoff in large reservoir systems of the world. Ambio 26: 210-219.

[20] Walling, D. E. (2006). Human impact on land-ocean sediment transfer by the world's rivers.Geomorphology,79 (3), 192-216.

[21] Taylor, S. R., andS. M. McLennan(1985),The Continental Crust: Its Composition And Evolution, Blackwell,Malden, Mass.

[22] Goldstein, S. J., and Jacobsen, S. B. (1988). Nd and Sr isotopic systematics of river water suspended material: implications for crustal evolution.Earth and Planetary Science Letters,87 (3), 249-265.

[23] Walling, D. E., and Fang, D. (2003). Recent trends in the suspended sediment loads of the world's rivers.Global and Planetary Change,39 (1), 111-126.

[24] Syvitski, J. P., Vorosmarty, C. J., Kettner, A. J., and Green, P. (2005). Impact of humans on the flux of terrestrial sediment to the global coastal ocean. Science,308 (5720), 376-380.

[25] Gaillardet, J., Dupre, B., Louvat, P., and Allegre, C. J. (1999). Global silicate weathering and CO 2 consumption rates deduced from the chemistry of large rivers.Chemical geology,159 (1), 3-30.

[26] Dessert, C., Dupre, B., Gaillardet, J., Frans, L. M., and Allegre, C. J. (2003). Basalt weathering laws and the impact of basalt weathering on the global carbon cycle.Chemical Geology,202 (3), 257-273.

[27] Gislason, S. R., Oelkers, E. H., and Snorrason, A. (2006). Role of river-suspended material in the global carbon cycle.Geology,34 (1), 49-52.

[28] Allegre, C. J., Dupre, B., Negrel, P., and Gaillardet, J. (1996). Sr Nd Pb isotope systematics in Amazon and Congo River systems: constraints about erosion processes.Chemical Geology,131 (1-4), 93-112.

[29] Nriagu, J. O., and Pacyna, J. M. (1988). Quantitative assessment of worldwide contamination of air, water and soils by trace metals.nature,333 (6169), 134-139.

[30] Audry, S., Blanc, G., Schafer, J., Chaillou, G., and Robert, S. (2006). Early diagenesis of trace metals (Cd, Cu, Co, Ni, U, Mo, and V) in the freshwater

reaches of a macrotidal estuary.Geochimica et Cosmochimica Acta,70 (9), 2264-2282.

[31] Rao, K. L. (1979).India's water wealth. Orient Blackswan.

[32] Goswami, D. C. (1998). Fluvial regime and flood hydrology of the Brahmaputra River, Assam.Memoirs-Geological Society of India, 53-76.

[33] http://www.grdc.sr.unh.edu

[34] De Vries, A., and Klavers, H. C. (1994). Riverine fluxes of pollutants: monitoring strategy first, calculation methods second.European Water Management,4 (2), 12-17.

[35] Phillips, J. M., Webb, B. W., Walling, D. E., and Leeks, G. J. L. (1999). Estimating the suspended sediment loads of rivers in the LOIS study area using infrequent samples.Hydrological processes,13 (7), 1035-1050.

[36] Rice, S. K. (2007).Suspended Sediment Transport in the Ganges-Brahmaputra River System, Bangladesh(Doctoral dissertation, Texas AM University).

[37] Bora, A. K. (2004). Fluvial geomorphology. InThe Brahmaputra Basin Water Resources. Springer Netherlands, 88-112.

[38] Datta, B., and Singh, V. P. (2004). Hydrology .In Singh V.P., Sharma N., Ojha C.S.P. (Eds.), The Brahmaputra Basin Water Resources, Kluwer Academic Publishers, Netherlands. 139-195.

[39] Subramanian, V. (1979). Chemical and suspended-sediment characteristics of rivers of India.Journal of Hydrology,44 (1-2), 37-55.

[40] Sarma, J. N. (2005). Fluvial process and morphology of the Brahmaputra River in Assam, India.Geomorphology,70 (3), 226-256.

[41] Viers, J., Dupre, B., and Gaillardet, J. (2009). Chemical composition of suspended sediments in World Rivers: new insights from a new database.Science of the total Environment,407 (2), 853-868.

Chapter 9

Organic Carbon Variation and Distribution in the Sediments

9.1 Introduction

The riverine export of carbon from land to the ocean represents a major link in the global carbon cycle. Within river drainage basins, atmospheric CO_2 is consumed by organic matter formation and chemical weathering and is transported by rivers as dissolved organic carbon, particulate organic carbon and dissolved inorganic carbon. Rivers contribute a large amount of ancient carbon and other bio-relevant materials either in a dissolved form (via chemical erosion) or solid form (via physical erosion) and annually deliver approximately 900 Tg total carbon to the world's oceans of which $\sim$ 500 Tg is organic carbon [1]. The role of continental erosion in the global carbon cycle and its influence on river carbon fluxes is likely to change with changing climates. The authors of [2] suggest that increased warming will increase run off for 75% of the world's major rivers. Estimates for the global flux of atmospheric C transported by rivers range between 500-700 Tg yr^{-1} , of which approximately 30% is DOC, 20% POC and 45% DIC. In addition to atmospheric C and estimated 80 Tg yr^{-1} of POC and 137 Tg yr^{-1} of DIC are discharged by rivers as a result of erosion of uplifted (primarily sedimentary) rocks.

9.2 Processes Controlling the Fate of Terrigenous Organic Matter

Lithology of the drainage basin , weathering rates, primary productivity, river run off and reworking of sediments influence the organic matter transport in the rivers In some studies tectonics is the major variable controlling the source of particles and solutes to rivers. Tectonic processes influence climate, the relief and degree of weathering within the drainage basin. It also impacts anthropogenic activity where people live and build roads. Particulate organic fluxes are principally governed by drainage intensity and sediments yields [3]. Vegetation and anthropogenic activities also play an important role in delivery of organic matter to the ocean. The contribution of ancient sedimentary organic carbon to suspended loads may also be higher because of anthropogenic activities and climate change [4], thereby influencing the age of the organic matter carried by rivers.

9.3 Sedimentological control of Corg loading

The amount of Corg exported by rivers results from a complex interaction between organic matter produced and decomposed within the basin and mineral particles derived from rock erosion. Physical and chemical properties of sediment must therefore exert a control on the Corg loading of sediments. However, in spite of several studies, the contribution of different factors to the control of Corg loading remains unclear. In addition, each river system is characterised by different source rocks, physical and chemical erosion rates or transport dynamics that must result indifferent Corg loading mechanisms.

Storage of organic carbon in floodplains

Floodplain storage of organic carbon is an aspect of the global carbon cycle which is not well studied or quantified [5]. Carbon is stored within the fluvial system decoupling it from the hydrologic transport in the channel. Whether erosion is a carbon source or sink depends on the relative CO_2 concentrations within the sediment and the channel. In cases of higher CO_2 concentrations in the sediment, sediment transport may result in a decrease of carbon within the sediments and therefore an export

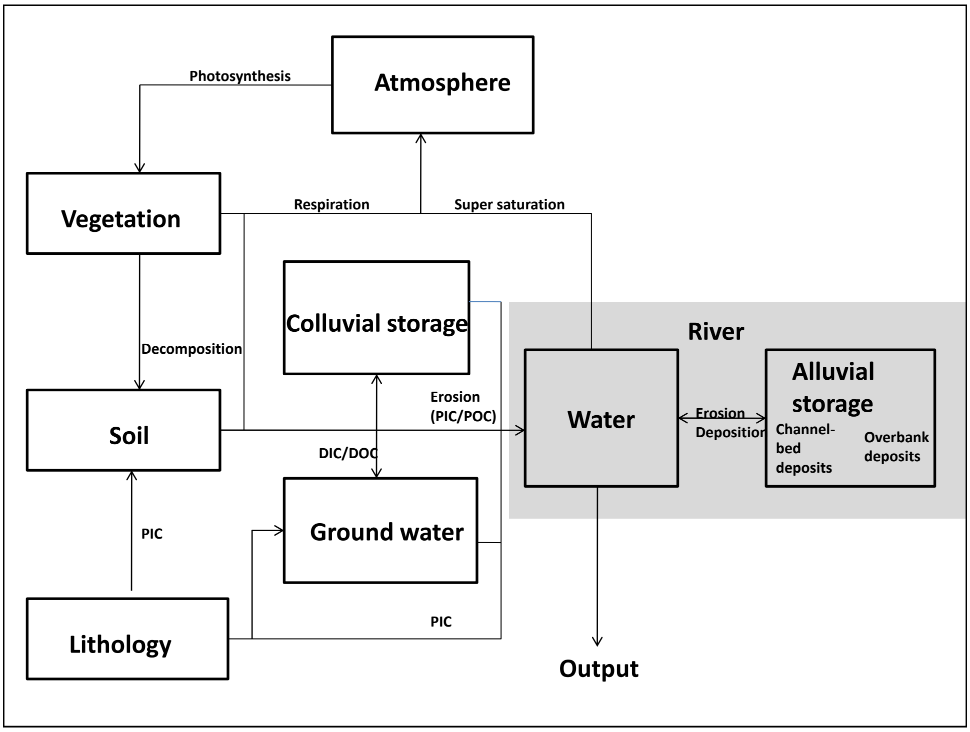

Figure 9.1: C-cycle with focus on the sediment transfer in fluvial systems. (Modified from [5]) PIC=particulate organic carbon, POC=particulate inorganic carbon, POC=particulate organic carbon, DIC=dissolved inorganic carbon, DOC=dissolved organic carbon.

to the channel. In cases of higher CO_2 concentration in the water, sediment may be enriched during the transport, resulting in a carbon sink. Due to the hillslope origin of Holocene floodplain fines and channel fill deposits, their long term storage on the floodplain lead to C sequestration within the fluvial system [5].

To date, there have been few attempts to couple investigation of overbank sediment deposition on river flood plains with an assessment of their resulting role as carbon sinks. Most assessments of the likely significance of flood plains as carbon sinks have been based on inference, that sediment deposition will result in deposition of POC. To develop an improved understanding of the role of river flood plains as carbon sinks, there is an important need to obtain more information on the organic carbon (OC) content of overbank and flood plain deposits and its spatial variability, as well as the deposition fluxes involved and rates of post-depositional oxidation or degradation of the deposited organic matter. Such work needs to be undertaken in different physiographic environments and over a range of spatial scales, in order to generate an improved understanding of the key controls and the potential for generalisation.

Himalayan erosion generates the largest sediment flux from a single continental drainage basin to the ocean. Each year 1-2 billion tons of particles are transported by the Ganga-Brahmaputra (G-B) fluvial system from the Himalayan range to the Bay of Bengal and deposited in the Bengal Fan turbiditic system. The global importance of Corg flux associated with sediment transport in the G-B fluvial system has been highlighted in previous studies on the basis of the modern river or the sedimentary record characterisations [6, 7, 8, 9, 10, 11]. The authors of [12] realised a comprehensive budget of Corg from Himalayan rocks to the Bengal Fan showing that modern burial flux of recent Corg generated by Himalayan erosion is $3.1 \pm 0.3 \times 10^{11}$ mol/yr and represents ca. 15% of the global flux and discovered that the Himalayan system is characterised by an extreme Corg burial efficiency, since almost 100% of Corg exported by G-B fluvial system is effectively buried in Bengal Fan sediments. This gives the G-B fluvial system a determinant role in terms of terrestrial Corg exportation and burial, and therefore in terms of atmospheric CO_2 sequestration.

Ganges is high (50 ± 60 mg/g) during periods of low sediment discharge and low (7.8 ± 9.0 mg/g) during high sediment discharge periods; in the Brahmaputra this fluctuation is not very significant, being below 30 mg/g throughout the year [9, 13]. These values are similar to those reported by [14] for the samples from tributaries of the Ganges and Brahmaputra in the Indian sector. Among world rivers the Ganga (or Ganges) and Brahmaputra rank first for sediment transport [15], with high erosion rates in the Himalayan range driving the high suspended sediment flux [16]. The annual sediment discharge is $400 - 600 \times 10^6$ tonnesyr^{-1} for the Brahmaputra and $330 - 550 \times 10^6$ tonnesyr^{-1} for the Ganga (River Survey Project, 1996 [17]). This generates an organic carbon (OC) burial flux that, associated with sediment trapping in the Bengal fan, has been estimated to be around 1.1×10^{12}molCyr^{-1} for the Neogene [18, 8]. Previous studies of OC in the Ganga and Brahmaputra have documented the concentration and composition of organic matter in the dissolved and suspended load in the Indo-Gangetic plain [9, 13, 14, 19]. They have provided insights into the sources and state of degradation of the organic matter near the mouth [13] and first estimates of particulate OC fluxes [14]. The authors of [10] measured a total flux of 0.5×10^{12}molCyr^{-1} for particulate OC in the Ganga-Brahmaputra transported as suspended load. This flux does not account for OC transported as bedload or sequestered in the plain.

In order to understand the composition characteristics and distribution pattern of organic carbon in river sediments we sampled sediments and soils from the channel, suspended, banks and floodplain of the Brahmaputra river (at 5 locations from upstream to downstream) and its tributaries rivers (before the confluence with the mainstream).

During the monsoon season in August 2013 river water (2L) bulk samples containing suspended sediments were collected from each sampling station in polypropylene bottles. Sampled water was passed through 500 μm sieve to remove any debris, if present. Samples were first filtered through 0.45 μm pre-combusted glass-micro fibre filters (GF/F Whatman) that had been pre combusted overnight at 450° C using vacuum pressure pump. After filtration, the filters were dried for 24 h at 50° C and POC was analysed in the laboratory using a TOC Analyser (Multi NC 2100S, HT 1300, Analytik Zena, Germany)-solid module in Tezpur University, Tezpur. Sediments samples (floodplain, overbank and channel sediments) were collected by channel sampling method, after removing the upper few centimeters layer, approximately 2 kg of sediment from selected locations. The collected sediment samples were then packed and sealed in polyethylene bags and transferred to the laboratory. After being air-dried, the sediment samples were crushed and ground to 200-mesh size and analysed for organic carbon.

9.4 Results

9.4.1 Longitudinal and lateral variation of organic carbon in the Brahmaputra

The organic C content (% OC) in the sediments of the Brahmaputra ranged from 0.01 to 0.04% , 0.08 to 0.53% , 0.08 to 0.20% and 0.20 to 0.82% in channel, overbank ,floodplain and suspended sediments ,respectively (table 9.1) and the particulate organic C content showed an almost uniform trend with only a slight increase downstream(0.33 to 0.68%; Figure 9.2).The overbank OC content also showed an almost

	Locations	LOI	TOC	% silt-clay	mean grain size
Channel	PSG	1.00	0.01	28.00	3.19
	DIB	3.46	0.02	35.30	4.16
	TEZ	2.00	0.03	40.50	3.35
	GHY	2.00	0.04	30.30	3.99
	DHBR	1.75	0.02	22.50	2.28
Bank	PSG	7.35	0.53	13.70	4.37
	DIB	3.40	0.11	84.60	5.69
	TEZ	3.61	0.19	54.20	4.41
	GHY	2.00	0.07	48.20	4.93
	DHBR	2.52	0.08	70.00	5.16
Floodplain	PSG	5.18	0.08	71.80	7.57
	DIB	4.07	0.12	99.30	5.84
	TEZ	10.52	0.20	93.00	6.11
	GHY	4.16	0.09	99.30	6.29
	DHBR	2.45	0.09	92.80	6.02
Suspended	PSG	4.80	0.33	na	Na
	DIB	1.89	0.20	na	Na
	TEZ	5.06	0.82	na	Na
	GHY	4.20	0.62	na	Na
	DHBR	5.53	0.68	na	Na

Table 9.1: Total organic carbon (wt %), LOI (Loss on ignition, %), % silt-clay and mean grain size(phi) in various locations in channel, bank, floodplain and suspended sediments in the Brahmaputra River. na ≡ not analysed.

	Rivers	LOI	TOC	%silt-clay	mean grain size
Channel	SBN	1.00	0.05	1.50	5.84
	JBR	1.77	0.01	34.50	3.32
	PGL	4.17	0.06	32.60	3.82
	BHD	1.48	0.00	34.40	3.72
	DKW	3.39	0.08	37.70	4.31
	KPL	2.00	0.00	32.60	4.14
Bank	SBN	6.11	0.05	53.20	4.67
	JBR	2.62	0.34	52.40	4.61
	PGL	4.45	0.88	53.60	4.48
	BHD	6.76	0.13	21.30	3.21
	DKW	4.20	0.30	37.70	4.30
	KPL	3.36	0.01	30.00	4.10
Floodplain	SBN	6.28	1.98	52.20	4.63
	JBR	4.38	0.24	39.50	4.10
	PGL	5.00	0.90	88.30	6.21
	BHD	2.31	0.10	74.80	4.96
	DKW	6.47	0.51	62.20	5.13
	KPL	3.62	0.04	85.00	5.63
Suspended	SBN	6.83	0.33	na	na
	JBR	6.83	0.33	na	na
	PGL	4.42	1.16	na	na
	BHD	4.42	1.16	na	na

Table 9.2: Total organic carbon(wt %), LOI (Loss on ignition, %), % silt-clay and mean grain size (phi) in various locations in channel , bank ,floodplain and suspended sediments in the tributaries. na ≡ not analysed.

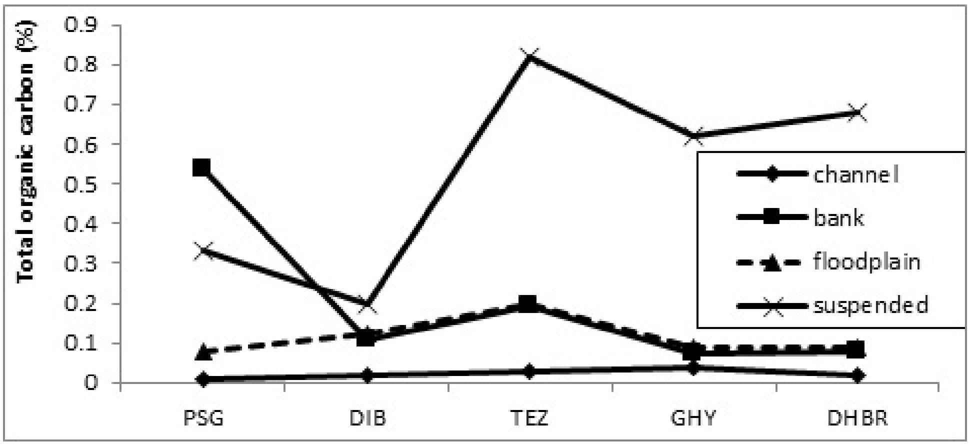

Figure 9.2: The lateral and downstream variation of organic carbon along the Brahmaputra.

uniform trend with a slight decrease downstream (7.35 to 2.52%; Figure 9.2). The channel and floodplain organic carbon did not show much variation along the river. We observed that both POC and overbank OC showed a decrease when the river entered the plains in Assam at DIB from PSG (which is at high altitude).

9.4.2 Relation between organic carbon content and % silt-clay and mean grain size in Brahmaputra

TOC content in the sediments were negatively correlated with % silt-clay. There was also no clear relationship (r=0.025) between the mean OC content and their mean grain size in the Brahmaputra river sediments.

9.4.3 Relation between organic carbon content and SPM (suspended particulate matter) in the Brahmaputra

The POC as well as LOI (Loss on ignition) displayed inverse relationship with SPM in the Brahmaputra River i.e. elevated concentrations of POC associated with low SPM and depleted concentrations of POC with high SPM at the sampling stations were seen. This observation is in agreement with [20].

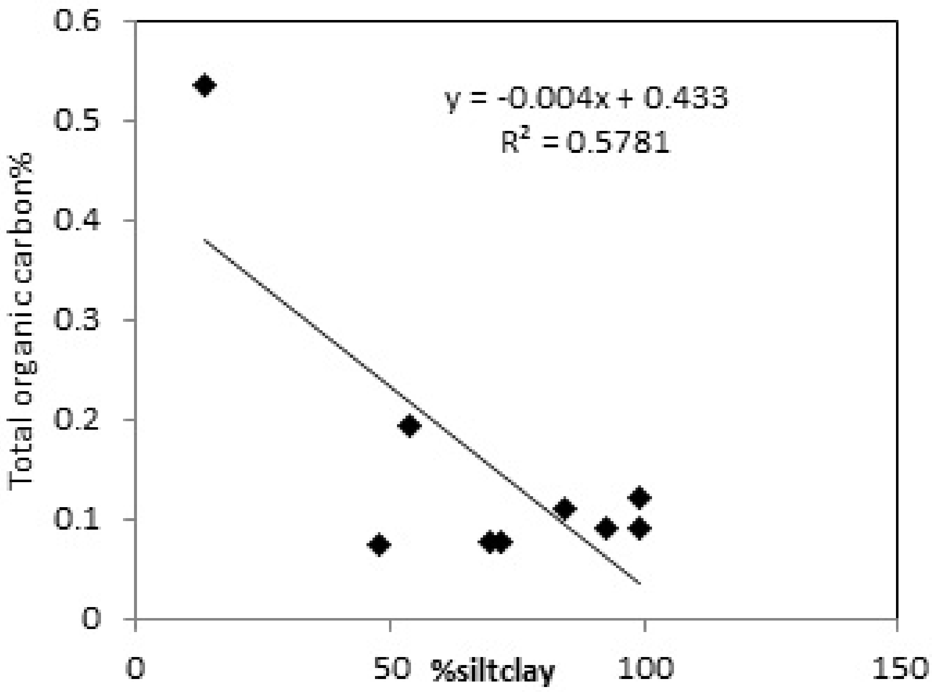

Figure 9.3: Plots showing the relationship between TOC versus % silt-clay.

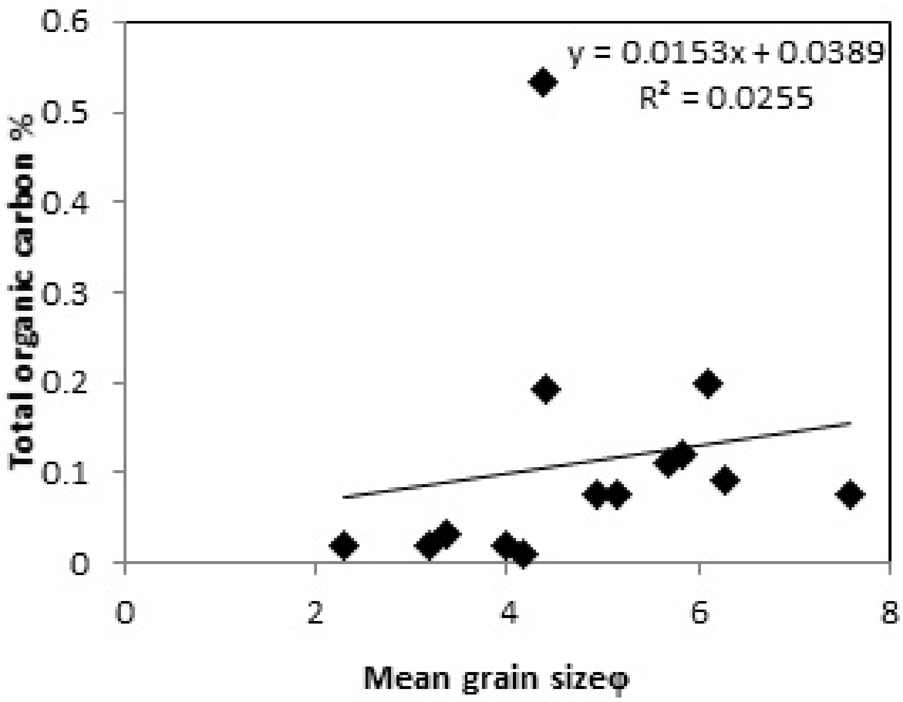

Figure 9.4: Plot showing the relationship between TOC and mean grain size (channel, overbank and floodplain).

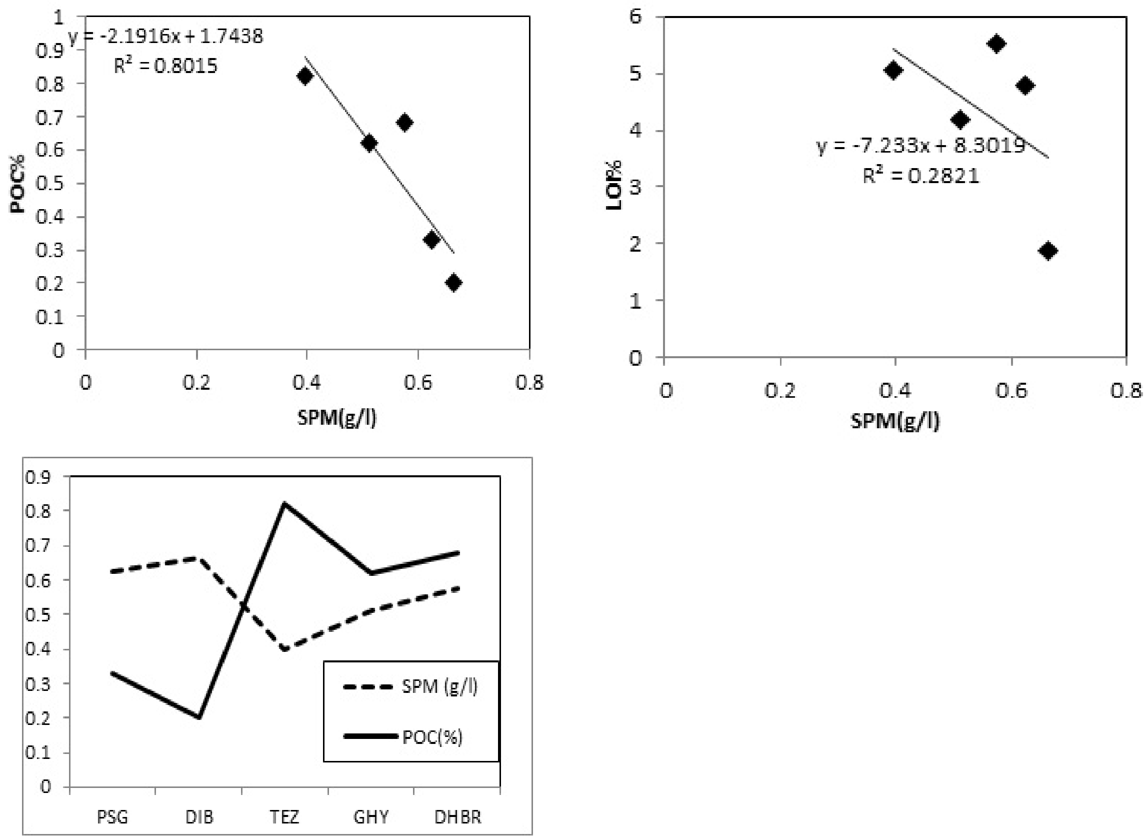

Figure 9.5: Plots showing the relationship between (a) POC versus SPM (Upper left panel) (b) POC versus LOI (Upper right panel) (c) variation of POC concentration with SPM (Lower panel) along the Brahmaputra River.

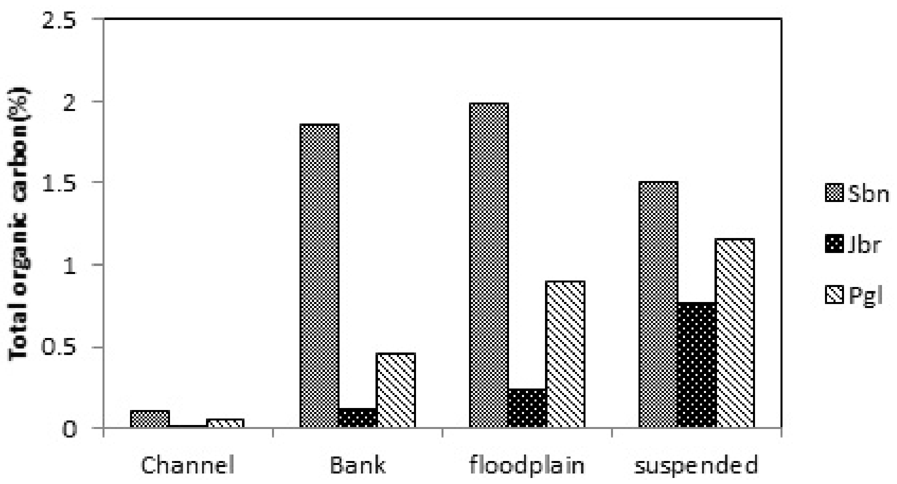

Figure 9.6: Variation of OC in the north bank tributaries.

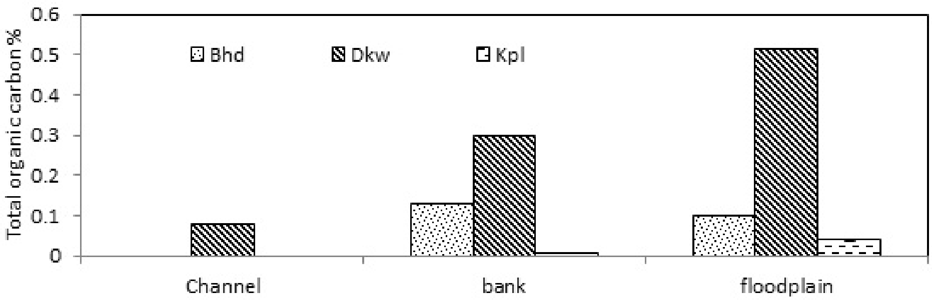

Figure 9.7: Variation of OC in the south bank tributaries.

9.4.4 Variation in OC in the tributaries

The organic content in the north bank tributaries (originating from the Himalayas) was found to be higher than the south bank tributaries originating in the Indo-Burma ranges and the Shillong plateau (Figure 9.6 and 9.7). The TOC content in the north bank tributaries ranged from 0.01 to 0.1%, 0.11 to 1.85%, 0.24 to 1.98% and 0.3 to 1% in channel, overbank, floodplain and suspended sediments respectively. The TOC content in the south bank tributaries ranged from 0.0 to 0.08%, 0.0 to 0.3% and 0.03 to 0.5% in channel, overbank and floodplain sediments respectively.

9.4.5 Relation between organic carbon content and % silt-clay and mean grain size in tributaries

Greater correlation was seen between TOC and grain size in the sediments in the north bank tributaries (r=0.869 with % silt-clay and r=0.841 with mean grain size) than in the south bank tributaries (r=0.038 with % silt-clay and r=0 .085 with mean grain size) and Brahmaputra (r=-0.578 with % silt-clay and r= 0.025 with mean grain size).

9.4.6 Description of statistical data

Statistical analysis was used in order to test a possible relationship between variations of depositional environments and organic carbon contents. The results of the statistical analysis of the TOC versus environmental classes are shown in Figure 9.12, 9.13, 9.14 and Table 9.4, 9.5. The four environmental classes available for all locations are: channel; overbank; floodplain and suspended. Box diagrams for

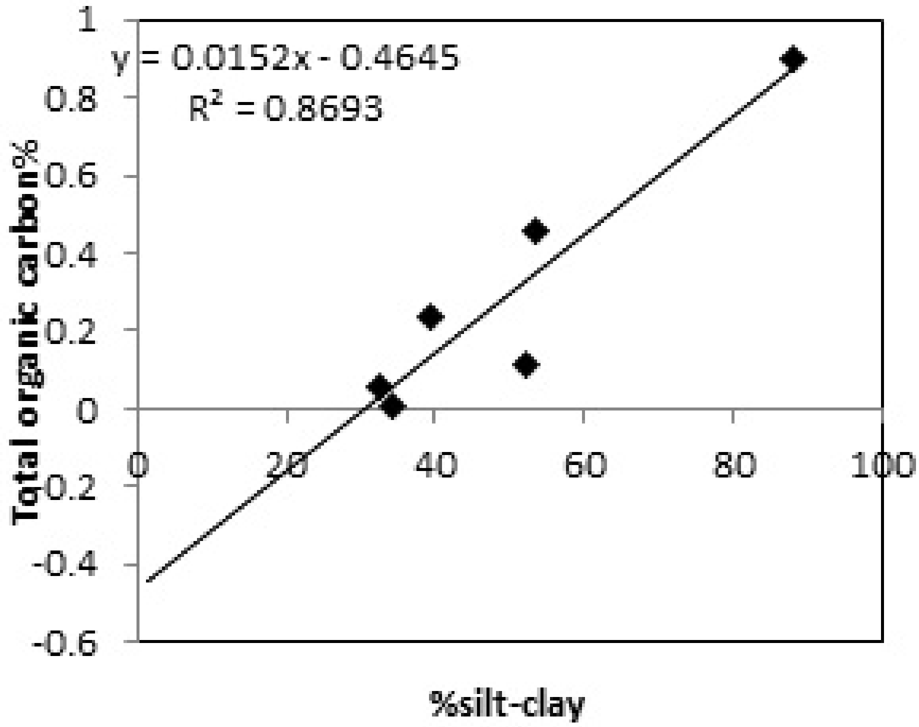

Figure 9.8: Plots showing the relationship between TOC versus % silt-clay in the north bank tributaries sediment (channel, overbank and floodplain).

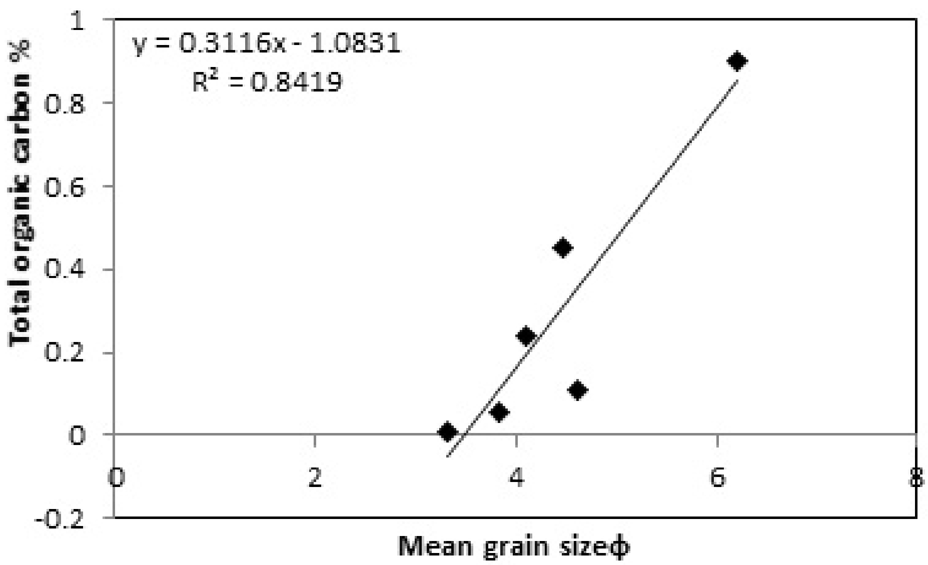

Figure 9.9: Plots showing the relationship between TOC (%) versus mean grain size in the north bank tributaries (channel, overbank and floodplain).

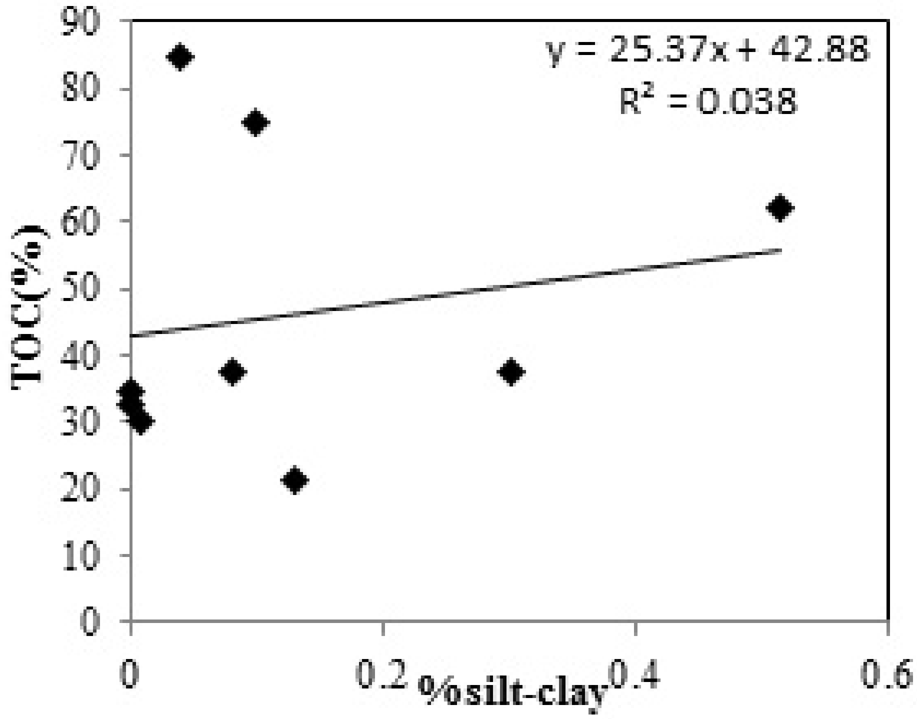

Figure 9.10: Plots showing the relationship betwee TOC versus % silt-clay in the south bank tributaries sediment (channel, overbank and floodplain).

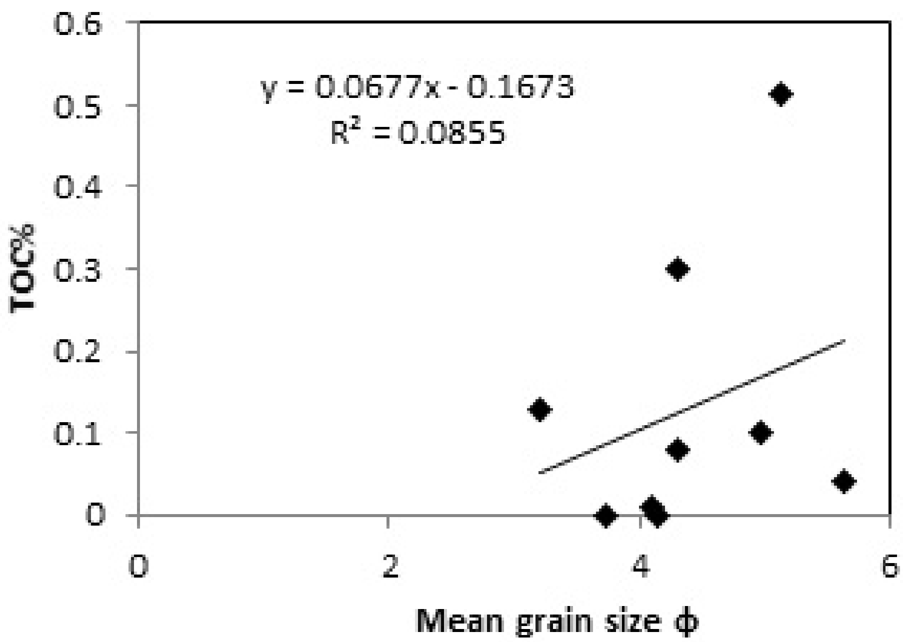

Figure 9.11: Plot showing the relationship between TOC versus mean grain size in the south bank bank tributaries (channel, overbank and floodplain).

samples	S%	I%	K%	C%
PSG	9.12	50.36	0.00	40.53
PSG	8.47	50.19	0.00	41.34
DBRG	6.57	49.29	15.55	28.59
DBRG	8.77	50.78	12.48	27.97
TEZ	7.43	58.38	10.79	23.40
GHY	7.87	55.67	18.80	18.80
DHBR	7.32	57.10	22.70	12.99
SBN	7.76	42.04	0.00	50.19
PGL	2.23	80.78	0.00	16.99
JBR	3.24	73.60	0.00	23.16
DKW	4.08	43.14	18.10	34.67
KPL	5.18	29.83	64.99	0.00
BHD	9.39	40.78	27.42	22.42

Table 9.3: Relative abundance of clay minerals smectite (S), illite (I), kaolinite (K) and chlorite (C) present in the sediments of the Brahmaputra and its tributaries.

LOI and OC illustrate both the median and interquartile of all depositional environments. The box-plots and the results of the analysis of variance ANOVA, which are summarised in Table 9.4, 9.5, suggest a significant influence of the depositional environments on the TOC content for the entire dataset at 0.05%-significance level.

TOC decreased from suspended to overbank to floodplain deposits(TOCss > TOCbnk > TOCfp > TOCch; Figure 9.12) in the Brahmaputra river whereas in the tributaries, the TOC contents increase significantly from channel bed deposits to overbank deposit to floodplain deposits (in the north bank tributaries: TOCfp > TOCbnk > TOCss > TOCch; Figure 9.13 and in the south bank tributaries: TOCfp > TOCbnk > TOCss; Figure 9.14). OC in suspended sediments was significantly higher in the Brahmaputra than in the Himalayan tributaries.

Testing the relationship between depositional environments and organic carbon: analysis of variance (ANOVA) A two-way ANOVA was conducted on all the samples arranged into four environmental classes in order to evaluate the effect of the depositional environment and locations on the OC and the interactions between locations and environment classes. When significant differences were observed, we

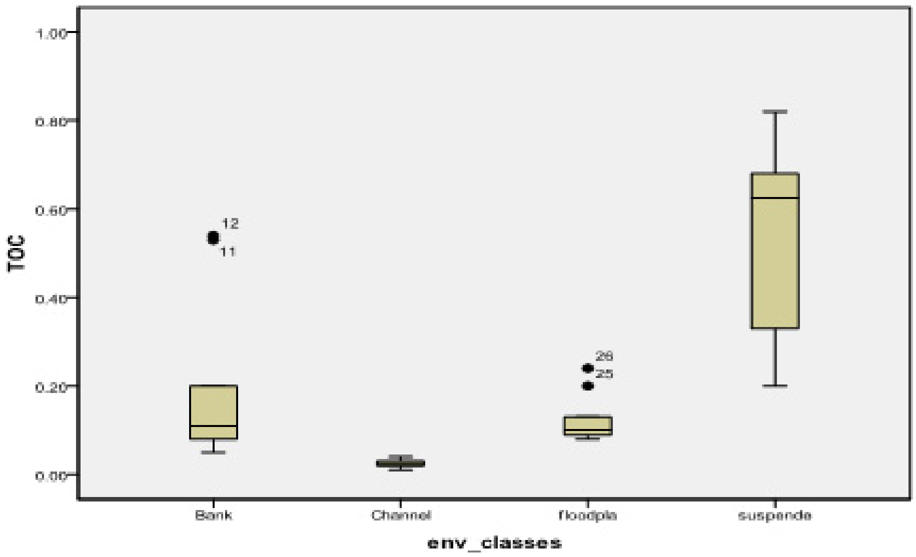

Figure 9.12: Box plot of TOC versus depositional environment in the Brahmaputra. Median, percentiles (10th, 25th, 75th and 90th) and error of the OC (channel, suspended, overbank and floodplain) of the different types of sedimentary deposits within the Brahmaputra catchment.

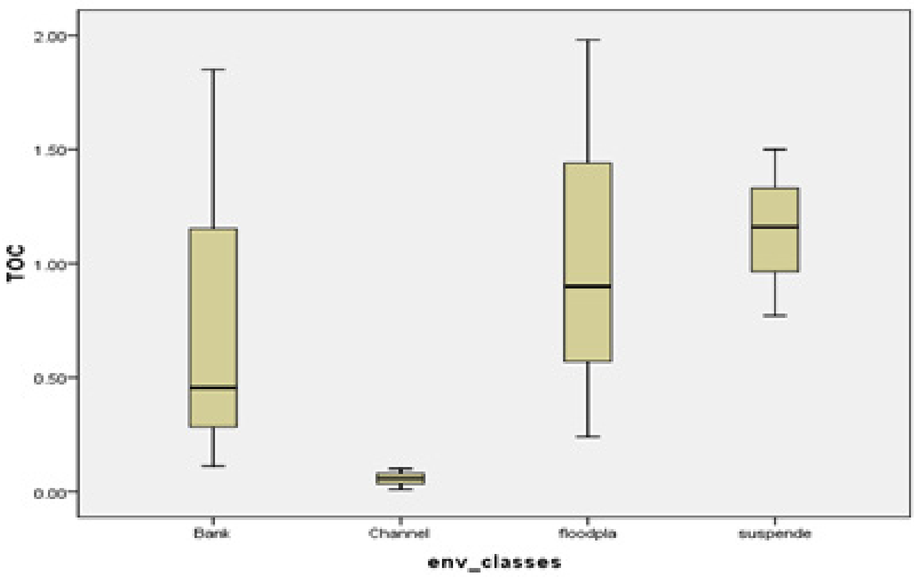

Figure 9.13: Box plot of TOC versus depositional environment in the North bank tributaries. Median, percentiles (10th, 25th, 75th and 90th) and error of the OC (channel, suspended, overbank and floodplain) of the different types of sedimentary deposits.

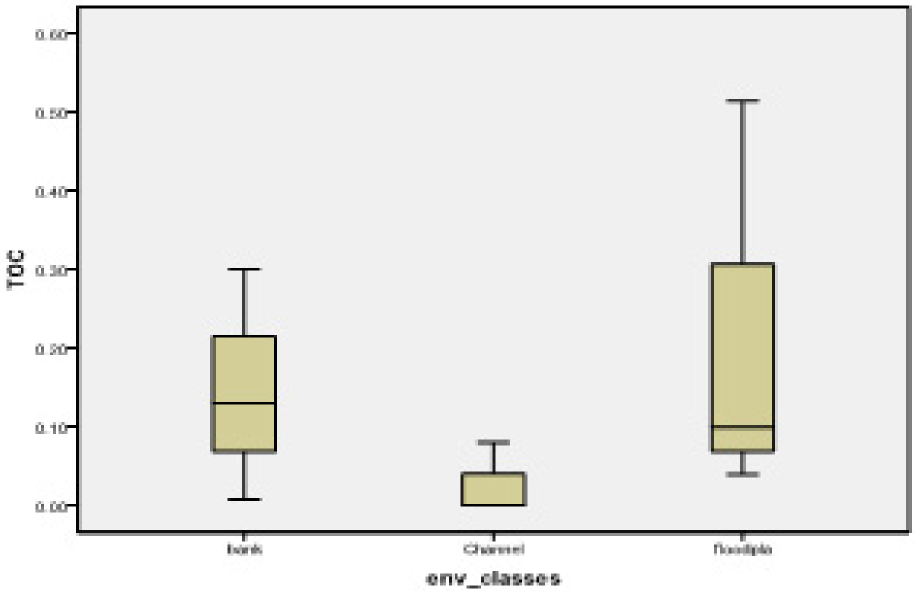

Figure 9.14: Box plot of TOC versus depositional environment in the South bank tributaries. Median, percentiles (10th, 25th, 75th and 90th) and error of the OC (channel, overbank and floodplain) of the different types of sedimentary deposits.

used LSD test for post hoc multiple comparisons. One way ANOVA was used to determine the significant differences between the environment classes and locations (Table 9.4, 9.5). The results confirmed that the there was no significant effect of environment of deposition and locations on the OC content.

9.5 Discussion

9.5.1 Sediment dynamics along the Brahmaputra River flow-path

Unlike major rivers, SPM concentrations decrease with a general trend of increasing particulate organic carbon (POC) in the Brahmaputra. This may be due to (1) increased turbidity (increase in SPM) with increasing discharge which decreases autochthonous primary production within the mainstream and tributaries and (2) high content of SPM is associated with high discharge when mobilization of sediment occurs, which is characterised by a low organic content.Almost uniform POC (0.33 to 0.68%) and LOI (4.8 to 5.5%) content at all the locations in the Brahmaputra

Pair wise comparisons (Dependent variable: TOC)			
(I) ENV_CLASSES	(J) ENV_CLASSES	Std. Error	Sig.
Bank	channel	.043	.000
	floodplain	.043	.000
	suspended	.049	.000
Channel	bank	.043	.000
	floodplain	.043	.000
	suspended	.049	.000
floodplain	bank	.043	.000
	channel	.043	.000
	suspended	.049	.000
suspended	bank	.049	.000
	channel	.049	.000
	floodplain	.049	.000

Table 9.4: Pair wise comparisons between the environmental classes.

Source	**df**	**Mean Square**	**F**	**Sig.**
ENV_CLASSES	3	1.289	87.048	.000
RIVERS	6	.598	40.338	.000
RIVERS * ENV_CLASSES	15	.436	29.447	.000

Table 9.5: Results of the ANOVA (analysis of variance) on all the samples from all the rivers arranged in 4 environmental classes. Effect of the rivers and environmental classes on the OC content.

indicates (1) a strong hydrodynamic condition along this transit (suggested by the poorly sorted sediments) and/ or (2) most particulate matter exported towards the coastal zone originated from headwater regions. The decrease in POC observed as the river entered the plains from higher altitude may be due to better preservation of the organic fraction in colder high altitude regions, with loss of carbon during downstream spiralling [21]. The subsequent little increase downstream may be due to the confluence of the tributaries and remobilisation of overbank deposits during monsoon (when the samples were collected).

9.5.2 Silt-clay, mean grain size and TOC

According to [20] positive co-variation between TOC content and the proportion of fine particles may result from at least two factors depending on how TOC is transported: (1) if TOC is mainly independent of minerals particles, its low density would tend to concentrate TOC in fine-grained sediments through hydrodynamic sorting, and (2) if TOC is mainly linked with minerals, both particle size and mineral composition must control the TOC loading in detrital sediments. In our study also we found that TOC was linked to both minerals and mean grain size. Poor correlation between particle size and TOC in the sediments of the Brahmaputra in all the environmental classes may be due to two reasons: (1) dominance of sand size particles in the sediments (2) due to a differing clay mineral composition in the sediments [22].
The observed weak or absent correlation between silt-clay and TOC content in the south bank tributaries could be due to a differing clay mineral composition between the north bank and south bank tributaries (Rasmussen et al., 2005). Specific surface areas of clays vary from 6-39 m^2g^{-1} for kaolinite [23] to 800 m^2g^{-1} for smectite and vermiculite and 50-100 m^2g^{-1} for illite [24].

9.5.3 SPM and TOC

In present study the riverine POC may be regulated by organic materials from soil erosion and bank remobilisation. Another possible impact factor may be the transport of sandy soils during flood periods (during high discharge when the SPM was measured) which contain less Organic matter. This may also be the reason for the absence of no correlation between TOC and mean grain size of the sediments. The POC content was found to be higher in the Himalayan tributaries (SBN, JBR and PGL) than in the south bank tributaries (BHD, DKW and KPL). With dams under construction at Thalkuchi in Pagladia and Gerukamukh in Subansiri River, the effect of dams on the SPM and POC need to be seen.

9.5.4 Statistics

The distribution of OC showed significant variation among the locations (PSG, DIB, TEZ, GHY and DHBR; p=0.000) and among the four environmental classes (suspended, overbank, channel and floodplain). The ANOVA Table 9.4 showed that there was significant difference between the OC content of the different environment classes. The ANOVA results (Table 9.5) showed significant difference among the TOC of all the rivers suggesting the different sources for the organic carbon in these rivers. Each river system is characterised by different source rocks, physical and chemical erosion rates or transport dynamics that have resulted in different TOC loading mechanisms.

9.6 Conclusions

In order to explore the composition characteristics and distribution pattern of organic carbon (OC) in the Brahmaputra catchment sediments from channel bed, riverbank, floodplain and suspended were sampled from upstream to downstream of the Brahmaputra mainstream in Assam Plains and its tributaries (Subansiri, Jiabharali, Pagladia, Burhidihing, Dikhow and Kopili), total organic carbon (OC), Particulate organic carbon (POC), mean grain size and clay were measured.

Uniform OC content suggest strong hydrodynamic conditions during transport (also suggested by the poorly sorted sediments). The relatively low OC concentrations found in overbank and floodplain sediments compared to the POC at the catchment scale suggest that erosion and sediment transport processes lead to C losses to the Brahmaputra River during transport in the Assam Plains.

The ANOVA results confirmed that the there was significant effect of environment of deposition and locations on the OC content which may be because each river

system is characterised by different source rocks, physical and chemical erosion rates or transport dynamics that must result in different TOC loading mechanisms.
This was a preliminary study to estimate the carbon variation in the Brahmaputra basin in Assam plains and the information in this study may benefit our understanding of the contribution of OC that Brahmaputra delivers to the global carbon budget.

Bibliography

[1] Milliman, J. D., and Meade, R. H. (1983). World-wide delivery of river sediment to the oceans.The Journal of Geology, 1-21.

[2] Miller, J. R., and Russell, G. L. (1992). The impact of global warming on river runoff.Journal of Geophysical Research: Atmospheres,97 (D3), 2757-2764.

[3] Ludwig, W., Probst, J. L., and Kempe, S. (1996). Predicting the oceanic input of organic carbon by continental erosion.Global Biogeochemical Cycles, 10 (1), 23-41.

[4] Blair, N. E., Leithold, E. L., Ford, S. T., Peeler, K. A., Holmes, J. C., and Perkey, D. W. (2003). The persistence of memory: The fate of ancient sedimentary carbon in a modern sedimentary system, Geochim. Cosmochim. Acta, 67, 63-73.

[5] Hoffmann, T., Glatzel, S., and Dikau, R. (2009). A carbon storage perspective on alluvial sediment storage in the Rhine catchment.Geomorphology, 108 (1), 127-137.

[6] Subramanian, V., and Ittekkot, V. (1991). Carbon transport by the Himalayan rivers.Biogeochemistry of Major World Rivers,42, 157-168.

[7] Datta, D. K., Gupta L. P. and Subramanian, V. (1999). Distribution of C, N and P in the sediments of the Ganga-Brahmaputra-Meghna river system in the Bengal basin. Organic Geochemistry, 30 (1): 75-82.

[8] France-Lanord, C., and Derry, L. A. (1997). Organic carbon burial forcing of the carbon cycle from Himalayan erosion.Nature,390 (6655), 65-67.

[9] Chowdhury, M. I., Safiullah, S., Iqbal Ali, S. M., Mafizuddin, M., and Enamul, S. (1982). Carbon transport in the Ganga and the Brahmaputra: preliminary results, Mitt. Geol. Palaeontol. Inst. Univ. Hamburg, 52, 457-468.

[10] Aucour, A. M., France-Lanord, C., Pedoja, K., Pierson, Wickmann, A. C., and Sheppard, S. M. (2006). Fluxes and sources of particulate organic carbon in the Ganga-Brahmaputra river system. Global Biogeochemical Cycles, 20(2).

[11] Singh, S. K., Sarin, M. M., and France-Lanord, C. (2005). Chemical erosion in the eastern Himalaya: major ion composition of the Brahmaputra and δ 13 C of dissolved inorganic carbon.Geochimica et Cosmochimica Acta,69 (14), 3573-3588.

[12] Galy, V., France-Lanord, C., Beyssac, O., Faure, P., Kudrass, H., and Palhol, F. (2007). Efficient organic carbon burial in the Bengal fan sustained by the Himalayan erosional system.Nature,450 (7168), 407-410.

[13] Ittekkot, V., Safiullah, S., Mycke, B. and Seifert, R. (1985) Seasonal variability and geochemical significance of organic matter in the River Ganges, Bangladesh. Nature 317, 800-3.

[14] Subramanian, V., J. E. Richey, and N. Abbas (1985), Geochemistry of river basins in the Indian subcontinent: Part II. Preliminary studies on the particulate C and N in the Ganga-Brahmaputra River system, Mitt. Geol. Palaeontol. Inst. Univ. Hamburg, 58, 513-518.

[15] Sarin, M. M., D. K. Krishnawami, L. K. Somayajulu, and W. S. Moore (1989), Major ion chemistry of the Ganga-Brahmaputra River system: Weathering processes and fluxes to the Bay of Bengal, Geochim. Cosmochim. Acta, 53, 997-1009.

[16] Galy, A., and France-Lanord, C. (2001). Higher erosion rates in the Himalaya: Geochemical constraints on riverine fluxes.Geology,29 (1), 23-26.

[17] River Survey Project (1996). Spatial representation and analysis of hydraulic and morphologic data: water resources planning organization, Dhaka flood plan

coordination organization, River Study Rep. 5, Water Resour. Planning Project, Gov. of Bangladesh, Dhaka.

[18] France-Lanord, C., and Derry, L. A. (1994). δ13C of organic carbon in the Bengal Fan: Source evolution and transport of C3 and C4 plant carbon to marine sediments. Geochimica et Cosmochimica Acta, 58 (21), 4809-4814.

[19] Safiullah, S., M. I. Chowdhury, M. Mafizuddin, S. M. Iqbal Ali, and M. Karim (1985). Monitoring of the Padma (Ganga), the Jamuna (Brahmaputra) and the Baral in Bangladesh, Mitt. Geol. Palaeontol. Inst. Univ. Hamburg, 58, 519-524.

[20] Galy, V., France-Lanord, C., and Lartiges, B. (2008). Loading and fate of particulate organic carbon from the Himalaya to the Ganga-Brahmaputra delta.Geochimica et Cosmochimica Acta,72 (7), 1767-1787.

[21] Tamooh, F., Meersche, K., Meysman, F., Marwick, T. R., Borges, A. V., Merckx, R., ... and Bouillon, S. (2012). Distribution and origin of suspended matter and organic carbon pools in the Tana River Basin, Kenya. Biogeosciences, 9 (8), 2905-2920.

[22] Rasmussen, C., Torn, M. S., and Southard, R. J. (2005). Mineral assemblage and aggregates control carbon dynamics in a California conifer forest.Soil Science Society of America Journal,69 (6), 1711-1721.

[23] Dixon, J. B. (1977) Kaolinite and serpentine group minerals: in Minerals in Soil Environments, J. B. Dixon and S. B. Weed, eds., Soil Science Society of America, Madison, Wisconsin, 357-403.

[24] Robert, M. and Chenu, C. (1992). Interactions between soil minerals and microorganisms. In: Stotzky, G. and Bollag, J-M., ed. Soil Biochemistry. New York: Marcel Deckker, 7:307-404.

Chapter 10

Conclusions and Future Scope

The present research study has been carried out along a stretch of 891 km of the Brahmaputra river in Assam, India. The study dealt with assessment of the textural, mineralogical and geochemical characteristics of the suspended, bed load, overbank and floodplain sediments of the Brahmaputra River in Assam and six of its major tributaries. It began with a systematic sampling and monitoring of the geochemical characteristics of the river. The findings of each chapter was summarised as follows:

The grain size analysis of the Brahmaputra River and its tributaries did not show downstream fining of sediment grain size which may be due to the tributary contribution. Rivers originating from the Himalayan orogenic belt region were characterised by the predominance of fine sand and very fine sand whereas the south bank tributaries bring much coarser sediments than the Himalayan rivers and were characterised by the high content of coarse- and medium-grained sand. Percentage silt-clay increased from bedload to bank to floodplain sediments due to the deposition of the finer fraction during floods and further weathering of the deposited sediments over time. The textural parameters clearly indicate the importance of source area in textural characteristics of sediments.

Mineralogy of the sediment samples have been studied using X-ray diffraction technique (XRD. Major and minor oxides in sediment samples were determined using X-ray fluorescence (XRF) and inductively coupled plasma-atomic emission spectrophotometer (ICP-AES) respectively. In our study, presence of hornblende, plagioclase, chlorite and orthoclase in downstream locations indicate the lesser intensity of chemical weathering in the mainstream. We found that the amount of kaonilite increased from Pasighat to Dhubri, while smectite and vermiculite decrease and illite remains stable. Illite and chlorite are higher in Brahmaputra than the Ganges (60% vs 42% and 17% vs 7% respectively), which may be due to the dominance of Himalayan tributaries in the Brahmaputra. Himalayan tributaries contain more micaceous minerals (with dominant biotite) south bank tributaries. More Illite in the north bank tributaries indicate more physical weathering and Himalayan uplift, whereas more smectite in the south bank tributaries are associated with more chemical weathering. From the geochemical data we found that in the Brahmaputra only the mobile elements are depleted in the channel and overbank sediments indicating low chemical weathering in the source area. In the suspended sediments, the concentrations of major and trace elements did not increase downstream and showed a conservative behaviour throughout the stretch of the river. In the A-CN-K ternary plots (showing the weathering trends) the Brahmaputra samples plot near to the granite-graniodiorite line (average upper continental crust composition) indicating very less chemical weathering in the source area (in the cold and dry Tibetan plains). The tributaries showed more chemical alteration and weathering compared to the Brahmaputra. In the South bank tributaries all the samples plot away from the plagioclase-K-feldspar line which indicates that they have undergone intense chemical weathering compared to the north bank tributaries. This is due to the flatter gradient and tectonically relaxed source area as compared to the north bank tributaries.

In order to explore the composition characteristics and distribution pattern of organic carbon (OC) in river sediments, we analysed OC content sediments and soils from the channel, suspended ,banks and floodplain of the Brahmaputra river (at 5 locations from upstream to downstream) and its tributaries rivers (before the confluence with the mainstream). The organic C content (% OC) in the sediments of the Brahmaputra ranged from 0.01 to 0.04% , 0.08 to 0.53%, 0.08 to 0.20% and 0.20 to 0.82% in channel, overbank, floodplain and suspended sediments, respectively. The POC as well as LOI (Loss on ignition) displayed inverse relationship with SPM in the Brahmaputra River i.e. elevated concentrations of POC associated with low SPM and depleted concentrations of POC with high SPM at the sampling stations were seen. Uniform OC content suggest strong hydrodynamic conditions during transport (also suggested by the poorly sorted sediments). The relatively low OC concentrations found in overbank and floodplain sediments compared to the POC at the catchment scale suggest that erosion and sediment transport processes lead to C losses to the Brahmaputra River during transport in the Assam Plains. It was found in our study that there was significant effect of environment classes and locations on the organic carbon content which may be because of contribution of different sources.

The Brahmaputra mainstream as well as the Himalayan tributaries of the Brahmaputra River that join from the north (the Subansiri, the Jia Bharali and the Pagladia) and south bank tributaries (the Burhi dihing, the Dikhow and the Kopili) were studied in terms sediment chemistry and associated particulate flux, and individual elemental contribution from each tributary into the Brahmaputra basin. Sediment discharge estimates are calculated to determine each tributary's contribution to the suspended load of the entire river system. The instantaneous suspended sediment loads during the monsoon season are used to estimate the annual suspended sediment load for the system. In the Brahmaputra though the river load increased downstream the individual signature of tributary inputs to the main channel were not clearly noticeable due to the high discharge and width of the main river. Heavy metal averages in the river were found to be lower than world average. It was observed that the elemental and particulate flux for north bank tributaries was more than the south bank tributaries- flux in the Subansiri River was found to be highest among the tributaries. With the dam under construction in this river, the effect on suspended flux on the Brahmaputra needs to be further investigated after the completion of the dam. In conclusion, the significant findings for the whole study are presented as follows:

1. The textural parameters clearly indicate the importance of source area physiography as well as tributary contribution in controlling textural characteristics of river sediments.

2. The north bank tributaries are characterised with high sediment fluxes and periods of physical weathering and Himalayan uplift, whereas the south bank tributaries is associated with more chemical weathering.

3. The Brahmaputra samples indicated very less chemical weathering in the source area. The tributaries showed more chemical alteration and weathering compared to the Brahmaputra.

4. Bank material of the Brahmaputra are mostly composed of dominant fine sand and silt with clay being less than 5% as found in our study which may explain the unstable banks and extensive erosion in the basin.

5. It was observed that the elemental and particulate flux for north bank tributaries was more than the south bank tributaries-flux in the Subansiri River was found to be highest among the tributaries.

The parameters analysed and discussed under this study is probably the first attempt to study the textural, mineralogical and geochemical characteristics of the Brahmaputra and its tributaries in detail in the Assam part of the river. This study provides some basic information that we need to plan and manage any water resource program and would be helpful for overcoming water management issues made critical by deterioration of river water and sediment quality.

Future Scope and Recommendations

- There is a need for systematic, regular and well-planned monitoring of sediment chemistry and sediment budget for sediment management programmes to be effective and sustainable. Monitoring studies at fixed sites over time are also necessary to study the effect of climate change.

- It is also necessary to recognise and include the different environments within river basins- terraces, floodplain etc. and the interconnectivity between these environments in integrated river basin management programmes. This will help to undertake and design specific sediment management options for different rivers.

- Most importantly from a geochemical and geomorphological perspective there is a need for more detailed understanding of the biogeochemical processes that govern generation , transport and deposition of riverine sediments at various scales.